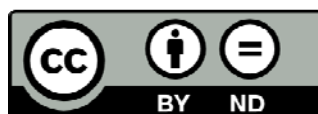




UNIVERSITAT DE
BARCELONA

Development of light-modulated allosteric ligands for remote, non-invasive control of neuronal receptors

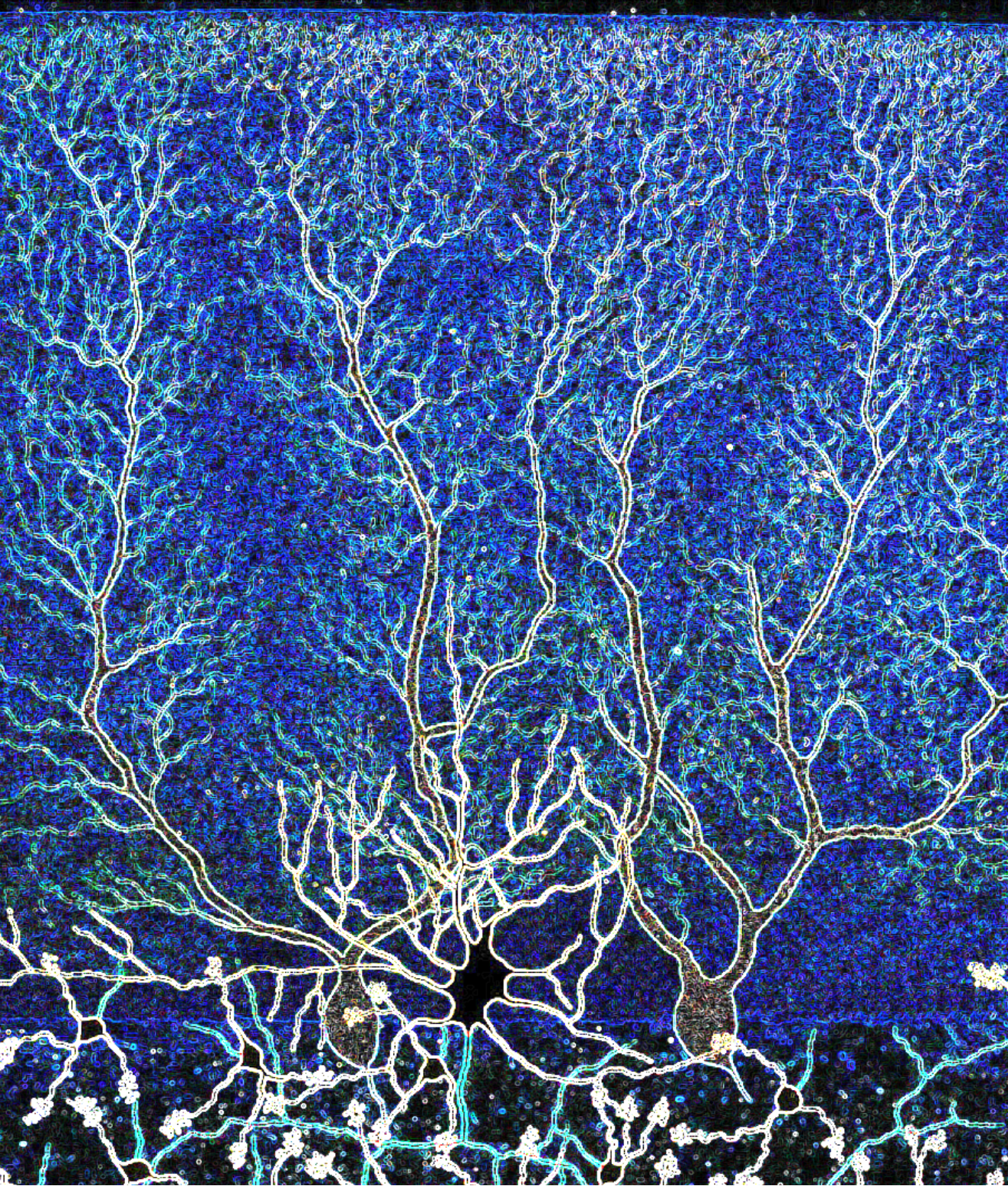
Silvia Pittolo



Aquesta tesi doctoral està subjecta a la llicència Reconeixement- SenseObraDerivada 3.0. Espanya de Creative Commons.

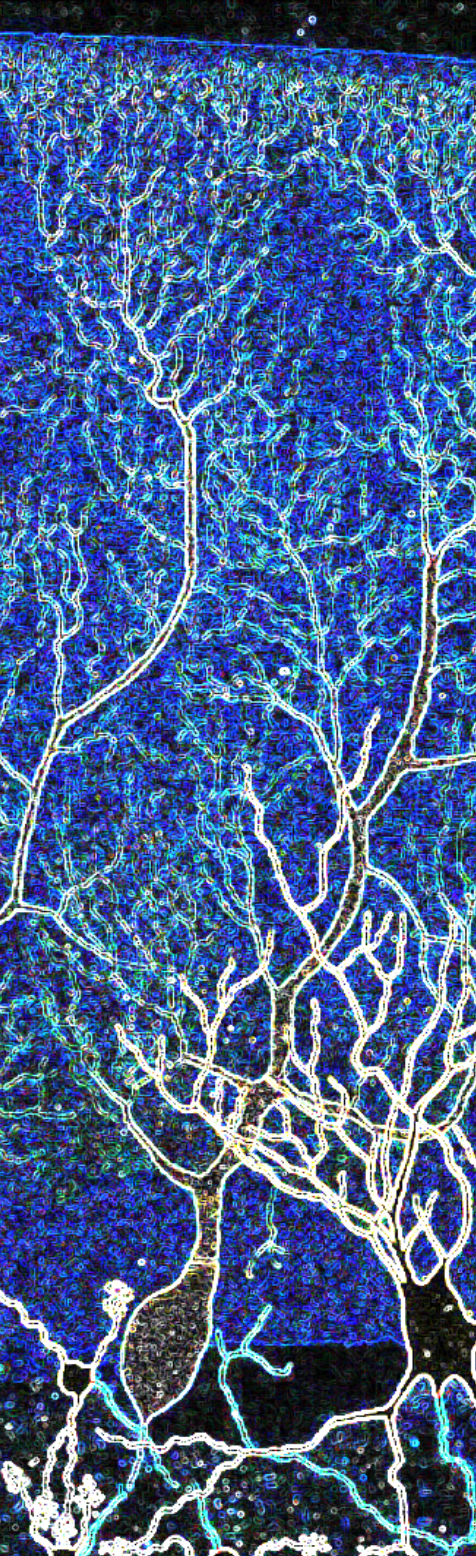
Esta tesis doctoral está sujeta a la licencia Reconocimiento - SinObraDerivada 3.0. España de Creative Commons.

This doctoral thesis is licensed under the Creative Commons Attribution-NoDerivatives 3.0. Spain License.



Development of light-modulated allosteric ligands
for remote, non-invasive control of neuronal receptors

Silvia Pittolo



Cover image adapted from:

Golgi, Camillo (1882–1883).
“Sulla fina anatomia degli organi
centrali del sistema nervoso”
Rivista sperimentale di Freniatria,
anni 1882–83” in *Tavola XIX*,
*Opera Omnia, Vol. I. Istologia
Normale* (1870–1883)
Milano, Ed. Hoepli, 1903, 295–393.



UNIVERSITAT DE
BARCELONA

Programa de Doctorat en Biomedicina
2011-2015

Memòria presentada per Silvia Pittolo a la Universitat de Barcelona per optar al títol de doctor
*This dissertation is submitted to the University of Barcelona for the degree of
Doctor of Philosophy*

Development of light-modulated allosteric ligands for remote,
non-invasive control of neuronal receptors

Silvia Pittolo

Nanoprobes and nanoswitches group
– Institute for Bioengineering of Catalonia –

Directors

Prof. Pau Gorostiza Langa

ICREA research professor at
Institute for Bioengineering of Catalonia
(IBEC)

Tutor

Prof. Francisco Ciruela Alférez

'Neuropharmacology and pain'
group leader
University of Barcelona

Dr. Amadeu Llebaria Soldevila

'Medicinal chemistry' group leader
Institute of Advanced Chemistry of Catalonia
(IQAC-CSIC)

Barcelona, September 2015

I am grateful to the Government of Catalunya and the Agency for Management of University and Research Grants (AGAUR) for helping funding my PhD studies with grant number 2012FI_B 01122.

I am also grateful to:

- Dr. Jean-Philippe Pin, for mentoring my stay at the Institute for Functional Genomics (IGF), CNRS, in Montpellier, France, between February and April 2013.

- Prof. Pedro de la Villa Polo, for hosting me at the University of Alcalá, in Alcalá de Henares, Spain, in November 2013.

- Dr. Eduardo Fernández Jover, for hosting me at the Institute for Bioengineering of the University Miguel Hernández, in Elx, Spain, in March, May, November and December 2014.

- Dr. Stephan Junek, for hosting me at the Max Planck Institute for Brain Research, in Frankfurt am Main, Germany, in July 2015.

Ai miei Genitori,

*Apri a la verità che viene il petto;
e sappi che, sì tosto come al feto
l'articular del cerebro è perfetto,*

*lo motor primo a lui si volge lieto,
sovra tant'arte di natura, e spira
spirito novo, di virtù repleto,*

*che ciò che trova attivo quivi, tira
in sua sustanzia, e fassi un'alma sola,
che vive e sente e sé in sé rigira.*

DANTE ALIGHIERI
La divina Commedia
Purgatorio, XXV, 67

TABLE OF CONTENTS

TABLE OF CONTENTS.....	9
INTRODUCTION	15
1 METABOTROPIC GLUTAMATE RECEPTORS.....	17
1.1 Structure and activation mechanism	17
Venus Flytrap (VFT) and Cysteine Rich Domain (CRD).....	18
Trans Membrane Domain (TMD).....	20
C terminal domain (CTD).....	21
1.2 Intracellular signaling.....	23
1.3 Localization and physiology of mGlu in the CNS.....	28
Localization.....	28
1.3.1 Role in neurotransmission.....	30
1.3.2 Role in glial cells	32
1.3.3 Role in synaptic plasticity	36
Short term plasticity (ms to s)	36
Long term plasticity (min to h).....	36
Future challenges	39
1.4 Relevance to neuropathologies	40
Animal models of mGlu ablation.....	40
Anxiety	43
Drug addiction.....	43
Schizophrenia	43
Fragile X syndrome and other autism spectrum disorders	44
Parkinson's Disease	46
Chronic pain.....	48
1.5 Conventional pharmacology in targeting mGlu receptors.....	48

2	OPTICAL TOOLS FOR MGLU RECEPTORS: SENSORS	56
2.1	Sensing the position of mGlu receptors with light	56
2.1.1	Non-covalent binding of fluorescent probes	56
2.1.2	Genetically encoded fluorescent proteins	57
2.1.3	Advances in fluorescence microscopy	59
	Two-photon microscopy	60
	Super-resolution microscopy	62
2.2	Sensing the receptor conformational and protein-protein interaction dynamics with light	63
	Time-resolved FRET	67
2.3	Sensing the signaling of mGlu receptors with light	69
2.3.1	Optical sensors of second messengers	69
	Calcium	69
	Chemical calcium indicators	70
	Genetically encoded calcium indicators (GECI)	72
	Inositol phosphate 3 (IP ₃)	72
	Genetically encoded IP sensors	73
	TR-FRET in IP accumulation assays	73
	Diacylglycerol (DAG)	75
	Cyclic AMP and GMP	75
2.3.2	Optical sensors of effectors	76
2.3.3	Interacting proteins to monitor receptor trafficking	76
	β-arrestin	76
	G protein-coupled receptor kinases (GRKs)	77
	Fusion to pHluorin	77
	Coordinators of vesicle trafficking	78
2.4	Future challenges	78
3	OPTICAL TOOLS FOR MGLU RECEPTORS: SWITCHES	80
3.1	Optogenetics	81
3.2	Optogenetic pharmacology	83
3.3	Optopharmacology	85
	Caged ligands	86
	Photochromic ligands	87
	Optopharmacological strategies for other neuronal receptors, pores, and ion channels so far	87

Caged ligands or irreversibly binding.....	88
3.4 Future challenges	94
OBJECTIVES	97
MATERIALS & METHODS	99
1 PHOTOCHEMISTRY OF OPTICAL SWITCHES.....	99
Absorption spectra.....	99
Kinetics of <i>cis-to-trans</i> relaxation.....	100
2 OPTOPHARMACOLOGY WITH IP-ONE HTRF ASSAY.....	100
2.1 Cell culture and electroporation.....	101
2.2 IP-One HTRF assay	101
2.3 Subtype-selectivity experiments with Alloswitch-1	102
3 SINGLE-CELL CALCIUM IMAGING AT SINGLE PHOTON STIMULATION.....	104
3.1 Cell culture and plasmid transfection.....	104
3.2 Neonatal rat cortical astrocyte cultures	104
3.3 Pre-incubation of G4optoNAM and derivatives	105
3.4 Ca ²⁺ indicator loading and bath solution.....	105
3.5 Single-cell calcium imaging	106
3.6 Photoisomerization of compounds	106
3.7 Addition of compounds during imaging	107
3.8 Data analysis	108
4 BEHAVIORAL TESTS IN <i>XENOPUS TROPICALIS</i> TADPOLES.....	110
5 BEHAVIORAL TESTS IN ZEBRAFISH LARVAE	111
6 TWO-PHOTON CALCIUM IMAGING AND EXCITATION	111
RESULTS	115
CHAPTER 1.....	117
1 DESIGN STRATEGY AND PHOTOCHEMISTRY OF ALLOSWITCH-1	117
2 OPTOPHARMACOLOGY OF ALLOSWITCH-1 WITH THE IP-ONE ASSAY	122
2.1 Potency of alloswitch-1 over mGlu ₅ in dark and under violet light.....	124
2.2 Selectivity of Alloswitch-1 over the rest of the mGlu receptors family.	126

3	REAL-TIME OPTOPHARMACOLOGY OF ALLOSWITCH-1	128
3.1	Alloswitch-1 in the absence of orthosteric agonist	135
	Future challenges.....	138
3.2	Effect of changing the illumination wavelength	139
3.3	Effect of changing the illumination pulse frequency	140
4	ALLOSWITCH-1 CONTROLS ENDOGENOUS MGLU ₅ RECEPTORS	141
5	ALLOSWITCH-1 CONTROLS MOTILITY IN <i>X. TROPICALIS</i>	143
CHAPTER 2		147
1	PHOTOCHEMISTRY AND PHARMACOLOGY OF G4OPTONAM	147
2	REAL-TIME OPTOPHARMACOLOGY OF G4OPTONAM	150
3	PROBING THE DURATION OF G4OPTONAM BINDING.....	152
4	G4OPTONAM AND ALLOSWITCH-1 IN ZEBRAFISH EMBRYOS	158
CHAPTER 3		161
1	DESCRIPTION OF THE LIBRARY OF ALLOSWITCHES	161
2	PHOTOCHEMISTRY OF ALLOSWITCHES.....	164
3	OPTOPHARMACOLOGY OF ALLOSWITCHES – IP-ONE ASSAY	165
4	REAL-TIME OPTOPHARMACOLOGY OF ALLOSWITCHES	165
4.1	SIB-1757	166
4.2	Wavelength-response relationship of alloswitches	167
CHAPTER 4		175
1	TWO-PHOTON EXCITATION OF ALLOSWITCH-1 IN HEK CELLS.....	176
2	TWO-PHOTON EXCITATION OF OTHER ALLOSWITCHES	180
3	AXIAL RESOLUTION WITH TWO-PHOTON EXCITATION OF ALLOSWITCH-1	181
DISCUSSION.....		183
CONCLUSIONS.....		193
RESUM EN CATALÀ		195
APPENDIX.....		201

AKNOWLEDGEMENTS213
BIBLIOGRAPHY215

INTRODUCTION

In the nervous system events happen in the scale of milliseconds, and the fine processes of neurons and neuroglia are highly compartmentalized at a microscopic level. These exclusive features of the brain define extremely precise temporal and spatial patterns of cellular activity, which are of fundamental importance for the proper functioning of the nervous system, since they allow the fast processing, sorting, integration, and flow of information with high reproducibility and precision.

To gain deeper understanding of how these patterns are organized in time and space, we need to observe the activity of the nervous system in unperturbed conditions and to artificially manipulate it at its own working frequency and spatial precision. For this purpose, new tools are needed to overcome the spatiotemporal limitations of the currently available techniques.

In neurobiology, observation of protein and cell function in real-time at high resolution is commonly achieved with imaging, which broadly speaking, is mainly limited by diffraction of light in thick samples. In recent years many new techniques were developed to break the diffraction limit of light, expanding the “visible” scale down to the 20 nm-range.

On the other hand, many strategies were conceived in recent years with the purpose of activating or deactivating remotely neuronal signaling (Alexander *et al.* 2009; Redfern *et al.* 1999; Rogan and Roth 2011), but the most outstanding approach has been by far the idea of using light to control neuronal proteins. Light can be manipulated with millisecond- and micrometer-precision using relatively simple devices, offering great opportunities for neurobiologists as demonstrated by the huge expansion of the field during the last decade.

Scientist pioneered this idea back in 1971 (Bartels *et al.* 1971), but it was not until the year 2005 that the application of light to stimulate neurons was quickly adopted worldwide. This was first achieved with what is now called optogenetics (Boyden *et al.*

2005), which consists of making neurons light sensitive by overexpressing exogenous genes coding for light-sensitive proteins. After more than a decade, the control of protein function with light has gone far beyond optogenetics and the need of genetic manipulations imposed by this technique. In fact, optopharmacology is now gaining importance in the field of optical control of neuronal proteins because of its complementary features. Optopharmacological tools are more suitable for controlling the physiology of endogenous proteins with light, and each year new compounds with enhanced photochemical and pharmacological properties are developed for the scientific community.

In the quest for both high-resolution imaging and stimulation of the nervous system activity, light has demonstrated to be a powerful tool. In the introduction to this experimental thesis we will review the most relevant optical sensors (probes) and optical actuators (switches) that have been developed so far to study with light a family of neuronal receptors called metabotropic glutamate (mGlu) receptors, with special emphasis on mGlu₅. We are interested in these proteins due to their physiological role in the modulation of neurotransmission, and their dysfunction being related to neuropathologies. The relevance of mGlu receptors in the functioning of the nervous system, and the possibility of manipulating them with a high-precision tool such as light, suggested intriguing possibilities for the optopharmacological control of neuronal function and neuropathologies, and was the starting point of the work presented in this thesis.

1 Metabotropic glutamate receptors

Glutamate is the major excitatory neurotransmitter of the central nervous system (CNS). It is released by the pre-synaptic neuron upon action potential firing, it diffuses in the synaptic cleft (space), and is then sensed by the postsynaptic neuron or the surrounding glial cells thanks to its binding to receptor proteins called glutamate receptors. These proteins are divided into two main groups: ionotropic (iGlu) and metabotropic (mGlu) glutamate receptors, which are respectively ligand-gated ion channels and class C G protein-coupled receptors (GPCRs). Ionotropic glutamate receptors include AMPA, NMDA, and kainate receptors, which are responsible for the fast synaptic transmission between neurons. The slow modulation of synaptic transmission is mediated by the eight members of the mGlu receptors superfamily (mGlu₁₋₈, Scanziani *et al.* 1997b), which are classified into three groups (I to III) mainly based on their localization, sequence homology, and the signal transduction pathway they are coupled to, and will be described in detail in the following section.

1.1 Structure and activation mechanism

All mGlu receptor subtypes form stable homodimers (Romano *et al.* 1996) and present a similar architecture (Rondard *et al.* 2011) schematically represented in **Figure 1a**. At the extracellular N-terminus of one protomer we find a large bi-lobed structure called the Venus Flytrap domain (VFT), where glutamate binding occurs and with reduced cysteine residues to allow dimerization of protomers. A cysteine-rich domain (CRD) connects functionally the VFT to the heptahelical transmembrane domain (TMD), which is the core of any GPCR, being responsible for the G protein activation. Finally, we find the regulatory intracellular C-terminal domain (CTD).

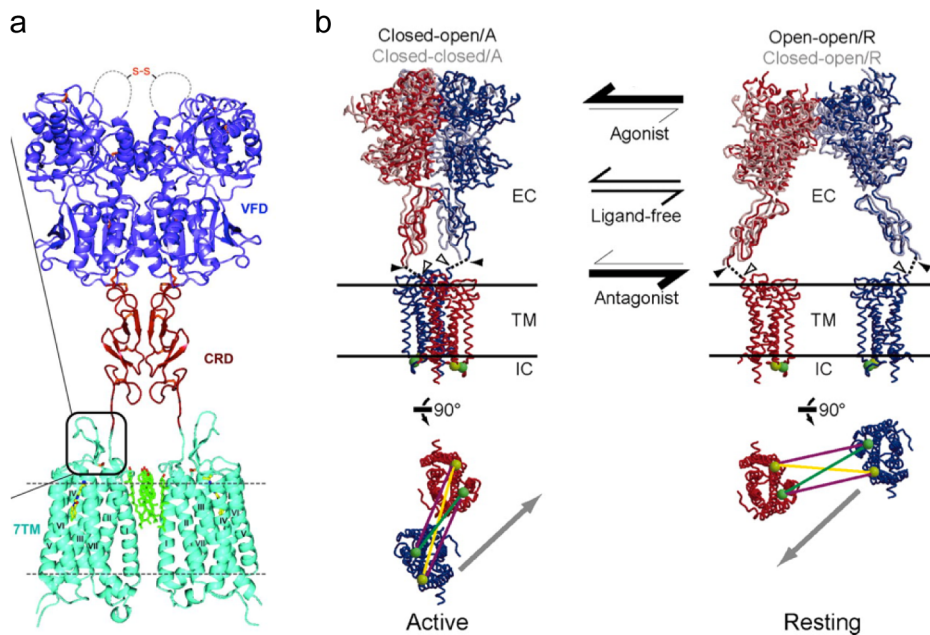


Figure 1 | Proposed models of mGlu receptors structure and activation mechanism.

(a) An mGlu₁ dimer model. Venus Fly Trap domains (VFT, alias VFD) are shown in blue, with reduced cysteine residues allowing dimerization indicated in red. In red is shown the cysteine rich domain (CRD), important for dimerization and allosteric activation of the transmembrane domain (TMD, alias 7TM, in cyan) by the VFT. The intracellular C-terminal domain (CTD) is not shown. Reproduced from Wu *et al.* Science 2014. (b) Proposed model for activation of group II and III mGlu receptor dimers, with single protomers painted red and blue. The dimer exists in dynamic equilibrium between an active (left) and a resting (right) state, characterized by a great conformational change occurring through the full-length of the receptor. Agonist or antagonist binding helps stabilizing the active and inactive receptor dimers, respectively. Each VFT cleft can be in the open or closed state, independent one from each other and from the receptor state. In this case, the closed-open VFT dimer for the active receptor, and the open-open dimer for the resting receptor are painted in dark colors, whereas other combinations are painted faint and specified in grey. Closing of a single protomer can induce the active configuration. The model receptor dimer in panel a is depicted in the active state, with the VFT dimer in the closed-closed conformation. Reproduced from Muto *et al.* 2007.

Venus Flytrap (VFT) and Cysteine Rich Domain (CRD)

The separation of the two lobes of the VFT forms a cleft, that constitutes the orthosteric binding site for glutamate. On the resting receptor, the relative position of the lobes of the VFT is constantly switching between an open and a closed conformation, but ligand binding to the cleft stabilizes the closed state (Quiococho 1990). The activation mechanism is not fully understood, but the models emerging from crystallographic studies point to receptor dimers existing in a dynamic equilibrium between a resting and an active state, with many possible conformations of open and closed states of each one of the two VFT

domains (Rondard *et al.* 2011), each of which is stabilized by antagonists or agonists, respectively (**Figure 1b**).

The TMD, just like for any GPCR, anchors the receptor to the plasma membrane, and is responsible for the transduction of the extracellular signal to the intracellular effectors. Briefly, binding of glutamate to the VFT induces a series of conformational changes in the protein – which are not fully understood yet – that end up in the activation of the bound G α protein for the nucleotide exchange, the release of the G protein subunits from the receptor, the binding to their effector proteins and the consequent activation/inhibition of the corresponding intracellular signaling pathways. Recently, the group of Ehud Isacoff discovered that the VFT of group II mGlu receptors can exist in three conformations: resting, activated and a short-lived intermediate state, and orthosteric agonists induce transitions between all these conformational states (Vafabakhsh *et al.* 2015). The occupancy of the active conformation by an agonist determines its efficacy.

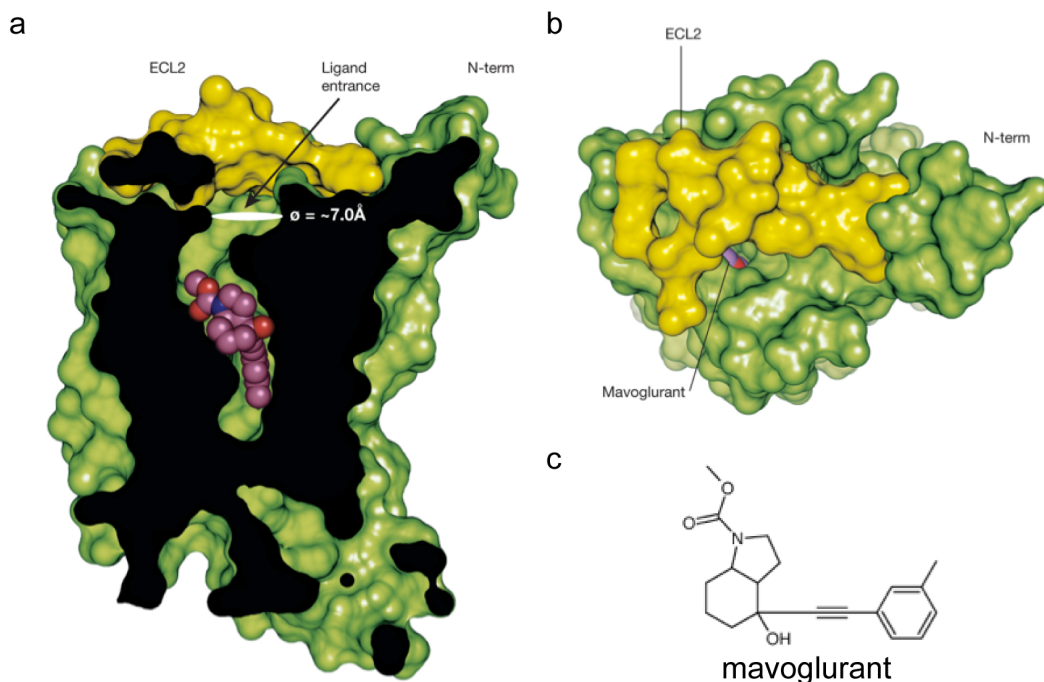


Figure 2 | Schematic representation of the mGlu₅ TMD crystal structure.

(a-b) Surface representation of mGlu₅ TMD with the mGlu₅ negative allosteric modulator mavoglurant (also known as AFQ056) sitting in the allosteric binding pocket, and viewed as a cross-section parallel to the membrane (a) or from the extracellular space (b), with the surface of the extracellular loop 2 colored yellow. Carbon, nitrogen, and oxygen atoms of mavoglurant are represented with magenta, blue, and red transparent balls, respectively. The theoretical dimension of the entrance for allosteric ligands is indicated in white, and

was found to be surprisingly narrow. Crystal structure resolved at 2.6 Å. Reproduced from Doré *et al.* Nature 2014. (c) Chemical structure of mavoglurant.

Trans Membrane Domain (TMD)

Inside the TMD domain hides a binding site for allosteric ligands, whose characteristics were recently unraveled by solving the crystal structure of mGlu₁ (Wu *et al.* 2014) and mGlu₅ TMDs (Doré *et al.* 2014) bound to negative allosteric ligands (**Figure 2**). An interesting point is that positive or negative allosteric modulators (PAMs and NAMs, respectively) can by themselves alter G protein activation. In fact, studies on mGlu receptors with mutated glutamate binding site (YADA) or deleted VFT (truncated receptors) showed that isolated TMDs oscillate between the active and inactive conformation, and are therefore fully functional units prone to G protein activation independent of the agonist (Goudet *et al.* 2004). This accounts for the observed constitutive activity of these mGlu receptors (Ango *et al.* 2001), and for the ability of some allosteric modulators to act independent of the orthosteric ligand (Schwartz and Holst 2007).

For the complete transmembrane transduction of the extracellular signal, a full-length monomer is not sufficient, but homo-dimerization is required (El Moustaine *et al.* 2012). It was demonstrated that glutamate, which binds to one or both VFT domains of a homo-dimer stabilizing its closed state (Kammermeier and Yun 2005; Kniazeff *et al.* 2004), causes a dimer interface reorientation an intersubunit rearrangement (Brock *et al.* 2007; Vafabakhsh *et al.* 2015) probably through the reduction of cysteine residues at the CRD interface of the dimer and on the extracellular portion of the TMD (Willard and Koochekpour 2013). These conformational changes end up in the symmetric activation of the two TMDs of the dimer, and consequently of the associated G protein (Brock *et al.* 2007). Although the exact ligand-activation mechanism is still not known (Rondard *et al.* 2011), new techniques provide new insights in the conformational changes underlying the activation of the TMD by the VFT dimers (Doumazane *et al.* 2013), and the crystal structures recently resolved would definitely prompt the unraveling of this fundamental signal transduction mechanism.

Heterodimerization has also been demonstrated for all mGlu receptors in transient expression systems (Beqollari and Kammermeier 2010) and for native receptors (Yin *et al.* 2014) with functional implications on dimer signaling (**Figure 6**, bottom panels), although incompatibility for heterodimerization exists between group I and groups II/III members (Doumazane *et al.* 2011). Heterodimerization and even oligomerization are

possible between mGlu receptors and other unrelated GPCRs (Cabello *et al.* 2009; González-Maeso *et al.* 2008).

C terminal domain (CTD)

In the intracellular CTD of mGlu receptors, the amino acid sequence is less conserved among subtypes than in the rest of the protein (Willard and Koochekpour 2013). The CTD is a quite long structure that contains the binding site for G proteins and other consensus sequences for binding to different regulatory proteins and the cytoskeleton (Enz 2012).

As GPCRs, all mGlu receptors can be regulated by GPCR kinases (GRKs) to induce homologous and heterologous desensitization and by regulators of G protein Signaling (RGS) that modulate G protein function (Thomsen and Behan 2007) GRKs may directly interfere in the interaction between activated mGlu receptors and the associated G protein (Gereau and Swanson 2008). Another possibility is that activated mGlu receptors are phosphorylated by GRKs, and this induces β -arrestin binding, which in turn promotes G protein uncoupling and receptor internalization and trafficking to the recycling endosome or the lysosomes for degradation (Pierce and Lefkowitz 2001). In fact, it was shown that agonist application causes rapid internalization of mGlu₁ (Doherty *et al.* 1999) through an arrestin- and dynamin-dependent process (Mundell *et al.* 2001). However, mGlu₅ was reported to internalize constitutively independent of activation by glutamate (Fourgeaud *et al.* 2003).

As an example of anchoring to the cytoskeleton, mGlu₅ can be associated with microtubules, and the CTD is required for this process, since receptors with truncated CTDs diffuse more freely in the membrane compared to wild-type receptors (Serge *et al.* 2003).

In the mGlu CTD there are also important sites for phosphorylation and dephosphorylation by different protein kinases and phosphatases. For instance, the mGlu₃ CTD is a substrate for PKA and PP2, whereas mGlu_{1/5/7} bind PP1 (Gereau and Swanson 2008). These binding sites for protein interactors might or might not be conserved between receptor subtypes, and this determines important differences in their signaling properties. For example, binding of PKC on a serine residue in the CTD of mGlu₅ but not in mGlu₁ determines differences in the features of the calcium signaling downstream the activation of the two receptor subtypes (Kim *et al.* 2005a).

Other proteins interacting at the mGlu CTD are signaling or receptor proteins as InsP₃ receptors in the case of mGlu₅ (Pierce *et al.* 2002), calmodulin (CaM) binding to mGlu₅

to dynamically regulate its trafficking (Lee *et al.* 2008), and to mGlu₄₋₇₋₈ (Enz 2012), or even ion channel subunits, like the Ca²⁺ channel subunit Ca_v2.1 binding to mGlu₁ (Fagni *et al.* 2004).

The literature about the specific interacting partners of group I mGlu receptors is much wider than that regarding group II and III receptors (Gereau and Swanson 2008). For instance, group I but not mGlu II/III mGlu receptors contain in their CTD the proline-rich sequence 'PPxxF', called Homer1 binding motif, through which they couple to the scaffolding proteins of the post-synaptic density (PSD) such as Homer1a or b/c (Ango *et al.* 2001; Brakeman *et al.* 1997), Preso1 (Hu *et al.* 2012), Shank3 (Tu *et al.* 1999), and via PSD-95 to AMPA and NMDA receptors (among other proteins) (Gao *et al.* 2013).

Proteins of the Homer family are particularly interesting, as they both regulate group I mGlu receptors signaling and localization at the PSD (**Figure 3**), and are rapidly induced during synaptic activity (Thomas 2002). They exist in long and short splice variants, which have differential roles in the trafficking and signaling of group I mGlu receptors. Long but not short Homer isoforms contain coiled-coil C terminals for tetramerization (Xiao *et al.* 1998), decrease the lateral mobility of mGlu₅ (Sergé *et al.* 2002), and are capable of connecting the receptors on the plasma membrane with proteins on intracellular organelles such as InsP₃ receptors on the ER (Kammermeier *et al.* 2000). Instead, the short isoform makes group I mGlu receptors preferentially bind to effectors on the plasma membrane like ion channels (Kammermeier and Worley 2007), and even induce constitutive activation of mGlu_{1/5} in the absence of glutamate (Ango *et al.* 2001). Interestingly, long Homer and Shank polymerize and form a network structure at the PSD, and this complex is one of the determinants of dendritic spine size in neurons and is destabilized by short Homer in a dose-dependent way (Hayashi *et al.* 2009). Short Homer is enriched after periods of synaptic activity, especially during development (Brakeman *et al.* 1997). Homer1a is also enriched during homeostatic scaling as an immediate early gene, it displaces long Homer isoforms disrupting the crosslinking, and thus induces activation of mGlu_{1/5} in the absence of glutamate, which increases the rate of AMPA receptors endocytosis through dephosphorylation of GluA2 subunits (Hu *et al.* 2010) and downregulation of synaptic activity. Interestingly, mGlu₅ and Homer interact with dynamin 3, whose altered expression causes remodeling of dendritic spines (Gray *et al.* 2003).

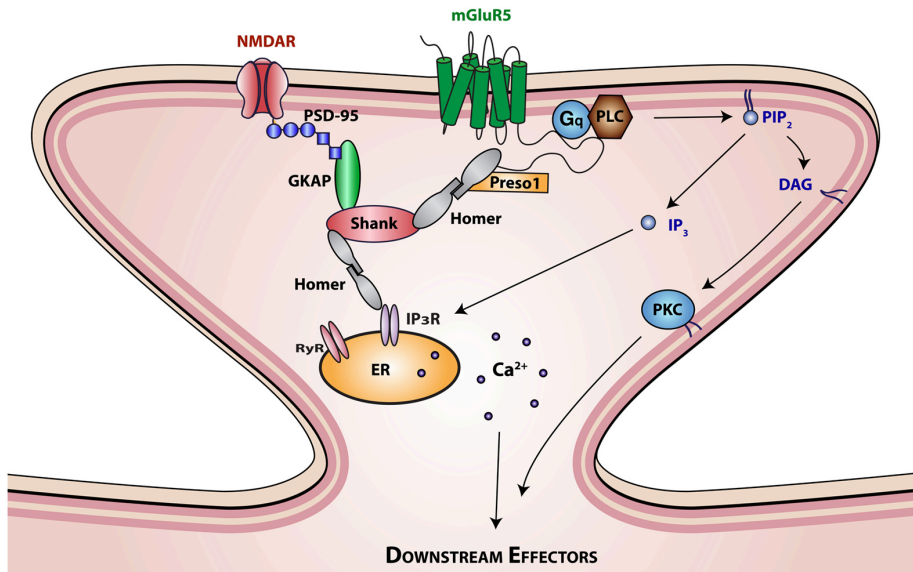


Figure 3 | Homer and mGlu₅ receptors interact at the postsynaptic membrane of dendritic spines.

Long Homer proteins form multimers through interactions of their coiled-coil domain, and bind Shank to form a polymeric network that physically links mGlu₅ receptors (through Preso-1) with the effectors inositol triphosphate (IP₃) receptors on the dendritic ER or NMDA receptors at the spine surface. The mGlu₅ intracellular signaling is also illustrated, but will be explained in more detail in **Figure 4** and **5**. Reproduced from Piers *et al.* (2012).

1.2 Intracellular signaling

Once glutamate binding to the VFT has initiated the conformational changes that lead to the stabilization of the active state of the receptor, different G α proteins can be activated and different signaling pathways initiated depending on the mGlu subtype involved (detailed in **Table 1**).

Table 1 | Classification and signal transduction pathways of mGlu receptors.

Group	Subtype	G prot.	Effector	2 nd messenger	Ref.
I	mGlu ₁	G _{q/11} α	↑PLC	↑[Ca ²⁺] _{ic} (trans.)	(Aramori and Nakanishi 1992; Kawabata <i>et al.</i> 1996)
		G _s α	↑AC	↑cAMP	(Tateyama and Kubo 2006)
	mGlu ₅	G _{q/11} α	↑PLC	↑[Ca ²⁺] _{ic} (oscill)	(Abe <i>et al.</i> 1992; Kawabata <i>et al.</i> 1996)

II	mGlu ₂	G _{i/o} α	↓AC	↓cAMP	(Flor <i>et al.</i> 1995a)
	mGlu ₃	G _{i/o} α	↓AC	↓cAMP	(Emile <i>et al.</i> 1996)
III	mGlu ₄	G _{i/o} α	↓AC	↓cAMP	(Flor <i>et al.</i> 1995b)
	mGlu ₆	Gβγ	cGMP	↑cGMP	(Nomura <i>et al.</i> 1994; Shen <i>et al.</i> 2012)
			PDE (TRPM1)		
	mGlu ₇	G _{i/o} α	↓AC	↓cAMP	(Okamoto <i>et al.</i> 1994)
mGlu ₈	G _{i/o} α	↓AC	↓cAMP	(Duvoisin <i>et al.</i> 1995)	

PLC, phospholipase C; AC, adenylate cyclase; cAMP, cyclic adenosin monophosphate; cGMP, cyclic guanosin monophosphate; PDE, phosphodiesterase; TRPM1, transient receptor potential cation channel subfamily M member 1.

Group I mGlu receptors (subtypes 1 and 5) couple to G_{q/11} proteins, which activate the enzyme phospholipase C (PLC) (**Figure 4**), although mGlu₁ was also shown to couple to G_sα protein subunits (Tateyama and Kubo 2006) that activate adenylate cyclase (AC) and increases cAMP in the cytoplasm.

PLC hydrolyzes phosphatidylinositol 4,5-bisphosphate (PIP₂) in inositol 1,4,5-triphosphate (IP₃) and diacylglycerol (DAG). IP₃ binds to IP₃ receptors (InsP₃) on the endoplasmic reticulum (ER), resulting in the opening of these Ca²⁺ channels and mobilization of Ca²⁺ ions from the intracellular stores. IP₃ is subsequently degraded into inositol 1,4-bisphosphate (IP₂) and inositol monophosphate (IP₁) by specific phosphatases for signaling termination. DAG and Ca²⁺ in turn activate protein kinase C (PKC), which phosphorylates different target proteins along the signaling cascade, the receptor itself among others. After that, downstream phosphatases are activated to terminate signaling, and the receptor can be eventually dephosphorilated. The concatenation of these phosphorylation/dephosphorilation events leads to sequential increase and decrease in the intracellular calcium concentration, giving rise to transient (mGlu₁) or oscillatory (mGlu₅) calcium responses, as explained in the following paragraph.

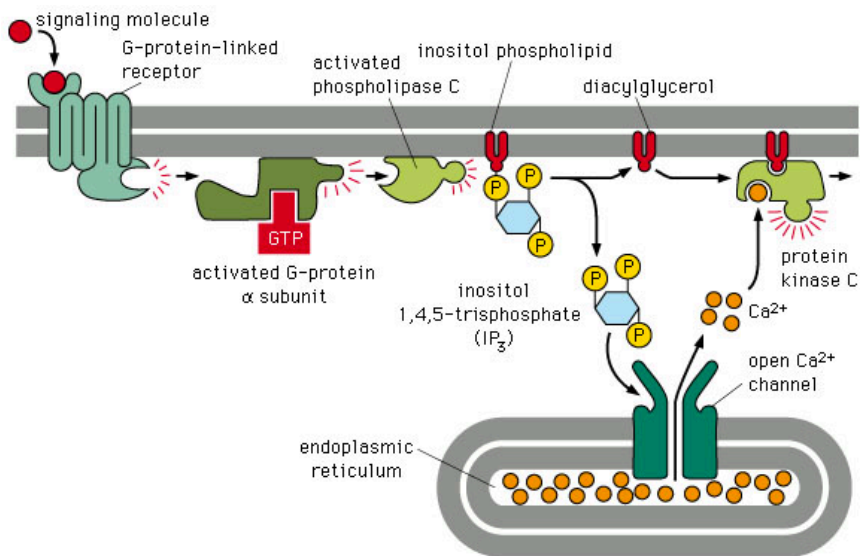


Figure 4 | The inositol phosphates signaling pathway.

An extracellular signal (neurotransmitter, hormone, etc.) binds to a GPCR, which activates the coupled G protein and induces GDP/GTP exchange on the $G\alpha$ subunit and its dissociation from $G\beta\gamma$. Activated $G\alpha$ subunits (GTP bound) activate PLC (phospholipase C), which hydrolyses PIP_2 in IP_3 and DAG. IP_3 opens IP_3 receptors on the endoplasmic reticulum that causes calcium release in the cytoplasm, and, jointly with DAG, activates PKC. Reproduced from Alberts *et al.* (2002).

Phosphorylation of the receptor induces its desensitization, whereas the opposite process induces its resensitization (Gereau and Heinemann 1998; Kim *et al.* 2008). When phosphorylation occurs at the amino acid residue Thr⁸³⁹ on mGlu₅ (Kim *et al.* 2005a), it starts a so-called “dynamic uncoupling” mechanism (Figure 5a) of receptor desensitizations and resensitizations through fast phosphorylation and dephosphorylation cycles (Nash *et al.* 2001). These cycles of feedback inhibition determine oscillations in the concentration of intracellular Ca^{2+} (Figure 5b), whose frequency is a function of receptor density and occupancy (Nash *et al.* 2002) and $G\alpha$ protein subunit expression levels (Atkinson *et al.* 2006). Instead, the amino acid analog to Thr⁸³⁹ on mGlu₁ (Asp⁸⁵⁴) is not conserved, and does not allow feedback phosphorylation of the receptor on the adjacent amino acid (Kim *et al.* 2005a). This explains why mGlu₁ activation results in Ca^{2+} transients rather than oscillations, in the form of a simple rise that can be followed or not by a sustained phase (peak or peak-and-plateau; Kawabata *et al.* 1996). Some deviations from this ideal model for mGlu₁ and mGlu₅ signaling patterns have been observed at high agonist concentration and after prolonged receptor stimulation (Kawabata *et al.* 1998). Depending on the cell type and the relative expression of other

downstream effectors of the G_q signaling pathway, group I mGlu can also activate the RAS/MAPK/ERK (Gallagher *et al.* 2004) and the PI3K/AKT/mTOR (Hou and Klann 2004) signaling pathways (see **Figure 6**).

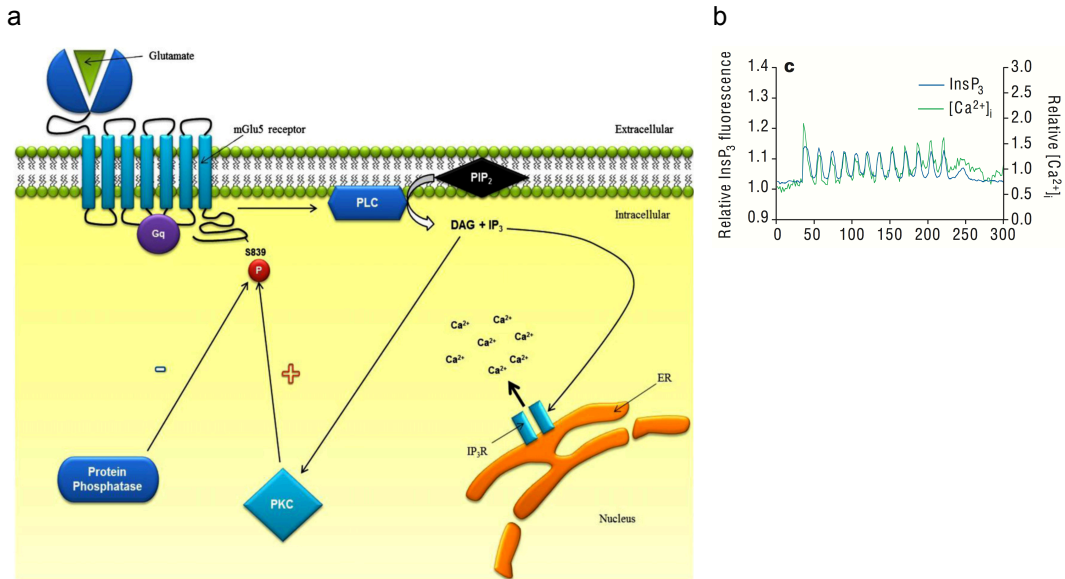


Figure 5 | Dynamic uncoupling mechanism and Ca^{2+} oscillations in the activation of mGlu₅.

(a) Glutamate binding to mGlu₅ at the cell surface activates the associated $G_{q\alpha}$ protein subunit, and by activating phospholipase C (PLC) induces formation of IP₃ and DAG. The first of these second messengers gives rise to a cytosolic Ca^{2+} increase through opening of the InsP₃ receptors on the ER. Instead, activation of protein kinase C (PKC) downstream mGlu₅ through DAG leads to feedback phosphorylation of the receptor at Ser⁸³⁹. Phosphorylation at this site disrupts coupling to the $G_{q\alpha}$ protein subunit and terminates the signaling, finally making Ca^{2+} levels decrease and stop PKC activation. Cytosolic protein phosphatases were proposed to remove phosphorylation of Ser⁸³⁹, restore G protein coupling and make a new cycle begin. Repeated cycles of receptor phosphorylation/dephosphorylation would translate into Ca^{2+} oscillations. Reproduced from Bradley and Challiss 2012. (b) Single-cell imaging of intracellular IP₃ and Ca^{2+} in Chinese Hamster Ovary (CHO) cells expressing mGlu₅ and the fusion protein GFP-PH_{PLC-1} and treated with 10 μ M quisqualate. Intracellular Ca^{2+} was measured using the calcium indicator Fura-2 and represented as the ratio of fluorescence at 340 and 380 nm. Reproduced from Nash *et al.* 2001.

Instead, group II (subtypes 2 and 3) and III (subtypes 4, 6, 7 and 8) mGlu receptors are recognized by the $G_{i/o\alpha}$ protein, which negatively couples to adenylate cyclase (AC), and inhibits the production of cyclic AMP (cAMP). However, for research purposes group II and III mGlu receptors can be artificially coupled to the G_q signaling pathway through a chimeric $G\alpha$ protein subunit called $G_{q/i}$, where few residues are exchanged to make the

$G_{q\alpha}$ protein recognize and bind the intracellular loops of $G_{1/0}$ coupled receptors without altering its coupling to PLC (Gomez *et al.* 1996).

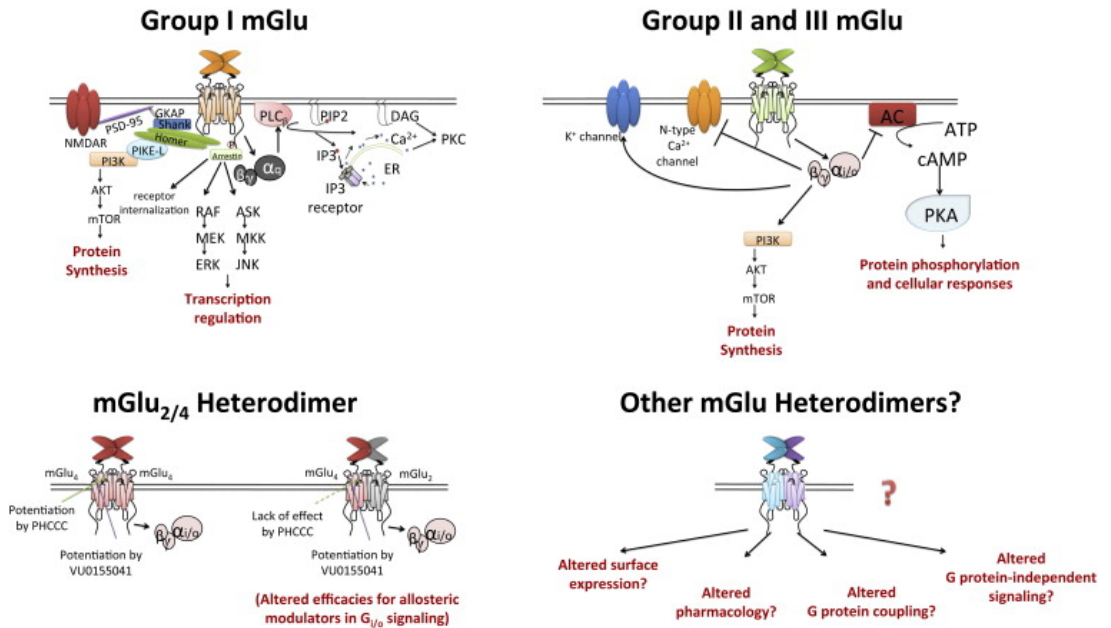


Figure 6 | Signaling pathways of group I versus group II/III mGlu receptors, and implications of receptor heterodimerization.

(**Top**) G protein-dependent and independent signaling pathways of group I (left) and II/III (right) mGlu receptors. (**Bottom**) Heterodimerization of mGlu_{2/4} receptors (left) differentially regulates the efficacies or binding of mGlu₄ PAMs, and remains unexplored for other mGlu receptors (right). GKAP, guanylate kinase-associated protein; PSD-95, postsynaptic density protein 95; NMDAR, N-methyl-D-aspartate receptor; PI3K, phosphatidylinositol 3-kinase; PIKE-L, phosphatidylinositol 3-kinase enhancer-long; AKT, protein kinase B; mTOR, mammalian target of rapamycin; ERK, extracellular signal-regulated kinase; ASK, apoptosis signal-regulating kinase; JNK, c-Jun N-terminal kinases; PIP₂, Phosphatidylinositol 4,5-bisphosphate; DAG, diacylglycerol; IP₃, inositol 1,4,5-trisphosphate; ER, endoplasmic reticulum; PKC, protein kinase C; AC, adenylate cyclase; PKA, protein kinase A. Reproduced from Yin and Niswender 2014.

The other side of the moon for GPCR signaling, which is usually forgotten or at least understated, is the fate of the $\beta\gamma$ subunits of the G protein once they have been released after dissociation of the trimeric G protein. We will not get into the details of this, but it is worth mentioning that free $G\beta\gamma$ protein subunits can modulate the activity of different effectors, such as ion channels and pumps (like G protein-gated inward rectifying potassium channels, GIRKs), protein kinases and phosphatases, promote β -Arrestin binding and internalization through GRKs, and many other targets (Pierce *et al.* 2002; **Figure 6**).

Another non-conventional aspect of mGlu receptors signaling is their modulation by extracellular ions, such as Ca^{2+} and Mg^{2+} for group I, chloride ions for group III, and both cations and anions for group II mGlu receptors (Francesconi and Duvoisin 2004; Gereau and Swanson 2008; Kuang and Hampson 2006). Finally, recent discoveries demonstrated that mGlu receptor signaling is not limited to surface receptors but can also occur from intracellular compartments (Jong *et al.* 2014; Jong *et al.* 2009; Kumar *et al.* 2012; Kumar *et al.* 2008). Signaling alternatives arising from heterodimerization of mGlu receptors will be discussed later on in **Section 1.4**.

1.3 Localization and physiology of mGlu in the CNS

Localization

Group I mGlu receptors are typically found on dendrites of neurons, postsynaptic to excitatory inputs, and perisynaptic to dendritic spines containing the ionotropic glutamate receptors (Luján *et al.* 1997). From immunoreactivity studies (**Figure 7a**) we know that mGlu₁ and mGlu₅ expression is almost complementary in the CNS. High expression of mGlu₁ was found in Purkinje cells of the cerebellar cortex, and in mitral/tufted cells of the main olfactory bulb, among others; mGlu₅ staining was found especially in the cerebral cortex, olfactory bulb, striatum, and extensively in the hippocampus (Ferraguti and Shigemoto 2006). In this last structure, pyramidal and granule cells express both mGlu₁ and mGlu₅, but mGlu₅ was found uniquely in their dendritic fields, whereas mGlu₁ was prevalent on the cell bodies (Lüscher and Huber 2010; Shigemoto *et al.* 1997). Subtype 5 is also extensively expressed by astrocytes (Miller *et al.* 1995), one of the glial cells present in the CNS, especially at early developmental stages (Sun *et al.* 2013); moreover, mGlu₅ is enriched on astrocytic processes rather than on the cell body (Arizono *et al.* 2012).

Among group II mGlu receptors, mGlu₂ is expressed at the presynaptic membrane far from active zones of neurotransmitter release, whereas mGlu₃ is found both pre- and postsynaptically (Petrálie *et al.* 1996), as well as on astrocytes, but in later development phases than mGlu₅ (Sun *et al.* 2013). Both mGlu₂ and mGlu₃ expression is widespread in the CNS, being that of subtype 2 less intense than that of subtype 3 (Ferraguti and Shigemoto 2006).

Members of group III are mostly presynaptic and quite widespread in the CNS (Niswender and Conn 2010), with the exception of mGlu₆ that is exclusively found in the

retina, and is expressed on the postsynaptic membrane of ON bipolar cells (Nakajima *et al.* 1993). The main site of mGlu₄ expression is found in the granule cells of the cerebellum, but it was found also in olfactory bulb, thalamus, dentate gyrus, and at corticostriatal, striatopallidal, and striatonigral (both SNc and SNr) synapses in the basal ganglia (Conn *et al.* 2005; Corti *et al.* 2002; Gubellini *et al.* 2014; Mercier and Lodge 2014). A peculiar member of the family is mGlu₇, due to its extremely low affinity for glutamate (guidetopharmacology.org). It is widespread in the CNS, being the most largely expressed group III receptor, although it can be highly compartmentalized depending on the postsynaptic neuron (Shigemoto *et al.* 1996). mGlu₇ is particularly prominent in the olfactory bulb, hippocampus, hypothalamus, and sensory afferent pathways (Mercier and Lodge 2014). This latter localization, together with its low agonist affinity, suggests a possible role in the desensitization linked to continuous or exceeding stimulation of sensory inputs (Pelkey *et al.* 2005). At the subcellular level, it is mainly presynaptic, but specifically abundant at the active zone of the presynaptic terminal (Shigemoto *et al.* 1997). Finally, mGlu₈ is expressed at much lower levels than mGlu₄ and mGlu₇, but as well widespread throughout the CNS and preferentially presynaptic. Presynaptic mGlu receptors not only inhibit neurotransmission at excitatory glutamatergic terminals, since they are also expressed presynaptically at inhibitory GABAergic, and neuromodulatory cholinergic and monoaminergic synapses (Niswender and Conn 2010; **Figure 7b**).

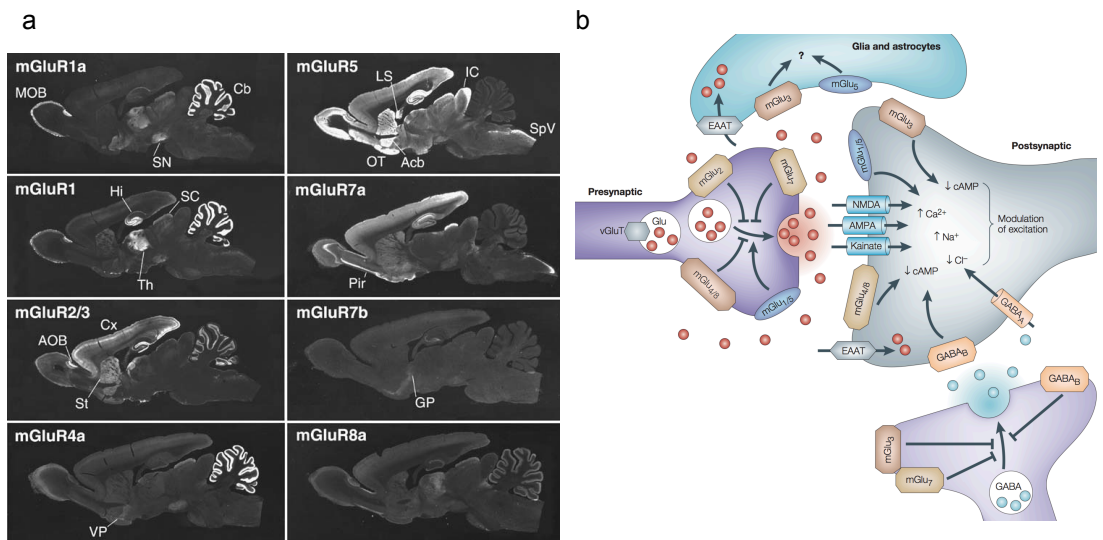


Figure 7 | Distribution of mGlu receptors in the brain at cellular and subcellular level.

(a) Immunoreactivity for mGlu receptors in parasagittal sections of the adult rat brain. AOB accessory olfactory bulb, Acb accumbens nucleus, Cb cerebellum, Cx neocortex, GP globus pallidus, Hi hippo-campus, IC inferior colliculus, LS lateral septum, MOB main olfactory bulb, OT olfactory tu-bercle, Pir piriform cortex, SC superior colliculus, SN substantia nigra, SpV spinal vestibular nucleus, St neostriatum, Th thalamus, VP ventral pallidum. Reproduced from Ferraguti and Shigemoto 2006. (b) Schematic representation of the tripartite synapse and the subcellular distribution of mGlu receptors. Reproduced from Swanson *et al.* (2005).

Table 2 | Sites of mGlu expression in the CNS at a subcellular, cellular, and brain region level.

receptor	Synaptic localization	Brain region	Cell type	Main function
mGlu ₁	post	Cerebellum hippocampus	Purkinjie cells Soma of pyr. neurons	Somatic Ca ²⁺ /depol
mGlu ₅	post/glia	Cortex hippocampus	Glia Apical dendrites of pyr. neurons	Inhib. I _{AHP}
mGlu ₂	pre	low but widespread	Cerebellum, Golgi cell	(Petralia <i>et al.</i> 1996)
mGlu ₃	pre/post/glia	widespread		(Tamaru <i>et al.</i> 2001)
mGlu ₄	Pre (active zone)	cerebellum striatum	Granule cells GPe interneurons (striato-pallidal synapse, indirect pathway)	(Conn <i>et al.</i> 2005; Corti <i>et al.</i> 2002)
mGlu ₆	post	only retina	ON bipolar cells	Inhib. TRPM1 (Nomura <i>et al.</i> 1994)
mGlu ₇	Pre (active zone; low expr.)	widespread		
mGlu ₈	Pre (active zone)	uneven; widespread		

Pre, presynaptic; post, postsynaptic; pyr., pyramidal.

1.3.1 Role in neurotransmission

Metabotropic glutamate receptors exert a variety of modulatory effects over synaptic transmission. As a general but reductionist rule, group I and group II/III receptors have

opposing roles in neurotransmission: activation of group I mGlu receptors is slowly excitatory, whereas activation of all other subtypes has inhibitory effects (Pin and Duvoisin 1995). Due to their different synaptic localizations already mentioned before, group I mGlu receptors tune neuronal excitability acting at the postsynaptic membrane, while groups II and III can modulate the release of neurotransmitter from the presynaptic neuron (**Figure 7b**).

Activation of group I mGlu receptors can regulate neuronal excitability by both increasing Ca^{2+} concentration in dendritic spines and by controlling a number of ion channel conductances, to ultimately depolarize the postsynaptic neuron (Niswender and Conn 2010). For instance, in the same pyramidal cell mGlu₁ and mGlu₅ depolarize the neuron through somatic calcium transients in the case of mGlu₁, and by inhibition of I_{AHP} (an inward K^+ current) and facilitation of NMDA currents in the case of mGlu₅ (Mannaioni *et al.* 2001) through a mechanism that still needs to be elucidated (Park *et al.* 2013). The regulation of NMDA receptors depends on Ca^{2+} -Calmodulin protein kinase II (CaMKII) and is specific of mGlu₅, since calmodulin (CaM) does not bind to mGlu₁ receptors (Choi *et al.* 2011). Activation of mGlu₅ generates a Ca^{2+} rise that makes CaMKII become active, dissociate from mGlu₅, recruit to adjacent GluN2B NMDA receptor subunits, and finally phosphorylate the receptor channels on a specific site (Jin *et al.* 2013) known to potentiate NMDA currents (Liao *et al.* 2001). Also, the overall result on synaptic transmission spans from robust excitation to more subtle changes in patterns or frequency of cell firing (Niswender and Conn 2010).

To explain the contribution of group II and III mGlu receptors, one explanation is that the released $\beta\gamma$ subunit of the G protein suppresses Ca^{2+} influx through presynaptic ion channels (Ikeda 1996; Takahashi *et al.* 1996), reducing the probability of neurotransmitter release (O'Connor *et al.* 1999). Another mechanism is the activation of presynaptic K^+ conductances to counteract depolarization of the presynaptic terminal (Dutar *et al.* 1999; Knoflach and Kemp 1998; Lüscher and Slesinger 2010), as well as direct interactions with proteins of the release machinery of synaptic vesicles, e.g. interference with the formation of the SNARE complex (Blackmer *et al.* 2005) and SNAP-25 being bound by G protein $\beta\gamma$ subunits (Gerachshenko *et al.* 2005).

In the case of mGlu₇, the release of $\beta\gamma$ is allowed by binding of Ca^{2+} -CaM to the CTD of the receptor (O'Connor *et al.* 1999), possibly subjecting the activation of signaling downstream mGlu₇ to the detection of a coincident activation of the presynaptic neuron (Caldwell *et al.* 2008). In accordance with this and as already mentioned before, the

localization of mGlu₇ at the site of neurotransmitter release, together with its low affinity for glutamate, suggested the hypothesis that it could work as a low pass filter for exaggerated synaptic transmission, being activated when there is an excess of glutamate to inhibit further glutamate release (Niswender and Conn 2010). This hypothesis is in accordance with experimental data showing increased spontaneous seizures in mice lacking this receptor (Sansig *et al.* 2001).

One interesting but still unanswered question is to what extent mGlu receptors are activated during normal synaptic transmission. Exocytosis of glutamate from the presynaptic neuron generates a fast millimolar-high concentration of the neurotransmitter inside the synaptic cleft, which is highly spatially confined thanks to fast active uptake mechanisms all around the synapse. Therefore, given the perisynaptic localization of most of the mGlu receptors, the probability of glutamate reaching and activating them during synaptic activity is low, unless the uptake mechanisms are dysregulated, or the rate of presynaptic input is fast enough to win over the uptake mechanisms. This happens when a relatively high-frequency stimulation generates a summation of glutamate in the synaptic cleft, and an increased diffusion to peri- or extrasynaptic sites (Scanziani 2002).

In line with these considerations, mGlu receptors have been found also on presynaptic GABAergic terminals, making contact with the granule cells of the cerebellum, where they decrease inhibitory neurotransmission (Mitchell and Silver 2000). These heterosynaptic mGlu receptors on inhibitory interneurons can be activated by glutamate spillover during high-frequency stimulation of the excitatory input, and lead to an additional release of the activity of the postsynaptic neuron; this might sound controversial, but it has been interpreted as a tool used by the network to increase contrast (Pinheiro and Mulle 2008).

1.3.2 Role in glial cells

Glial cells are divided into microglia and macroglia, the latter comprising two cell types: astrocytes and oligodendrocytes. Microglial cells are the immune cells of the mature nervous system and collaborate in circuit shaping during development (Schafer *et al.* 2012), whereas oligodendrocytes are implied in the production of myelin in the CNS. Astrocytes are the most abundant glial cell in the CNS, and entangle thousands of fine

processes in close proximity with neuronal synapses. They are probably the most interesting glial cell type: initially believed to have simple structural roles, but lately gaining more and more importance because of their homeostatic functions, their active participation in synaptic and basal transmission (Gourine *et al.* 2010; Martin *et al.* 2015; Panatier *et al.* 2011; Perea and Araque 2007; Perea *et al.* 2014), in the genesis and pruning of synapses (Eroglu and Barres 2010; Tsai *et al.* 2012), and the still unraveled spatio-temporal properties of the astrocyte-neuron interactions (Allen 2014; Araque *et al.* 2014). Because of the important modulation of synaptic transmission mediated by astrocytes, the concept of 'tripartite synapse' was recently introduced (Araque *et al.* 1999). Based on this theory, a third element (the astrocyte) participates in the communication between the two generally acknowledged elements of the synapse, that is the pre- and the postsynaptic neuron (**Figure 9**).

Group I mGlu receptors have not been found on microglial cells, and there are contrasting results about the presence of group II/III mGlu receptors, but there is evidence for the presence of mGlu_{2/3} in microglia derived from autoptic preparations of patients with multiple sclerosis (Geurts *et al.* 2003). In astrocytes of the CNS *in vivo* only two mGlu receptors have been identified, namely subtypes 3 and 5 (4 and 8 were found in some studies in culture), whereas mGlu_{1a} was detected in astrocyte cultures from spinal cord. Finally, group I and II mGlu receptors, and mGlu₄ were detected only in cultured oligodendrocytes (D'Antoni *et al.* 2008). We will focus now on mGlu receptors expressed by astrocytes and their roles in neurotransmission (reviewed in De Pittà *et al.* 2015).

Group I mGlu receptors in astrocytes

In cultured astrocytes mGlu₅ can be enriched by adding trophic factors in the culture medium (Miller *et al.* 1995). Glutamate stimulation of cultured astrocytes was long ago demonstrated to engender (besides activation of Kainate receptors) intracellular calcium oscillations (Cornell-Bell *et al.* 1990; Nakahara *et al.* 1997) such as those observed in cell lines transiently overexpressing the mGlu₅ receptor. These oscillations likely result from the same process of dynamic uncoupling described in **Section 1.2**, and show the same dependence of oscillatory frequency from receptor expression levels (Bradley and Challiss 2012).

During *in vivo* neuronal activity, Ca²⁺ rises that occur in astrocytes and depend on mGlu₅ activation (Wang *et al.* 2006) induce the release of ATP, which then acts on purinergic

receptors expressed by neurons, and serves as a scaling factor to increase the strength of synaptic connections and basal transmission (Gordon *et al.* 2009; Panatier *et al.* 2011; **Figure 8**).

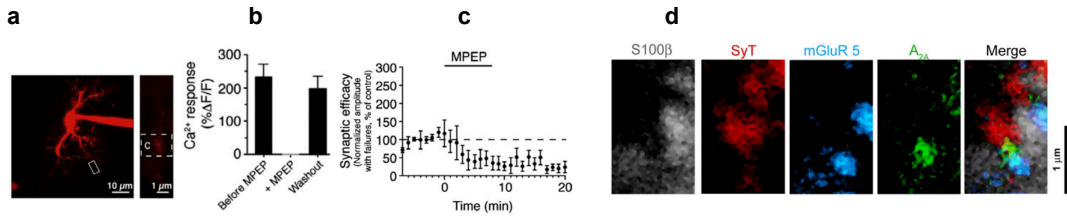


Figure 8 | Astrocytic processes are in close proximity with presynaptic terminals, and contain clusters of mGlu₅ receptors that regulate basal transmission.

(a) Astrocyte in adult rat hippocampal slice, and imaged astrocytic compartment (inset). (b) Single-pulse stimulation-induced Ca²⁺ responses in an astrocytic compartment are blocked by the selective antagonist of mGlu₅, MPEP (25 µM); this effect is reversible upon washout. Data are reported as mean ± s.e.m. (c) Inhibition of mGlu₅ decreases synaptic efficacy (amplitude of postsynaptic currents). (d) Confocal images of immunolabeled adult rat hippocampal slices showing a S100β-positive astrocyte process (gray), synaptotagmin-positive presynaptic elements (SyT, red), mGlu₅ (cyan), and A_{2A} receptors (green), as well as the four channels merged. Clusters of mGlu₅ receptors are on astrocyte processes facing purinergic receptors juxtaposed to presynaptic elements. Reproduced from Panatier *et al.* 2011.

More recently, group I mGlu receptors were demonstrated to play a physiological role in astrocytic functions, such as glutamate and K⁺ uptake from the synaptic cleft to maintain homeostatic levels of these substances (Devaraju *et al.* 2013). Astrocyte mGlu₅ seems to play a role also in functional hyperemia. In fact, antagonists of group I mGlu receptors that block Ca²⁺ rises in astrocytes but not in neurons are able to suppress activity-dependent vasodilation in slices (Zonta *et al.* 2003).

Furthermore, a model emerged based on experiments from different research groups proposing that mGlu₅ receptors on astrocytes ensheathing CA1-CA3 synapses of the hippocampus can discriminate between different frequencies of presynaptic activity (Panatier and Robitaille 2015) (**Figure 9**). mGlu₅ was proposed to respond to low or high input frequencies with local or somatic Ca²⁺ signaling. This would induce the astrocyte to release purines or glutamate, and thus activate presynaptic purinergic or postsynaptic NMDA receptors, finally increasing neurotransmitter release or regulating postsynaptic excitability and synchronization. Based on this model, Panatier and Robitaille highlight that **“it is crucial to adapt the time and space domains of the experimental paradigm to fit the kinetics and properties of the astrocytes in a given physiological condition”** to better understand the role of mGlu₅ in astrocyte-to-neuron

communication. Such spatiotemporal control of mGlu₅ is possible with light stimulation, which has been achieved with glutamate photo-uncaging (Bernardinelli *et al.* 2014) and in this thesis with reversible photochromic ligands.

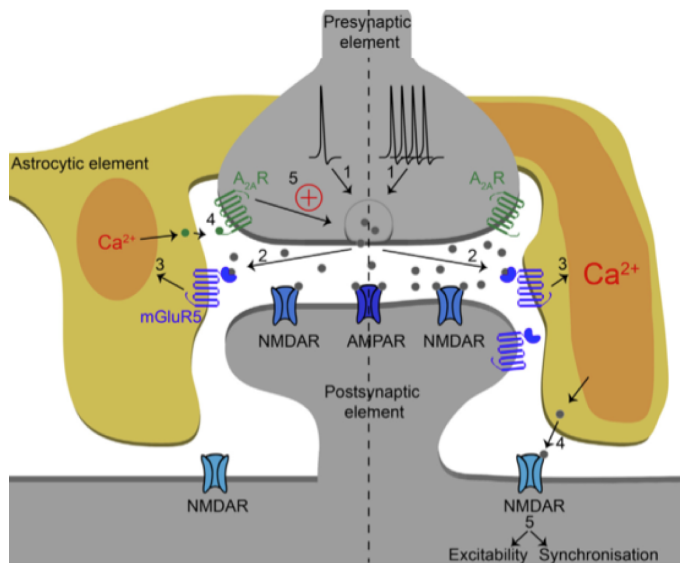


Figure 9 | Model showing how astrocyte mGlu₅ receptors can differentially integrate low- and high-frequency synaptic transmission on hippocampal CA3-CA1 tripartite synapses.

(Left) Glutamate released by a single action potential (1) activates mGlu₅ receptors on an astrocyte process (2) and generates a local increase of Ca²⁺ in the astrocyte (3), which in turn triggers purine release that activates presynaptic A_{2A} receptors (4), increasing neurotransmitter release (5). (Right) Trains of action potentials

(1) make the presynaptic neuron release a higher amount of glutamate that activates astrocyte mGlu₅ receptors (2) leading to a generalized increase in cytosolic Ca²⁺ (3). Now glutamate instead of adenosine is released from the astrocyte, and activates extrasynaptic NMDARs (4) to modulate excitability and synchronization of the postsynaptic neuron (5). Reproduced from Panatier and Robitaille 2015.

Group II mGlu receptors in astrocytes

In contrast to mGlu₅, mGlu₃ expression levels in astrocytes *in vitro* are enhanced by both trophic factors and proinflammatory cytokines (Berger *et al.* 2012). In cultured murine astrocytes, activation of mGlu₃ induces a reduction in cAMP formation only in the absence of extracellular Ca²⁺, while in the presence of the ion cAMP concentrations increase. This is something peculiar, but probably to be referred to the autocrine activation of A_{2A} adenosine receptors, which are expressed by astrocytes and couple to G_sα subunits to induce a rise in cAMP (Moldrich *et al.* 2002). Group II mGlu agonists induce expression of glutamate transporters on astrocytes (Aronica *et al.* 2003; Boer *et al.* 2010), and this explains the neuroprotective potential shown by mGlu₃ (Bradley and Challiss 2012). Another reason for this is the release of neuroprotective factors such as NGF (Ciccarelli *et al.* 1999) or TGF-β (Bruno *et al.* 1998) downstream MAPK. As well as mGlu₅, astrocytic mGlu₃ has been found to sense synaptic activity, but in different brain regions than the other mGlu subtype (Haustein *et al.* 2014).

Both mGlu₃ and mGlu₅ have been shown to induce fast remodeling of fine peripheral astrocyte processes (PAP) in the minute timescale (Laviolle *et al.* 2011). This remodeling likely occurs *in vivo* in response to synaptic activity to promote coverage of synaptic boutons by astrocytes and thus enhancing spine stability (Bernardinelli *et al.* 2014).

1.3.3 Role in synaptic plasticity

The ability of synapses to undergo changes in their strength in response to specific patterns of synaptic activity is called synaptic plasticity. It is mediated by both pre- and postsynaptic mechanisms, and it is generally expressed as changes in the amount of neurotransmitter released or the number of postsynaptic neurotransmitter receptors, respectively. Plasticity can be short (ms to s) or long (tens of minutes or more) term, and can both potentiate (short/long term potentiation, STP/LTP) or depress (short/long term depression, STD/LTD) synaptic transmission. Plastic changes allow processes for which brain adaptation is required, such as the processes of sensory adaptation, learning and memory storage, and the stabilization or pruning of strong or weak synapses during development (Kauer and Malenka 2007).

Short term plasticity (ms to s)

Short-term plasticity is mediated by pure biophysical mechanisms, usually at the presynaptic terminal by modulating the residual calcium after synaptic activity and the properties of the releasable pool of vesicles, although postsynaptic neurotransmitter receptor saturation and desensitization also play a role (Regehr 2012). Therefore, mGlu receptors can induce short-term plasticity in terms of frequency facilitation and synaptic depression to the same extent they can modulate presynaptic calcium channels and vesicle release and act on receptor channels desensitization states, as already discussed in this section (Cosgrove *et al.* 2011; Pinheiro and Mulle 2008).

Long term plasticity (min to h)

Long-term plasticity is a more complex event requiring not only initiation of plastic changes but also the active maintenance of these modifications through structural changes of the synapse architecture (Yuste and Bonhoeffer 2001). The details of this process are beyond the scope of this experimental thesis, but a few examples can illustrate the roles of mGlu receptors in this phenomenon.

LTP/LTD has been described for all groups of mGlu receptors (Lodge *et al.* 2013; Mukherjee and Manahan-Vaughan 2013). As well as for short-term plasticity, presynaptic mGlu_{2/3/7} can induce persistent modifications in the amount of neurotransmitter release by regulating Ca²⁺ influx through VGCCs or release vesicle properties (Atwood *et al.* 2014; Bellone *et al.* 2008; Castillo 2012), consistent with the observation that Gβγ subunits and SNAP-25 are necessary for LTD (Zhang *et al.* 2011), and that RIM1α is involved in many forms of LTP/LTD (Castillo 2012). This highlights a double mechanism by which presynaptic mGlu receptors activation could directly or indirectly decrease neurotransmission.

However, presynaptic mechanisms of LTP/LTD can also be initiated postsynaptically, by glutamate binding on group I mGlu receptors and subsequent release of endocannabinoids (eCB) for retrograde signaling (Heifets and Castillo 2009). These substances act on presynaptic CB1 receptors, which are metabotropic receptors also coupling to the cAMP/PKA signaling pathway and modulating RIM1α phosphorylation (Chevalleyre *et al.* 2007; Kiritoshi *et al.* 2013).

Postsynaptic LTP/LTD in first instance involves changes in the trafficking or lateral diffusion of postsynaptic AMPA and NMDA receptors (Groc and Choquet 2006; Morishita *et al.* 2005; Peng *et al.* 2010), and only later relies on structural changes of dendritic spines (Matsuzaki *et al.* 2004). The best studied form of postsynaptic plasticity dependent on mGlu receptors is the LTD involving group I mGlu receptors. It was first described long time ago in the cerebellum (Ito 1989) for mGlu₁, and later for other brain areas, especially the hippocampus CA1 where mGlu₅ is the main actor involved (Huber *et al.* 2000). The process of mGlu-LTD can be induced by application of the group I mGlu selective agonist DHPG, and is also called chemical-LTD (Palmer *et al.* 1997; Schnabel *et al.* 1999). Chemical-LTD is mediated by distinct signaling mechanisms for different receptor subtypes and localizations (Lüscher and Huber 2010), but both pathways ultimately converge to modified phosphorylation states and trafficking of AMPA and NMDA receptors (Collingridge *et al.* 2010; Jin *et al.* 2015; Snyder *et al.* 2001) and spine shrinkage (Oh *et al.* 2013). In line with this, a recent study demonstrated that activation of group I mGlu receptors localized onto dendritic ER compartments restricts the lateral mobility of ER cargo including AMPA receptors, acting in a fast and PKC-dependent way through increases in ER spatial complexity mediated by phosphorylation of the microtubule-binding ER protein CLIMP63 (Cui-Wang *et al.* 2012). This is in accordance with the observation that spines of CA1 neurons without an ER are

refractory to mGlu-LTD induction (Holbro *et al.* 2009; Lüscher and Huber 2010). Notably, group I mGlu receptors are required for both homosynaptic and heterosynaptic structural plasticity (Oh *et al.* 2015).

Moreover, mGlu-LTD requires local translation and degradation of proteins (Klein *et al.* 2015), and synthesis of specific AMPAR subunits (GluA2) and their insertion on the post-synaptic membrane (Huber *et al.* 2000; Mameli *et al.* 2007). GluA2-lacking AMPA receptors are Ca^{2+} permeable (CP-AMPA) and shape excitatory postsynaptic currents (EPSCs), whereas insertion of GluA2 subunits makes these receptors impermeable to Ca^{2+} (CI-AMPA). This subunit change is mediated by coincident activation of CP-AMPA and group I mGlu receptors (Hainmüller *et al.* 2014; Kelly *et al.* 2009). This subunit switch occurs also during homeostatic scaling of synaptic activity (Turrigiano 2008) and is considered as one of the principal factors mediating this type of plasticity (Lee 2012). GluA1 translation is induced locally in inactive synapses, increasing the proportion of surface CP-AMPA receptors to allow adaptation of neurons to periods of reduced input. An increase in neuronal activity induces the translation of immediate early genes such as Arc, which induces internalization of AMPARs, and Homer1a, leading to agonist-independent activation of group I mGlu receptors (Hu *et al.* 2010) and down-regulation of synaptic activity.

Another postsynaptic mechanism for long-term plasticity involves NMDA receptors, which undergo a developmental switch in subunit composition that is highly conserved throughout evolution and species, and apparently coincides with the critical periods of the sensory systems. This switch changes the biophysical properties of these channels, influencing the neuronal response to synaptic activity on a long-term basis (Paoletti *et al.* 2013). This mechanism is also critical for the postnatal experience-dependent shaping of mature synapses in response to different frequencies of afferent fibers activity (**Figure 10**, Lau and Zukin 2007). This mechanism was shown to depend on mGlu₅ *in vivo* (Matta *et al.* 2011).

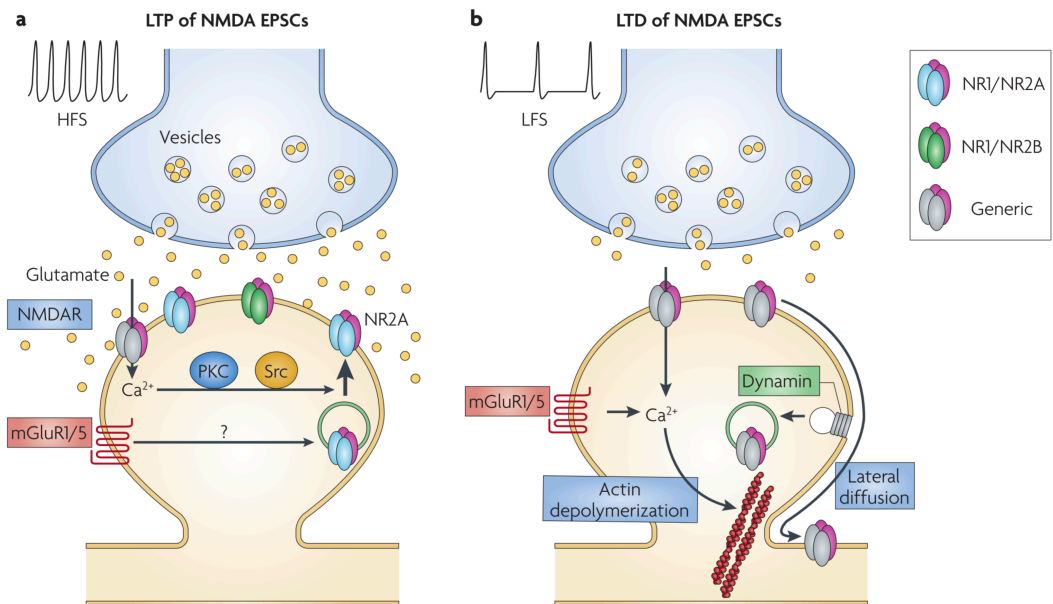


Figure 10 | Different activation frequencies are required for induction of LTP and LTD.

In the CA1 of adult hippocampus high-frequency stimulation (HFS) of the input fibers (SC) induces LTP through rapid insertion of NR2A-containing NMDARs (a), whereas low-frequency stimulation (LFS) induces LTD by removing NMDARs from synaptic sites through actin depolymerization and lateral diffusion of the receptors (b). Reproduced from Lau and Zukin (2007).

Future challenges

From these studies a general picture emerges depicting common subcellular pathways of mGlu regulation of synaptic activity, with different and possibly opposing outcomes at the neuronal network level depending on the activated subtype and the temporal activation pattern, its localization on dendritic compartments, and the specific protein expression pattern of single neurons. It becomes evident that research tools that could dissect the contribution to synaptic plasticity of individual mGlu subtypes depending on their spatial and temporal activation patterns would be of extreme interest in the unraveling of these complex mechanisms of brain function.

Unfortunately, the individual contribution to synaptic transmission of each member of the mGlu family has been difficult to determine, because even though these receptors regulate ion channel conductances, they are not ion channels themselves and cannot be studied with electrophysiology, which has long been the gold standard in the study of neurotransmission. So how to study the modulation of neurotransmission operated by mGlu receptors with at least the same cell-specificity and high temporal resolution provided by electrophysiology? A classical strategy consists in the selective

pharmacological inhibition or activation of mGlu subtypes, with drugs that could be locally applied or directly dialyzed into the chosen neuron (Pineiro and Mülle 2008). However, this is not yet possible nowadays. Besides the intrinsic spatiotemporal limitations of using diffusible pharmacological ligands, truly selective ligands are not available for every single mGlu subtype and especially for group II/III receptors (see **Table 5** and discussion in **Section 1.5**).

In this context, optical activation of neurons and neuronal proteins by means of light allows investigating the roles of synaptic receptors in neurotransmission, and circumvents the spatial limitations of electrophysiology by giving access to small compartments such as the synapse or dendritic spines (Scanziani and Häusser 2009). These novel tools will be reviewed in **Sections 2 and 3**.

1.4 Relevance to neuropathologies

We have summarized so far that mGlu receptors are involved in the modulation of synaptic transmission. Thus, it is not surprising that impaired function of these receptors leads to cognitive disorders. The major evidences are outlined below.

Animal models of mGlu ablation

Phenotypic analysis of knockout mice strains for mGlu receptors (**Table 3**) has highlighted the individual roles of receptor subtypes in higher brain functions. Although studies of mGlu₈^{-/-} animal models are incomplete and mGlu₃-lacking mice have not shown any obvious cognitive deficit so far, the general picture confirms mGlu receptors as fundamental players in synaptic plasticity, with different receptor subtypes having differential roles in different cell types, in either short- or long-term plasticity, and potentiation or depression. Overall, these animal models confirm experimental data on functional implications of mGlu receptors in the CNS that were already discussed in previous sections.

Table 3 | Phenotype of mGlu-lacking animal models.

Group	Subtype	Phenotype	Reference
I	mGlu ₁	Premature death; ataxia, impaired spatial learning/ MF-LTP/ cerebellar LTD	jaxmice.jax.org; (Conquet <i>et al.</i> 1994)

	mGlu ₅	abnormal fear conditioning and spatial learning; reduced NMDA-dependent LTP in CA1 and DG; increased spine density	(Lu <i>et al.</i> 1997) (Chen <i>et al.</i> 2012)
II	mGlu ₂	no obvious cognitive deficits; disrupted MF-CA3 LTD; impaired addictive behavior	(Morishima <i>et al.</i> 2005; Yokoi <i>et al.</i> 1996)
	mGlu ₃	no evident effects	jaxmice.jax.org
III	mGlu ₄	abnormal motor learning; impaired PP facilitation at PF- Purkinje cell synapse	(Pekhletski <i>et al.</i> 1996)
	mGlu ₆	lost response to light in ON bipolar cells	(Masu <i>et al.</i> 1995)
	mGlu ₇	reduced anxiety; alteration of hippocampal theta rhythms; deficits in spatial working memory (short-term)	(Cryan <i>et al.</i> 2003; Hölscher <i>et al.</i> 2004; 2005)
	mGlu ₈	Only preliminar results	infrafrontier.eu

References from the OMIM database (www.omim.org; website accessed on 26 Aug 2015), obtained searching for GRM1 to 8 in the database, under the 'Animal Model' section, unless differently specified.

Metabotropic glutamate receptors are functionally linked to many CNS disorders, such as anxiety (Pitsikas 2014; Swanson *et al.* 2005), drug addiction (Pomierny-Chamiolo *et al.* 2014), schizophrenia: (Conn *et al.* 2009b; Hermann and Schneider 2012); depression (Pilc *et al.* 2008; Pilc *et al.* 2013); epilepsy: (Alexander and Godwin 2006); pain (Bleakman *et al.* 2006; Palazzo *et al.* 2014); Alzheimer's Disease (AD): (Caraci *et al.* 2012; Lee *et al.* 2004); Parkinson's Disease (PD): (Conn *et al.* 2005; Finlay and Duty 2014) and Fragile X syndrome (Darnell and Klann 2013). The references indicated review the role of all mGlu receptors in the specified pathologies.

Many drugs that activate or inhibit specific mGlu receptors have been used to treat a range of neurological and psychiatric disorders (summarized in **Table 4**) at preclinical and clinical phases. Hereafter, we will briefly introduce the implication of mGlu receptors in brain disorders, and review some of the most successful examples in the pharmacological targeting of the abovementioned neuropathologies.

Table 4 | Neurological disorders related to dysfunctions of mGlu receptors.

Group	Subtype	CNS pathology	Reference
I	mGlu ₁	inherited ataxia	(Conti et al. 2006)
		autoimmune cerebellar disorder	(Fazio et al. 2008)
		<i>schizophrenia</i>	(Frank et al. 2011)
		pain (amygdala)	(Han and Neugebauer 2005)
	mGlu ₅	Anxiety (-)	(Spooren et al. 2000)
		schizophrenia (+)	(Matosin and Newell 2013)
		depression	
		drug addiction (-)	(Chiamulera et al. 2001)
		PD (-)	(Battaglia et al. 2001)
		Fragile X syndrome (-)	(Conn et al. 2005)
	pain (PAG)	(de Novellis et al. 2005)	
	(amygdala)	(Han and Neugebauer 2005)	
II	mGlu ₂	anxiety (+)	(Schoepp et al. 2003)
	mGlu ₃	schizophrenia (+)	(Patil et al. 2007)
	*	depression	
		drug addiction (+)	(Morishima et al. 2005)
		pain (+)	(Jones et al. 2005)
III	mGlu ₄	chronic pain (+)	
		PD (+)	(Marino et al. 2003)
		Schizophrenia (+)	(Slawinska et al. 2013)
		<i>Depression</i>	(Lopez et al. 2014)
	mGlu ₆	<i>missing in the CNS</i>	
	mGlu ₇	<i>underdeveloped topic</i>	
	mGlu ₈	<i>underdeveloped topic</i>	

* Group II mGlu receptors are listed jointly since no truly selective ligands are available to dissect individual subtype contributions (see **Section 1.5**), although genetic analysis can provide critical discussion on this (see Nicoletti et al. 2015).

Plus (+) and minus (-) signs indicate the direction of the receptor modulation (activation or inhibition, respectively) needed to correct the indicated disorder.

Sources: Nicoletti et al. 2011, Nicoletti et al. 2015, or PubMed.com (accessed on 28 August 2015).

Anxiety

Fenobam was discovered as an anxiolytic in the 70s. Its molecular target remained unknown until it was found to inhibit mGlu₅ (Porter *et al.* 2005), but the drug was never approved for clinical use due to its side effects (Jacob *et al.* 2009). Since then, other inhibitors of mGlu₅ were used in preclinical and clinical trials for the treatment of anxiety (Swanson *et al.* 2005). An advantage over benzodiazepines (usually administered in the treatment of anxiety) is that mGlu₅ modulators seem to induce no tolerance in preclinical models (Nordquist *et al.* 2007).

Group II mGlu receptors regulate synaptic transmission and plasticity in the amygdala, an area of the CNS playing a central role in anxiety disorders (Nicoletti *et al.* 2011). The mGlu_{2/3} receptor agonist LY354740 emerged as a novel approach to treat anxiety (Schoepp *et al.* 2003) and progressed into phase II clinical trials, but was then withdrawn because found to be epileptogenic (Dunayevich *et al.* 2008).

Drug addiction

As anticipated by studies showing elevated cocaine reinforcement (Morishima *et al.* 2005) and alcohol consumption (Zhou *et al.* 2013) in mGlu₂ knockout mice, this receptor negatively regulates the activity of the reward pathway that plays a central role in drug self-administration. The mGlu₂ potentiator N-Acetylcysteine is under clinical development for the treatment of cocaine, nicotine, cannabis and methamphetamine addiction (reviewed in Nicoletti *et al.* 2015). The opposite was observed for mGlu₅^{-/-} mice, which fail to self-administer cocaine (Chiamulera *et al.* 2001), and a drug inhibiting mGlu₅ is under clinical development for the treatment of tobacco smoking (Kenny 2009).

Schizophrenia

Schizophrenia is a disabling mental illness of yet unidentified etiology. The glutamatergic hypothesis of schizophrenia is based on hypofunction of NMDA receptors (Snyder and Gao 2013), particularly in fast-spiking interneurons of the prefrontal cortex (Kinney *et al.* 2005) that is a key brain region for cognition. This leads to disinhibition of glutamatergic neurons in this area and to cognitive dysfunctions. Since NMDA receptors cannot be targeted directly due to the risk of inducing excitotoxicity (Stone 1988), the indirect targeting of NMDAR through activation of mGlu₅ receptors, which were demonstrated to be physiologically and physically linked to NMDAR (Matta *et al.* 2011), emerged as a promising tool for the treatment of schizophrenia (Matosin and Newell 2013). Potentiators of mGlu₅ have shown good efficacy in preclinical studies of schizophrenia

treatment (Moghaddam and Javitt 2012; Noetzel *et al.* 2012), but with novel concerns for excitotoxicity being induced by mGlu₅ through direct induction of NMDA currents. However, it was recently demonstrated that the relief of symptoms induced by mGlu₅ activation is NMDA-independent (see **Section 1.5**) with mechanisms not completely understood. Recently, mGlu₅ activation was found to upregulate microRNA miR137 levels, which binds the mRNA encoding for GluA1 and converts silent synapses into active ones, and whose downregulation has been linked to schizophrenia (Olde Loohuis *et al.* 2015).

The exact implication of group II mGlu receptors in the pathophysiology of schizophrenia is unknown, but a large body of evidence shows that agonists of mGlu_{2/3} have antipsychotic efficacy. Some of these drugs have reached clinical trials, although with varying successes in treating this disorder (Kinon *et al.* 2011; Patil *et al.* 2007), that finally caused the discontinuation of the programme (Nicoletti *et al.* 2015).

An antipsychotic efficacy for mGlu₄ activation was recently suggested, but the mechanisms of such effects are not known yet (Slawinska *et al.* 2013).

Finally, mGlu₁ was recently identified through genetic studies as a possible mutated receptor in schizophrenic patients (Frank *et al.* 2011), but these results are not yet validated.

Fragile X syndrome and other autism spectrum disorders

Fragile X syndrome (FXS) is caused by mutations in the gene encoding for the RNA-binding and translational suppressor fragile X mental retardation protein (FMRP), whose loss provokes developmental delay, severe intellectual disability, autistic-like behaviors, attention deficit and hyperactivity, and epileptiform activity (Bhakar *et al.* 2012).

The first demonstration of a dysfunction of mGlu₅ in Fragile X syndrome was an enhanced mGlu₅-LTD (but not NMDA-LTD) in the hippocampus of FXS mouse models (Huber *et al.* 2002). Since then, lots of evidences have demonstrated that many pathways downstream of mGlu₅ are abnormal in FXS mice (Darnell and Klann 2013), and led to the development of the so-called 'mGluR theory of Fragile X' (Bear *et al.* 2004; Bhakar *et al.* 2012). According to this theory, absent or non-functional FMRP fails to regulate local transcription downstream of mGlu₅ activation, generating an excessive translation of LTD-associated proteins in dendritic spines (**Figure 11**).

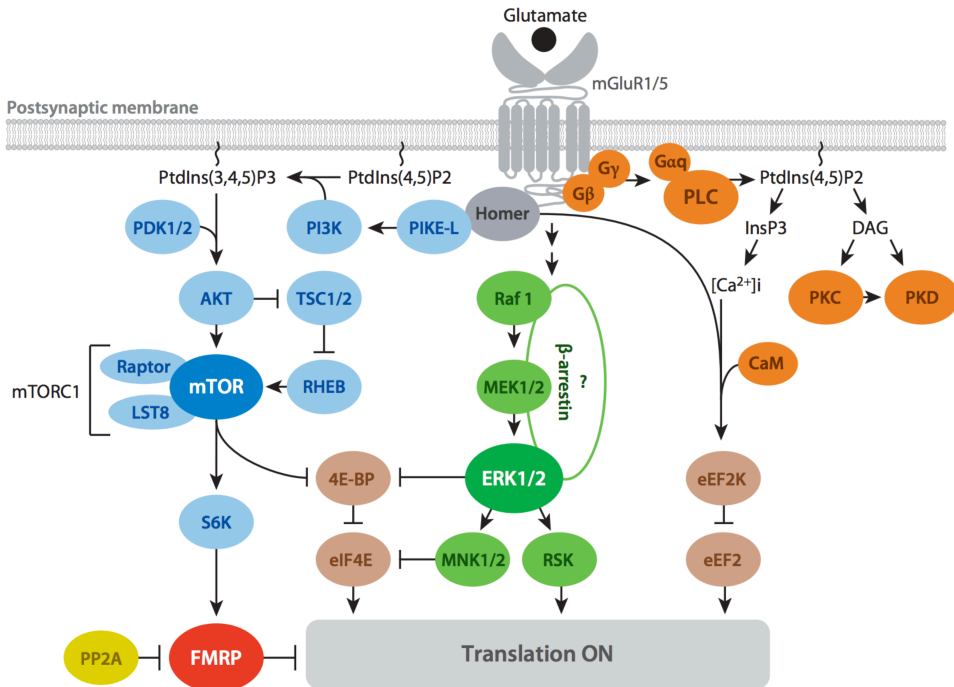


Figure 11 | The mGlu₅ signaling pathways relevant to the mGluR theory of Fragile X syndrome.

Protein translation can be regulated by activation of group I mGlu receptors through three pathways: (1) the PLC/calcium-calmodulin pathway (orange ovals), (2) the mTOR pathway (blue ovals), and (3) the ERK pathway (green ovals). Brown ovals indicate key translational regulatory components. Group I mGlu activation may also inhibit FMRP (red oval) function to regulate translation through a fourth pathway requiring stimulation of PP2A (yellow oval).

[Ca²⁺]_i, calcium release from intracellular stores; CaM, calmodulin; ERK, extracellular signal-regulated kinase; FMRP, fragile X mental retardation protein; InsP3, inositol-1,4,5-triphosphate (InsP3); mTOR, mammalian target of rapamycin; PtdIns, phosphoinositides; PLC, phospholipase C; PP2A, protein phosphatase 2A; Raptor, regulatory-associated protein of mTOR. Reproduced from Bhakar *et al.* 2012.

This theory was later confirmed by studies in which chronic pharmacological inhibition of mGlu₅ was shown to correct FXS symptoms even in adult mice (Michalon *et al.* 2012). Unfortunately, clinical trials of these drugs in FXS patients gave unsatisfactory results when compared with placebo and were recently discontinued (Nicoletti *et al.* 2015).

Another inherited intellectual disability with autism-like symptoms and caused by mutation of the tuberous sclerosis complex (TSC) produces abnormalities in synaptic protein synthesis and plasticity that are diametrically opposed to those observed in FXS. Interestingly, it was successfully corrected with drugs that activate mGlu₅ (Auerbach *et al.* 2011), suggesting the existence of an ‘optimal range’ of mGlu₅-dependent protein synthesis in normal synaptic plasticity and cognition.

Recently, mGlu₄ was identified as a potential target for autism-like disorders (Becker *et al.* 2014). However, mGlu₅ remains undoubtedly the most important mGlu drug target so far for autism spectrum disorders, given its importance in FXS and the demonstration of its upregulation in *post mortem* frontal cortexes of children with autism (Fatemi and Folsom 2011).

Parkinson's Disease

PD is caused by the progressive degeneration of nigro-striatal dopaminergic neurons in the substantia nigra *pars compacta*. This determines a reduction and eventually a complete loss of dopamine (DA) for stimulating D1 receptors on the “direct” inhibitory pathway, and for inhibiting D2 receptors on the “indirect” excitatory pathway, which both innervate the output nuclei of the basal ganglia motor circuit. This decreased and increased activity of the direct and indirect pathways, respectively, results in inhibition of thalamo-cortical neurons and the motor dysfunctions typically associated with PD. Even though DA replacement therapy with L-DOPA is effective in treating PD symptoms, its long-term administration determines the insurgence of L-DOPA-induced dyskinesias (LIDs). These severe side effects induced researchers to look for drugs for parallel administration, and the attention focused on mGlu₄ PAMs and mGlu₅ NAMs (Nickols and Conn 2014), due to their expression at almost all synapses in the basal ganglia motor circuit (for an excellent review see Conn *et al.* 2005, **Figure 12**).

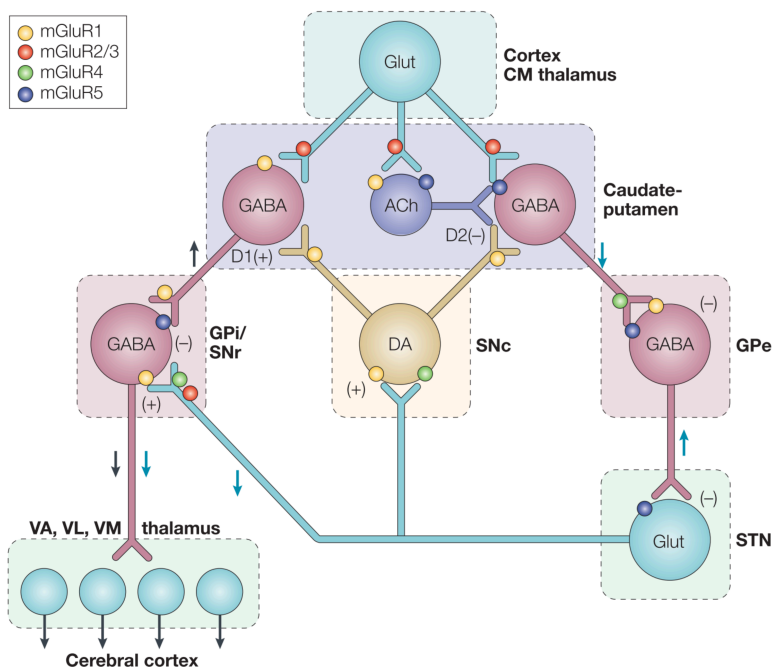


Figure 12 | Distribution of mGlu receptors in the basal ganglia motor circuit.

Dopaminergic neurons of the SNc release DA on GABAergic neurons of the striatum (caudate-putamen) of the direct and indirect pathways (black and blue arrows, respectively), which converge to regulate the output of thalamus to the cortex. In the striatal neurons of the direct pathway, DA activates excitatory D1 receptors, which results in inhibition of GABAergic neurons in the GPi and SNr. In the indirect pathway, DA activates inhibitory D2 receptors, which inhibits these striatal neurons that project to the GABAergic neurons in the (GPe). This results in the sequential inhibition of glutamatergic neurons in the STN and GABA neurons in the GPi/SNr. The net effect downstream DA in the basal ganglia is the release of thalamocortical activity. Group I mGlu receptors counterbalance the action of DA across the direct pathway, and mimic it in the indirect pathway. Group II mGlu receptors mimic the action of DA by reducing glutamate release at corticostriatal and STN-GPi/SNr synapses. Activation of mGlu₄ receptors mimics the action of DA in the indirect pathway. ACh, acetylcholine; CM thalamus, thalamic centromedian nucleus; Glut, glutamate; GPe, external globus pallidus; GPi, internal globus pallidus; SNc, substantia nigra pars compacta; SNr, substantia nigra pars reticulata; STN, subthalamic nucleus; VA, VL, VM thalamus, ventral anterior, ventrolateral and ventromedial thalamic nuclei. Reproduced from Conn *et al.* (2005).

Specifically, mGlu₄ is expressed on striato-pallidal GABAergic neurons of the indirect pathway, which is upregulated in PD. Its stimulation with PAMs causes inhibition of inhibitory signals controlling the glutamatergic output, leading to a net reduction in the activity of the indirect pathway, and relieve of motor symptoms in parkinsonian animal models (Jones *et al.* 2012; Marino *et al.* 2003).

The distribution of mGlu₅ in the basal ganglia is more widespread compared to that of mGlu₄ (Conn *et al.* 2005), and its contribution to the functioning of the motor circuit more complex. On striatal neurons, mGlu₅ counteracts the activity of D1 (Liu *et al.* 2001) and D2 receptors (Ferre *et al.* 2002; Nishi *et al.* 2003). Moreover, it inhibits neurons of the external globus pallidus (Poisik *et al.* 2003), and increases firing of the subthalamic nucleus (Awad *et al.* 2000). In all these cases, blocking mGlu₅ should favor dopaminergic pathways, and this has been demonstrated by pharmacologic inhibition of mGlu₅ (e.g. by mavoglurant). This treatment is highly effective in alleviating motor symptoms of LIDs and parkinsonism in animal models (Breyse *et al.* 2002), although mavoglurant was discontinued in clinical trials (Nicoletti *et al.* 2015).

Interestingly, Yin and colleagues (Yin *et al.* 2014) were able to demonstrate the existence of mGlu₄ homodimers at striato-pallidal synapse, whereas mGlu₄ formed heterodimers with mGlu₂ at cortico-striatal synapses, thanks to application of drugs that selectively activate one and/or another dimer type. This is an interesting point for reconsidering past studies treating animal models of PD with such molecules, and needs to be taken into account in the future development of pharmacological strategies for PD treatment.

Indeed, this suggests that activating one receptor type might be beneficial in one area whilst undesired in a different area nearby, and that therefore we might need space-specific drugs for the correct treatment of these pathologies. For instance, inhibiting mGlu₅ at striatal neurons does produce the intended therapeutic effect, but the widespread expression of this target in the brain poses a great difficulty to alleviate the disease using a purely pharmacologic approach, even with an ideally specific drug. One possibility is endowing very specific drugs with an additional feature: the ability to remotely activate and deactivate them, in order to focus their action in the target receptor *located exclusively in a certain region or organ*, while avoiding the inhibition of the same receptor in other regions. This strategy, which we tested with light-regulated NAMs of mGlu₅ (**Chapters 1 and 3**), provides a new source of drug specificity and might help reduce therapeutic side effects.

Chronic pain

Metabotropic glutamate receptors are implicated in the processes of nociception and pain occurring at the peripheral nervous system (Neugebauer 2001). However, group I and II/III mGlu receptors are expressed also in supraspinal pain centers such as those of the thalamus, the amygdala and the PAG, with the different subtypes having opposing pro- and antinociceptive roles, respectively (Goudet *et al.* 2009). The implications of group III mGlu receptors in the central mechanisms of pain are not much documented, also due to lack of selective ligands for these receptor subtypes. Fear has a central role in the affective and emotional components of pain that are processed in the amygdala, and mGlu₄ was recently proposed to play a role in this brain region for the acquisition of fear learning and memory (Davis *et al.* 2013).

1.5 Conventional pharmacology in targeting mGlu receptors

The therapeutic strategies for the pharmacological targeting of GPCRs can be divided into two major categories: orthosteric and allosteric. Orthosteric drugs mimic or competitively antagonize the actions of the endogenous ligand through binding to the endogenous ligand-binding site. In the specific case of glutamate receptors, orthosteric drugs must have amino acid-like polar or charged structures, which represents a problem for a drug bioavailability and permeability through the hematoencephalic barrier. Moreover, the proteins containing the highly conserved glutamate binding-site are many

and diverse, ranging from ion channels to metabotropic receptors and even amino acid transporters. Therefore, orthosteric drugs lack the selectivity and medicinal chemistry properties required for pharmacological targeting of mGlu receptors, and allosteric drugs binding to the allosteric site in the mGlu TMD are preferred (Urwyler 2011).

Allosteric drugs may boost or hamper affinity and/or efficacy of the orthosteric ligand, thus modulating rather than controlling the orthosteric signaling through the receptor. This property is called cooperativity, and can be positive, negative, or neutral depending on the nature of the allosteric modulator: positive, negative, and silent allosteric modulators are called PAM, NAM, and SAM, respectively. Since cooperativity is saturable, allosteric modulators are considered safer in case of overdose with respect to orthosteric ligands (Gregory and Conn 2015). Another advantage of allosteric over orthosteric drugs is the enhanced subtype selectivity, due to more divergent protein structures in the TMD than in the glutamate-binding pocket. Finally, allosteric modulators usually depend on when and where the orthosteric ligand is bound to the target, and thus regulate receptor activation while maintaining it among spatio-temporal physiological ranges (Nussinov and Tsai 2013). However, some allosteric modulators possess either intrinsic agonist or inverse efficacy, which allows them to activate or inhibit the receptor in the absence of glutamate; these ligands are called agoPAM or inverse agonists, respectively (Conn *et al.* 2009a). A summary of the different types of allosteric modulators, and a model depicting their effect on the target receptor are represented in **Figure 13**.

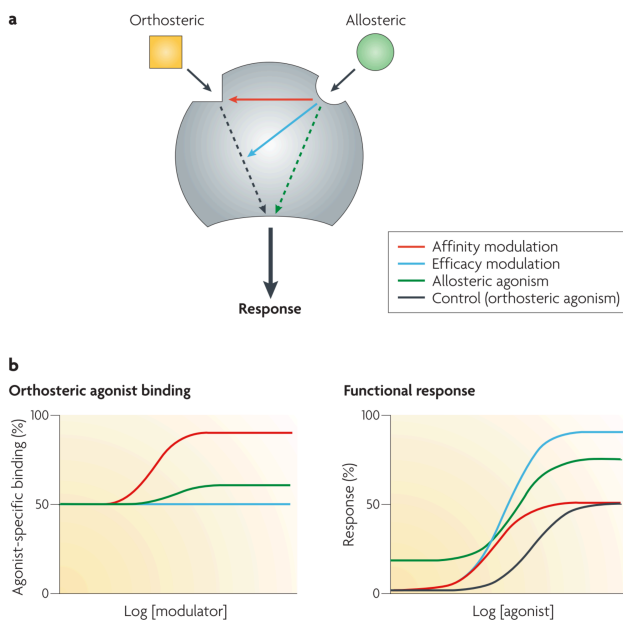
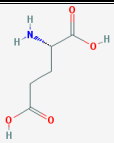
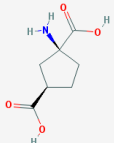
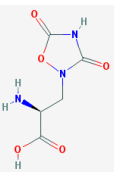
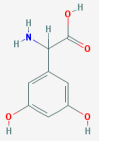
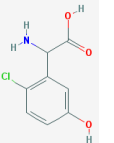


Figure 13 | Allosteric modulation of receptors. (a) Orthosteric ligands bind to the endogenous agonist binding site, and induce a control response (black curve). Allosteric ligands bind to a distinct site, and can modulate in different ways the receptor response to the orthosteric agonist. They can either modulate its affinity for the binding pocket (red) or the efficacy by which it induces the receptor signaling (cyan), or induce directly a response (green). (b) Models showing these effects in terms of agonist binding (left) or functional response (right). Reproduced from Conn *et al.* 2009a.

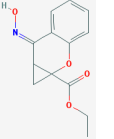
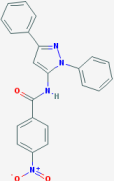
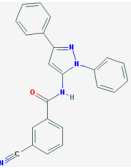
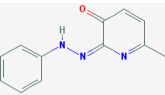
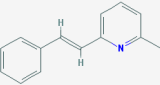
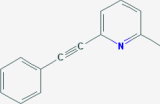
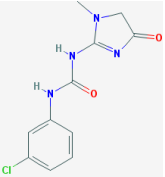
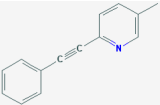
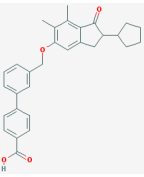
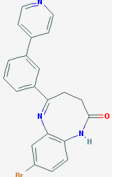
A quite unknown type of allosteric drugs is the one that reacts with the target receptor to create a covalent bond that links the drug and its effect to the receptor until this is degraded into the lysosomes. Unlike covalent orthosteric drugs (e.g. aspirine), covalent allosteric drugs are a nascent idea (Nussinov and Tsai 2013), and despite obvious concerns about safety issues and possible off-target reactivity, they are being reconsidered as promising pharmacological agents for overcoming poor selectivity and low potency of drugs, as well as drug resistance (Singh *et al.* 2011). They are also considered the perfect candidate for addressing the so called ‘ultimate physiological goal’ of a pharmacological agent, that is to exert an effect with a single dose for the entire life-time of its target (Lewandowicz *et al.* 2003).

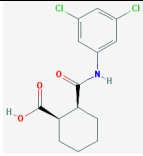
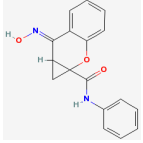
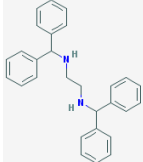
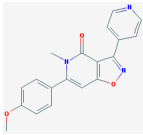
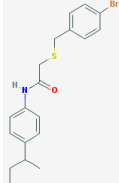
A selection of the most important orthosteric and allosteric ligands available for mGlu receptors is listed in the following table (**Table 5**).

Table 5 | Most used ligands of mGlu receptors.

Ligand		Group I		Group II		Group III			
name	structure	mGlu ₁	mGlu ₅	mGlu ₂	mGlu ₃	mGlu ₄	mGlu ₆	mGlu ₇	mGlu ₈
L-Glu ⁻		(E)	(E)	(E)	(E)	(E)	(E)	(E)	(E)
ACPD		ago	ago	ago	ago	ago	ago	ago	ago
L-Quis		ago	ago						
3,5-DHPG		ago	ago						
CHPG			ago						

name	structure	mGlu ₁	mGlu ₅	mGlu ₂	mGlu ₃	mGlu ₄	mGlu ₆	mGlu ₇	mGlu ₈
LY367385		<i>antag</i>							
NAAG					(E)*				
DCG-IV		<i>antag</i>	<i>antag</i>	ago	ago		<i>antag</i>		
LY379268				ago	ago		ago		
LY354740				ago	ago				
EGLU				ago	ago				
L-AP4						ago	ago	ago	ago
XAP 044								ago	
CCPG						<i>antag</i>	<i>antag</i>	<i>antag</i>	<i>antag</i>
LY341495		<i>antag</i>	<i>antag</i>	<i>antag</i>	<i>antag</i>	<i>antag</i>	<i>antag</i>	<i>antag</i>	<i>antag</i>
VU71		PAM							

name	structure	mGlu ₁	mGlu ₅	mGlu ₂	mGlu ₃	mGlu ₄	mGlu ₆	mGlu ₇	mGlu ₈
CPCCOEt		NAM							
VU-29			PAM						
CDPPB			PAM						
SIB-1757 (1 st)			NAM						
SIB-1893			NAM			PAM			
MPEP			NAM			PAM			
Fenobam			NAM						
5-MPEP			SAM						
BINA				PAM					
MNI-136				NAM	NAM				

name	structure	mGlu ₁	mGlu ₅	mGlu ₂	mGlu ₃	mGlu ₄	mGlu ₆	mGlu ₇	mGlu ₈
VU0155041						PAM			
PHCCC		NAM				PAM	<i>PAM</i>		
AMN082								Ago- PAM	
MMPIP								NAM	
AZ12216052									PAM

(E) stands for endogenous ligand; *italics* = marginal effect or low potency.

NAAG = N-Acetylaspartylglutamate; eGlu = Ethylglutamic acid.

All entries of the table have been taken from the IUPHAR (guidetopharmacology.org) or the Tocris company (tocris.com) websites; accessed on the 26 August 2015. Images of chemical structures were from pubchem.ncbi.nlm.nih.gov.

It is worth pointing out that this table is not reflecting the amount of ligands available for each receptor subtype, being the most abundant the ligands developed for mGlu₁ and mGlu₅ (Urwyler 2011). As for orthosteric ligands, only CHPG is truly selective for a single subtype (mGlu₅). Interestingly, the group I mGlu selective agonist quisqualate is also an agonist of AMPA receptors (guidetopharmacology.org). Notably, an endogenous orthosteric ligand was described to activate selectively mGlu₃ (Wroblewska *et al.* 2002), but there is still controversy about these results (Johnson 2011). No selective allosteric ligands have been achieved so far for mGlu₆. There are no PAMs available for mGlu₃ and mGlu₇. No NAMs exist so far for mGlu₄ and mGlu₈, and no true selective ones for group II mGlu receptors (Sheffler *et al.* 2012). However, the recently resolved crystal

structures of mGlu₁ (Wu *et al.* 2014) and mGlu₅ TDM in complex with a NAM (Doré *et al.* 2014) pave the way for a rational design of mGlu allosteric modulators, that hopefully will soon lead to the identification of more potent and selective compounds targeting these receptors.

A last thing worth pointing out is the promiscuity observed among mGlu₅ NAMs and mGlu₄ PAMs: SIB-1893, not shown in table, and MPEP, initially characterized as mGlu₅ NAMs, were later discovered to be also low potency mGlu₄ PAMs (Urwyler 2011). This phenomenon was also observed for other GPCRs (mAChR), and prompted the idea of allosteric modulators being “molecular switches” (Wood *et al.* 2011), meaning that small changes in their chemical structures can lead to great variations in their mode of pharmacology (e.g. NAM to PAM) and selectivity for a given mGlu subtype (e.g. mGlu₅ to mGlu₄, **Figure 14**).

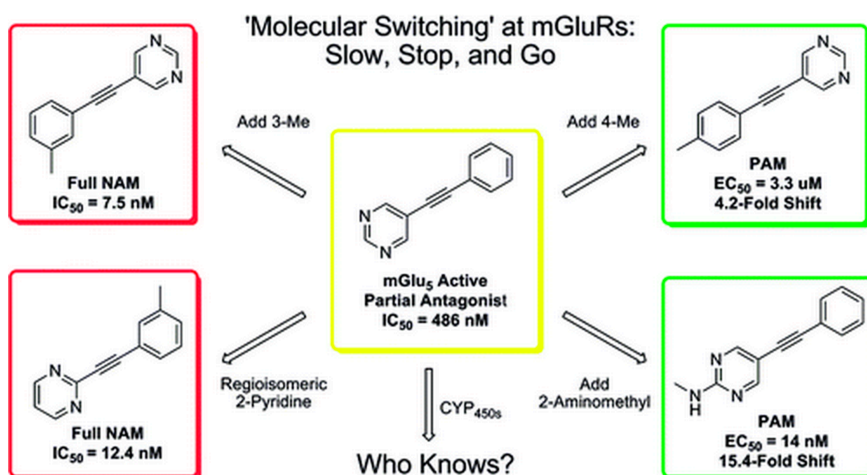


Figure 14 | Molecular switching in mGlu receptor allosteric modulators.

Scheme depicting the chemical structure of a partial antagonist of mGlu₅ (yellow), and the effect of adding different chemical substituents on the scaffold of the parent allosteric modulator, leading to a phenomenon called “molecular switching” whereby modest structural changes can modulate the mode of pharmacology, i.e. from PAM to NAM (green, red), or even selectivity for a given subtype (not represented). Reproduced from Wood *et al.* 2011.

From the therapeutic point of view, allosteric ligands are way more attractive than drugs targeting the orthosteric binding pocket for the reasons already mentioned above. Moreover, they bind to a quite hydrophobic pocket inside the TDM that requires lipophilic allosteric modulators, which have better pharmacokinetic profiles than amino acid-like drugs. However, one therapeutic disadvantage of PAMs is that many of them are ago-PAMs and act in the absence of the endogenous ligand, thus going beyond the

physiological activation of the target receptor. This is not only a theoretical problem, since the basal concentration of glutamate in the brain is sufficient by itself to reach the activation threshold of the receptor when combined with a PAM (Amalric *et al.* 2013). In the particular case of mGlu₅, PAMs of this receptor subtype had emerged as promising antipsychotic drugs for the treatment of schizophrenia as an alternative to NMDA agonists (Matosin and Newell 2013), since NMDA receptors cannot be targeted directly due to the risk of inducing excitotoxicity (Stone and Burton 1988). However, there was concern about whether targeting mGlu₅ with ago-PAMs could also activate NMDA receptors directly, as already discussed before. This concern was lately proved correct (Parmentier-Batteur *et al.* 2014; Rook *et al.* 2013), but luckily another property of allosteric ligands called ‘biased agonism’ came to help. Biased agonism (also called ‘stimulus-trafficking’ or ‘functional selectivity’) is defined as the ability of a ligand to preferentially activate a discrete subset of intracellular effectors through induction of a unique conformational state in a GPCR different from the one induced by normal ligands (Conn *et al.* 2009a). Thus, biased ligands have signaling profiles downstream GPCR activation that diverge from the usual ones, and recently biased mGlu₅ PAMs were described (Noetzel *et al.* 2013; Rook *et al.* 2015), one of them preferentially activating the G_qα signaling pathway without inducing NMDAR currents. Biased agonism provided a good strategy to prevent possible side effects of mGlu₅-targeted antipsychotics, as nicely demonstrated on animal models (Rook *et al.* 2015).

This uncommon activation process is only one example of how complex is the functioning of a receptor, and this must be multiplied by the possibilities of receptor heterodimerization (Yin *et al.* 2014), and the variety and variability of protein interactors and intracellular effectors (plus all downstream proteins) specific to different cell types and regulating the receptor localization and signaling (Enz 2012; Ritter and Hall 2009). In the context of the complexity of GPCR activation and signaling pathways in space and time, it will be very interesting to consider the possibility offered by light-regulated drugs to actually emulate these complex patterns at high resolution (potentially millisecond and subcellular) better than how the mode of action of conventional pharmacological agents does. These issues will be considered in the **Discussion** session.

2 Optical tools for mGlu receptors: sensors

In the following section we will review which are the most relevant tools currently available as optical sensors for the study of mGlu receptor localization, regulation of trafficking, dimerization, interaction with other proteins, dynamic changes in their intra- and intermolecular conformational states, and their mechanisms of activation and intracellular signaling. We will also point out some other interesting methods that, despite their demonstrated power in the study of other GPCRs, have not been applied to mGlu receptors, but seem to offer promising potential applications in the understanding of how mGlu receptors contribute to the physiology of the CNS in health and disease.

2.1 Sensing the position of mGlu receptors with light

2.1.1 Non-covalent binding of fluorescent probes

Classical techniques of light microscopy such as phase contrast do not allow directly visualizing receptor proteins.

The localization of proteins by means of light was first made possible by both the construction of the first fluorescence light microscope by Lehmann and von Prowazek in 1913 and the advent of immunolabeling by **conjugating antibodies with organic fluorophores** such as AlexaFluor and CyDyes, first conceived by Albert Coons in 1941 (Chiarini-Garcia *et al.* 2011). Later, chemiluminescent or bioluminescent enzymes were also fused to antibodies for imaging proteins with optical microscopy (Roda *et al.* 2004). This combination of techniques has long been applied in neuroscience to identify localization of proteins at subcellular level, and specific antibodies are available for all mGlu receptor subtypes.

The main limitation of this approach is that antibodies do not permeate into cells, so they only allow labeling receptors at the cell surface, while intracellular trafficking of receptors in living cells remains unexplored with this technique (Fernández-Suárez and Ting 2008). Studies about the internalization and intracellular trafficking of mGlu receptors with this technique were only possible on fixed, permeabilized samples, generating incomplete information about the fourth dimension of biological processes, that is their time course (Mahato *et al.* 2015). Another drawback of antibodies is they can cause aggregation of receptors and stabilization of big complexes due to their dual-binding

nature, and this raises concerns on experimental results when studying internalization and trafficking of mGlu receptors. Finally, despite their wide application in neurobiology, antibodies are quite big structures, ranging 10 to 20 nm, more less the size of the receptor itself, and are not suited for the study of receptor localization and trafficking at a spatial resolution smaller than double their size (Fernández-Suárez and Ting 2008). In the quest for smaller probes, very recently researchers started to use antibodies from camelids, known as nanobodies, which lack light chains and are smaller than full-length antibodies (Fridy *et al.* 2014). Interestingly, nanobodies were successfully applied in a recent study to follow signaling complexes formed after GPCR internalization, and demonstrated that GPCRs interact with their G proteins also in the early endosome (Irannejad *et al.* 2013). Unfortunately, no nanobodies are available for mGlu receptors yet.

Another way for non-covalently targeting a receptor would be to label it with a **fluorescent ligand**. This approach has a very high spatial precision, given the very small size of ligands (about 1 nm). Despite the promising potential of this technique, fluorescent ligands have been synthesized for many GPCRs, but not for mGlu receptors (fluorescent ligands for GPCRs are reviewed in Sridharan *et al.* 2014). Future development of such ligands for mGlu receptors would be of great interest, because they would help in clarifying the interaction between mGlu protomers in native tissues (Albizu *et al.* 2010), and fluorescent ligands with subtype-specificity would even shine light on the controversial question of heterodimerization of native mGlu receptors.

In a similar approach, the receptor is selectively targeted with a reactive ligand bearing the fluorophore, and made fluorescent by affinity labeling (Tsukiji *et al.* 2009), but was not implemented for mGlu receptors yet.

2.1.2 Genetically encoded fluorescent proteins

Another breakthrough in the field came from advances in molecular biology. By applying the technology of recombinant DNA, receptors can now be cloned and covalently fused to proteins that are able to fluoresce, and can be visualized directly under the microscope. The classical example is fusion to fluorescent proteins (FPs) such as green fluorescent protein (GFP) and its homologs presenting different spectral properties (Dean and Palmer 2014), which have a size smaller than that of antibodies (around 4 nm, Hink *et al.* 2000). The reproducibility of DNA cloning and the commercial availability

of many FPs allows the successful fusion of these optical sensors with potentially any mGlu receptor of interest (Coutinho *et al.* 2001), despite some technical challenges related to the big size of mGlu receptors and the length of their cDNA. A disadvantage of FPs is their tendency to aggregate, even when expressed in fusion with the proteins of interest (Verkhusha and Lukyanov 2004), and this was observed especially in the case of RFP (Costantini and Snapp 2013).

Self-labeling enzymes

More recently, other slightly smaller proteins were identified that could be used to fluorescently label proteins of interest without the risk for aggregation (Dean and Palmer 2014). These are self-labeling enzymes – mainly SNAP-tag (Keppler *et al.* 2003), CLIP-tag (Doumazane *et al.* 2011) and Halo-tag (Los *et al.* 2008) – which are fused to the protein of interest and are incubated with a fluorescent substrate or mix of reagents that ultimately leads to the covalent tethering of a classical organic fluorophore to the fusion protein tag (Dean and Palmer 2014).

These enzymatic tags present a series of advantages with respect to FP tags. First of all, the same substrate is available in combination with many color fluorophores, so there is no need for cloning different constructs for each desired color like for FPs (Lohse *et al.* 2012). Second, since they have the high substrate specificity typical of enzymes, labeling two or more proteins with different self-labeling tags is possible with no concerns for cross-reaction. Also, we need to point out that not all fluorescent reagents for enzymatic reactions are membrane permeable and therefore only suited for labeling of surface receptors or fixed samples (Liu *et al.* 2015), but this can in turn be exploited to target specifically all receptors in a cell or only the ones present at the cell surface. For instance, a recent study shows that chemical pulse-chase labeling of SNAP-tagged proteins with either cell-permeable or impermeable reagents can be used *in vivo* to study the differential half-life of intra- and extracellular proteins with more temporal definition (Bojkowska *et al.* 2011). This would not be possible with FPs, since they fluoresce during the entire lifetime of the receptor they are attached to, and do not allow discrimination between cell-surface or intracellular localizations.

One general advantage of creating chimeric proteins is that you can add to the construct a sequence for subcellular localization, and this is a nice strategy to ‘zoom in’ a cellular compartment, plus avoiding fluorescence background from non-relevant cellular localizations. Moreover, since they are expressed alongside with the protein itself, they

admit the visualization of receptors both on the cell surface and in the intracellular milieu or organelles. On the other hand, a general disadvantage that limits the application of FPs and tags for the study of any native protein is the need for exogenous expression, which can alter network dynamics. However, they provide excellent tools to study many of the dynamics of proteins, and by using viral vectors they can be induced *in vivo*, and be expressed under endogenous promoters to limit interference with the network (Gross *et al.* 2013). In the specific case of mGlu receptors, one relevant question is to what extent the fusion of proteins can alter the normal functioning of the receptor. Both their NTD and CTD are very important domains, the first mediating ligand binding and receptor activation, and the second allowing their intracellular signaling and their coupling to regulatory or interactor proteins (e.g. Homer). Therefore, in-frame fusion of mGlu receptors with FPs or self-labeling enzymes would possibly modify their signaling properties depending on the site elected for protein fusion.

Auto-fluorescent proteins can be used to localize the receptors, but also to track their membrane dynamics, study conformational changes, and detect protein–protein interactions, as will be discussed later on in **Sections 2.2** and **2.3**.

2.1.3 Advances in fluorescence microscopy

The main spatial limitation of the techniques presented above is not the labeling itself, but the intrinsic resolution of light microscopy. In fact, optical resolution does not correspond to the size of the smallest fluorescent particle, but to “the radius of the image formed by the objective that represents that self-luminous point” (Chiarini-Garcia *et al.* 2011). The explanation for this was formulated long time ago by Ernst Abbe in 1873, who stated that any optical imaging instrument, ranging from telescopes to microscopes, has a fundamental limit that resides in the phenomenon of light diffraction, and depends only on the wavelength of light and the numerical aperture (NA) of the lens used. On a perfectly aligned optical microscope with high NA, this limit is about 200 nm (Huang *et al.* 2010). This implies that particles smaller than this are seen as all having the same size, and molecules at a distance lower than 200 nm cannot be seen as separate structures.

The precise spatial localization of an mGlu receptor, whose size is less than 10 nm, cannot be determined precisely using classical optical approaches. A challenge for optical microscopy was to achieve nanoscale imaging, and early progress towards this

goal was made in the 1980s with the 'optical sectioning' of the image, using techniques such as confocal microscopy, total internal reflection fluorescence (TIRF) microscopy (Axelrod *et al.* 1984), or two-photon excitation (2PE) microscopy (Svoboda and Yasuda 2006). These techniques image only a thin section of the sample, either by eliminating the fluorescence coming from out-of-focus planes of the specimen with a pinhole (confocal microscopy), or avoiding the excitation of fluorophores outside the focal plane using evanescent waves adjacent to the glass interface (TIRF) or pulsing light with two-photon lasers (2PE). All these techniques yield clearer images with less background, and, since there is no need of mechanically slicing the sample, they are compatible with live cell applications.

Two-photon microscopy

Excitation of fluorophores with femtosecond pulsed laser beams provides another interesting advantage. This technique is based on the two-photon absorption of molecules (**Figure 15**), which was theoretically predicted by Maria Goeppert (1931) and experimentally verified by Wolfgang Kaiser (1961). A fluorophore can be promoted to its excited state with one photon using a certain light wavelength, usually in the visible range, and will emit light of a second and usually longer wavelength while going back to its ground state. However, the same fluorophore can be excited by two consecutive photons bearing in total the same energy as the light used for normal one photon excitation, which means about double the wavelength for one photon excitation (if using one single laser for 2PE), therefore usually in the near infrared (NIR) or infrared (IR) part of the spectrum. The light emitted by the excited fluorophore will be of the same wavelength for both one and two-photon stimulation, but with 2PE the emission will be focused in a submicrometric volume at the focal point of the objective. This is explained by 2PE being a non-linear process that decays quadratically with light intensity, which in turn is highest at focus and drops off quadratically with distance above and below the focal plane (Denk *et al.* 1990). The probability of coincident absorption of two photons by the same molecule $1 \mu\text{m}$ above and below the focal plane approaches zero. This results in efficient energy yield for excitation of the fluorophore only in a volume as tiny as $0.1 \mu\text{m}^3$ (Cahalan *et al.* 2002).

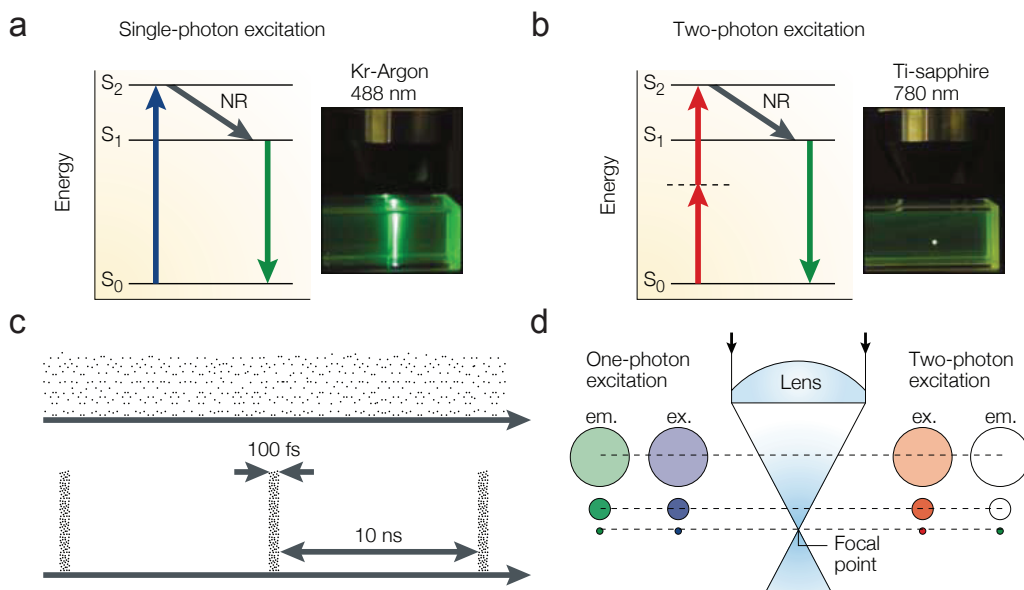


Figure 15 | The principle of temporal and spatial compression in two-photon excitation with pulsed femtosecond lasers.

(a-b) Single-photon (a) and two-photon (b) excitation of a fluorescent sample. (a) An electron in the fluorophore is excited from its ground state (S_0) to the excited state (S_2) by one photon of high-energy blue light ($\lambda = 488 \text{ nm}$, blue arrow) from a krypton-argon laser (Kr-Argon). This electron rapidly loses energy by non-radiative relaxation (NR, black line), and eventually goes back to the ground state and emits fluorescence (green arrow). Fluorescence emission occurs along the whole path of a laser beam going through a fluorescent sample (inset). (b) The same process occurs when two photons of low-energy infrared light ($\lambda = 780 \text{ nm}$, red arrows) from a pulsed titanium-sapphire laser (Ti-sapphire) are absorbed simultaneously and achieve exciting the fluorophore to the S_2 state. However, fluorescence is emitted only at the focal point of the laser beam (inset) because of the quadratic relationship between light intensity and two-photon excitation. (c) Schematics showing the temporal compression of photons in pulsed laser beams (bottom), versus continuous laser beams (top). In a pulsed laser having the same average power as a continuous laser, the same amount of photons over a time interval (10 ns) is packed in short femtosecond pulses (100 fs). This temporal compression generates a higher photon density at concrete times and therefore higher instantaneous powers. These instantaneous high powers allow 2PE with NIR light wavelengths. (d) Schematics showing the spatial compression of photons by an objective lens, and excitation (ex.) and emission (em.) intensities in the light cone for one and two-photon laser beams. In a laser beam focused through an objective lens, the density of photons (and the excitation of the fluorophore) is greatest at the focal spot and declines away from this point (blue and red circles). For one-photon excitation, fluorescence emission (green circles) is linearly proportional to excitation, and occurs along the whole laser beam. For two-photon excitation, efficient excitation is restricted to the focal point of the laser beam. The rest of the sample is exposed to single low-energy infrared photons that fail to excite the fluorophore and thus cause neither background fluorescence nor photobleaching. Adapted from Cahalan *et al.* 2002.

Scanning with two-photon lasers allows using longer NIR light wavelengths, which have deeper penetration in thick samples (Papagiakoumou *et al.* 2013) and therefore are compatible with *in vivo* imaging of neuronal structures (Svoboda and Yasuda 2006). This 2PE process is theoretically possible with all kind of molecules assumed they can absorb light at single photon, although with varying efficiencies depending on the molecule cross-section (Xu and Zipfel 2015).

Two-photon lasers can be combined with diffractive spatial light modulators (SLM) to boost the spatial definition of the imaging or stimulation of molecules (Nikolenko *et al.* 2007; Nikolenko *et al.* 2008). SLMs are devices that apply a physical filter to the incoming light beam, so that this is shaped in an arbitrary image of the desired illumination pattern, while maintaining the full power of the original light beam. This method allows avoiding the scanning of the whole image with the laser, so that simultaneous illumination of different regions in the 3D space becomes possible.

Super-resolution microscopy

The adoption of optical sectioning methods provided lateral resolution of 200 nm, and an improved axial resolution approaching half a micrometer (Fernández-Suárez and Ting 2008), but it was not until the mid 1990s that the advances in microscopy revolutionized the field. In 2014, Eric Betzig, William Moerner and Stefan Hell were awarded the Nobel Prize in Chemistry for the development of far-field super-resolution fluorescence microscopy techniques, namely STED (Hell and Wichmann 1994), STORM (Rust *et al.* 2006) and PALM (Betzig *et al.* 2006), which allowed for the first time breaking the diffraction barrier.

STED (stimulated emission depletion) uses patterned light to excite and then deplete different sets of fluorescent molecules at distances below the diffraction limit, which generates a fluorescence emission of a size smaller than the diffraction barrier. The other two super-resolution techniques (stochastic optical reconstruction microscopy, STORM; photoactivated localization microscopy, PALM) image at single-molecule resolution thanks to photoswitchable fluorescent probes that are bound to individual proteins, and only a fraction of them is stochastically switched on and off at each imaging frame, allowing their sub-diffraction localization. Reiteration of the process allows reconstruction of the frames in an overall image with single-molecule resolution (Huang *et al.* 2010). Unfortunately, these techniques are limited by photobleaching and long integration times, therefore localization of single molecules with high precision is not possible over long time courses or at high frames rates (Jones *et al.* 2011). Moreover, *in*

in vivo localization is challenging due to the high degree of light scattering in thick samples (Liu *et al.* 2015).

Among all mGlu receptors, only mGlu₅ has been investigated using super resolution techniques. In a recent study Westin and colleagues used a construct where the receptor was fused with a FP to elucidate its colocalization in dendritic spines with PSD95, actin, Homer and Norbin, another of the mGlu₅ accessory proteins (Westin *et al.* 2014).

Despite their limitations, these are interesting techniques offering unprecedented resolution, which are likely to improve in the near future with the development of new mGlu optical sensors, higher-speed optics, better camera sensitivities and higher dye brightness in order to approach imaging in the time scale of single-protein dynamics (Liu *et al.* 2015).

2.2 Sensing the receptor conformational and protein-protein interaction dynamics with light

In **Section 1** we introduced the hypothesis about the intra- and intermolecular rearrangements that accompany the activation of mGlu receptors. Most of the studies that helped elucidating these mechanisms explored these conformational changes by using biosensors that combine some of the fluorescent sensors introduced in the previous section with a phenomenon called fluorescence resonance energy transfer (FRET, also known as Förster resonance energy transfer; Miyawaki 2011).

FRET is based on a radiationless transfer of energy between an excited donor and an acceptor fluorophore. When the donor and the acceptor are far away from each other, the irradiated donor emits fluorescence at its characteristic wavelength. However, when the donor and the acceptor come close enough, energy absorbed by the donor is transferred from the excited donor to the acceptor, which in turn becomes excited and can emit fluorescence at its own characteristic wavelength. In this process, the emission of the donor is reduced (see **Figure 16**). These changes in fluorescence emission can be measured with an appropriate microscope setup on very short time scales, usually less than 5 ms, depending on the brightness of the fluorophores and the sensitivity of the camera used (Ambrosio and Lohse 2011). The fluorescence emission of each

fluorophore relative to the excitation intensity provides a measurement of the distance between the fluorophores that has nanometric precision (see next paragraphs for details) and is very fast and compatible with live cell preparations.

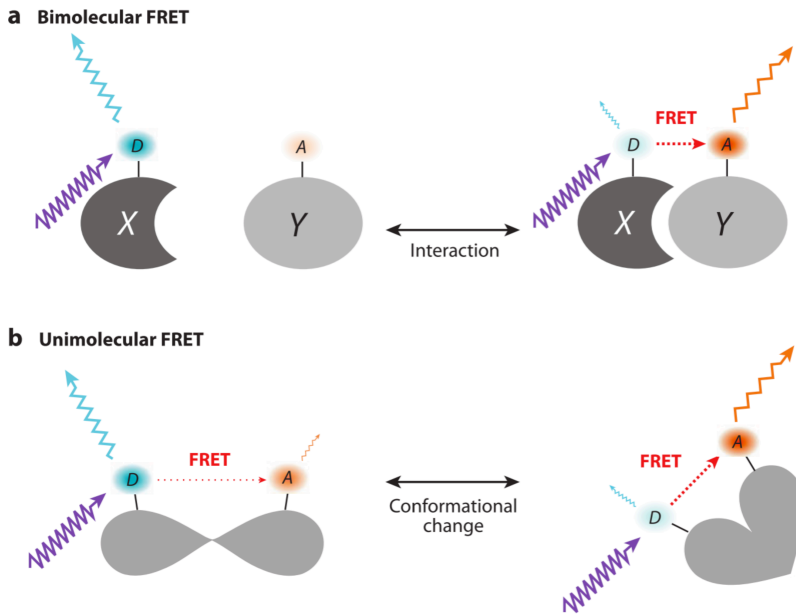
An alternative to FRET that is based on bioluminescence instead of fluorescence is BRET (bioluminescence resonance energy transfer). In BRET, the energy emitted by a luminescent moiety is transferred to a fluorophore, which can emit detectable fluorescence depending on the close proximity of the two molecules. Despite offering lower background, BRET emits lower light intensities than FRET, thus requiring longer acquisition times and compromising the temporal resolution of the technique (Ambrosio and Lohse 2011).

FRET efficiency depends on the spectral overlap between donor (emission) and acceptor (excitation), the relative orientation of the fluorophores, and the distance r between the donor and acceptor. An important feature of FRET is that its distance dependence is inversely proportional to r^6 , and this explains its outstanding sensitivity to the donor-acceptor distance and why effective FRET works only over a range of 10 nm or less (Gandía *et al.* 2008). This implies that FRET is highly dependent on orientation and distance of the two fluorophores, and this property has been exploited in the design of different GPCR biosensors.

A biosensor is a protein that is able to sense some physical or chemical property. FRET-based GPCR biosensors consist of a donor and an acceptor labeling the same GPCR on two different sites. Thanks to their ability in changing their emission depending on the relative position of the differentially labeled parts of the receptor (**Figure 16b**), they have been exploited mainly to unravel the conformational changes at the basis of GPCR activation and inactivation mechanisms and the time constants that govern these processes, both in real-time and in living cells (for a comprehensive review, see Lohse *et al.* 2012).

Figure 16 | Schematics of uni- and bimolecular FRET mechanism of action.

Two possible mechanisms of fluorescence resonance energy transfer (indicated with red arrows) between an excited (violet arrows) donor (D) and an acceptor (A). In both cases, the emission of the donor (blue arrows) is lowered when FRET takes place, whereas the acceptor only emits (yellow arrows) as a consequence of a FRET event. (a) In bimolecular FRET donor and acceptor are bound to two distinct proteins (X and Y); FRET only takes place when donor and acceptor are brought close one to each other by direct interaction of proteins X and Y. (b) In unimolecular FRET donor and acceptor are conjugated to separate parts inside the same protein. FRET becomes more efficient when a conformational change in the protein makes the two fluorophores come closer. Reproduced from Miyawaki 2011.



This technology was first developed in the laboratory of prof. Lohse to study the activation kinetics of two GPCRs, an adrenergic and the parathyroid hormone (PTH) receptors (Vilardaga *et al.* 2003). Unimolecular FRET between a CFP cloned at the CTD and a YFP inserted at the third intracellular loop of the receptor allowed the discovery of unexpectedly fast kinetics of agonist-induced activation for adrenergic receptors but not for PTH ones. By means of a fast superfusion device (with complete washout in less than 10 ms), they were able to determine that the agonist-induced activation of the adrenergic receptor required only 40 ms, whereas that of the PTH receptor was 25-fold slower. This provided a kinetic proof of the different physiological roles underlying neurotransmitter versus hormone signaling with a temporal precision that could not be achieved before. This type of biosensor made possible studying what kind of conformational changes were induced in GPCRs upon binding of different types of ligands (e.g. full or partial agonist, antagonists, or inverse agonists) as reviewed in Newman *et al.* (2011).

Another class of biosensors consists of the donor and the acceptor being localized on two different proteins (**Figure 16a**). Unlike previous protein-protein interaction assays such as pull-down and coimmunoprecipitation experiments, bimolecular FRET provides spatiotemporal information about intermolecular dynamics in living cells. Depending on the labeled proteins one can study for instance where and when GPCR

homo/heterodimers or oligomers form (Gandía *et al.* 2008); by labeling a receptor and its coupled G protein, we can investigate the kinetics of dissociation from the activated receptor (Hein *et al.* 2005) or the signal bias; by labeling β -arrestin, the rates of receptor desensitization (Lohse *et al.* 2012).

Applications with mGlu receptors

For instance, mGlu₂ and 5-HT receptors, which were known to heteromerize and interact in schizophrenia, were labeled with distinct FPs to monitor how mutations of selected residues affected FRET between the two receptors in living cells, and therefore the formation of heteromers. This allowed identifying the transmembrane segments responsible for the interaction between protomers (Moreno *et al.* 2012).

In another study, BRET between mGlu and NMDA receptors, which are functionally coupled, was used to assess the existence of physical interaction between these receptors in the case of subtypes 1 and 5, but not 7, mGlu receptors (Perroy *et al.* 2008). By combining FRET and BRET in sequence (called sequential RET, SRET), Cabello and colleagues obtained an elegant demonstration of mGlu₅ receptors forming oligomers with dopamine D2 and adenosine A_{2A} receptors in transfected cells (Cabello *et al.* 2009). In the specific case of mGlu receptors, bimolecular FRET can be used to investigate the activation of the receptor. Since structural studies predicted that mGlu₁ receptors form dimers whose activation brings together the TMDs of each protomer (Kunishima *et al.* 2000), Marcaggi and colleagues constructed a biosensor dimer of mGlu₁ protomers fused with FPs of different colors to their second intracellular loop, whose conformational changes following application of ligands were reflected in changes in the FRET ratio. With this system they were able to observe surprisingly fast kinetics of activation (around 10 ms) and slower deactivation (40 ms; Marcaggi *et al.* 2009).

Combining uni- and bimolecular FRET to differentially target individual protomers or parts of a protomer with FPs of different colors provided unique insight in the mechanism of mGlu₁ activation. By using this complex strategy followed by agonist application to mGlu₁ dimers, two facts emerge, that are: first, sequential inter- and then intrasubunit rearrangements take place, and, second, only one subunit at a time assumes the 'active' conformation within an mGlu₁ dimer (Hlavackova *et al.* 2012).

Very recently, a new FRET biosensor was developed based on mGlu₂ and mGlu₃, and helped clarifying the conformational changes and kinetics that underlie mGlu receptors activation (Vafabakhsh *et al.* 2015). A SNAP and a CLIP tag were placed at specific

positions of two VFT domains and each labeled with a FRET pair. Receptor homodimers immunopurified from cell lysates were analyzed with TIRF microscopy for single-molecule FRET (smFRET). Thanks to this novel approach, the authors of this study demonstrated that the VFTs of mGlu dimers exist in three conformations (resting, activated, and a short-lived intermediate state), and that mGlu₃ is Ca²⁺-sensitive and therefore displays basal activity in physiological conditions. The temporal resolution of this biosensor also allowed discovering that the activation kinetics of mGlu₂ are faster (80 ms) and less stable than those of mGlu₃ (180 ms).

The continuous development of novel FRET technologies to gain insight in single receptor events with more and more temporal resolution demonstrates the interest of this research topic, and anticipates important discoveries in the field in the next years.

Time-resolved FRET

Initially the FRET biosensors were based on FPs, but major disadvantages of these proteins as fluorophores led to the development of better FRET systems. First, overexpressed proteins tend to be misfolded and accumulate in intracellular compartments, and this, in addition to the tendency to aggregate of FPs, could give rise to FRET independent of real donor-acceptor interaction. Second, FPs as FRET pairs can suffer from the so-called 'crosstalk' and 'bleedthrough', *i.e.* overlap between donor and acceptor excitation or emission spectra, respectively (Ciruela *et al.* 2010), and lead to low signal-to-noise ratios. This last problem was solved by developing the so-called time-resolved FRET (TR-FRET).

TR-FRET uses lanthanides caged into cryptands (e.g. europium cryptate) as FRET donors. Cryptands are synthetic molecular cages that bind strongly cations. Lanthanides are rare earth metals with luminescence half-lives longer than 1 ms, in contrast to conventional fluorophores whose fluorescence usually decays in 20 ns (Cottet *et al.* 2013). Their long-lived photoluminescence is exploited in FRET assays to separate temporally the excitation of the donor from the acquisition of the fluorescence emitted by the acceptor (**Figure 17**; Bazin *et al.* 2002). The light source to excite the donor can be switched off before collecting the acceptor fluorescence, since europium cryptate will still be transferring energy to the acceptor for FRET, to finally eliminate crosstalk (Cottet *et al.* 2012). During this 'waiting time' contaminating fluorophores that are naturally present in samples will also switch off, contributing to the reduction of the background. Moreover, these donors usually do not present bleedthrough (*i.e.* interference with the emission spectrum of the acceptor) when used in combination with acceptors such as AlexaFluor

or d2 (a fluorophore developed by Cisbio Bioassays for optimized TR-FRET; Maurel *et al.* 2008). To conclude, the TR-FRET approach offers a much higher signal-to-noise ratio, and has been used mainly for experimental approaches where reproducibility has great importance, such as medium or high-throughput screenings (one of these techniques will be detailed later on in **Section 2.3**).

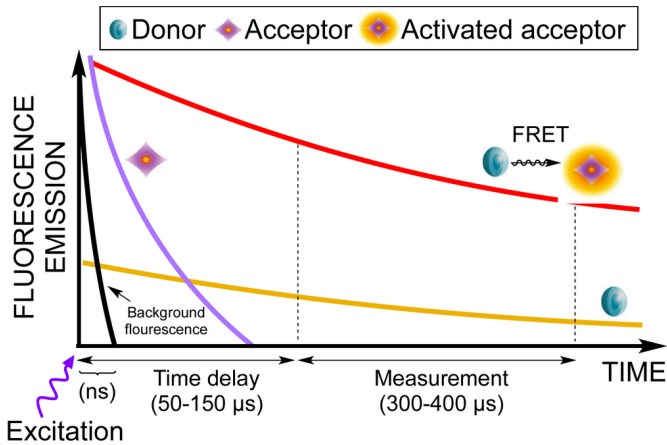


Figure 17 | Fluorescence emission in time-resolved FRET.

Light wavelengths used to excite the FRET donor (violet arrow) also excite the acceptor (this phenomenon is referred to as 'crosstalk' in the text) and natural fluorophores present inside cells, which therefore emit some amount of fluorescence (violet and black lines, respectively). Normally fluorescence decays in a short time (< 200 μs), whereas lanthanide-

cryptate donors have much longer photoluminescence half-lives (up to 1 ms; yellow line). Therefore, acceptor excitation and the consequent fluorescence emission through TR-FRET (red line) happen over longer time scales than with classical FRET. This allows the experimenter to add a time delay after the excitation of the donor and before measuring the fluorescent readout as a result of FRET, and leads to a cleaner signal devoid of crosstalk from acceptor and natural fluorophores. Reproduced from Nørskov-Lauritsen *et al.* 2014.

These new generation FRET pairs were initially used to label antibodies (Kniazeff *et al.* 2004; Maurel *et al.* 2004). Even though time-resolved, the use of antibodies for FRET studies does not guarantee the specificity of FRET. In fact, antibodies are not bound to a single label but to many of them, and this increases the probability of getting FRET by random collision between fluorophores, just like for overexpressed FPs. Moreover, antibodies can stabilize large complexes of proteins and lead to unwanted perturbations of the system, as already discussed in **Section 2.1**. Combining europium cryptate with SNAP-tagged GPCRs for bimolecular TR-FRET has solved these inconveniences, because only one donor or acceptor is conjugated to one protein. In the first study using this technology, Maurel and colleagues (Maurel *et al.* 2008) demonstrated that members of both class A and C GPCRs form oligomers, whereas mGlu receptors assemble strictly into dimers. In a later work by the same group, they also demonstrated that agonist application induces nanometric displacement between two labeled VFT domains inside

an mGlu₂ dimer, and that this movement is ligand-type and G protein-binding dependent (Doumazane *et al.* 2013).

A last and very appealing use of these long-emitting lanthanide compounds is their conjugation to receptor ligands (reviewed in Cottet *et al.* 2013). Although the fluorophore is bigger in size than the ligand itself, the labeling worked unexpectedly well for peptidic ligands (*i.e.* hormones) and also for small amines. The FRET pair can consist in the ligand and the GPCR for high-throughput drug screening, or a mixture of the ligand half marked with the donor and the other half marked with the acceptor. This second option constitutes the elective strategy for studying oligomerization of native receptors inside tissues (Albizu *et al.* 2010). However, data interpretation would not be univocal in the absence of FRET, since negative cooperativity could prevent the second ligand from binding to the oligomer.

To conclude, FRET-based biosensors have better spatial and temporal precision than most super-resolution microscopes, and have offered unprecedented accuracy in the study of mGlu receptor dynamics and protein-protein interactions so far.

2.3 Sensing the signaling of mGlu receptors with light

In **Section 1.2** we introduced the effectors, second messengers and downstream pathways involved in the intracellular signaling of mGlu receptors. The effectors can be enzymes (PLC β , AC, PKC), ion channels (VGCC, GIRK, TRPM1) or interactor proteins (Homer, β -arrestin, GRK, *etc.*); the second messengers IP₃, DAG and Ca²⁺, cAMP and cGMP. A number of optical sensors are available to investigate the intracellular signaling pathways initiated by mGlu receptors activation, and will be reviewed hereafter with special emphasis on the ones used in the experimental part of this thesis.

2.3.1 Optical sensors of second messengers

Calcium

Calcium is a crucial ion for intracellular signaling, involved in the regulation of fundamental cellular functions as diverse as egg fertilization or cell death (Berridge *et al.* 2003), and many reporters are available to sense this important second messenger.

Among them, the optical ones can be divided into two main categories: the chemical or synthetic fluorescent indicators and the genetically encoded ones.

Chemical calcium indicators

The first chemical Ca^{2+} indicator to be synthesized was Quin-2 in 1980 (Tsien 1980), which represented a real revolution in the field compared to previous methods used to sense Ca^{2+} inside cells or organisms. Earlier methods were either not sensitive, such as the Ca^{2+} -sensitive luminescent protein aequorin, or too invasive. For example, alizarin sulfonate is a natural pigment that forms red crystals upon Ca^{2+} binding, and was injected in *Amoeba* to demonstrate that Ca^{2+} ions were fundamental for movement; also, Ca^{2+} -selective microelectrodes were used in direct contact with the cytoplasm, but damaged cells due to their dimensions (Petersen *et al.* 2005). In contrast, Quin-2 was soluble, non-toxic, and membrane-permeable in its acetoxymethyl ester (AM) formulation (Tsien 1981). Unfortunately, its excitation required deep ultraviolet radiation, which also excited cellular autofluorescence that interfered with the measurements. Moreover, its fluorescence yield was low, so that bulk loading was needed to obtain satisfactory signals, which in turn induced buffering of the low-concentration (and most interesting) calcium events (Petersen *et al.* 2005). The second generation of indicators developed by Tsien and colleagues included Fura-2 and Indo-1, and solved the problems of cellular autofluorescence and calcium buffering (Grynkiewicz *et al.* 1985). Thirty years after its synthesis, Fura-2 AM is still one of the most used chemical calcium indicators worldwide.

Fura-2 is a fluorescent calcium chelator, whose emission spectrum changes in amplitude and peak when it is bound to the ion (**Figure 18**). These variations in fluorescence reflect the amount of free calcium the indicator can bind, and can be measured with cameras or other types of photodetectors to estimate the calcium present inside a cell or a population of cells.

To allow easy loading into cells, Fura-2 is made temporarily membrane-permeable by masking the non-permeable carboxylates that chelate calcium ions with esterifying groups, converting it into Fura-2 AM. Then, esterases present in the cytoplasm of the cell are in charge of its hydrolysis to Fura-2, restoring the chelating properties of the molecule and its membrane impermeability, thus trapping it inside the cell (Tsien 1981). The advantage of this is that the residual indicator in the extracellular solution can be washed out, thus reducing background.

Another interesting property of Fura-2 is that upon calcium binding not only the fluorescence intensity changes, but also the peak of excitation moves towards shorter wavelengths (**Figure 18b**). In absence of free calcium the peak is above 360 nm, and as the calcium increases the peak progressively moves towards 340 nm. The isosbestic point is the excitation wavelength at which the fluorescence emission is constant regardless of the calcium concentration, and corresponds to 360 nm.

This characteristic makes Fura-2 suitable for ratiometric measurements. The molecule is excited at two light wavelengths, one above and one below the isosbestic point (usually 340 and 380 nm), and fluorescence emission at 510 nm is collected after each excitation. The ratio between the two fluorescence emissions (F_{340}/F_{380}) represents an estimate of calcium inside the cell that is 'corrected' for intensity changes. The use of ratiometric measurements is preferred because it cancels out artifactual variations in the signal due to local differences in Fura-2 concentration, which could come from photobleaching of the indicator, uneven loading, membrane leakage, and unequal cell thickness (thermofisher.com, accessed on 11 Sept 2015, **Figure 18d**).

The last advantage of Fura-2 is that it has a good two-photon cross section (Xu *et al.* 1996; **Figure 18e**), which makes it suitable for imaging calcium *in vivo* (Sohya *et al.* 2007). However, its absorption at two-photon is so broad that ratiometric imaging would be too challenging. Despite this, Fura-2 excitation at a single NIR wavelength is sufficient to monitor qualitatively calcium dynamics in neurons *in vivo*.

Fura-2 and many other indicators with manifold calcium affinities and spectral characteristics are commercially available.

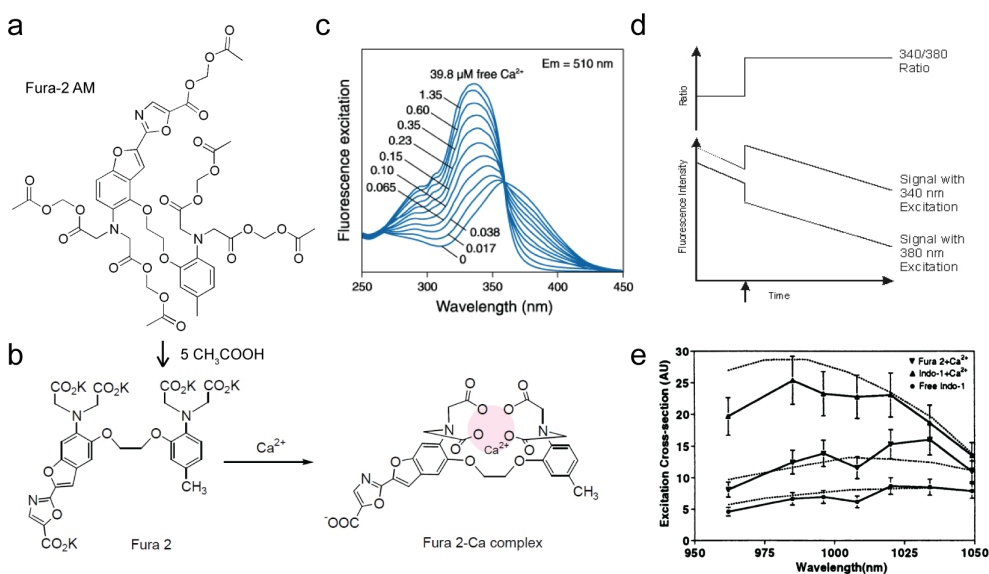


Figure 18 | Fura-2 AM structure and excitation spectrum.

(a) Chemical structure of Fura-2 acetoxymethyl ester (Fura-2 AM). (b) Structure of Fura-2 pentapotassium salt on the left, and Fura-2 in coordination with a calcium ion on the right. (c) Excitation spectra of Fura-2 in solution with indicated concentrations of free calcium; fluorescence emission was collected at 510 nm. In absence of calcium, peak emission occurs above 360 nm. By increasing the amount of free calcium, the peak progressively moves towards shorter light wavelengths. At saturating concentrations of the ion, the peak emission is around 340 nm. The isosbestic point for Fura-2 excitation is 360 nm. (d) Model showing how changes in absolute fluorescence of Fura-2 signals can be corrected by applying ratiometric measurements. (e) Two-photon excitation cross-section of Ca^{2+} -bound Fura-2 represented by the lower solid line in graph (the other traces representing other indicators can be ignored). Panel a from en.wikipedia.org, b from dojindo.com, c from thermofisher.com, and d from mktg.biotek.com; accessed on 11 Sept 2015. Panel e reproduced from Xu *et al.* 1996.

Genetically encoded calcium indicators (GECI)

About two decades after the synthesis of Quin-2, the same research group generated a new class of calcium indicators, now called GECI.

The first members of this class of biosensors were a series of proteins called cameleons. They were obtained by fusion of the calcium-sensitive protein calmodulin (CaM) with the CaM-binding peptide M13 and two different FPs, in a way that FRET between FPs was allowed upon Ca^{2+} binding (Miyawaki *et al.* 1997). Unfortunately, the first cameleons had low signal-to-noise ratios and slow response kinetics, making them unsuitable for many applications (Grienberger and Konnerth 2012). Later on, similar GECIs were created whose calcium sensitivity was reflected in changes in their fluorescence intensity rather than on a FRET mechanism. The most famous are GCaMP and its derivatives, available (most of them commercially) in different colors, calcium affinities and binding kinetics, and cloned under normal or cell type-specific promoters for both infecting with viral vectors and creating transgenic mice (Grienberger and Konnerth 2012). GCaMPs, thanks to their unprecedented calcium sensitivity paralleled by advances in imaging techniques, have been widely used in acute or chronic studies *in vivo* (Tian *et al.* 2009). Very recently, a family of photoactivatable GECIs was generated by the group of Isacoff, which is optimized for super-resolution microscopy at the single protein level (Berlin *et al.* 2015).

Inositol phosphate 3 (IP_3)

Inositol phosphates (IPs) are located upstream of calcium in the signaling cascade initiated by group I mGlu receptors. Measuring IPs is particularly challenging due to the

variety of isoforms in which they exist and the labile nature of these compounds (Irvine and Schell 2001), which are rapidly degraded by cellular enzymes as explained in **Section 1.2**. Lithium ions can be used to decrease the rate of degradation of IP₁ (Benjamin *et al.* 2004), which leads to accumulation of IP₁ in the cytosol. Traditional methods to measure IPs are chromatography or radiolabeling, but these lack spatiotemporal definition. Very few light-based methods for analyzing IPs are available, and all of them are based on FRET mechanisms.

Genetically encoded IP sensors

By fusing FPs with the ligand binding domains of InsP₃ receptors, researchers created genetically encoded indicators selective for IP₃, namely Libra (ratiometric and plasma-membrane targeted, Tanimura *et al.* 2004), Fretino (Sato *et al.* 2005), FIRE (Remus *et al.* 2006), and IRIS (Matsu-ura *et al.* 2006).

Fretino was used to study the real-time kinetics of IP₃ production in the dendrites of cultured hippocampal neurons following glutamate application (Sato *et al.* 2005). Notably, the lower affinity sensors IRIS exhibit low IP₃ buffering, and this allows to monitor simultaneously both IP₃ and Ca²⁺ dynamics in real-time in individual cells. This was demonstrated in heterologous cells expressing the mGlu₅ receptor during Ca²⁺ oscillations induced in these cells by application of glutamate, but unfortunately the sensors failed to detect IP₃ oscillations due to their slow off-rates (Matsu-ura *et al.* 2006). Improved versions of these IP₃ sensors having even lower IP₃ affinity and faster off-rates were created (Gulyás *et al.* 2015; Tanimura *et al.* 2009), so that IP₃ dynamics can now be monitored with more temporal precision than before.

TR-FRET in IP accumulation assays

One way to optically measure accumulation of IPs with high-throughput efficiency is the IP-One HTRF assay developed by the company CisBio Bioassays in collaboration with the laboratory of Jean-Philippe Pin at the IGF in Montpellier, France, by exploiting the TR-FRET technology (**Figure 19**).

The IP-One HTRF assay is a high-throughput homogeneous time-resolved fluorescence (HTRF) competition immunoassay that uses anti-IP₁ antibodies labeled with europium- or terbium-cryptate, and synthetic IP₁ labeled with the TR-FRET-optimized d2 fluorophore. Cells expressing the G_q-coupled GPCR of interest are seeded in multi-well plates, and stimulated with the agonist in presence of the drugs under screening, which activates PLC and triggers the IPs cascade. This is done in a solution containing LiCl,

which makes IP₁ (a subproduct of the degradation of IP₃) stable, and allows its accumulation during the stimulation of the receptor. Cells are then lysed and incubated with a mixture of the labeled FRET-pair of IP₁-d2 and αIP₁-Ab-EuCryptate. The resulting FRET is read with a fluorescence plate reader that introduces a time delay between fluorescence excitation and detection (see **Figure 17**) and allows determining the amount of IP₁ accumulated during the stimulation with drugs under study, which is in turn a measure of GPCR activation.

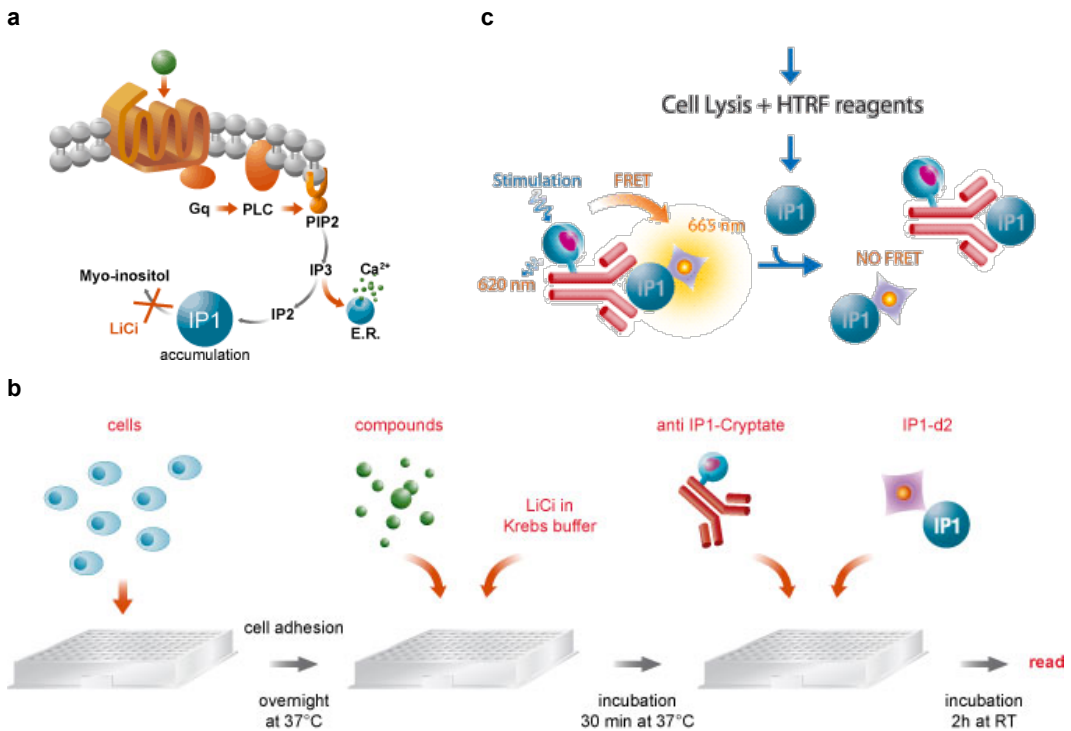


Figure 19 | IP accumulation assay by CisBio Bioassays.

(a) Agonist activation of a G_q-coupled GPCR activates PLC and hydrolysis of PIP₂ in IP₃. IP₃ is quickly degraded into IP₂, IP₁ and myo-inositol. Lithium chloride inhibits the last step of the IP₃ cascade, making IP₁ stable and allowing its intracellular accumulation. (b) For IP-One assay cells expressing the desired receptor are seeded in a multi-well plate one day before the competition assay. Once adhered, cells are stimulated with the appropriate receptor agonist plus the drugs under study, in a buffer containing LiCl. After 30 minutes, the cells are lysed and incubated with the TR-FRET pair IP₁-d2 and αIP₁-Ab-EuCryptate. After two hours the TR-FRET efficiency is read in a fluorescence plate-reader that allows time-delayed fluorescence measurements. (c) Time-resolved FRET is induced by excitation of the Eu-Cryptate donor, which labels α-IP₁ antibodies, when this is bound to the FRET acceptor d2-IP₁, so that the short distance between the donor and the acceptor allows RET. The IP₁ produced by the cells as a consequence of GPCR activation competes with the synthetic d2-labeled IP₁ for binding of the FRET-donor. Therefore, low FRET indicates high production of IP₁ by the cells, and high GPCR activation. Reproduced from cisbio.com and bmglabtech.com, accessed on 12 Sept 2015.

This is a straightforward method for cell populations expressing group I mGlu receptors, whose activation naturally induces the hydrolysis of IP₃ by PLC β through coupling to G_q α protein subunits. To measure the activation of group II and III mGlu receptors, which couple to G_i α proteins, this is done indirectly, thanks to co-transfection with a chimeric G_{i/q} α protein that recognizes G_i α -coupled receptors but activates G_q α instead (Gomez *et al.* 1996). This simple but effective strategy allows the high-throughput screening of ligands for all mGlu receptors simultaneously using the same assay in one single multi-well plate.

Diacylglycerol (DAG)

DAG is the other second messenger that is generated together with IP₃ following hydrolysis of PIP₂. DAG is a membrane-anchored lipid, which diffuses laterally in the membrane to contribute to the activation of PKC by Ca²⁺ ions (Carrasco and Mérida 2007). The domains of PKC that recognize DAG and make the enzyme associate to the plasmalemma were fused with FP-pairs to create FRET-based DAG sensors that translocate from the cytoplasm to the cell membrane (Sato *et al.* 2006). Other FRET-based biosensors for DAG are reviewed in Ueda *et al.* (2013).

Cyclic AMP and GMP

Among the first FRET-based sensors for real-time cAMP detection we find FICR_hR, which was based on regulatory and catalytic subunits of PKA chemically labeled with different fluorophores. Binding of cAMP induced the dissociation of the regulatory subunits from the catalytic ones, producing a decrease in FRET. Later, chemical labeling was substituted by genetic labeling with FPs to obtain Epac (Zaccolo and Pozzan 2002), and other sensors with better dynamic ranges and lower affinities were also designed (Gorshkov and Zhang 2014). Since expression of exogenous biosensors is not the elective method to study the physiological mechanisms of cell signaling, a research group developed a curious system called CANDLES (from Cyclic AMP iNdirect Detection by Light Emission from Sensor cells) whereby cAMP from *naïve* primary cell cultures can be measured with a luminescent assay. Sensor cells expressing a luminescent cAMP sensor are co-cultured with primary cells, which then communicate with gap junctions and cAMP diffuses into sensor cells and generates a luminescent read-out (Trehan *et al.* 2014).

Endpoint HTRF assays for measuring cAMP accumulation similar to those used for detecting IPs are available from CisBio bioassays.

As for cGMP, since its concentration in neurons is lower than that of cAMP, optical sensors for this cyclic nucleotide, although existing, are challenging. A list of them is also reviewed in Gorshkov and Zhang (2014).

As far as we know, none of these sensors has been applied to monitor intracellular signaling of mGlu receptors.

2.3.2 Optical sensors of effectors

Among the effectors of mGlu receptors we find PKC, PKA, ERK, ion channels, and more downstream CaMKII (among others). Optical sensors are available for detection of voltage, chloride ions, and activation of all the mentioned kinases, and were recently reviewed by Ueda *et al.* (2013).

However, changes in membrane voltage, ion composition, and kinases and transcription factors represent points of convergence among many signaling pathways downstream of different GPCRs, that could result from activation of different types of GPCRs and tyrosine kinase receptors (TRK). This makes the probing of these effectors not really specific to mGlu receptors, and won't be treated here.

2.3.3 Interacting proteins to monitor receptor trafficking

β -arrestin

β -arrestins are endocytic adaptors involved in the desensitization and internalization of GPCRs. These proteins were named after their ability to sterically hinder the coupling of G proteins to activated receptors (DeWire *et al.* 2007). Later on they were discovered to function also as adaptors for signal transduction in the non-classic and G protein-independent signaling of GPCRs from intracellular compartments (Lefkowitz and Shenoy 2005).

FRET has been extensively used to study the interaction between β -arrestins and many GPCRs (reviewed in Lohse *et al.* 2012). Basically, this was done by positioning one FP of the FRET pair at the CTD of the GPCR, and the other FP at the C terminal of β -arrestin (Vilardaga *et al.* 2003), so that recruitment of β -arrestin resulted in increased

FRET. As for GPCR activation mechanisms, FRET resulted particularly suited to study the kinetics of β -arrestin binding and dissociation, and helped define the delay time for its recruitment after binding of the agonist to the receptor (Lohse *et al.* 2012). To date, no study has addressed with FRET-based optical probes the interaction between β -arrestins and mGlu receptors.

A high-throughput assay that uses GFP-tagged β -arrestin for screening GPCR drug targets is available from Molecular Devices. In this assay, called TransFluor, the translocation of β -arrestin along with the activated receptor from the membrane to the cytosol and then to vesicles is monitored and quantified by automated microscopes to estimate receptor activation.

G protein-coupled receptor kinases (GRKs)

GRKs are membrane bound kinases that are recruited by active forms of GPCRs and phosphorylate them on sites of β -arrestin binding. By RET experiments it was clarified that the nature of GRK/GPCR interaction is transient, and has not been extensively investigated (Lohse *et al.* 2012).

Fusion to pHluorin

pHluorin is a fluorescent protein that was originally developed to study endo- or exocytosis processes and can be exploited to study the intracellular trafficking of proteins. It is a GFP mutant whose fluorescence is pH-dependent, being minimal at acid pH values (Miesenböck *et al.* 1998). This protein becomes a sensor of protein localization when it is fused to the N-terminal of the protein of interest, so that pHluorin is exposed to the extracellular medium or the lumen of organelles once internalized. Since pH is different in the different steps of the internalization and recycling/degradation pathway (Mellman 1992), proteins fused to pHluorin emit varying amounts of fluorescence depending on their localization. Phluorin was fused to mGlu receptors in a number of studies for visualization purposes (Arizono *et al.* 2012; Pelkey *et al.* 2007; Wilkinson and Henley 2011), but only in one of them used to assess the internalization of mGlu₇ following application of a PAM or an antagonist (Pelkey *et al.* 2007).

Coordinators of vesicle trafficking

As far as mGlu receptors are considered, one interesting but unexplored way for the monitoring of receptor trafficking is the FRET-based biosensor 'Raichu-Rab5'. Rab5 is a Rab GTPase known as a key protein for cargo sequestration, assembly of clathrin-coated pits at the plasma membrane, and a regulator of the early endocytic pathway (Stenmark 2009). Raichu-Rab5 comprises Rab5, a Rab5-binding domain and two FPs; increase in activated Rab5 (Rab5-GTP) results in increased FRET of the biosensor (Kitano *et al.* 2008). In our opinion, an interesting application of Raichu-Rab5 could be its use in combination with mGlu receptor agonists, antagonists and other types of ligands. The appearance of FRET indicating Rab5 activation could be monitored with spatiotemporal resolution to check if the internalization that has been observed following activation of mGlu receptors is a general mechanism involving the whole membrane or is somehow compartmentalized in space or time. Other FRET sensors that could be applied in the study of receptor internalization are reviewed in Ueda *et al.* (2013).

2.4 Future challenges

Spatial compartmentalization of proteins or signals seems to be an issue in many signaling cascades (partitioning in lipid rafts, membrane anchoring of proteins or second messengers, buffering of ions...). Temporal patterning of signals is also emerging as an important characteristic of signaling, as many second messengers or enzymes have been shown to operate in an oscillatory-coded way (Ca^{2+} , IP_3 , cAMP, PKC, CamKII...). Recent advances in high-resolution imaging together with the technology of recombinant DNA provided scientists with useful tools for the optical probing of neuronal proteins and their functions.

However, to image simultaneously *in vivo* multiple proteins at single-molecule resolution remains an unmet goal. For this, we need to expand the colors of the fluorophores toolbox for multiple recording, and to create red-shifted sensors for the induction of FRET at two-photons. Moreover, since super-resolution imaging techniques have not reached sufficient spatial and/or temporal resolution for interrogating single FRET-pairs with light, the questions that have been answered until now only represent the average response of hundreds of these biosensor, so that we have no means to know if the kinetic data reflect reality or just the slower average of possibly much faster events. As

imagined by Lohse, one of the pioneers of the FRET biosensors, these questions will be satisfactorily answered when optical sensors with better spatiotemporal characteristics and faster super-resolution microscopy techniques will be developed for the single-receptor interrogation, or by “triggering the synchronous activation of all receptors simultaneously [...] with ultrarapid techniques of agonist delivery to receptors” (Lohse *et al.* 2012). An alternative possibility is synchronous receptor stimulation by light, which is the focus of this thesis.

In the present section we reviewed the most important optical sensors for mGlu receptors. There are a number of still open questions that we might be able to answer in the near future thanks to optical switches for the activation of single receptors with light, at fast rates and with single-molecule resolution. In the next section we will present the optical switches that are available to date for the interrogation of mGlu receptors by means of light.

3 Optical tools for mGlu receptors: switches

A switch is by definition “a device for making and breaking the connection in an electric circuit” (google.com, accessed on 13 Sept 2015), for example the button next to the door of a room that is used to turn on a lamp from the distance. Applied to neuroscience, a switch would consist in the application of a remote signal (electricity, magnetic field, light) to activate a specific protein in a living cell. In this way, the protein of interest is ‘electrically or optically switched’ on or off by arbitrarily manipulating the remote signal. This generates a response in the protein that can be measured as a read-out thanks to a certain activity sensor (the probe).

For example, the application of a membrane potential to a portion of membrane where one single voltage-gated ion channel is present makes current flow through the channel with amplitude and kinetics that can be estimated with a patch-clamp amplifier. The electrical activation and inactivation of voltage-gated proteins at single-channel resolution has been extensively used to study their properties since the development of patch-clamp techniques for electrophysiology in the late 1970s.

Almost simultaneously, scientists started to develop switches for proteins that were based on light as the activation mechanism. This was first achieved through a chemical reaction that conjugated a light-sensitive ligand to a susceptible residue close to the binding-site of the receptor protein, so that the ligand could be optically delivered for the activation of the receptor (the PTL approach, detailed in **Section 3.2**, Bartels *et al.* 1971). Nowadays, the definition of optical switches has broadened to comprise all methods that use light to regulate remotely and non-invasively specific events in cells (Gorostiza and Isacoff 2008). As we already mentioned, light is fast and spatially precise, and by gaining optical control over proteins and neurons we gained insight into many biological processes that were unthinkable with the techniques available only a decade ago.

In the following section, we will review the optical switches currently available for the control of native or engineered mGlu receptors with light (recently reviewed by Reiner *et al.* 2015). They are classified based on the three possible strategies for generating optical switches for ion channels and receptor proteins, which are introduced in **Figure 20**.

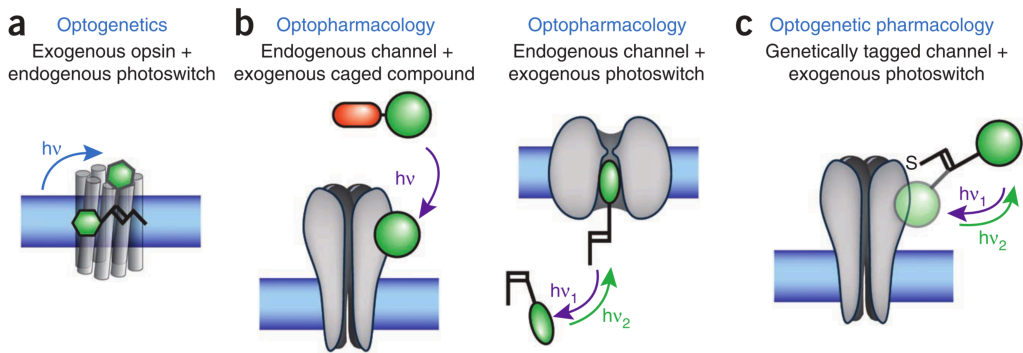


Figure 20 | Design strategies for optical switches.

(a) Optogenetics rely on genetic manipulation of neurons to introduce a gene encoding for an opsin and make them sensitive to light. (b) Optopharmacology uses light-sensitive pharmacological agents to activate native proteins by uncaging or reversibly photoswitching ligands. (c) Optogenetic pharmacology is a hybrid method that targets proteins with light-sensitive reactive compounds, which additionally conjugate to the protein thanks to a residue genetically modified to make the protein susceptible of modification. Reproduced from Kramer *et al.* 2013.

3.1 Optogenetics

One way to make mGlu receptors light sensitive is through optogenetics, which combines genetics with optics to create optical switches. This method dates back to 2005, when Boyden and colleagues (Boyden *et al.* 2005) genetically induced in neurons the expression of the recently discovered and naturally light-sensitive protein Channelrhodopsin-2 (ChR2) from *algae* (Nagel *et al.* 2003), and used it as an optical switch of neuronal firing with high spatiotemporal precision. Later on, this and other opsins were successfully expressed with cell-type specificity in mammals, and used to achieve optical control of specific behaviours in freely moving mammals (Adamantidis *et al.* 2007). In just a ten years time the field has seen a huge expansion, which proves how powerful and promising this technique is to decipher how the neuronal circuits are wired (Deisseroth 2015).

The creation of genetically encoded optical switches for GPCRs was pioneered in 2005 with the design of rhodopsin-GPCR chimaeras. These were initially tested *in vitro* (Kim *et al.* 2005b) and later used *in vivo* and called optoXRs (Airan *et al.* 2009). These engineered receptors were inspired at a naturally light-sensitive GPCR opsin called rhodopsin, which is a protein responsible for light-transduction during night vision in the vertebrate retina (Palczewski 2006). In these studies, the intracellular loops of rhodopsin

were replaced with those specific to adrenergic receptors, so that light induced the activation of the intracellular signaling pathways initiated by adrenergic ligands. The second of these studies theorized that this technology would allow unprecedented insights into the effects of space- and time-specific patterned activation of GPCRs, but in the practice this has not been investigated yet, despite the optogenetic toolbox for GPCRs has expanded in the last years (Masseck *et al.* 2014; Oh *et al.* 2010; Siuda *et al.* 2015; Spoida *et al.* 2014).

The only study applying optogenetics to mGlu receptors was a recent one by Van Wyk and colleagues (van Wyk *et al.* 2015). Here, the intracellular loops of an opsin were substituted by those of mGlu₆, to obtain the Opto-mGluR6 chimera, which upon illumination initiated the intracellular signaling downstream of mGlu₆. As already mentioned in **Section 1**, mGlu₆ is selectively expressed in the retina and is functionally implicated in the process of vision (Masu *et al.* 1995). The transgenic expression of this optical switch under the GRM6 promoter in blind animals successfully restored vision. Interestingly, these researchers used melanopsin instead of rhodopsin. Melanopsin is a blue light-sensitive GPCR expressed by a subpopulation of vertebrate retinal ganglion cells whose functions are not related to vision, such as regulation of pupillary reflex and circadian rhythms (Fu *et al.* 2005). This opsin is particularly attractive for therapeutic applications due to its naturally high sensitivity to light, which makes it compatible with normal daylight vision.

A related form of remote but non-optical switches that allow activating GPCRs with spatiotemporal precision is the RASSL/DREADD approach. Briefly, this consists in generating mutant GPCRs that are no more activated by their endogenous ligand, but only by synthetic ligands. These substances are added as inert ligands and are active only on the mutant receptors. This approach represents the only alternative method to engineer GPCRs and make them spatio-temporally controllable, but has not been applied to mGlu receptors yet and won't be further treated here (reviewed in Masseck *et al.* 2011).

Finally, another optogenetic strategy to induce intracellular signaling pathways normally initiated by GPCRs is to exploit the coupling of different non-rhodopsin opsins to different G proteins. By selecting the appropriate opsin and expressing it in cells, the researchers were able to induce with light in selected cells or regions of cells the specific second messenger (IP₃/DAG/Ca²⁺ or cAMP) with the desired spatiotemporal pattern dictated by light (Beiart *et al.* 2014; Karunaratne *et al.* 2013).

3.2 Optogenetic pharmacology

A hybrid method to create optical switches is the one called optogenetic pharmacology. In this approach, proteins are made light sensitive by two simultaneous conditions: first, and which we already mentioned in the introduction to **Section 3**, a reactive ligand is conjugated to the receptor protein through a light-sensitive linker (photoswitchable tethered ligand, PTL) whose length can be controlled with light; second, the PTL must be attached to the protein on an appropriate site, whereby the distance between the ligand and its binding pocket on the receptor is optimal for its light-dependent delivery.

In the work by Bartels and colleagues, this second condition was accomplished by conjugating the PTL to cysteines nearby the acetylcholine-binding site, which were known to form a disulfide bond and allow the tethering of fixed-length ligands for the permanent activation of the nicotinic acetylcholine receptor (nAChR; Karlin and Winnik 1968). Since such suitable cysteines were only known for the nAChR, in the following attempts of addressing receptor proteins with PTLs the receptors had to be mutated on one critical residue to insert an amino acid (usually a cysteine) susceptible for reaction with the PTL. Therefore expansion of this strategy to other receptor classes was delayed until receptor cloning and site-directed mutagenesis were made available. Due to the requirement of a receptor mutation for PTL conjugation, this method is considered a hybrid in that it uses both synthetic ligands and genetic engineering.

The first optical switch created by optogenetic pharmacology of an mGlu receptor was described two years ago by Levitz and colleagues and called LimGluR (from light-mGlu receptor, **Figure 21d**, Levitz *et al.* 2013). The originality of their work consisted in the identification of the residues on mGlu₂, mGlu₃ and mGlu₆ where an amino acid could be mutated to cysteine without altering the protein functionality plus allowing the reaction with analogs of a PTL, which had been described previously by the same group for light-engineering ionotropic glutamate receptor channels (LiGluRs, Volgraf *et al.* 2006). The PTL, called MAG, was composed by glutamate (G) plus a reactive group (maleimide, M) at the two ends of the molecule, linked by a moiety containing azobenzene (A).

Azobenzene consists of two phenyl rings linked by an N=N double bond (**Figure 21**). The molecule exists in a thermally stable *trans* configuration, which under illumination with violet light (380 nm) reversibly isomerizes to *cis*. This light-induced switch in configuration induces important changes in polarity (**Figure 21b**), geometry, end-to-end distance (**Figure 21a**) and absorption spectrum (**Figure 21c**). The reverse isomerization takes place either by thermal relaxation (Δ) or by illumination with visible light

wavelengths (> 400 nm). Importantly, azobenzenes are versatile photoswitches, since photoisomerization wavelengths and thermal relaxation rates can be customized by adding or changing substituents at the phenyl rings (reviewed in Beharry and Woolley 2011).

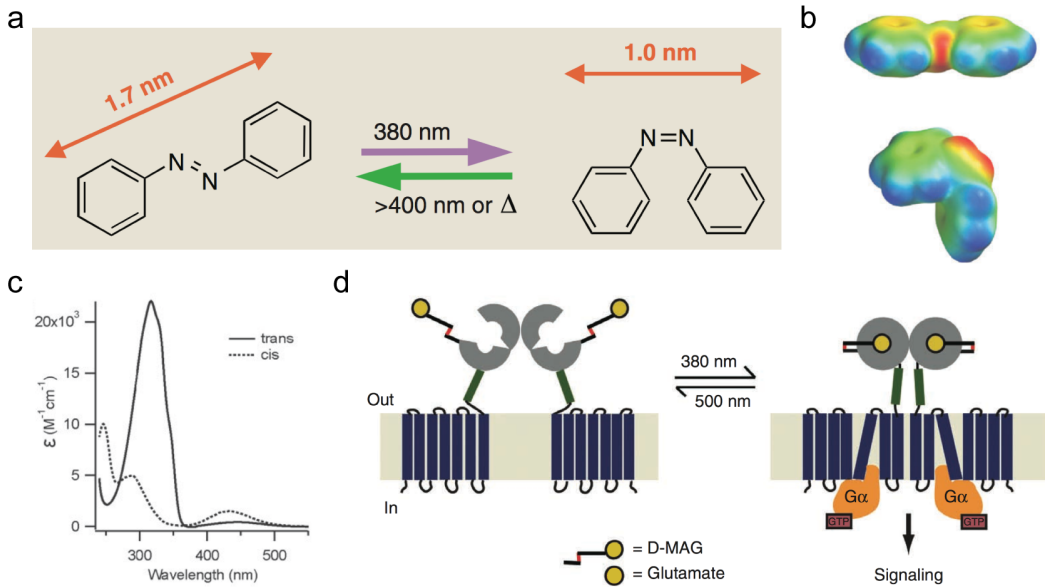


Figure 21 | Schematics of azobenzene light-sensitivity and optogenetic pharmacology for mGlu receptors.

(a) Azobenzene can reversibly photoisomerize between an extended and thermally stable *trans* configuration (left) to a bent *cis* configuration (right) following illumination with violet light (violet arrow, 380 nm). The *cis* to *trans* isomerization can happen spontaneously by thermal relaxation (Δ indicates thermal energy) or under illumination with visible light (green arrow). The *cis* isoform is shorter than the *trans* one by ~ 7 Å. (b) Spacefilling model of *trans* (top) and *cis* (bottom) azobenzene coloured by electrostatic potential (red to blue represents negative to positive). (c) Typical absorption spectra of the *trans* and *cis* isomers of azobenzene dissolved in ethanol. (d) Schematics of a LimGluR dimer conjugated with D-MAG at the VFT, with the azobenzene bond depicted in red. In the *trans* state (left) azobenzene maintains the glutamate inside D-MAG far away from its ligand-binding site. Illumination with 380-nm light induces the *cis* isomer, so that the glutamate inside MAG can bind to the clamshell and induce receptor activation and intracellular signaling. Adapted from (a) Gorostiza and Isacoff 2008, (b-c) Beharry and Woolley 2011 and (d) Levitz *et al.* 2013.

In the LimGluR, the reactive part of the PTL was conjugated to a mutated cysteine on the mGlu receptor, and this generated a local concentration of ligand that was particularly high at the receptor surface and at permitted positions based on the length of the PTL. In analogy with the strategy previously used with light-gated ionotropic glutamate receptors (LiGluR; Volgraf *et al.* 2006), the extent of light-induced changes in azobenzene length were sufficient to allow or hamper the accessibility of glutamate to

the VFT cleft of LimGluR. In this way, the intracellular signaling of the engineered mGluR was made optically switchable (**Figure 21d**).

This interesting approach offers an intrinsic spatially resolved system, where spatial resolution can be further enhanced by exciting the azobenzene-based photoswitch at two-photon with NIR light. Two-photon excitation of azobenzene-based optical switches was demonstrated only recently in our laboratory for a PTL conjugated to an ionotropic glutamate receptor (Izquierdo-Serra *et al.* 2014), and then demonstrated for LimGluRs by the Isacoff group (Carroll *et al.* 2015).

The study from Levitz and colleagues was the first one where the activation and the intracellular signaling of an mGlu receptor could be selectively activated with high temporal resolution. Thanks to coupling of LimGluR to ion channel effectors, the authors observed activation and inactivation kinetics of less than 1 ms, which demonstrated that mGlu receptors coupled to an optical switch enable signaling on a timescale relevant for synaptic transmission.

Unfortunately, the authors observed that light acting on LimGluR induced an incomplete agonism compared to the full activation obtained by applying glutamate. This is probably due to an incomplete tethering of the PTL on the full set of recombinant receptors expressed by the cell, or partial steric hindrance of the PTL with certain conformations assumed by the active receptor. These issues could be solved by more efficient labeling and/or attaching the PTL to residues enabling configurations compatible with full ligand binding and receptor activation.

3.3 Optopharmacology

The names optopharmacology or photopharmacology were proposed recently to distinguish synthetic chemical photoswitches from those obtained by genetic manipulation of proteins, i.e. by optogenetics or optogenetic pharmacology (Broichhagen *et al.* 2015; Kramer *et al.* 2013). Optopharmacology has been the first and for long time the only source of optical switches for neuronal receptors, such as the freely diffusible photolabile ligands (usually referred to as caged ligands) or photochromic ligands (PCLs, sometimes called 'reversibly caged ligands') that are widely used to regulate optically native receptors, and will be introduced in the following paragraphs. The most important feature of these optical switches is that since they are pharmacologically based there is no need for genetic manipulation, which makes them suitable for understanding the

functioning of receptor proteins, neurons and circuits in a fully physiological context. Although freely diffusible ligands lack the cell-type specificity provided by optogenetics or optogenetic pharmacology, it is possible to combine them with two-photon excitation in order to obtain a volume-defined optical control over the receptor.

Caged ligands

Caged ligands are chemical molecules where the ligand for a given receptor is trapped into a photolabile protecting group. Light is then used to uncage the molecule at the desired time or place, and the released active ligand is free to access its binding site on the receptor. The first caged ligand available for stimulation of glutamate receptors was glutamate itself (Callaway and Katz 1993). Despite its lack of selectivity (Ellis-Davies 2007) caged glutamate has been extensively used because its uncaging with two-photon light offered the spatial precision needed for activating single dendritic spines in brain slices (Matsuzaki *et al.* 2001; Nikolenko *et al.* 2007) and *in vivo* (Noguchi *et al.* 2011). Caged ligands with subtype-specificity for mGlu receptors became available only recently, such as NPEC-DHPG for group I mGlu receptors activation (Palma-Cerda *et al.* 2012), NPEC-LY379268 for group II (tocris.com), and NPEC-DCPG, which is selective for mGlu₈ activation (tocris.com). NPEC-ACPD is a wide-spectrum mGlu agonist, with decreasing affinity for groups II, I and III mGlu receptors (Palma-Cerda *et al.* 2012).

Despite the great spatial and temporal resolution offered by caged ligands in controlling neuronal receptors, researchers should beware of undesired off-target effects of both the caged compound (Fino *et al.* 2009; Fino and Yuste 2011) and the byproducts released after uncaging. Care should be taken in the pharmacological characterization of the inertness and safety of the caged compound, the cage, and the possible metabolites.

A last consideration regards the irreversibility of the uncaging process. When ligands are uncaged by two-photon, the amount of active molecule released is very limited, and its rapid diffusion in the extracellular solution will abruptly lower its concentration to negligible concentrations. Instead, when the photolysis of the cage is obtained with single photon light, uncaging is not spatially limited, and this has also temporal consequences on the activation of the receptor. Uncaging in the whole illumination field could gradually increase the concentration of active molecule in solution, possibly to levels exceeding the threshold for receptor activation, and thus inducing receptor activity in the absence of photolysis.

Photochromic ligands (PCLs)

PCLs are freely diffusible ligands linked to a light-sensitive moiety, typically azobenzene. The ligands can be orthosteric agonists and antagonists, or allosteric modulators, or other chemicals such as pore blockers. Light regulates their affinity for the receptor protein through physical changes in the attached azobenzene, e.g. by steric clash between ligand and receptor or incompatibility with activating conformations. Given the reversible nature of the photoisomerization of azobenzenes, photoswitchable ligands offer a better temporal control over the receptor than caged ligands, whose uncaging is irreversible. Moreover, photoisomerization might be regarded as a 'clean' reversible process that does not generate byproducts with unknown effect on the cellular environment. However, it is challenging to estimate the actual fraction of photoconverted PCLs, as well as to characterize the extent of PCL binding and receptor activation when the PCL is in either configuration. In addition, as for every pharmacological ligand, off-target proteins could also be activated or inhibited by the PCL.

To date, three PCLs are available for the light-control of mGlu receptors. The first, which consisted in a molecule of glutamate linked to an azobenzene, was developed in 2007 by the group of Isacoff and called GluAzo (Volgraf *et al.* 2007). This photoswitchable glutamate derivative was shown to modulate its affinity for kainate receptors in a light-dependent way, but its use to reversibly control with light mGlu receptors has not been reported. However, the applications of GluAzo are limited by its partial selectivity being an orthosteric ligand. The other two PCLs are allosteric modulators selective for mGlu₄ and mGlu₅ that we developed and characterized in collaboration with the research group in Medicinal Chemistry of Dr. Amadeu Llebaria at the IQAC-CSIC, Barcelona, and will be presented respectively in **Chapters 1** and **2** of this experimental thesis.

Optopharmacological strategies for other neuronal receptors, pores, and ion channels so far

In this section we will briefly present the optopharmacological design strategies used to gain optical control on pore blockers, as well as orthosteric or allosteric ligands of both ionotropic and metabotropic neuronal receptors other than mGlu.

Caged ligands or irreversibly binding

Irreversibly caged agonists other than glutamate are commercially available for other neurotransmitter receptors, such as GABAergic, dopaminergic, noradrenergic, cholinergic, serotonergic, and purinergic receptors (tocris.com). Caged opioids are also available. One must remember that orthosteric agonists target both ionotropic and metabotropic receptors for a given neurotransmitter. Caged agonists with better selectivity were developed to differentially target the three main classes of ionotropic glutamate receptors, that is AMPA, NMDA and kainate receptors (reviewed in Reiner *et al.* 2015).

A special class of optopharmacological tool is the photoreactive AMPA antagonist ANQX. This molecule binds to surface AMPA receptors, and then light can be used to permanently conjugate the antagonist to the receptors, so that the receptor is irreversibly silenced (Adesnik *et al.* 2005). This strategy was adopted for the monitoring in real-time of the lateral trafficking of native receptors, but the temporal control over the receptors is lost after the photoreaction has taken place, similarly to what happens with caged agonists.

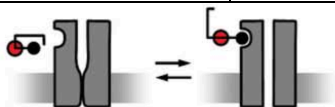
PCLs

Previously in this section we presented GluAzo, a PCL of kainate receptors containing azobenzene. The design of optical switches might be based on a light-sensitive moiety different from azobenzene, such as spiropyrans or stilbenes (extensively reviewed in Szymański *et al.* 2013). In this section we will only review the PCLs containing azobenzene, which is the molecule adopted in this thesis to create optical switches for mGlu receptors.

We can classify PCLs for neuronal proteins in three main classes, depending on the type of ligand they bear: orthosteric agonists or antagonists, allosteric modulators of receptor proteins, and pore blockers. The structures and design strategies of these compounds are summarized in **Table 6**.

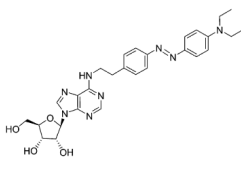
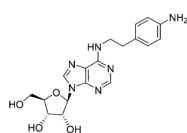
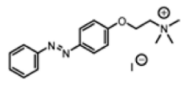
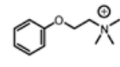
Table 6 | Optopharmacological tools for reversible control over neuronal proteins.

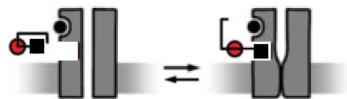
Photochromic ligand (PCL)	Parent compound	Target protein	Design strategy	Ref:
---------------------------	-----------------	----------------	-----------------	------



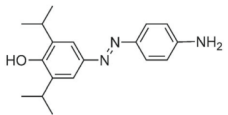
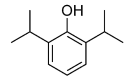
Orthosteric agonists/antagonists

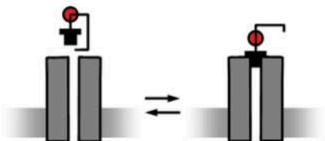
<p>BisQ</p>	<p>benzyltrimethyl ammonium</p>	nAChR	Phenyl ring available at one end	Bartels <i>et al.</i> 1971
<p>GluAzo</p>	<p>LY339434 (glu analog)</p>	GluK1/2	Substituted phenyl ring available at one end	Volgraf <i>et al.</i> 2007
<p>ATA-1</p>	<p>BnTetAMPA (AMPA analog)</p>	AMPA	Phenyl ring available at one end	Stawski <i>et al.</i> 2012
<p>azo-capsazepin</p>	<p>Capsazepin (antag.)</p>	TRPV1	Substituted phenyl ring available at one end	Stein <i>et al.</i> 2013
<p>photofentanyl-2</p>	<p>Fentanyl (agonist)</p>	μ OR	Phenyl rings available at two ends	Schonberger <i>et al.</i> 2014

MRS5543 	APNEA (non selective agonist) 	A _{2A} /A ₃	Substituted phenyl ring available at one end	Bahamonde <i>et al.</i> 2014
AzoCholine 	Phenylcholine ether (agonist) 	nAChR α7 (neuronal)	Phenyl ring available at one end	Damijonaitis <i>et al.</i> 2015

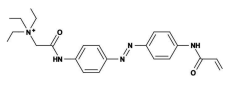
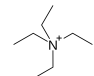
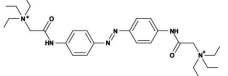
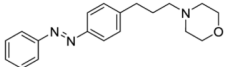
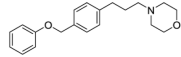


Allosteric modulators

azopropofol 	Propofol (*allosteric) 	GABA _A	Substituted phenyl ring available	Stein <i>et al.</i> 2012
--	--	-------------------	-----------------------------------	--------------------------



Pore blockers

AAQ 	Tetraethylamm onium (TEA) 	K _v	Attachment of azobenzene through an amide linker	Banghart <i>et al.</i> 2009
QAQ 		Na _v /K _v /Ca _v		
fotocaine 	fomocaine 	Na/K/Ca _v	'Azologization'	Schönberger <i>et al.</i> 2014

Chemical structures are from indicated references or from google images. Insets illustrating the functioning of the PCL strategy for light-control of orthosteric/allosteric ligands and pore blockers are adapted from Gorostiza and Isacoff (2007).

Orthosteric PCLs

Azobenzene can be attached to one end of orthosteric agonists or antagonists so that the changes in configuration occurring into azobenzene during photoisomerization are hopefully reflected in a changed affinity of the orthosteric ligand for its receptor protein. This was first done with the already mentioned GluAzo (Volgraf *et al.* 2007), and before that with the orthosteric cholinergic BisQ (Bartels *et al.* 1971). Later it was also demonstrated for the AMPA agonists ATAs (Stawski *et al.* 2012), the TRPV1 antagonist azo-capsazepin (Stein *et al.* 2013), the μ -opioid receptor agonist photofentanyl (Schönberger and Trauner 2014), the partial agonist/antagonist of A_{2A}/A_3 receptors MRS5543 (Bahamonde *et al.* 2014), and the nAChR α_7 agonist AzoCholine (Damijonaitis *et al.* 2015).

Notably, photofentanyl (PF) was the first azobenzene-based PCL targeting a GPCR (**Figure 22**). M-opioid receptors (μ ORs) are class A GPCRs that play important roles in pain and are the major target of morphine. Unlike the mGlu-like class G GPCRs, they lack the extracellular VFT domain, so that opioids bind directly to the TMD of μ ORs. Schönberger and colleagues created the optical switch photofentanyl by attaching azobenzene to a parent μ OR agonist called fentanyl. The agonist fentanyl was preferred to derivatives of morphine because of his simpler structure and the presence of two phenyl rings that could be used as starting points for easily attaching azobenzene to either end of the molecule. Only one of the two resulting molecules, PF-2, was functional *in vitro* in cells transfected with the μ OR and a reporter channel, suggesting a 'functional polarity' in the ligand that was or was not permissive for chemical modifications.

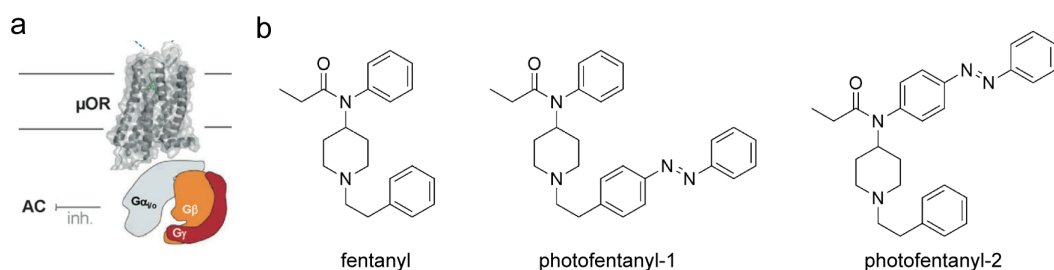


Figure 22 | Design strategy of photofentanyl, a photoswitchable agonist of μ -opioid receptors.

(a) Ribbon representation of the class A GPCR μ opioid receptor (μ OR) and cartoon of the coupled G protein. The agonist fentanyl bound to the orthosteric binding pocket of the μ OR is outlined in green. (b) Chemical structure of fentanyl, the precursor μ OR agonist, and its azo-derivatives photofentanyl 1 and 2. The two phenyl rings of the parent compound were used as scaffolds for the lateral addition of azobenzene. From fentanyl the authors derived photofentanyl 1 and 2, but only PF1 was found to be active as a μ OR agonist in its *trans* configuration, and inactive in the *cis* one. Adapted from Schönberger *et al.* 2014.

A similar design strategy was adopted for the synthesis of all the other PCLs mentioned, whereby an active ligand for the desired receptor is identified on the basis of a phenyl ring available at one end of his structure for the easy insertion of azobenzene.

Allosteric PCLs

The same successful strategy was applied to generate an optically switchable propofol (Stein *et al.* 2012; Yue *et al.* 2012). Propofol is a small molecule used in the clinics as a general anaesthetic, and although the mechanism by which it potentiates ionotropic GABA_A receptors currents has not been elucidated, it is considered to act allosterically. Using the only phenyl ring of propofol, Stein and colleagues generated the azo-propofol, an azobenzene compound that potentiates the ligand-gated ion channel GABA_A in the *trans* configuration, and becomes inactive upon violet light illumination. This compound was shown to induce light-dependent anesthesia in *Xenopus laevis* tadpoles. To our knowledge, this is the only study describing a reversibly caged allosteric modulator of an ionotropic receptor.

Pore blocker PCLs

Several light-sensitive pore blockers of voltage-gated ion channels were obtained by attaching azobenzene in different ways to a tetraethylammonium (TEA) molecule, which blocks the pore of K⁺ channels from the inside. Many variations of this optical switch have been described by the groups of Richard Kramer and Dirk Trauner, and are reviewed in Kramer *et al.* 2013. All these works used a similar approach whereby azobenzene or substituted azobenzenes were appended at one side of the molecule through a short amide linker, allowing TEA to be exposed at the other end for interaction with the pore (AAQ, BENAQ, PhENAQ, DENAQ; Banghart *et al.* 2009; Mourot *et al.* 2011). An interesting variation to this scheme is the symmetric addition of TEA at both ends of a central azobenzene (QAQ; Banghart *et al.* 2009). Due to their ability to enter cells through TRPV1 and P2X channels and their versatility as pore blockers of many channels (K⁺, Na⁺, Ca²⁺), they have found application in a number of interesting fields, of which two particularly interesting are the optical control of nociception (Mourot *et al.* 2012) and the photosensibilization of degenerated retinas in animal models of blindness (Polosukhina *et al.* 2012). However, since they are not really selective for one particular type of ion channel, they are not relevant to the experimental work presented in this thesis and won't be discussed further.

Recently, another strategy was adopted to create a light-sensitive pore blocker from a molecule of fomocaine, a local anesthetic introduced in the 1960s. Schönberger and colleagues found that the structure of fomocaine contained a benzyl-phenyl ether moiety, structurally similar to azobenzene. Replacement of this moiety by azobenzene afforded an azobenzene-analog of fomocaine, which they named ‘fotocaine’ (**Figure 23b**). Additionally, they identified many scaffolds that resemble azobenzene (listed in **Figure 23a**) and seem good targets for generating azobenzene-analogues (azologues) from existing drugs, a strategy which they called ‘azologization’. The azologization of fomocaine resulted in an active pore blocker that provided light control over action potential firing in cultured hippocampal neurons (Schönberger *et al.* 2014).

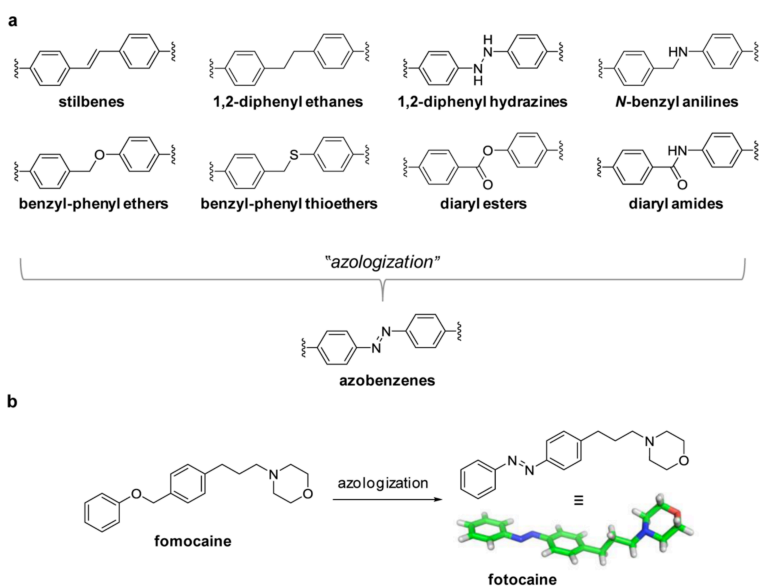


Figure 23 | Principle of ‘azologization’ and the example of fotocaine.

(a) List of ‘azologizable’ chemical scaffolds, consisting of two phenyl rings separated by a linker of length two atoms. (b) Example of azologization of the local anesthetic fomocaine into fotocaine by substitution of a benzyl-phenyl ether for an azobenzene. Reproduced from Schönberger *et al.* 2014.

The rationale behind this successful approach is that azologization of an active compound should preserve the pharmacological properties of the parent compound into the ‘azologue’, given the initial structure is sufficiently similar to azobenzene. To generalize, this should be possible with all drugs presenting two phenyl rings linked at a distance of two carbon (or substituted) atoms. In turn, light should isomerize the azo-

logue to the cis configuration, acting as a switch that disrupts the similarity between the azologue and the parent compound.

A survey of databases revealed that many drugs contain one or more of the moieties susceptible of azologization indicated in **Figure 23** (Schönberger *et al.* 2014). Hopefully many optical switches for the control of neuronal proteins will become available with little effort in the next future.

3.4 Future challenges

We presented here an array of optical switches for the control of mGlu receptors with light. Strategies requiring genetic manipulation such as optogenetics and optogenetic pharmacology offer the unique advantage of being targetable to defined cell types and even subcellular compartments. This is done by selecting the promoter under which they are to be expressed and eventually the targeting sequences encoded in the cloned DNA. On the other hand, creating transgenic animals or delivering DNA by infection with viral vectors for any research problem raises practical and ethical questions. At the cellular level, overexpression of proteins causes physiological distortions in neurons, especially at synaptic compartments (Miyashita *et al.* 2013) and give rise to compensatory mechanisms that may further alter the system under study. While there are several viral vectors that are considered safe for therapeutic use and are under clinical trials, less is known about immune reactions against overexpressed opsins, which are largely of microbial origin. In the perspective of therapies based on the optical targeting of dysfunctional mGlu receptors, these irreversible genetically based-approaches require extensive trials before translation into clinics.

The elective strategy for more physiological applications in research and safe clinical trials has ever been the pharmacological approach. However, at the system level the delivery of drugs with conventional pharmacology follows temporal paradigms that are not in accordance with emerging concepts of pulsatile or patterned activation of receptors. As for localized therapeutic effects, the spatial precision of classical pharmacology is limited to the lipophilicity of the drug and the targeted delivery with chemical strategies. At the cellular and subcellular level, the spatial component becomes even more important, as demonstrated by some studies introduced in **Section 1**

showing differential effects of the same drug on different cell-types or subcellular compartments.

Optopharmacology takes advantage of the selectivity of pharmacological ligands for their receptors, and implements their specificity with the precision provided by light for switching on and off reversibly their activity in a space- and time-defined way. Optopharmacology can overcome the limitations of conventional pharmacology in studying neuronal receptors in physiology and disease, although parallel advances in stimulation and recording of neuronal proteins activity at higher spatiotemporal resolution and *in vivo* will be necessary.

OBJECTIVES

Despite the relevance of mGlu receptors to neuronal and astroglial communication, as well as their implication in the basic processes of neurotransmission and synaptic plasticity, the mechanisms that govern their functioning are still partially understood.

Advances in optical imaging at high resolution and sensitivity allowed the implementation of optical techniques to probe by means of light many features of mGlu receptors activation and signaling at increasing spatiotemporal precisions. Thanks to these techniques, it is now emerging that mGlu receptors follow activation mechanisms different from those initially imagined for GPCRs. Still, it is not clear what their exact kinetics are, or the functional consequences of temporal and spatial patterns of mGlu activity, and this is probably due to the scarcity of tools for activating mGlu receptors with spatiotemporal precision. Observing mGlu activity elicited by a poorly defined stimulation can be compared to listening to an answer without knowing what the question was. The current spatiotemporal precision of optical sensors (the listeners) can only be fully exploited by using optical switches (the inquirers) matching their performance.

In this thesis we aimed at **expanding the toolbox of optical switches for mGlu receptors**, with particular interest in respecting the physiological context of their activation. For that purpose, we discarded approaches based on genetic engineering of receptors, as well as on the irreversible uncaging of compounds. We preferred the use of optopharmacology, and specifically applied it to allosteric modulators, which have displayed higher selectivity and more physiological activation than orthosteric ligands. This objective involved technical challenges due to the structural restrictions of mGlu allosteric binding pockets, but at the same time offered potentially high gains to spatiotemporally control these receptors both in therapeutic and basic research applications.

Therefore, we set the following main objectives of this thesis:

1. To develop the first light-regulated allosteric modulators targeting metabotropic glutamate receptors. The molecular design, *in vitro* and *in vivo* characterization of alloswitch-1 and G4optoNAM is presented in **Chapters 1 and 2**.
2. To expand the knowledge about this new class of compounds by synthesizing and characterizing a library of compounds derived from substitutions in alloswitch-1. The inferred data about structure-activity relationship and optimal optopharmacological characteristics for allosteric photoswitches of mGlu receptors are shown in **Chapter 3**.
3. To demonstrate the functional photoisomerization of alloswitch-1 by using two-photon stimulation, with the aim of exploring the resolution limits of reversible optical switches (**Chapter 4**).

MATERIALS & METHODS

1 Photochemistry of optical switches

We characterized the photochemical properties of the compounds mainly using UV-visible spectroscopy.

Absorption spectra

Alloswitch-1

Absorption spectra of 25 μM alloswitch-1 in DMSO in dark or after illumination were obtained with a Helios Gamma UV-Vis spectrophotometer (Thermo Scientific) scanning at 1 nm intervals. The effect of repeated 390 and 490 nm light cycles over absorbance of 25 μM alloswitch-1 in DMSO was evaluated by measuring absorbance at 360 nm after illuminating for 3 min at wavelengths indicated in figure. In all cases, *trans*-to-*cis* isomerization (or *vice versa*) was achieved by illuminating specimens placed in 10 mm Quartz Suprasil cells (Hellma Analytics) with a Polychrome V light source (Till Photonics) set to a potency of 100% and bandwidth of 15 nm, and coupled to an optic fiber placed at a distance of 5 cm from the specimen.

G4optoNAM

Absorption spectra of 50 μM G4optoNAM in DMSO were recorded on a Varian Cary 300 UV-Vis spectrophotometer (Agilent Technologies) using a 0.01 cm path-length quartz cuvette, scanning between 550 nm and 300 nm with an average time of 33 ms at 5-nm intervals for full absorption spectra. Photoisomerization was obtained by irradiating G4optoNAM with a 430 nm-LED array (FCTecnics) for 3 min or 630 nm-LED (Photo Activation Universal Light, Geniul) for 1 min.

Kinetics of *cis*-to-*trans* relaxation

Alloswitch-1

The relaxation plot of 25 μM alloswitch-1 in either DMSO or aqueous solution (1% DMSO in a solution containing, in mM: 140 NaCl, 5.4 KCl, 1 MgCl_2 , 10 HEPES, 10 glucose and 2 CaCl_2 , pH adjusted to 7.40 with NaOH) was built from absorbance readings at 360 nm collected with a Helios Gamma UV-Vis spectrophotometer (Thermo Scientific) every 2 s versus time. The time constant of alloswitch-1 relaxation (half-life, $t_{1/2}$) was calculated by fitting the collected data with an exponential decay function using IgorPro (WaveMetrics). Illumination for *trans*-to-*cis* photoisomerization lasted 7 min, and was done in a quartz cuvette and with a monochromator light source as already explained in the previous section for acquisition of absorption spectra of alloswitch-1.

G4optoNAM

The fast relaxation kinetics of 50 μM G4optoNAM in PBS/DMSO 98:2 were evaluated using a ns laser flash-photolysis system (LKII, Applied Photophysics) equipped with a Nd:YAG laser (Brilliant, Quantel) as pump source ($\lambda_{\text{exc}} = 355 \text{ nm}$), a Xe lamp as probe source and a photomultiplier tube (Hamamatsu) coupled to a spectrograph as detector. Data were fit with a monoexponential function with Prism (GraphPad).

2 Optopharmacology with IP-One HTRF assay

We characterized the pharmacological properties with a high-throughput assay that was set up by the company CisBio Bioassays in collaboration with the laboratory of Jean-Philippe Pin (IGF, Montpellier, France). The principle of the technique is detailed in **Figure 19**.

All experiments were done in HEK 293 cells, cultured and transfected by electroporation as previously described for expression of rat metabotropic glutamate receptors (Brabet *et al.* 1998).

2.1 Cell culture and electroporation

Briefly, cells were maintained in 15-cm Petri dishes in Dulbecco's Modified Eagle Medium (DMEM, Life Technologies) with 10% Fetal Bovine Serum (FBS, Life Technologies) and 1% antibiotics (Penicillin/Streptomycin, Sigma-Aldrich), at 37 °C and in 5% CO₂ humidified atmosphere in the cell incubator.

For transfection, the cells were trypsinized and suspended at 10⁷ cells/ml in the electroporation buffer. Note that a correction factor was applied for resuspending cells, which consisted in subtracting 1/3 of the resuspension volume to account for the volume occupied by cells. The cells were then mixed with the appropriate amounts of cDNAs and 1 M MgSO₄ again in electroporation buffer, and electroporated with a GenePulser Xcell electroporator (Bio-Rad). Transfected cells were seeded in black clear-bottom 96-well plates pre-treated with poly-L-Ornithine (30 min at 37 °C) at a concentration of 1.5·10⁵ cells/well. At least 6 hours later, the medium was changed to glutamate-free DMEM GlutaMAX-I.

A chimeric G_{i/q}-protein was co-transfected for the mGlu receptors that are not naturally linked to the phospholipase C (PLC) signaling pathway (all except mGlu_{1/5}) to couple receptor activation to the PLC pathway and to obtain inositol phosphates (IP) production. To maintain ambient glutamate at minimal concentrations, the excitatory amino-acid transporter 1 (EAAC1) was co-transfected for all mGlu receptors. All receptors contained an HA tag in N-terminal to monitor their cell surface expression by ELISA.

2.2 IP-One HTRF assay

The day after transfection, IP accumulation was estimated using the IP-One HTRF assay kit (CisBio Bioassays, France) according to the manufacturer's instructions. Cells were stimulated to induce IP₁ accumulation during 30 minutes, at 37°C and 5% CO₂, in a lithium-containing buffer, where the agonists and test compounds were solubilized at concentrations indicated in figures. For testing simultaneously dark and illumination conditions, 96-well plates were placed over a rectangular LED array (FCTecnics) at a distance between 3 and 4 cm and continuously illuminated; one half of the 96-well plate bottom was covered with aluminum foil for the dark condition.

After 30 minutes, cells were lysed in a lysis buffer. For experiments under continuous illumination, cells were washed once in stimulation buffer alone after the 30 min stimulation, before continuing with the lysis step of the assay protocol. This was done in

order to avoid artifacts derived from the fast relaxation of the *cis* isomers in aqueous solution. Cell lysates were mixed with IP₁-d2 ($\lambda_{em} = 665$ nm) and anti- IP₁ -cryptate antibody ($\lambda_{em} = 620$ nm) and incubated during 2 hours at RT, and after this transferred to a black opaque-bottom 96-well plate for fluorescence readings.

Time-resolved FRET fluorescence readings were obtained with a RUBYstar HTRF HTS microplate reader (BMG Labtech) with a delay time of 150 μ s between donor excitation and fluorescence readings, as FRET ratio (Ratio 665/620). Efficient FRET occurs when IP₁-d2 is bound to anti-IP₁-cryptate, and gives high FRET ratio. Stimulation of mGlu receptors with increasing agonist concentrations results in the production of increasing amounts of endogenous IP₁, which competes with labeled IP₁-d2 for FRET, and FRET ratio progressively decreases. High FRET ratios indicate low levels of mGlu receptor activation.

For comparison among different experimental days, FRET ratios were normalized against maximum and minimum FRET measured, to obtain the 0 and 100% receptor activation, respectively. All points were realized in duplicate or triplicate. Data were analyzed using the Prism software (GraphPad). Dose-response data from IP accumulation assays in dark or illuminated cells were normalized by the dose-response to agonist or a reference allosteric modulator in dark conditions, and then fitted with a standard Hill equation using Prism.

2.3 Subtype-selectivity experiments with Alloswitch-1

For determining the selectivity of alloswitch-1 across the eight members of the mGlu receptors family, we transfected the cells as previously described with the individual receptors. A high concentration of the compound (5 μ M, 200-fold compared to its potency over mGlu₅) was tested for its ability to either potentiate or inhibit the activation of any of the mGlu receptors by an orthosteric agonist, in both dark conditions and under violet light illumination. Illumination conditions were as described in the previous paragraph (**Section 2.2**). To investigate a possible allosteric potentiation (that is, if alloswitch-1 exerted a PAM effect over an mGlu receptor), we measured the activation of the receptors in the presence of both low and saturating concentrations of agonist (which were used as reference values for normalization). If the compound were a PAM of a given receptor, it would increase the activation observed at low agonist concentration. To determine allosteric inhibition instead (that is, if alloswitch-1 exerted a NAM effect over an mGlu), we measured the response of the receptors to high agonist

concentrations in both the presence and absence of a competitive antagonist (values used for normalization). If the compound were a NAM at a given receptor, it would inhibit its orthosteric activation in a way similar to the competitive antagonist. Low, high, and saturating concentrations of agonists, as well as antagonist concentration used for experiments are listed in **Table 7**.

Data were normalized either by the response to low and saturating concentrations of agonists for allosteric receptor activation, or by the absence or presence of antagonist for allosteric receptor inhibition. The compound was considered inactive at a given receptor when it induced less than 50% of activation or inactivation.

Table 7 | Concentrations of agonists and antagonist used in selectivity experiments.

Compounds and relative concentrations used for monitoring the selectivity of 5 μ M alloswitch-1 across the mGlu receptors subfamily in transiently transfected HEK 293 cells with the IP-One HTRF assay.

	Agonist			Antagonist
	Low	High	Saturating	
Receptor				
Group I				
	Quisqualate			
mGlu ₁	20 nM	2 μ M	200 μ M	
mGlu ₅	0.5 nM	100 nM	5 μ M	
Group II				
	LY354740			
mGlu ₂	0.5 nM	100 nM	5 μ M	LY341495
mGlu ₃ *	2 nM	200 nM	20 μ M	100 μ M
Group III				
	L-AP4			
mGlu ₄	5 nM	500 nM	50 μ M	
mGlu ₆	100 nM	10 μ M	1 mM	
mGlu ₇	5 μ M	500 μ M	10 mM	
mGlu ₈	10 nM	1 μ M	100 μ M	

* An additional 100 nM LY341495 was added to counteract the high constitutive activity of mGlu₃.

3 Single-cell calcium imaging at single photon stimulation

3.1 Cell culture and plasmid transfection

We maintained HEK tsA201 cells in Dulbecco's Modified Eagle Medium: Nutrient Mixture F-12 (DMEM/F12, 1:1, Life Technologies) with 10% Fetal Bovine Serum (FBS, Life Technologies) and 1% antibiotics (Penicillin/Streptomycin, Sigma-Aldrich), at 37 °C and in 5% CO₂ humidified atmosphere in the cell incubator. We used X-treme GENE 9 DNA Transfection Reagent (Roche Applied Science) to induce transient expression of the cDNAs. Following manufacturer's instructions, 1 µg cDNA and 3 µl X-treme GENE 9 were mixed in a volume of 100 µl in culture medium devoid of FBS and P/S, and incubated during 20 minutes at RT. After this, 10⁶ cells were resuspended in 2 ml of complete culture medium and plated in a 6-multiwell plate together with the transfection mix. One or two days after, we harvested the cells with accutase (Sigma-Aldrich) and seeded them onto 15-mm borosilicate glass coverslips (Fisher Scientific) pre-treated with Poly-L-Lysine (Sigma-Aldrich) to allow cell adhesion, at concentrations suitable for obtaining pre-confluent cultures on the days of experiments. We performed calcium imaging experiments on pre-confluent cultures at 2 to 3 days after transfection.

Transient transfection of mGlu₅

For testing alloswitch-1 and its derivatives or any mGlu₅ ligand we transfected the cells with rat mGlu₅-SNAP, which was a gift from prof. Francisco Ciruela (UB).

Transient transfection of mGlu₄

For coupling of mGlu₄ to the intracellular Ca²⁺ signaling pathway, we induced co-expression of the rat mGlu₄ and the chimeric G_{i/q}-protein in a proportion of 2:1 (the total amount of cDNA was kept to 1 µg).

3.2 Neonatal rat cortical astrocyte cultures

Procedures were conducted in accordance with the European guidelines for animal care and use in research, and were approved by the Animal Experimentation Ethics Committee at the University of Barcelona (Spain). Sprague-Dawley rat pups (1 to 4 day

old) were decapitated and their neo-cortices removed in ice-cold phosphate buffered saline (PBS, Life Technologies) containing 0.3% bovine serum albumine (BSA, Sigma-Aldrich) and 0.6% glucose. Tissue was dissociated by proteolysis (5 min at 37 °C in trypsin-EDTA with DNase I from bovine pancreas, Sigma-Aldrich) and mechanical disaggregation with pipette tips, and centrifuged at 1500 rpm for 10 min. Pellets were resuspended in astrocyte medium (DMEM with GlutaMAX, high glucose and pyruvate from Life Technologies, supplemented with 15% heat-inactivated FBS and 1% penicillin/streptomycin), filtered and plated in cell culture flasks. Medium was changed the day after dissection and every 4 days. Once at confluence (7 to 9 days-in-vitro, DIV), the cells were subcultured by overnight shaking and trypsinization (Trypsin-EDTA), and seeded onto Poly-D-Lysine (Sigma-Aldrich) coated coverslips. Maturation and mGlu₅ expression were induced by addition of G-5 supplement (Life Technologies) at DIV 9-11. Astrocytes were used for experiments from DIV 11 on.

3.3 Pre-incubation of G4optoNAM and derivatives

For pre-incubation experiments, we pre-treated the cells with 30 μM of either compound in bath solution (see below) containing 2% DMSO, in the cell incubator. After 10-30 minutes we removed the compound, and rinsed the cells with fresh solution containing 2% DMSO for three times, and three times more with fresh solution without DMSO. After that, cells were loaded with the calcium indicator as described below, and then rinsed three more times.

3.4 Ca²⁺ indicator loading and bath solution

We loaded the cells with the calcium indicator Fura-2 AM (10 μM, Life Technologies) in Ca²⁺-free bath solution and 1% DMSO for 30 minutes in the incubator (37 °C and 5% CO₂), and rinsed with fresh solution. We used a ratiometric indicator in order to avoid artifacts due to fluorescence bleaching during the illumination intervals needed for the photoisomerization. The composition of the bath solution was as follows (in mM): 140 NaCl, 5.4 KCl, 1 MgCl₂, 10 HEPES, 10 glucose and 2 CaCl₂; pH was adjusted to 7.40 with NaOH.

3.5 Single-cell calcium imaging

Coverslips were mounted on an imaging chamber (Open Diamond Bath Imaging Chamber for Round Coverslips, or Fast Exchange Open Diamond Bath for fast washout experiments, both from Warner Instruments). The imaging chamber filled with 940 μ l bath solution, or 1 ml for experiments in which the perfusion system was used; perfusion was not used unless otherwise indicated in the figure notes.

Cells were then placed on an inverted fully-motorized digital microscope (iMic 2000, Till Photonics) controlled with the Live Acquisition 2.1 software (Till Photonics). Fura-2 was excited at 340 and 380 nm using a Polychrome V light source (Till Photonics) and a 505 nm dichroic beam splitter (Chroma Technology). Emission at 510 nm for both channels (F_{340} and F_{380}) was filtered by a D535/40nm emission filter (Chroma Technology) and finally collected by a cooled CCD camera (Interline Transfer IMAGO QE, Till Photonics). Images were acquired at room temperature with a UV Apochromat 40 \times oil objective lens (Olympus), with an exposure time of 10 ms and at a 0.5 Hz frame rate. The fluorescence ratio (F_{340}/F_{380}) for each cell profile was automatically calculated and stored by the Arivis software (LA Arivis Browser 1.6, Arivis).

3.6 Photoisomerization of compounds

To photoisomerize the compounds during image acquisition, we used the same light source as for the excitation of the calcium dye. We illuminated the cells in the field of view with discontinuous light flashes of a given wavelength, with duration < 1.5 s and periodicity of 2 s. This protocol resulted in one illumination step intercalated between two pairs of Fura-2 images, and it was repeated in loop for the total duration of the illumination period with that given light wavelength. These illumination periods lasted 1.7 min for G4optoNAM, 5 min for alloswitch-1 derivatives, 6.7 min for alloswitch-1, unless otherwise indicated in the text or figures. Duration, frequency, and intervals between light patterns were the same for all light wavelengths tested within the same experiment.

Alloswitch-1

For *trans*-to-*cis* and *cis*-to-*trans* isomerization we used light flashes of violet (390 nm, 1 s duration) and green (490 nm, 0.1 s duration) light, respectively. The light periods lasted 6.7 min for all experiments shown, except for experiments with Fenobam (5 min), and for

experiments where alloswitch-1 was added under violet light (13.7 min). For experiments in astrocytes, light periods lasted between 3.5 and 5 min, as indicated in figures.

Alloswitch-1 derivatives

We illuminated the cells with light flashes of 0.5 s duration (0.1 s was used only for 500 nm light), during a period that lasted in total 5 minutes (3.3 for compound **2**). Starting at minute 13.3, the cells received illumination with 6 different light wavelengths (eight in the case of compound **6**), organized in eight consecutive light periods (ten for compound **6**). For compound **2** the order of light wavelengths applied was 360, 370, 380, 390, 400, 500, 380, 500, 380 nm. For all other compounds tested, the first four light periods were 380 nm the first and third, and 500 nm the second and fourth. The rest of light periods were, in order, as follows: 370, 390, 400, 410 nm for compounds **1a** to **1l**, **3a** and **5**; 390, 400, 410, 430 nm for compound **3c**; 370, 390, 400, 410, 430, 450 nm for compound **6**. In one experiment with compound **3a** the 370 nm light period was missing. In one experiment with compound **6** the trial finished before the two last light periods.

G4optoNAM and derivative

To photoisomerize G4optoNAM we illuminated the cells with flashes of 430-nm blue light, of 1.5 s duration, and with a period of 2 s for a total duration of 1.7 minutes.

3.7 Addition of compounds during imaging

Experiments with alloswitch-1 and derivatives

Agonists and compounds (1 μ M, or otherwise indicated) were added during image acquisition into the accessory pool of the imaging chamber, by pipetting 30 μ l of an initial 1:30 dilution of the compounds, for a final dilution of approximately 1:1000 (final amount of DMSO was 0.1%). A thorough pipetting assured a good mixing of the solutions.

The agonist used to stimulate mGlu₅ in HEK tsA201 cells was quisqualate (3 μ M, Sigma-Aldrich), and for astrocytes preparations the mGlu_{1/5}-selective agonist 3,5-dihydroxyphenylglycine hydrate (DHPG, 50 μ M; Sigma-Aldrich).

Experiments with G4optoNAM

For dose-response experiments were G4optoNAM or its –OH substituted derivative had been pre-incubated, the imaging chamber was filled with 940 μ l washing solution, and the mGlu₄ agonist L-AP4 (Tocris) was added during image acquisition directly into the

accessory pool of the chamber. Approximately 0.1, 0.4, and 1 μM concentrations of L-AP4 were obtained by successive additions of 0.1, 0.3, and 0.6 pmol respectively, in a volume of 20 μl each.

For real-time incubation experiments, the chamber was filled with 1 ml washing solution, and connected to a perfusion system. L-AP4 was perfused through this system, except during incubation of the mGlu₄ NAMs. For NAMs incubation during image acquisition, the perfusion was stopped and the NAMs added to the accessory pool of the imaging chamber similarly to what is described above for L-AP4 addition in pre-incubation experiments. The final NAM concentration was obtained by pipetting 30 μl of an initial 1:30 dilution of the compound, to obtain a final dilution of approximately 1:1000 (the final amount of DMSO was lower than 1%). L-AP4 addition during NAMs incubation was done in the same way. To washout the NAMs, we restored the perfusion and dropped onto the imaging chamber more than 4 ml of washing solution using a disposable Pasteur pipette. Perfusion was kept on during the rest of the experiment.

3.8 Data analysis

Analysis of calcium responses from mGlu₅-transfected HEK cells. (Alloswitches)

Cells showing no sustained oscillatory responses following activation of mGlu₅ were excluded from the analysis. Frequency of intracellular calcium oscillations was counted as number of oscillations per minute during agonist application, during compound application, or during an illumination period in Excel (Microsoft Office). The frequencies of calcium oscillations were calculated over the entire period of time for each condition with no exception, and dose-response data were fitted with the Hill equation using Prism (GraphPad).

To compare data from different compounds in **Chapter 3**, the oscillatory frequencies were normalized to the initial oscillatory frequency in response to agonist, and expressed as 'fold to agonist'. The normalized responses under different light conditions were averaged and plotted as mean \pm s.e.m. against the corresponding illumination wavelength, in order to visualize the wavelength-activity relationship. These data were then fitted to a Gaussian function in Prism 6.01 (GraphPad). We inferred three parameters describing a Gaussian in Prism: maximum, peak, and standard deviation (SD). We used SD to obtain the half width at half maximum (HWHM) values, being HWHM equal to $\sqrt{2 \cdot \ln 2 \cdot \text{SD}}$.

Graphs were created with IgorPro, from Wavemetrics (time course of intracellular calcium) or Prism (dose-response and wavelength-activity relationships). Images were processed with Adobe Illustrator.

Analysis of calcium responses from mGlu₄/G_{iq}-transfected HEK cells. (G4optoNAM)

Sustained variations in intracellular calcium resulting from activation of mGlu₄ were evaluated from the fluorescence ratio traces by calculating the area under the curve of the response with a custom-made macro (Amperometric Spike Analysis, v. 8.15, written by Eugene Mosharov, <http://sulzerlab.org/download.html>) in IgorPro 6.0.5 (WaveMetrics). Each cell was analyzed independently. Cells that did not respond to all initial applications of agonist were excluded from the analysis. Responses to light in presence of agonist arising more than 20 s after the beginning of the illumination were not taken into account.

In real-time incubation experiments, the three initial responses to application of agonist were averaged, and this value was used for normalization. In pre-incubation experiments, responses to a certain agonist concentration and/or to light were normalized to the maximum response obtained. Responses to the following concentration tested were considered null after the maximum response had been obtained.

Graphs were created with IgorPro (intracellular calcium time course) or Prism 6.01 (GraphPad). Dose-response curves were fitted with a standard Hill equation using Prism. The video of single cell calcium imaging was edited from raw images using Fiji (ImageJ). Statistical differences from the baseline (average of three initial responses to agonist) were assessed with the non-parametric Friedman test for repeated measures, with Dunn's correction for multiple comparisons in Prism.

Single-cell traces drift correction

We corrected eventual increases in the fluorescence ratio observed at resting states only for visualization purposes and after data collection. We did this by applying a custom-made macro for drift correction (CorrectDrift, written by Mike Johnson, mike-johnson@lnl.gov) in IgorPro (WaveMetrics).

4 Behavioral tests in *Xenopus tropicalis* tadpoles

This section describes experiments set up and done entirely by Dr. Kay Eckelt.

All animal procedures were approved by the animal care and Ethics committee for animal experimentation at the University of Barcelona. For experiments, *X. tropicalis* tadpoles of stage 47 to 50 were placed in a 24-well plate at a density of 3 animals/well in *Xenopus* water (referred as water) and video recorded at indicated time points. Motility of the animals was measured after an initial adaptation period of 15 minutes (baseline). Water was replaced by water containing either alloswitch-1 at the indicated concentrations, 100 μ M fenobam, or vehicle (1% DMSO) and motility after 30 min incubation was measured again (dark). Light-dependent behavior was induced by changes in illumination between violet (380 nm) and green (500 nm) light using a LED plate⁸ placed at a distance of approximately 30 cm from the animals. Tadpole motility was monitored during 60 s during violet light illumination (violet) starting after a 10 s adaptation period and during 60 s in ambient light after a 10 s pulse of green light. Light cycles were repeated consecutively for 3 times. Tadpoles were returned to water after pharmacological treatments. The day after, animals were observed for abnormalities and behavioral tests were repeated as described to evaluate compounds washout. Animal tracking and trajectory images were obtained from 60 s binarized video sequences using a custom ImageJ macro based on the wrMTrck methodology (<http://www.phage.dk/plugins/wrmtrck.html>). Motility was measured as normalized distance, calculated as moved distance at a given condition (measured as total animal displacement per well within 60 s) divided by the mean of the moved distance of the baseline condition for each treatment condition.

Data processing and statistical analysis of motility of *X. tropicalis* tadpoles was carried out with homemade software scripts in R (version 2.15.2, R Foundation). Data were first normalized to basal motility, and then tested for normality with the D'Agostino and Pearson omnibus test. Statistical differences relative to baseline between light conditions were assessed separately for each of the compounds and for each light condition using a Wilcoxon signed rank test and a p-value correction for multiple testing. Statistical significance was set to $p < 0.05$. All reported values are represented as mean \pm s.e.m.

5 Behavioral tests in Zebrafish *larvae*

This section is reproduced from a manuscript in preparation by Dr. Xavier Rovira, who also did the experiments with zebrafish shown in **Chapter 2**.

Zebrafish were maintained under standardized conditions and experiments were conducted in accordance with the European Communities council directive 2010/63. Embryos were staged according to Kimmel *et al.* (1995). Wild-type TL (Tupfel long fin) specimen used for these experiments were provided by the Zebrafish International Resource Center (ZIRC). Monitoring of the animal motility was made with a new prototype of the high-throughput enclosure to analyze the zebrafish behavior with a controllable source of light (Opto-Zebrabox, Viewpoint life sciences). The Opto-Zebrabox was used to test the photoswitchable molecules in a 96-well plate format with a complete control of the different light parameters. One embryo per well was placed in E3 medium (5 mM NaCl, 0.17 mM KCl, 0.33 mM CaCl₂, 0.33 mM MgSO₄, 100 µl). For the adaptation of the animals, the plate was kept in the same environmental conditions of the experiment for 30 min previous to the beginning. The compounds were diluted in E3 medium at the double of the final assayed concentration. The addition of compounds (100 µl/well) was done with a multichannel pipette to minimize time differences between wells. One minute after the addition, the recording of animals' movements was started for 25 min in dark and the data accumulated every 5 minutes. Right after, a protocol with 3 cycles of dark-light (1 min per condition) was started. All data were accumulated every minute for this last protocol. The analysis of the results was performed Prism software (GraphPad).

6 Two-photon calcium imaging and excitation

Two-photon experiments were done at the Advanced Digital Microscopy core facility of IRB (PCB, Barcelona), with the kind assistance of Dr. Anna Lladó.

Cell culture and transfection

HEK tsA201 cells were maintained and transfected as described above in **Section 3.1 of Materials & Methods** with minor modifications. For two-photon experiments we transfected a plasmid kindly offered by prof. Francisco Ciruela that encodes for the

mGlu₅ receptor in fusion with eYFP instead of SNAP-tag (mGlu₅-eYFP). This was done for double-check of the 2PE stimulation of mGlu₅ responses, since eYFP allows a straightforward identification of cells expressing mGlu₅.

In experiments where intracellular calcium was monitored with GCaMP6s, the calcium reporter was co-transfected with the mGlu₅-SNAP plasmid in a ratio 1:1, maintaining all other transfection conditions unchanged. Cells were plated onto 21-mm instead of 15-mm coverslips.

Calcium indicator and bath solution

Loading of calcium dye and the bath solution used were as already detailed in **Section 3.4 of Materials & Methods**, except incubation of Fura-2 AM was in culture medium instead of bath solution. Cells expressing GCaMP6s were not loaded with Fura-2. Fura-2 was used as a single-wavelength calcium indicator, since ratiometric imaging would have required slow frame rates, which were incompatible with the time resolution needed for imaging successfully the calcium oscillations. The wavelengths used for imaging Fura-2 were between 760 and 820 nm, therefore approximately corresponding to 380-410 nm for single-photon stimulation. Thus, increases in intracellular calcium were displayed as decreases in the fluorescence emission of Fura-2.

Two-photon calcium imaging of Fura-2 in HEK cells

Coverslips were mounted in a round Attofluor cell chamber (Thermo Fisher scientific), which was placed on an inverted Leica TCS SP5 MP Confocal system (Leica Microsystems) equipped with a HCX PL APO 40×/1.25-0.75-NA oil objective. Light sources for 1P were a 405 nm diode laser and an Argon laser set at 514 nm for eYFP imaging; the light source for 2P was an IR laser MaiTai Wide Band (710nm-990nm). Emitted fluorescence was collected with hybrid detectors ranging 420 to 515 nm. Since true confocal images were not acquired, the pinhole was kept wide open throughout experiments, unless otherwise specified. Imaging of Fura-2 was done at either 760, 780, 800, or 820 nm. Scanning times (346 ms) and frame rates (< 0.2 Hz) were kept to the lowest values compatible with image pixel size (256 x 256) and scanning frequency (400 Hz, bidirectional). Also, the laser power for imaging was set to the minimal value allowing satisfactory imaging, which was usually between 3-5 mW on sample for all wavelengths tested. This was done to reduce to the minimum the exposure of the photochromic compounds to multiphoton light during imaging.

Singe-photon calcium imaging with the calcium reporter GCaMP6s

Cells expressing GCaMP6s were imaged with the same equipment as described in the previous paragraph, except for the light source. Fluorescence of GCaMP6s was stimulated with an Argon laser set at 488 nm and at the lowest power possible, to avoid *cis-to-trans* isomerization of alloswitches, and detected in the range 490 to 550 nm. Two-photon images of GCaMP6s were collected with the IR laser MaiTai Wide Band by illuminating at 900 nm.

Two-photon excitation (2PE) of alloswitch-1 and derivatives

Photoisomerization of the optical switches with two-photon light was achieved by bidirectional scan of the entire field of view at a higher laser power and longer duration than those used for imaging calcium. Laser power was adjusted to be around 20 mW on sample. The duration of the high power scan for 2PE of alloswitches was 4.453 s. Due to an unexpected delay introduced by the setup for the execution of the power switch, the imaging rate of Fura-2 during 2PE of alloswitches was on average 6.6 s (instead of 5 s). The overall duration of a 2PE period was 90 frames unless otherwise specified, which corresponds to about 10 min. To check for the wavelength dependence of 2PE of alloswitches, we repeated the same stimulation for different light wavelengths, in steps of 20 nm ranging 760 to 820 nm.

Control one-photon excitation (1PE) during 2P imaging

In some experiments we did control 1PE of photoswitches using a 405 nm diode laser set at 20 % of its nominal power, with scan time and all parameters equal to those used for 2PE. However, the imaging rate of Fura-2 during 1PE of alloswitches was on average 8.6 s (instead of 6.6 s obtained during 2PE). The overall duration of a 1PE period was 90 frames unless otherwise specified, which corresponded to about 13 min.

Addition of compounds during 2P imaging

Addition of compounds was done directly in the imaging chamber as already described in **Section 3.7 of Materials & Methods**, or, for some experiments and when indicated in figure, before mounting the coverslips on the microscope.

Image analysis

Images were exported in the Leica image format (.lif) and analyzed offline with Fiji (ImageJ, release Nov 2013). The raw fluorescence intensity was extracted for each cell

profile and plotted in Excel with a custom-written macro. Whenever oscillations were observed, the number of peaks was counted, together with the peak time (time when the minimum fluorescence was observed, corresponding to the observed peak in intracellular calcium).

Cells showing calcium variations or oscillations after Alloswitch-1 had already been added, if any, were excluded from analysis. Cells displaying one single calcium rise during 2PE were not considered as successfully excited. Only cells showing two or more calcium oscillations were taken into account for calculating rise time and frequency of calcium oscillations.

After all responding cells had been assigned a rise time and oscillatory frequency, we loaded the eYFP channel images and checked for expression of mGlu₅ in the responding cells. No responding cells were found to be non-transfected.

RESULTS

The results section is divided into four chapters, according to the different aims of this thesis and as anticipated in the **Objectives**.

Chapter 1

We addressed the challenge of developing light-regulated allosteric modulators of mGlu receptors in two ways.

In this first chapter of results we describe a rational design strategy that proved successful in reaching our goal, which consists in the ‘azologization’ of a known allosteric modulator of mGlu receptors, as already mentioned in **Section 3** of the **Introduction**. We show the characterization of the obtained compound, which we called alloswitch-1, *in vitro* and *in vivo*, and finally consider its possible applications as a research tool and in the clinics in the **Discussion**.

In contrast, **Chapter 2** illustrates the discovery of another light-regulated allosteric modulator of mGlu receptors, which was identified after screening a library of azobenzene derivatives. This compound is also extensively characterized *in vitro* and *in vivo*, and its binding and activation mechanisms are investigated.

1 Design strategy and photochemistry of alloswitch-1

When this project was started, the only optopharmacological design approach that had been explored and successfully applied to ion channels and ionotropic receptors (Banghart *et al.* 2009; Bartels *et al.* 1971; Mourot *et al.* 2012; Stein *et al.* 2013; Stein *et al.* 2012; Volgraf *et al.* 2007; Yue *et al.* 2012) and to one class A GPCR (Schönberger and Trauner 2014) was based on the attachment of azobenzene at permissive positions in orthosteric ligands. Almost all of them were obtained by identifying a ligand bearing a phenyl group, and using this as a building block for the introduction of azobenzene to one end of the parent compound. This implied the addition of at least 8 atoms to the initial

molecule, whose size ranged between 9 and 28 atoms (not counting hydrogens), and in most cases the addition almost doubled the size of the compound. Notably, all these switches acted at the orthosteric binding site of the receptors or ion channels, or at an unidentified site in the case of azopropofols (Stein *et al.* 2012).

Instead, our purpose was to develop optical switches acting at the allosteric binding site of mGlu receptors, which were advantageous pharmacologically due to higher receptor subtype selectivity and physiological regulation. The mGlu₅ models available at the time pointed at a very deep pocket with a narrow entrance, almost buried in the TMD, and lately this hypothesis was confirmed by structural data (**Figure 2, Section 1** of the **Introduction**; Doré *et al.* 2014). This tight binding pocket put strong constraints on the substitutions available, and practically ruled out the possibility of finding a position in a ligand model that was sufficiently permissive to tether an azobenzene.

Design strategy

We hypothesized that adding the azobenzene at one side of a parent mGlu allosteric compound would corrupt the pharmacology of the ligand, by hampering its entrance or fitting into the allosteric pocket. This was confirmed by evidence showing that small changes in the structure of mGlu allosteric modulators produce big changes in their pharmacological properties (Wood *et al.* 2011).

Therefore, we adopted a different strategy that was aimed at fully embedding the light-switch into the functional core of the parent compound, rather than only using one phenyl ring of the initial molecule for building azobenzene beside it. The advantage of such an approach is twofold. On one hand, we aimed at preserving the drug-like characteristics of the parent compound, avoiding the addition of unnecessary chemical groups that could break Lipinski's rule of five for drug-like compounds (Lipinski *et al.* 2001) and make the molecule bigger, unselective, probably insoluble, and finally unsuitable for *in vivo* applications. On the other hand, we expected that isomerisation between the *trans*- and *cis*- configurations of the azobenzene derivative would break the 'functional core' of the molecule and thus produce a dramatic change over the resulting receptor activity.

In brief, azobenzene consists of two phenyl rings connected by an N=N bond, and we screened existing allosteric modulators of mGlu receptors for chemical scaffolds presenting two aryl rings at a distance of exactly two bonds, just like azobenzene. We identified in the literature an allosteric modulator of mGlu₄ with the desired characteristics (VU0415374, **Figure 24**, left, from Engers *et al.* 2011), presenting three

aryl rings separated two by two by amides. Few chemical modifications in VU0415374 were necessary to replace one of the two amides by an azo group (-N=N-). This led to two new molecules containing intrinsically a light-sensitive moiety, one in the form of a phenylazopyridine and the other as a proper azobenzene, that we called respectively alloswitch-1 and compound **2** (**Figure 24b** and **24c**). These compounds were synthesized by Xavier Gómez i Santacana, a PhD student in the group of Dr. Amadeu Llebaria at iQAC-CSIC (Barcelona). This design strategy was later described by the group of Dirk Trauner as ‘azologization’ (Schönberger *et al.* 2014).

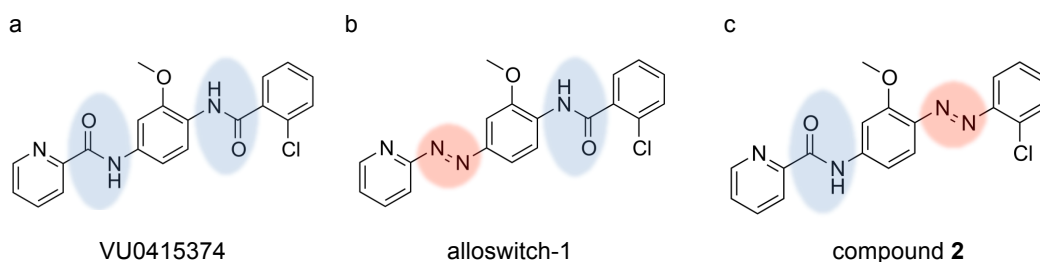


Figure 24 | Azologization of an mGlu allosteric modulator.

Chemical structures of the parent compound VU0415374 (**a**) and the azobenzene derivatives alloswitch-1 (**b**) and compound **2** (**c**), with amide bond and azo-bonds highlighted by blue and red ovals, respectively. The parent compound presented two phenyl rings and a pyridine, which were maintained in the azologues and gave rise to a phenylazopyridine in **b** and a substituted azobenzene in **c**. Schematics adapted from Pittolo *et al.* (2014).

Initial screening of pharmacological activity

A plate-reader based assay was used to assess the activity of these compounds as mGlu₄ PAMs. To do this, Dr. Xavier Rovira from the group of Jean-Philippe Pin and Laurent Prézeau at the IGF in Montpellier, France, measured the cumulative IP production in HEK cells transfected with mGlu₄ and a G_{1/q}α chimeric protein, for coupling mGlu₄ with the IP-production pathway with the IP-One HTRF assay by CisBio Bioassays described in **Section 2.3.1** of the **Introduction**.

Although our allosteric precursor used as a scaffold for azologization is a potent nanomolar-range PAM of mGlu₄, the derived azologue-compounds showed only marginal activity in this receptor (**Figure 25a**). This was disappointing, but given the pharmacological promiscuity of mGlu₄ PAMs and mGlu₅ NAMs that we discussed previously (Urwyler 2011), we decided to assay the compounds also for negative modulation of mGlu₅ receptors. Compound **2** showed no inhibitory activity over mGlu₅

when compared with the potent mGlu₅ NAM MPEP (**Figure 25b**; Gasparini *et al.* 1999). Alloswitch-1, instead, showed nanomolar potency at inhibiting this receptor (see **Figure 31**), and was used for all further characterizations.

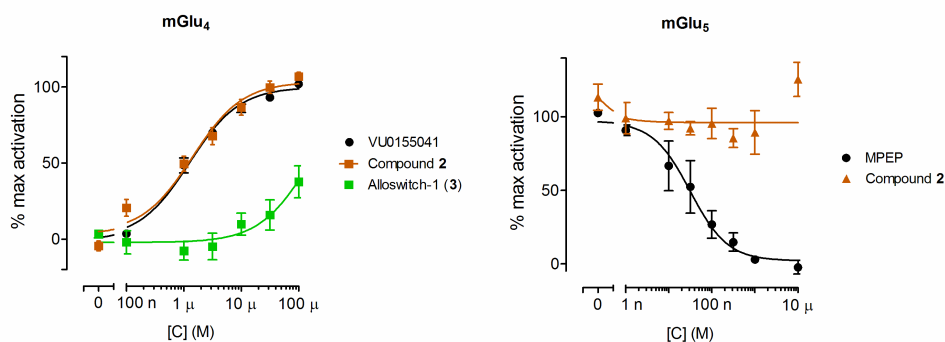


Figure 25 | Compound 2 and alloswitch-1 are weakly active in mGlu₄, and compound 2 has no effect on mGlu₅.

We monitored the effect of alloswitch-1 and compound 2 by measuring the accumulation of inositol phosphates (IP) in HEK 293 cells transiently expressing mGlu₄/G_{iq}α (a) or mGlu₅ (b), and stimulated with orthosteric agonists L-AP4 (10 nM, a) or quisqualate (300 nM, b). (a) Normalized activation of mGlu₄ by L-AP4, in presence of 2 (brown) and alloswitch-1 (green), showing the compounds are weak PAMs of mGlu₄ (EC₅₀ 2 = 1.8 ± 0.5 nM). The activity of the mGlu₄ PAM VU-0155041 (black) is shown for comparison (EC₅₀ = 834 ± 106 nM). (b) Normalized effect of 2 (brown) over mGlu₅ activation, showing the compound is inactive in this receptor, unlike the mGlu₅ NAM MPEP (black, IC₅₀ = 45 ± 21 nM). Data are presented as mean ± s.e.m. from at least 3 independent experiments. Data from Dr. Xavier Rovira, IGF, Montpellier, France.

Photochemical characterization of alloswitch-1

As most azobenzene-based compounds, alloswitch-1 isomerises to its *cis* configuration under illumination with violet light (390-390 nm), and quickly returns to the *trans* configuration upon green light illumination (490-500 nm) or slowly by thermal relaxation (**Figure 26a**). These changes in configuration are reflected in changes in the absorption spectrum of the molecule. By UV-vis spectroscopy, we can monitor the efficiency of the photoisomerization in different conditions (e.g. different solvents or after illumination with different light wavelengths). We first measured the absorption of alloswitch-1 in the organic solvent DMSO (**Figure 26b**), in the dark and after 10 minutes illumination with 380- or 500-nm light, and could see the typical absorption peak of azobenzene-like compounds at 380 nm. We chose a long time of illumination to be sure that we reached the photostationary state of the azo-compound. This is specific for every azo-molecule, and consists in the equilibrium between *trans* and *cis* isomers, and no further photoisomerization is possible beyond this point (Rau 1990). We repeated these

measures in the aqueous buffer (**Figure 26c**) where we solubilize the molecules for studies with living cells, and we were able to observe only partial changes in absorption upon illumination with 380-nm light. Since acquiring a UV-vis spectrum takes almost a minute, we thought this difference was attributable to faster relaxation kinetics of the *cis* isomer in aqueous buffers than in DMSO, which wade the molecule relax thermally before we could measure its full absorbance spectrum.

Therefore, we monitored the kinetics of *cis*-alloswitch-1 relaxation in DMSO and in buffer (**Figure 26d** and **26e**) by measuring the absorbance at a fixed wavelength (360 nm), and saw that it relaxes at a slow rates in DMSO, and with a shorter half-life of about 2 minutes in physiological buffer, indicating that continuous illumination is not necessary for maintaining the molecule in the *cis* isoform.

Finally, since azobenzenes are reversible photoswitches, we checked the reproducibility of the photoisomerization by measuring the absorbance of the molecule at 360 nm after alternate illumination with violet or green light (**Figure 26f**), and we saw it was stable along at least 5 illumination cycles (more than used in experiments in cells).

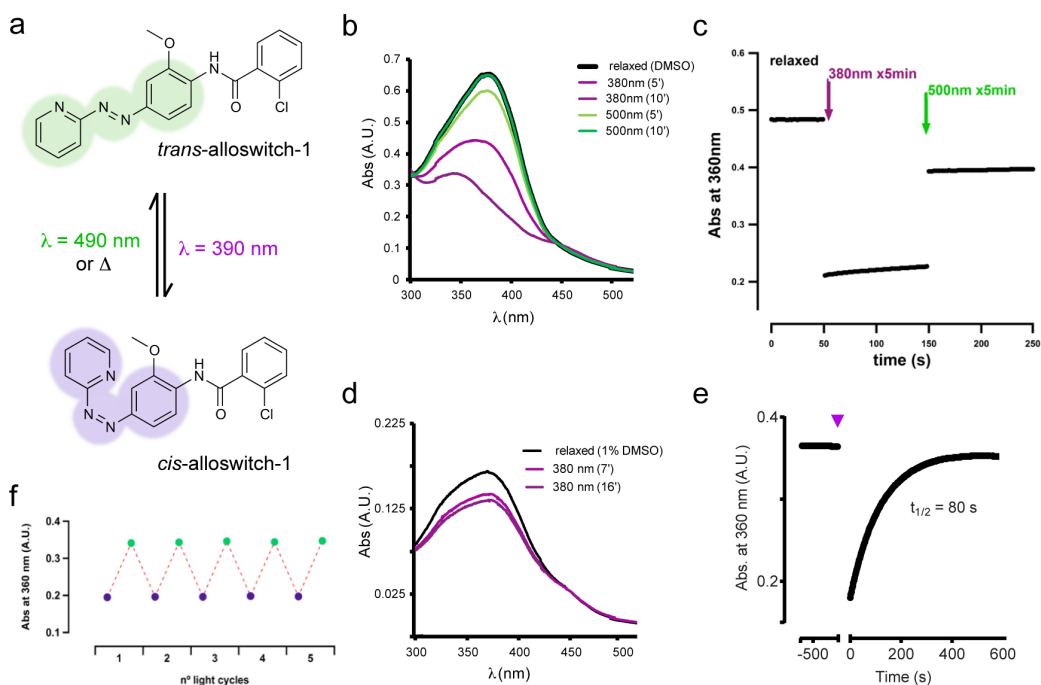


Figure 26 | Photoisomerization of alloswitch-1.

(a) Schematics of alloswitch-1 photoisomerization. (b, c) Absorption spectra of 25 μM alloswitch-1 in DMSO (b) and aqueous buffer (c). (d-e) Kinetics of thermal relaxation of alloswitch-1 in DMSO (d) and aqueous buffer (e). (f) Stability of the reversible photoisomerization of alloswitch-1 during 5 illumination cycles with 380 and 500 nm light. Graph shows absorbance of alloswitch-1 (25 μM in DMSO) at 360 nm during five illumination

cycles. Absorbance was measured after 3 minutes illumination with either 390 or 490 nm light (violet and green dots respectively). In part reproduced from Izquierdo-Serra *et al.* (2014).

2 Optopharmacology of alloswitch-1 with the IP-One assay

We performed a more detailed pharmacological characterisation of alloswitch-1 in collaboration with the group of Jean-Philippe Pin in Montpellier, under the supervision of Dr. Xavier Rovira and Dr. Cyril Goudet. All experiments were done in cells overexpressing mGlu₅, as high-throughput screenings in 96-well plates, using the IP-One HTRF kit assay, that was a technique initially developed by CisBio Bioassays in collaboration with the laboratory of Jean-Philippe Pin and later commercialized by the same company. However, this experimental procedure had never been used before to screen the optopharmacological profile of molecules in the dark or under constant illumination, so we did preliminary experiments to optimize the technique.

First, we checked if the illumination with violet (380-nm) LED arrays could affect the response of mGlu₅-expressing cells to mGlu₅ agonists such as the endogenous agonist glutamate, or other orthosteric ligands such as quisqualic acid and DHPG. No agonist degradation was observed in these experiments (**Figure 27**).

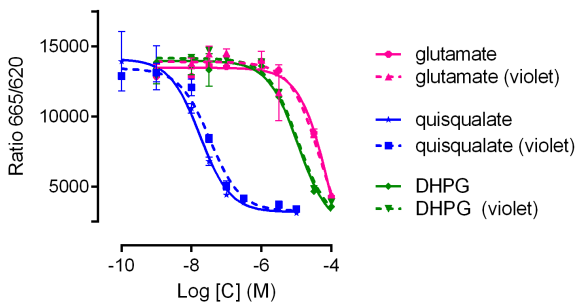


Figure 27 | Photostability of mGlu₅ agonists under continuous illumination at 380 nm during 30 minutes.

IP-One HTRF assay in HEK cells expressing mGlu₅, challenged with a dose-response to three different mGlu₅ orthosteric agonists (glutamate, quisqualate and DHPG), in dark conditions (solid lines) or under illumination with violet light (380 nm, dashed lines). FRET efficiency expressed

as ratio between fluorescence emission after excitation of donor and acceptor (665 and 620 nm respectively). Efficiency of FRET indicates low production of IPs and therefore low receptor activation. Log EC₅₀ for glutamate was -4.02 ± 0.15 M in dark conditions and -4.32 ± 0.26 μ M under violet light; log EC₅₀ for quisqualate was -7.76 ± 0.09 M in dark conditions and -7.47 ± 0.08 μ M under violet light; log EC₅₀ for DHPG was -4.96 ± 0.12 M in dark conditions and -4.95 ± 0.12 μ M under violet light. Data indicated as mean \pm s.e.m.; experiments done in duplicate.

Based on some incongruences observed in the results of the first experiments between the cells challenged with alloswitch-1 in dark conditions or the ones challenged with the compound but under constant violet illumination, we hypothesized that the LED array used for the illumination could be heating up the samples. An increased temperature could affect the cell metabolism and bias the results. To test this, we performed two sets of experiments, where the dark and the violet light condition were tested whether on different 96-well plates or in the same plate, half covered with aluminum foil to obtain the 'dark' condition (**Figure 28**). This way, if the illumination was affecting the temperature of the sample and consequently the cellular response to the stimulation, this should be reflected in a different potency of the mix of agonist and compound used to stimulate the cells.

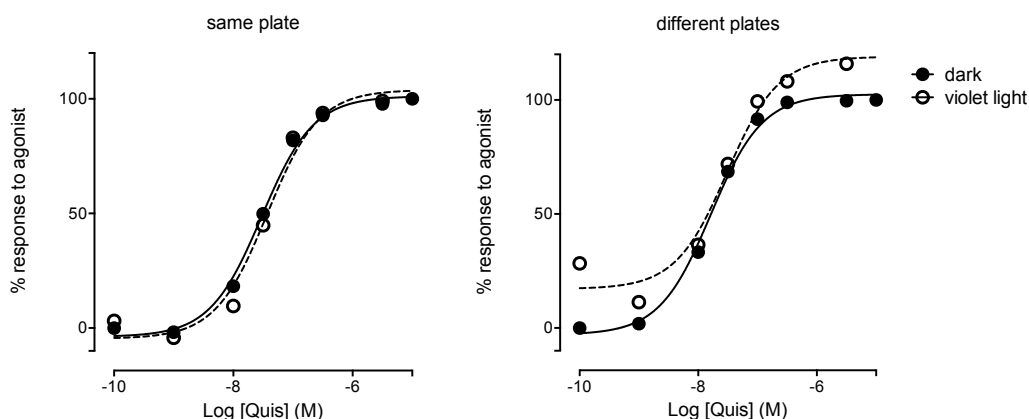


Figure 28 | Testing dark and light conditions on different plates provokes artifacts.

Normalized dose-response to indicated concentrations of the orthosteric agonist quisqualate from IP-One HTRF assay in mGlu₅-expressing HEK cells, in dark conditions or with violet light illumination. (**left**) Dose-responses on the left were obtained on the same 96-well plate, placed over an LED array for illumination and half covered with aluminum foil to create the 'dark' condition. (**right**) Dark and light conditions on the right were obtained from different 96-well plates. The agonist EC₅₀ is unchanged, but the basal receptor activation is increased when cells are placed over an LED array.

In these experiments we observed that the agonist-induced activity was unchanged between the dark and violet light condition when these were tested simultaneously on the same plate, whereas it was different when tested on two separate plates (**Figure 28**). We also noticed that alloswitch-1 was more effective in inhibiting mGlu₅ when the dark condition was tested on a separate plate. This was evidently an artifact, and we decided to perform all further experiments with dark and light conditions on the same plate.

2.1 Potency of alloswitch-1 over mGlu₅ in dark and under violet light

We performed experiments of dose-response to the orthosteric mGlu₅ agonist quisqualate in the presence of increasing concentrations of Alloswitch-1 or the mGlu₅ inverse agonist fenobam, both in the dark and under violet light (**Figure 29**). This analysis evidenced that in dark conditions both *trans*-Alloswitch-1 and fenobam antagonised the accumulation of IP induced by the agonist in an allosteric way. Moreover, we observed that even in the absence of orthosteric stimulation (at low or null concentrations of quisqualate) both molecules induced a decrease in the accumulation of IPs, indicating that these compounds inhibit the constitutive activation of mGlu₅, and therefore act as inverse agonists at this receptor.

In contrast, when we illuminated the cells with violet light the antagonism of *cis*-Alloswitch-1 almost disappeared, indicating that the optical switch loses potency when switching from the *trans* to the *cis* configuration. This light-dependent loss-of-function was not observed with the non-photoswitchable fenobam or in the absence of any compound, suggested it was not an effect caused directly by illumination.

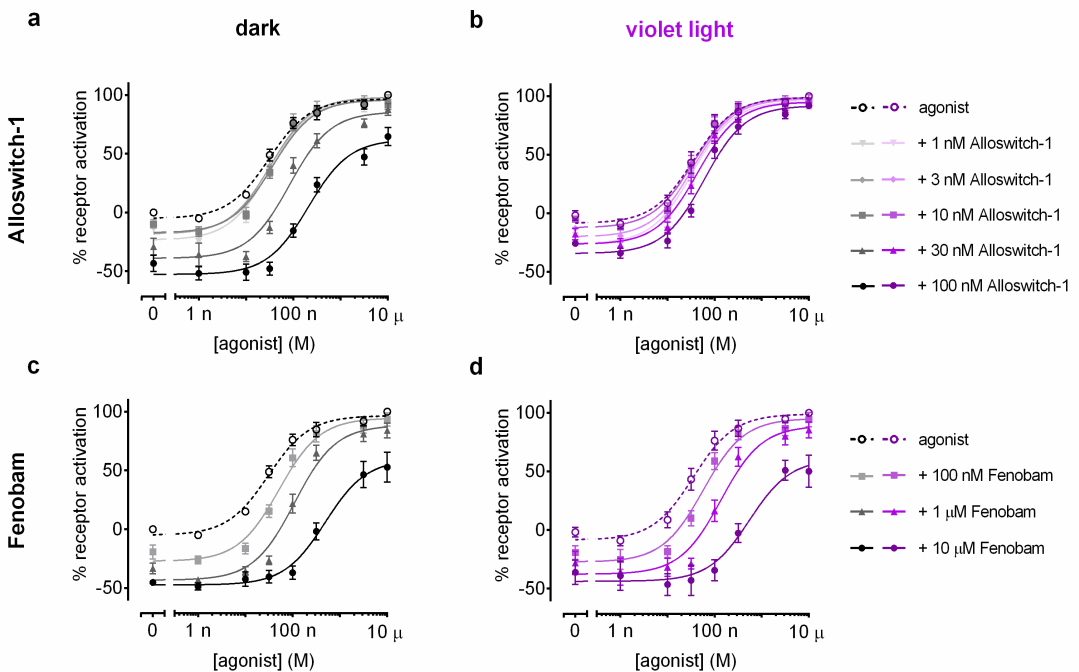


Figure 29 | Antagonism of Alloswitch-1 over mGlu₅ is concentration-dependent and light-sensitive.

Agonist dose-response relationship showing the effect of different amounts of Alloswitch-1 (a,b) and Fenobam (c,d) over agonist potency and efficacy, in dark conditions (a,c) or under constant illumination with violet light (b,d). Receptor activation was measured by IP accumulation assay in mGlu₅-transfected HEK 293 cells stimulated with increasing concentrations of the orthosteric agonist quisqualate (open dots and dashed lines). (a) In dark conditions, increasing Alloswitch-1 concentrations up to 100 nM reduces the evoked activation of the receptor and its constitutive activity (rightward and downward shift, respectively). This effect is comparable to that induced by the mGlu₅ NAM Fenobam (c). (b) Under violet light, equal concentrations of Alloswitch-1 have little effect on the activation profile of mGlu₅. (d) The efficacy and potency of Fenobam do not change under violet light. Data are normalized to values from IP accumulation in absence or saturation of agonist, and presented as mean ± s.e.m. for at least three independent experiments performed in duplicate.

The results shown in **Figure 29** are summarized in **Figure 30**, which shows how the response to the agonist is affected in a light-dependent manner by the presence of 100 nM Alloswitch-1, and in a light-independent way by the presence of 10 μM fenobam.

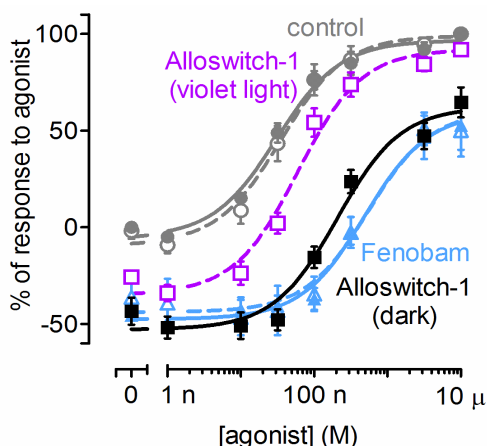


Figure 30 | Alloswitch-1 optically modulates mGlu₅ *in vitro* (summary of Figure 29).

IP₁ accumulation assay in HEK cells transiently expressing mGlu₅. Normalized dose-response to indicated concentrations of the orthosteric agonist quisqualate in absence (control, grey, dots) and presence of Alloswitch-1 (100 nM, violet and dark, squares) or fenobam (10 μM, cyan, triangles), either in dark (solid lines and filled symbols) or under violet light conditions (dashed lines and open symbols).

Finally, we quantified the loss of potency induced by violet light illumination (**Figure 31**). To do this, we challenged the cells with a fixed amount of agonist and we did a dose-response to increasing concentrations of Alloswitch-1, either in dark conditions or under violet light.

The concentration of quisqualate was set around its EC₈₀ (100 nM, as inferred from **Figure 29**), in order to better see the effects induced by the addition of an inhibitor. The fitting of the obtained dose-response curves with a standard Hill equation indicated that *trans*-Alloswitch-1 had a measured potency of approximately 25 nM, and that this potency could be scaled down optically by a factor of 1.5 log. Dose-response to fenobam is shown in **Figure 31** for comparison.

We believe that the reduction of Alloswitch-1 potency elicited by violet light has to be attributed to a drop in concentration of the active *trans* isomer at the photostationary state. Despite this is a major question about the functioning of optical switches based on azobenzene, we have not performed yet any experiment to confirm this. In fact, there are technical limitations in the coupling of illumination with experimental setups that could clarify this issue, and moreover reaching a condition where only the *cis* isomer is present in solution is not possible because of the photostationary state of azobenzenes (see **Section 3** of this Chapter and **Figure 37** for detailed explanation and further discussion).

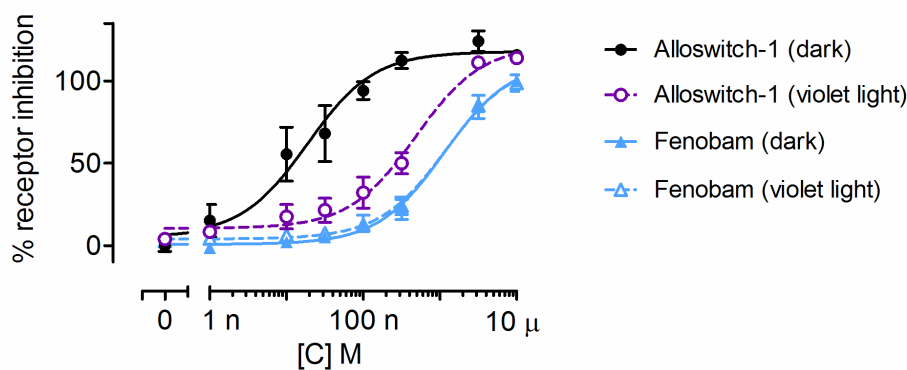


Figure 31 | Potency of Alloswitch-1 over mGlu₅.

IP accumulation assay in mGlu₅-transfected HEK 293 cells stimulated with an EC₈₀ of agonist (100 nM quisqualate, see **Figure 29**) and normalized against absence or saturation of a reference NAM (Fenobam). Dose-response curves show the inhibitory effect of increasing concentrations of compounds in dark conditions or under violet light. IC₅₀ for Alloswitch-1 shifts from a value of 25 ± 19 nM in dark conditions to 0.5 ± 0.1 μM under violet light. Data shown as mean ± s.e.m. from at least three independent experiments done in duplicate.

2.2 Selectivity of Alloswitch-1 over the rest of the mGlu receptors family.

Selectivity for their molecular target is probably the most important reason why allosteric ligands are acquiring more and more importance as drug targets (Conn *et al.* 2009a). We screened the activity of 5 μM Alloswitch-1 across the eight members of the mGlu receptors family with the IP-One assay. We did experiments to check for possible NAM or PAM activity of our optical switch on mGlu receptors (**Figure 32a** and **32b**, respectively). We did this under either illumination condition, to discard any possible unexpected effect of the *cis* isoform. In order to determine possible effects on other

mGlu receptors, alloswitch-1 was applied at a 200-fold concentration with respect to its potency over mGlu₅. At this high concentration, no differences over mGlu₅ inhibition can be obtained between the dark and violet light conditions (see saturation of inhibition at high concentrations of alloswitch-1 in **Figure 31**). Alloswitch-1 can be considered selective for mGlu₅ since at this high concentration it elicits less than 50% of activity on all mGlu receptors except mGlu₅. Therefore this thorough study revealed that the molecule was active only as a NAM of mGlu₅ receptors, with no significant cross-reactivity with other members of the family.

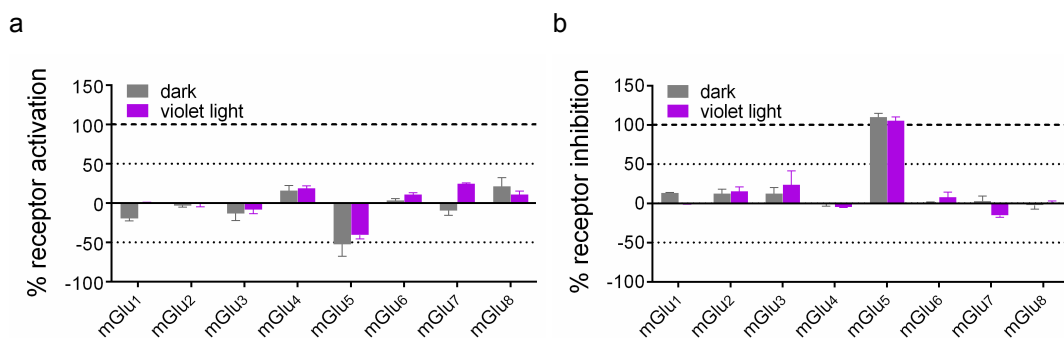


Figure 32 | Alloswitch-1 is selective for mGlu₅ across the metabotropic glutamate receptor family (mGlu₁₋₈) in the dark and under violet light.

We monitored the activity of all metabotropic glutamate receptors (subtypes 1 to 8), by measuring the accumulation of inositol phosphates (IP) in HEK cells transiently expressing the individual receptors. A high concentration of alloswitch-1 (5 μ M) was tested for its ability to either potentiate (a) or inhibit (b) the activation of the mGlu receptors induced by low (a) or high (b) agonist concentration, in dark (black bars) and under violet light (see **Table 7** in **Materials and Methods** for detailed information about ligands and concentrations used). (a) Alloswitch-1 does not significantly potentiate receptor activation regardless of illumination. (b) Alloswitch-1 inhibits selectively the activation of mGlu₅ at both light conditions, while not significantly inhibiting other mGlu subtypes. To determine possible effects on other mGlu receptors, alloswitch-1 was applied at a 200-fold concentration with respect to its potency over mGlu₅. At this high concentration, no differences over mGlu₅ inhibition can be obtained between the dark and violet light conditions (see saturation of inhibition at high concentrations of alloswitch-1 in **Figure 31**). Alloswitch-1 can be considered selective for mGlu₅ since at this high concentration it elicits less than 50% of activity on all mGlu receptors except mGlu₅. Data represent normalized receptor activation or inhibition for at least 3 independent experiments, done in duplicate, and are represented as mean \pm s.e.m.

Finally, we wanted to check how using different light wavelengths for the photoisomerization of Alloswitch-1 could affect the efficacy of the optical switch. Sticking to the availability of LED arrays we had, we used 430-nm light as an alternative red-shifted illumination wavelength, but we were unable to see any relevant difference with this method (**Figure 33**).

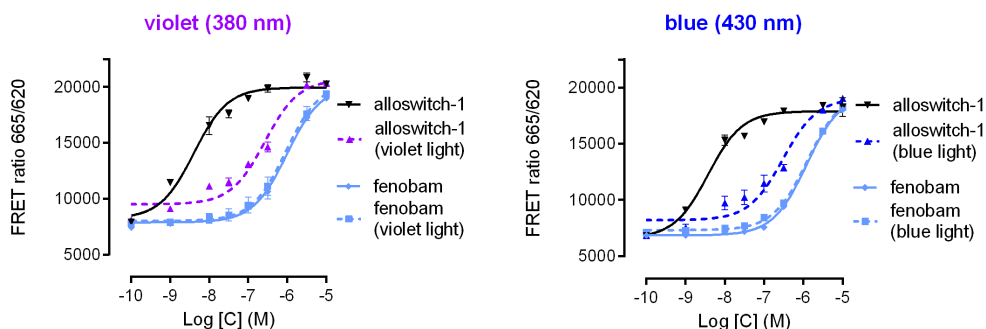


Figure 33 | Effect of alloswitch-1 over mGlu₅ activation and inhibition under illumination with 380 and 430 nm.

IP-One HTRF assay in mGlu₅-expressing HEK cells stimulated with an EC₈₀ of agonist (100 nM quisqualate). The effect of the mGlu₅ NAM fenobam is shown for comparison. FRET efficiency expressed as ratio between fluorescence emission after excitation of donor and acceptor (665 and 620 nm respectively). Efficiency of FRET indicates low production of IPs and therefore low receptor activation. Log IC₅₀ for alloswitch in dark for both experiments was -8.4 ± 0.1 M, and -6.6 ± 0.1 and -6.5 ± 0.1 M for cells illuminated with violet and blue light, respectively. Log IC₅₀ for fenobam was unchanged for both experiments. Experiments were done in duplicate.

3 Real-time optopharmacology of Alloswitch-1

Reversibility is a fundamental characteristic of azobenzene-based optical tools, which makes them suitable for the control of proteins with high temporal resolution. However, IP-One experiments we could not check the reversibility of the light-induced shift in Alloswitch-1 potency, since this is an end-point assay in which cells must be lysed in order to collect the read-out. Therefore, we decided to move to an experimental setup that allowed monitoring mGlu₅ responses in real-time. We used HEK cells overexpressing mGlu₅, and monitored variations in intracellular calcium using an inverted microscope coupled to a monochromator light source for both imaging and stimulation. The software allowed us to create patterns of different light wavelengths of a defined duration and an imaging rate compatible with the calcium events induced in cells by activation of mGlu₅ receptors.

These experiments showed that by applying an mGlu₅ agonist (quisqualate, 3 μ M) we could induce cytosolic calcium oscillations (**Figure 34**), as previously reported (Bradley *et al.* 2009). This characteristic cellular response was fully blocked by addition of alloswitch-1 at concentrations above 100 nM, in agreement with what emerged from IP-One assay experiments. Calcium oscillations were resumed in presence of *cis*-

Alloswitch-1 during illumination with violet light (390 nm, example of a cell receiving 100 nM Alloswitch-1 in **Figure 34b**), and were stopped by illumination with green light (490 nm), indicating the recovery of Alloswitch-1–antagonistic action. The light-dependent activity of the receptor was reversibly switched off and on several times by simply changing the light wavelength that illuminated the sample. Violet light *per se* had no effect on the response of mGlu₅ in control cells (0.1 % DMSO, **Figure 34c**). The on-off switching of mGlu₅ activity was not seen in cells treated with vehicle or fenobam (10 μM, **Figure 34d**).

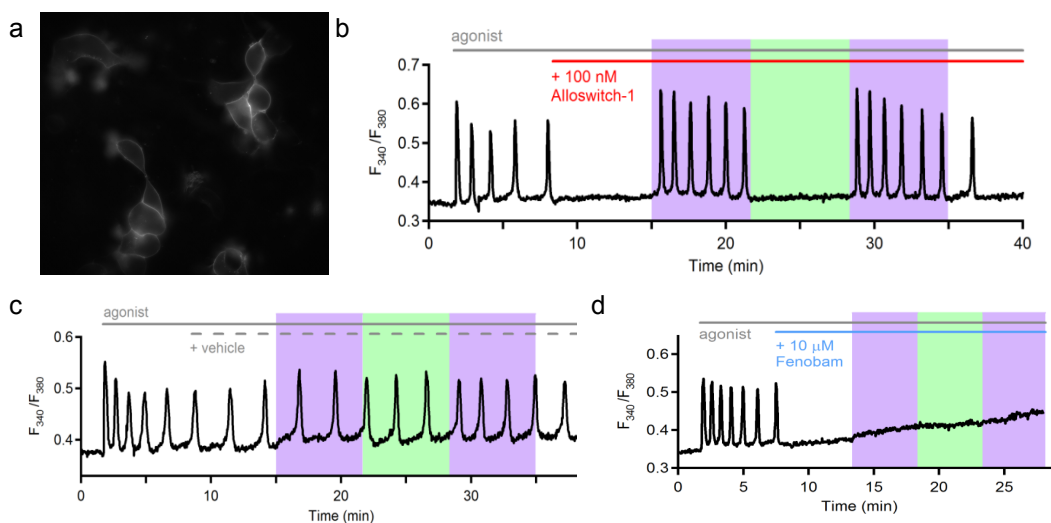


Figure 34 | Alloswitch-1 optically activates mGlu₅-expressing cells.

(a) Image of mGlu₅-SNAP-expressing HEK cells, labeled with SNAP-Surface 647 and loaded with the Fura-2 calcium indicator. (b) Alloswitch-1 (red line) inhibits calcium oscillations induced in cells by application of an mGlu₅ agonist (grey line, 3 μM quisqualate), but this inhibition can be reversibly switched off and on by violet or green light (colored boxes). (c) Treatment of cells with vehicle (0.1% DMSO, dotted line) had no effect on mGlu₅ responses. (d) Application of the mGlu₅ NAM Fenobam (10 μM, blue line) resulted in inhibition of calcium oscillations regardless of illumination.

The application of control compounds (DMSO or fenobam) was also repeated preceding or following addition of Alloswitch-1, respectively (**Figure 35**). Thanks to these experiments, we demonstrated that the same cell could be made light-switchable (**Figure 35a**) or light-unswitchable (**Figure 35b**) in real-time.

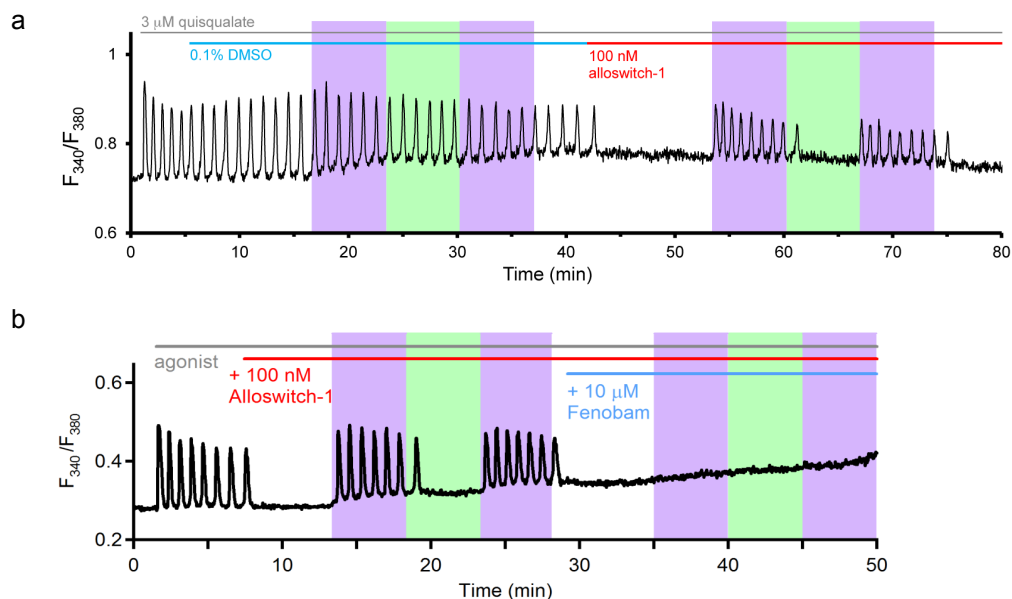


Figure 35 | Cells can be made light-switchable or light-unswitchable in real-time.

(a) HEK cells expressing mGlu₅ and treated with agonist (3 μ M quisqualate, grey line) and vehicle (0.1% DMSO, cyan line) show calcium oscillations that are not naturally light-sensitive, but when Alloswitch-1 is added (100 nM, red line) these oscillations can be stopped in a light-dependent way. (b) Fenobam is non-photoswitchable and inhibits Alloswitch-1-dependent calcium oscillations. The calcium oscillations induced by light in the presence of agonist (3 μ M quisqualate, grey line) and Alloswitch-1 (100 nM, red line) were abolished in the presence of Fenobam (10 μ M, cyan line). Violet and green boxes in both panels indicate illumination with 390 and 490 nm light, respectively.

Further characterization of Alloswitch-1 properties at different concentrations (in log proportion ranging 0.01 to 1000 nM) revealed that the orthosteric activation of mGlu₅ was antagonised in a concentration-dependent manner by *trans*-Alloswitch-1 in dark conditions or under green light (**Figure 36**), in agreement with the NAM behavior of Alloswitch-1. Unexpectedly, under violet light this NAM activity was replaced by a dose-dependent increase in calcium oscillations (**Figure 36c**, violet curve), in contrast with the optopharmacological profile obtained with IP-One assays.

The trend in the dose-response curve corresponding to illumination with violet light suggested that the *cis* isomer could act as a PAM at the binding pocket of mGlu₅. To test this hypothesis, we repeated the single-cell experiments, but added Alloswitch-1 directly under violet light illumination instead of in the dark. If *cis*-Alloswitch-1 was a PAM, its addition should increase the oscillatory frequency (de Paulis *et al.* 2006), similarly to what we observed with the mGlu₅ PAM VU29 (**Figure 38c**).

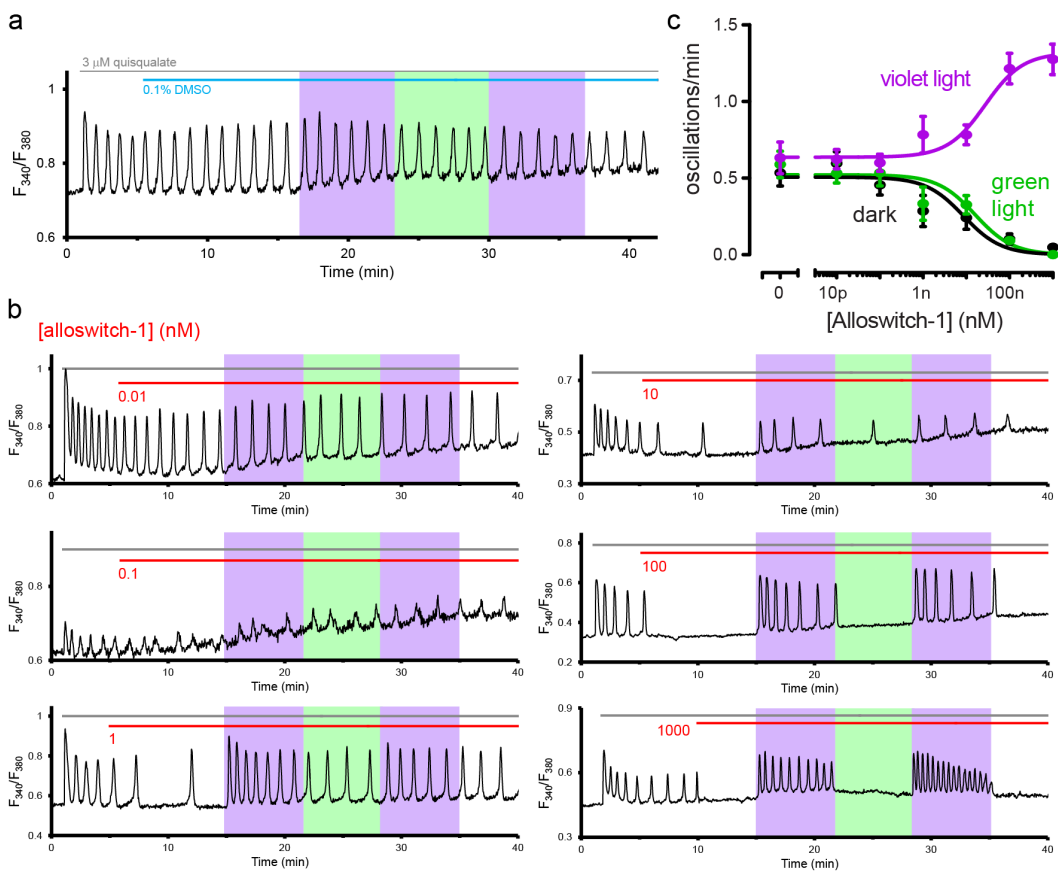


Figure 36 | Dose-response relationship and light-dependent activity of alloswitch-1 from real-time experiments.

(a, b) Example traces of calcium imaging experiments as in **Figure 34b**, with vehicle (0.1% DMSO, a) or alloswitch-1 concentrations ranging 10 pM to 1 μ M, with steps of 1 Log each (b). (c) Light and dose-dependent effects of alloswitch-1 on agonist-induced calcium oscillations in real-time experiments in individual cells as exemplified in b. [Alloswitch-1] = 0 corresponds to data from a. Values represent mean \pm s.e.m. from at least three independent experiments. IC_{50} dark = 8.6 ± 1.6 nM; IC_{50} green = 16.0 ± 1.5 nM; half-maximum effective concentration (EC_{50}) violet = 27.2 ± 1.9 nM; $n = 9-23$ cells for each concentration. All three light conditions were tested in the same cell for one concentration of the tested compound.

In these experiments, the combined action of alloswitch-1 and violet light did not result in an increased oscillatory frequency, thus supporting the idea that *cis*-alloswitch-1 is not an mGlu₅ PAM (**Figure 37**).

We need to consider that azobenzenes never reach a full conversion to the *cis* isomer at the photostationary state, and a residual percentage of the *trans* isomer at equilibrium, although varying, is always present. The results of the previous experiment were not conclusive then, since the residual *trans* in solution could have been inhibiting mGlu₅, thus masking the PAM activity of the *cis* isomer.

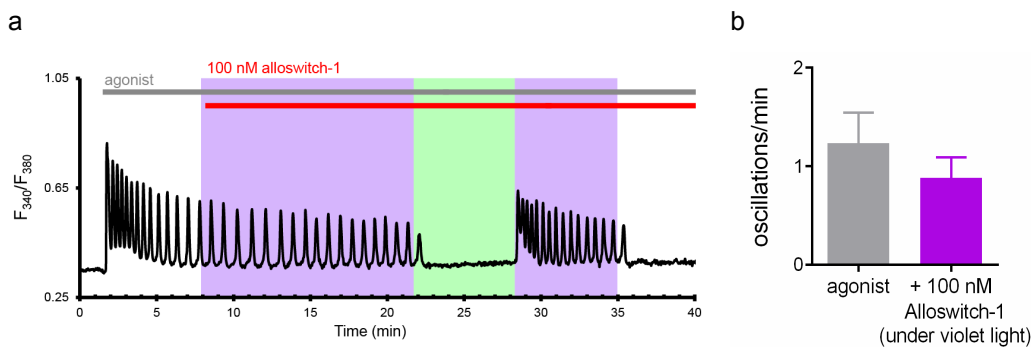


Figure 37 | Alloswitch-1 added under violet light does not affect calcium oscillation frequencies.

(a) Example trace of intracellular calcium time-course in an mGlu₅-transfected HEK cell loaded with Fura-2 (F_{340}/F_{380}) and responding to agonist application (3 μ M quisqualate, black line) with calcium oscillations. Illumination with violet light (violet boxes) started before addition of alloswitch-1 (100 nM, red line). Light was switched from violet to green (green boxes), and back to violet light. After that, experiment was conducted in the dark during 6.7 minutes, and another violet-green-violet light cycle was repeated. (b) Quantification of calcium oscillations frequency after agonist application, and after application of 100 nM alloswitch-1 directly under violet light (violet bar). Data are represented as mean \pm s.e.m. $n=4$ cells from two independent experiments.

Since the possibility of *cis*-alloswitch-1 being a PAM could not be discarded due to uncertainty in the composition of the *cis-trans* solution, we next made an attempt to separate the *cis* from the *trans* isomer, and test the pure *cis* on cells. This is not possible for azobenzenes, which always exist in equilibrium, so Xavier Gómez i Santacana synthesized a stilbene derivative whereby the azo-group of alloswitch-1 was replaced by alkyls. Stilbenes as well exist in *trans* and *cis* isomers, but these configurations they can assume are more stable than those of azobenzenes and can be separated one from another. Although different chemically from alloswitch-1 because of two nitrogen atoms substituted by carbons, the *cis*-stilbene derivative is geometrically similar to *cis*-alloswitch-1 (**Figure 38a**) and we aimed to use it as a model for a chemically pure *cis*-alloswitch. We tested it in cells to assess a possible PAM activity over mGlu₅ receptors, but calcium oscillations induced by quisqualate were inhibited upon addition of the *cis*-stilbene derivative (**Figure 38b**). In a second experiment, we were able to revert the inhibition of mGlu₅ operated by the *cis*-stilbene derivative by delivering to the cells a high concentration of the mGlu₅ PAM VU29 (20 μ M, **Figure 38c**). This demonstrated that the *cis*-stilbene derivative of alloswitch-1 was binding at the allosteric binding pocket of mGlu₅ receptors and was acting as a NAM, which does not support the hypothesis of *cis*-alloswitch-1 being a PAM.

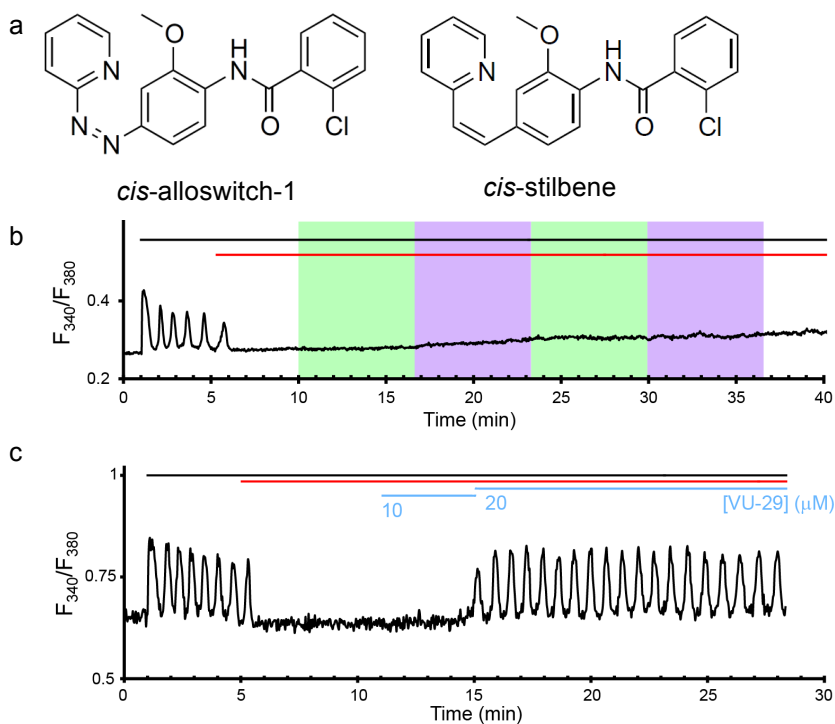


Figure 38 | A pure *cis*-stilbene derivative of alloswitch-1 is not a PAM of mGlu₅.

(a) Chemical structures of *cis*-alloswitch-1 and *cis* isomer of its stilbene derivative. Although they bear chemical differences due to the absence of the nitrogen atoms in the stilbene, the latter can be purified in a stable *cis* form and be used as a structural model of *cis*-alloswitch, which can only exist in a mixed form with its trans isomer (b, c) Intracellular calcium time-course in mGlu₅-transfected HEK cells loaded with Fura-2, challenged with the agonist (3 μ M quisqualate, black line) and (b) 1 μ M or (c) 10 μ M of the *cis*-stilbene derivative (red lines), followed by (b) violet/green illumination or (c) application of increasing concentrations of an mGlu₅ PAM (10 and 20 μ M VU29, cyan lines). The cell shown in panel b was also stimulated with light periods of green (100 ms/2 s) and violet (390 nm, 100 ms/2 s) light indicated in figure by color boxes.

Nevertheless, the ‘apparent PAM’ behaviour of alloswitch-1 under violet light observed in **Figure 36c** remained an intriguing issue, so we designed different experiments from which we built a second dose-response relationship. In this second round of experiments, a full dose-response to alloswitch-1 was tested in the same experiment (see example trace, **Figure 39a**), instead of coming from separate experiments as shown in **Figure 36**. The light-dependency of the dose-response was evaluated by realizing the whole experiment under either illumination condition (dark, green or violet light).

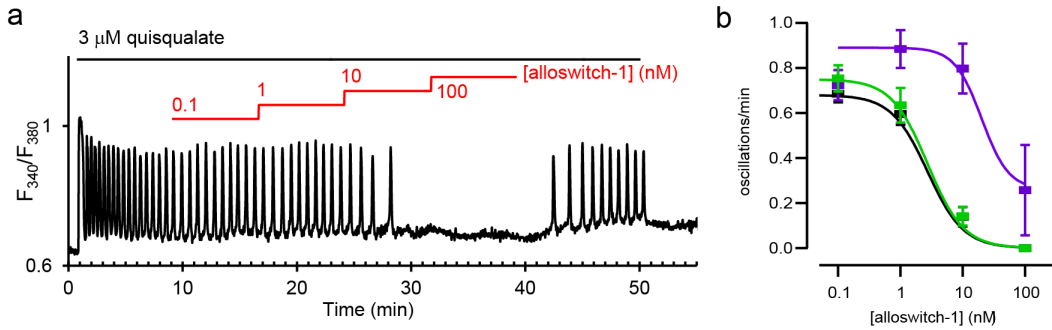


Figure 39 | Dose-response to alloswitch-1 in an individual cell, and light-dependence of this effect.

(a) Example trace of an individual cell stimulated in dark conditions with the mGlu₅ agonist quisqualate, and then challenged with increasing amounts of alloswitch-1, with concentrations ranging 0.1 to 100 nM with three steps of 1 Log each. (b) Dose-response to alloswitch-1 in presence of 3 μM quisqualate and under indicated light conditions (dark, $n = 12$; violet, 380 nm, $n = 9$; green, 500 nm, $n = 18$, from two independent experiments). Data are from experiments performed entirely either in the dark (as exemplified in a; black), or under violet (380 nm; violet) or green (500 nm; green) light pulses of 0.5 s duration and 0.5 Hz frequency.

What emerged from these alternative dose-response experiments in the absence of light switching was a completely different trend. In dark conditions or under green light, alloswitch-1 evoked a similar dose-dependent inhibition of mGlu₅, and illumination with violet light only induced a rightward shift in the potency of the NAM, similar to what observed with end-point IP-One experiments.

Then, the unexpected results observed in **Figure 36c** should be attributed to some other factor at play. Taking into account that the receptor over-activation was only observed when violet light was switched on after the initial dark condition or a green light period, we thought that overactivation could be related to the transient, rapid nature of the switching events. Violet light promotes a fast photoisomerization of *trans*-alloswitch-1 to the *cis* isoform, which results in a sudden drop in concentration of the *trans* isomer. If we assume that the *trans*-isoform is the active-NAM, and the *cis* isoform is not an active-PAM as we initially thought, but an inactive-NAM, then photoisomerization of alloswitch-1 could result in the ‘apparent PAM’ effect due to an abrupt receptor reactivation occurring when the *trans*-NAM was withdrawn. In other words, *trans*-to-*cis* isomerization could be inducing a ‘rebound effect’ on the receptor function, but only when the receptor has been inactive for some time before the withdrawal of the active-NAM.

The possible effects of such a sudden change in allosteric modulator concentration were difficult to address with non-photoswitchable allosteric modulators in calcium imaging experiments. We tried to mimic such a situation by perfusing a control mGlu₅ NAM through a fast-washout chamber that allowed exchanging the chamber volume in a few

seconds. This relatively rapid washout of fenobam failed to evoke a comparable ‘rebound effect’ after persistent inhibition (**Figure 40**), but faster methods (e.g. local perfusion using a pipette or a piezo-actuated perfusion barrel) should be tested to investigate such ‘rebound effect’.

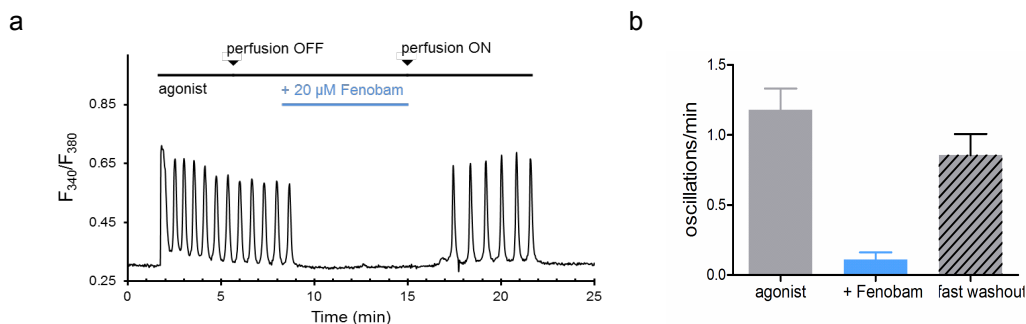


Figure 40 | Fast washout of Fenobam does not increase frequency of calcium oscillations. (a) Example trace of intracellular calcium (fluorescence ratio F_{340}/F_{380}) of an mGlu₅-transfected HEK cell loaded with Fura-2 and imaged under continuous perfusion (except in between arrowheads). Presence of agonist (3 μ M quisqualate) corresponds to black line. Presence of 20 μ M Fenobam corresponds to blue line. Perfusion of agonist is switched back on in correspondence to second arrowhead, to induce the fast washout of Fenobam. No line corresponds to perfusion with bath solution. (b) Frequency of calcium oscillations (oscillations/min) after agonist application and until addition of Fenobam (3 μ M quisqualate, grey bar), during Fenobam application (10 or 20 μ M, blue bar), and after fast washout of Fenobam (dashed bar). Data are represented as mean \pm s.e.m.; n=8 cells from 4 independent experiments.

Overall, these results defined relevant questions regarding photoswitchable ligands, which were beyond the scope of this thesis, and will be addressed in future research (see **Appendix – III** for further discussion).

3.1 Alloswitch-1 in the absence of orthosteric agonist

Another type of experiment that we initially performed in the attempt to solve the ‘apparent cis’ problem, raised instead another interesting question.

We did real-time experiments to see the eventual effects of alloswitch-1 over mGlu₅-expressing cells in the absence of orthosteric stimulation (**Figure 41**). At the beginning of the calcium imaging experiments the cells were challenged with the orthosteric ligand quisqualate to check their oscillatory response. Then, the agonist was washed away and calcium went back to basal values. After washout of the agonist, alloswitch-1 was added to the bath in dark conditions, and after some minutes light was switched on, consisting in 3 periods of violet light alternated with 2 periods of green light. As expected, when

alloswitch-1 was delivered to the cells nothing happened, in accordance with its NAM nature. Unexpectedly, under violet light calcium oscillations were restored in the cells initially responding to quisqualate, and were terminated by green light. Moreover, the experiment continued with a thorough washout of alloswitch-1, after which the cells were stimulated again with the agonist, and with the same light periods as in the case of alloswitch-1. The results were even more surprising: the response to the agonist was now reduced compared to the initial one (**Figure 41b**), and the photoswitchable control over the calcium oscillations persisted even in the absence of alloswitch-1.

From this set of experiments we hypothesized two issues. First, that alloswitch-1 could be acting over mGlu₅ independently of the agonist and induce a 'rebound effect' that was released upon withdrawal of the *trans* isomer under violet light, and, second, that its binding to the receptor is permanent, and we did further experiments to clarify these issues.

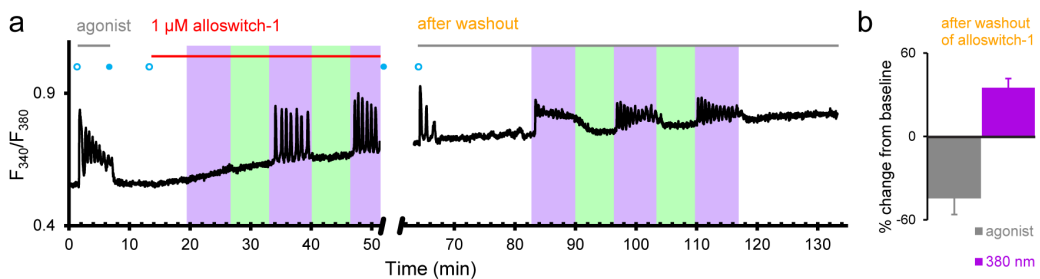


Figure 41 | Alloswitch-1 activates optically mGlu₅ even in the absence of agonist, and light responses are maintained after washout.

(a) Example trace of an individual cell transiently expressing mGlu₅, challenged with the mGlu₅ agonist quisqualate (3 μM; grey lines), and then washed out. Cyan dots indicate washout perfusion turned off (open) or on (filled). Cell was then incubated with alloswitch-1 alone (1 μM; red line), and violet (380 nm) or green (500 nm) illumination was switched on during times indicated by color boxes to check for optical control of mGlu₅. After thorough washout of alloswitch-1, the same amount of agonist was applied again, and stimulations with light were repeated like in the first part of the experiment. Perfusion was used only during the washout steps. (b) Quantification of the cell response to agonist (3 μM quisqualate; grey bar) or agonist and light (380 nm; violet bar) after the washout of alloswitch-1 (n = 2). Only oscillating cells were used for this quantification.

Initially, we attributed the agonist-independent effect of alloswitch-1 to the known constitutive activity of mGlu₅ (Ango *et al.* 2001). However, HEK cells are known to extrude a considerable amount of glutamate in few hours-time, which could accumulate in the extracellular medium and account for the oscillations seen in presence of alloswitch-1 and violet light. So we repeated the experiment with continuous perfusion of alloswitch-1 (**Figure 42**), to discard any possible accumulation of the endogenous ligand

of mGlu₅ interfering with our test. Actually, when alloswitch-1 was continuously perfused the light-dependent oscillations disappeared, therefore our hypothesis of alloswitch-1 regulating the constitutive activation of mGlu₅ might be wrong. In contrast, in the second part of the experiment the agonist response was still reduced after removal of alloswitch-1, and the light-dependent responses still present, supporting the idea of alloswitch-1 having an off-rate of many minutes or even permanently binding to mGlu₅ receptors. However, the slowing down of the oscillatory frequency during the last cycle of violet light strongly indicates that this long-lasting effect of alloswitch-1 results from a transient rather than permanent interaction with the receptor.

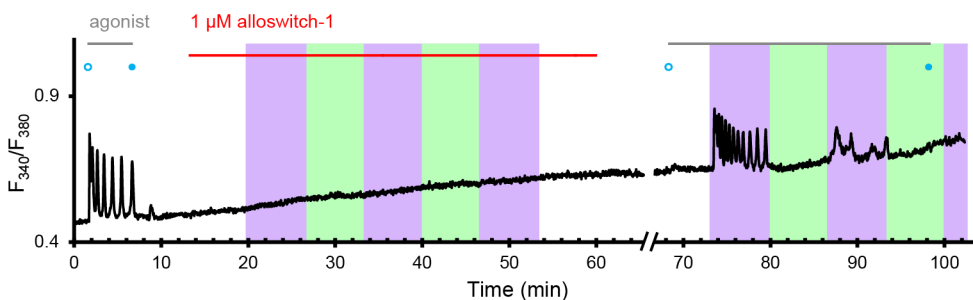


Figure 42 | Optical activation of mGlu₅ is not possible when alloswitch-1 is continuously perfused in the absence of agonist, but is persistent after its washout in the presence of agonist.

Example trace of an individual mGlu₅-expressing cell treated as shown in **Figure 41**, but with perfusion on at all times except during addition of agonist. Cyan dots indicate washout perfusion turned off (open) or on (filled). Alloswitch-1 (1 μ M; red line) was constantly perfused to avoid accumulation of glutamate in the bath upon extrusion by cells.

To finally check this, we repeated the whole experiment but adding a final step where the cells were perfused with a high concentration of MPEP (**Figure 43**). This potent mGlu₅ NAM was meant to displace any residual but unbound alloswitch-1, and should have had no effect on permanently bound alloswitch-1 molecules. After perfusing and washing MPEP, the cells were stimulated one more time with agonist and violet and green light. If alloswitch-1 was permanently bound to mGlu₅, the light-responses should still be present. However, this was not the case, although the results are not convincing since the cells failed to respond to the last application of agonist. This could depend both on the technical difficulties of performing such long experiments on living cells, or on the possibility of MPEP masking the alloswitch-1 binding in some unpredictable way.

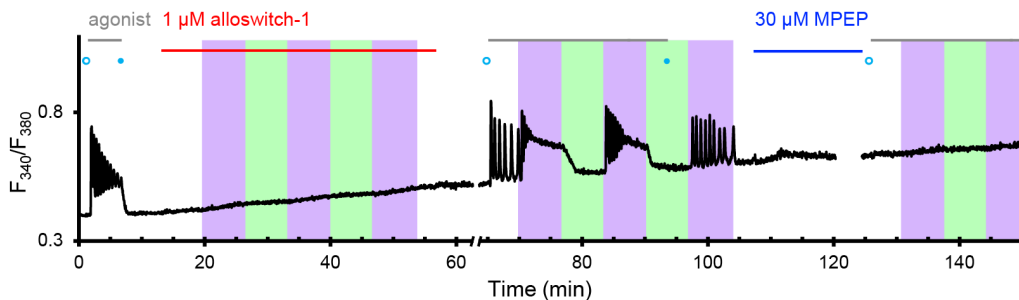


Figure 43 | Optical activation of mGlu₅ after washout of alloswitch-1 is absent after displacement by MPEP.

Example trace of an individual mGlu₅-expressing cell treated as shown in **Figure 42**, but with an additional incubation with an excess of the mGlu₅ NAM MPEP (30 μM; blue line) that was meant to displace the residual alloswitch-1. After about 20 min, MPEP was washed out and cells treated again with agonist and illumination as indicated in figure. Cyan dots indicate washout perfusion turned off (open) or on (filled).

Future challenges

Several open questions remain, including whether *cis*-alloswitch-1 can bind the receptor, and what is the affinity of its eventual binding, and the off-kinetics of its unbinding. An unequivocal answer could come from radioligand binding experiments, where an allosteric ligand labeled with a radioactive atom could be incubated in cell membranes containing mGlu₅ together with different amounts of alloswitch-1 under violet light. Radioactivity would then be assessed to estimate the displacement of the probe, and thus the effective binding of the *cis* isoform to mGlu₅ together with the kinetics of this process. However this presented some technical difficulties, both for doing the experiment under a light source and for finding a radiolabeled non-photolabile mGlu₅ NAM with potency similar to alloswitch-1, and these experiments were not tried.

Another possibility would be doing this with a FRET biosensor, whereby *cis*-alloswitch-1 binding to the sensor could induce conformational changes.

However, no sensors are available for testing allosteric activation of mGlu receptors, and their development would be challenging because FRET pair should be formed by two red-shifted fluorophores to avoid overlap between their excitation or emission wavelengths and the absorption spectra of *trans* and *cis*-alloswitch-1. Note that azobenzenes are well-known fluorescence acceptors, *i.e.* quenchers (Chevalier *et al.* 2013), and since alloswitch would be located in the nanometric range from FRET donor-acceptor pairs, its phenylazopyridine could interfere with the FRET structural dynamics experiment even in the case of using sequential photostimulation.

Therefore, to respond these important questions we will need to wait for novel techniques for the measurement of the binding kinetics of reversible optical switches.

3.2 Effect of changing the illumination wavelength

By analyzing the absorption spectrum of alloswitch-1 after illumination with light between 300 to 550 nm, Xavier Gómez i Santacana established that the maximum *trans*-to-*cis* photoisomerization for alloswitch-1 was reached by illuminating the molecule at 390 nm (Pittolo *et al.* 2014). We performed calcium-imaging experiments in which alloswitch-1 was photoisomerized at light wavelengths above and below the established maximum of photoisomerization, to check if this peak was comparable in functional assays, and whether it was possible to modulate optically the frequency of calcium oscillations by simply changing the illumination wavelength.

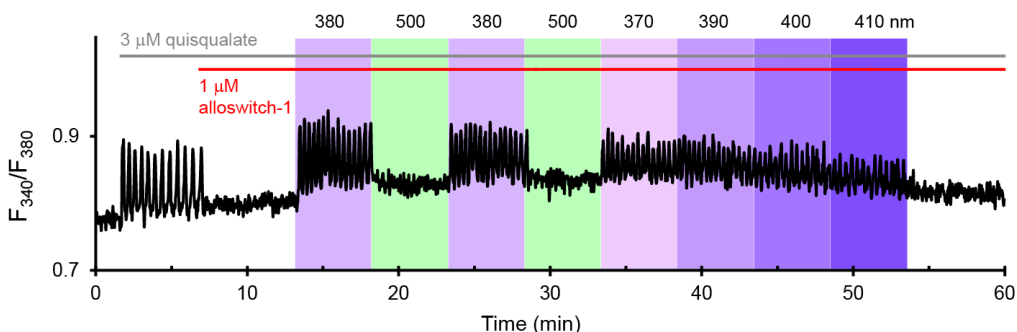


Figure 44 | Wavelength-dependence of alloswitch-1 effect.

Example trace of calcium imaging of an mGlu₅-expressing cell loaded with Fura-2 and challenged with the agonist (3 μM quisqualate, black), alloswitch-1 (1 μM, red) and different light wavelengths (color boxes and numbers expressing wavelengths in nm).

The results of the experiment depicted in **Figure 44** are summarized in **Chapter 3**, **Figure 62** and **Table 9**, where alloswitch-1 is referred to as compound **1a**. The peak inferred from functional experiments correlated well both with the absorption maximum of the *trans* isomer (380 nm) and the optimum wavelength for photoisomerization *in vitro* (390 nm). However, the FWHM was quite wide (85 nm, see **Table 9**), so that huge differences in activity were only found for 500 nm (**Figure 62**). Therefore, the frequency of calcium oscillations could not be significantly tuned by means of light at the wavelengths tested here.

3.3 Effect of changing the illumination pulse frequency

For calcium imaging experiments the same light source was used for both photoisomerization and imaging, so that constant illumination of alloswitch-1 was technically impossible. Unless otherwise indicated in the figure notes, for all experiments violet light was on during one second out of two seconds for the whole light period, so that 1 s of light on was followed by one second of darkness. We wanted to assess if this intermittent photoisomerization of alloswitch-1 could be affecting the functional response of the receptor. To do this, we designed experiments where two 5-minute periods of violet light were used to induce photoisomerization of alloswitch-1, each having different light-pulse frequencies (5 and 0.5 Hz) but equal amount of total light delivered (2.5 min). We did not notice relevant changes in the functional response of the receptor by applying this different illumination paradigm (**Figure 45a**), neither we did when inverting the order in the illumination frequencies (0.5 and 5, **Figure 45b**).

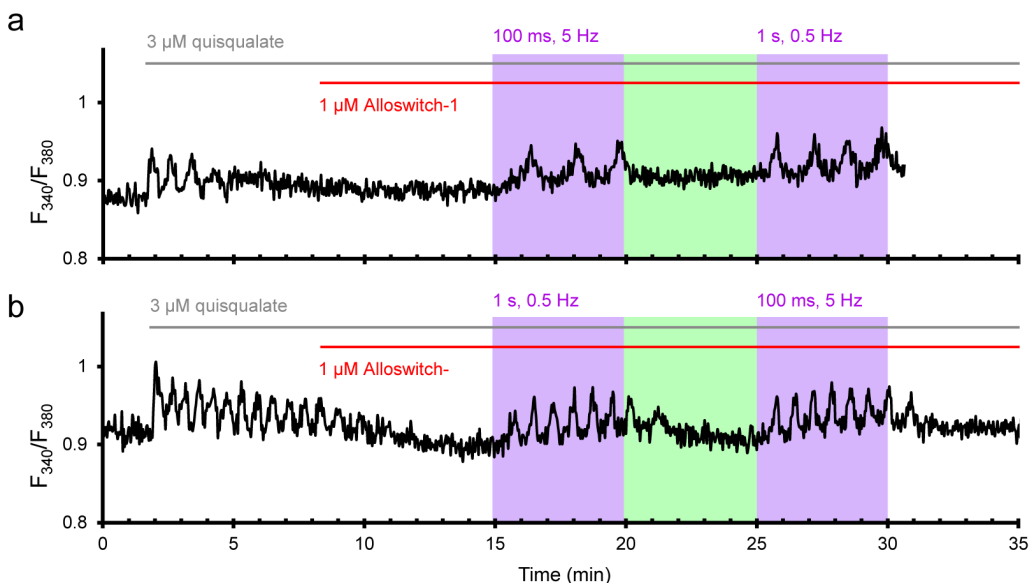


Figure 45 | Different illumination frequencies have no effect on the light-dependent activation of mGlu₅ by alloswitch-1.

Time course of intracellular calcium in mGlu₅-expressing cells, stimulated with agonist (3 μM quisqualate, black line) and alloswitch-1 (1 μM , red line), and illuminated with 5-min light periods of violet and green light (colored boxes). Frequency of violet illumination in the first and second light period was respectively 5 and 0.5 Hz in panel **a**, and the reverse in panel **b**.

These results were quite predictable, because the half-life of *cis*-alloswitch-1 in buffer is longer than the period we used for the intermittent photoisomerization. Therefore, it was

unlikely that once *cis*-alloswitch-1 had been induced in solution and the receptor activated, the isomer could undergo thermal relaxation to the *trans* inhibiting isomer before the following light period was switched on.

However, thanks to time-resolved techniques such as smFRET biosensors, we now know that the lifetime of the active conformation for mGlu₂ receptors is in the timescale of tens of milliseconds (Vafabakhsh *et al.* 2015), below the frequency of illumination that we tested here. Therefore, we believe that further characterization with techniques offering high temporal definition would be better suited to answer the important question raised here.

4 Alloswitch-1 controls endogenous mGlu₅ receptors

The results shown until now are based on the activation of mGlu₅ receptors overexpressed in a cell line. In the pursuit of more physiological contexts, we repeated real-time calcium imaging experiments with alloswitch-1 in secondary cultures of differentiated rat cortical astrocytes (**Figure 46a**). These cells endogenously express mGlu₅ receptors (Miller *et al.* 1995), and its orthosteric stimulation results in intracellular calcium oscillations (Nakahara *et al.* 1997). As astrocytes can also express mGlu₃ receptors (Bradley and Challiss 2012), the orthosteric stimulation by quisqualate was replaced by application of the more selective group I mGlu agonist dihydroxyphenylglycine (DHPG). The results were qualitatively comparable to those obtained with the overexpressed receptor. Alloswitch-1 blocked the calcium oscillations induced by DHPG in dark conditions and under green light but not under violet light, and fenobam inhibited the light-dependent activation of astrocytes (**Figure 46b**).

We then checked if the optical modulation of the response could fail in the presence of the endogenous ligand, so we repeated experiments in presence of glutamate. Although the response to glutamate differed from the one obtained with DHPG, the optical modulation of these cells was still possible in the presence of alloswitch-1 (**Figure 46c**).

Finally, control experiments in the presence of vehicle (0.1% DMSO, **Figure 46d**) were done to rule out any interference of light with astrocyte activation.

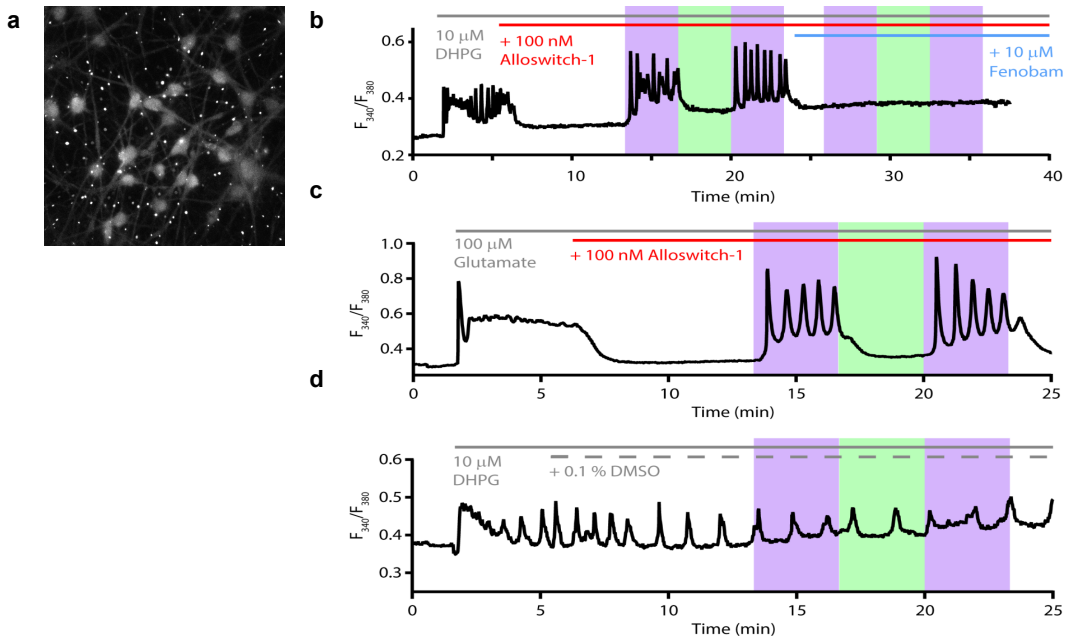


Figure 46 | Alloswitch-1 optically controls intracellular calcium signaling in astrocytes endogenously expressing mGlu₅.

(a) Image of Fura-2 loaded rat cortical astrocytes in culture as used for real-time experiments. (b-d) Representative traces of intracellular calcium time-course from astrocytes represented in a (calcium shown as fluorescence ratio F_{340}/F_{380}). Violet and green boxes indicate violet and green light illumination respectively. (b) Application of the mGlu_{1/5} selective-agonist DHPG (10 μ M, black line) induces calcium signaling in astrocytes, which is blocked by addition of 100 nM alloswitch-1 (red line), and is reversibly switched on and off with violet and green light, respectively. A non-competitive mGlu₅-selective NAM (10 μ M Fenobam, blue line) abolishes the optical control over the astrocyte in the presence of alloswitch-1. (c) Activation of an astrocyte with the endogenous ligand glutamate results in calcium mobilization and can be optically regulated using alloswitch-1. (d) Control experiment showing that agonist-induced (10 μ M DHPG, black line) calcium oscillations were not affected by application of vehicle (0.1% DMSO, grey line) and light.

With another set of experiments conducted in the absence of orthosteric ligands, we aimed at checking if alloswitch-1 could serve as an optical switch for astrocytes by acting on their basal activation. The results, although encouraging (**Figure 47**), are far from being conclusive since the experiments were not conducted under continuous perfusion. Similarly to experiments in cell lines, the absence of perfusion could bias the data, since there could be an accumulation of glutamate released by astrocytes in the imaging chamber (Perea and Araque 2007).

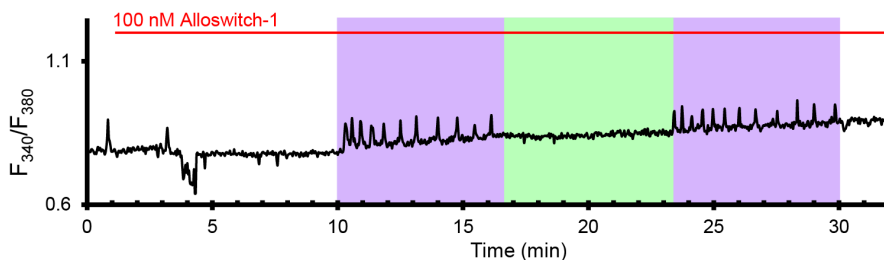


Figure 47 | Alloswitch-1 optically controls astrocytes with no need for addition of agonists. Representative trace of time course of intracellular calcium in a cultured rat cortical astrocyte loaded with Fura-2 (calcium shown as F_{340}/F_{380}) and only treated with 100 nM alloswitch-1 and violet or green light, as indicated by color boxes. The astrocyte shows some degree of spontaneous activity, as demonstrated by calcium oscillations occurring before and during the application of alloswitch-1.

We also tested alloswitch-1 in cultured hippocampal neurons. These cells are known to express $mGlu_5$, although at lower extent than astrocytes (Sun *et al.* 2013), and their electrical activity be modulated by group I $mGlu$ receptors (Graves *et al.* 2012). Although these were only preliminary experiments, we were not able to induce light-dependent calcium events in neurons. However, upon illumination with violet light we observed calcium transients in astrocytes contaminating the neuronal culture, indicating that the imaging conditions were adequate and alloswitch-1 was not degraded. Astrocyte responses might be due to $mGlu_5$ expression levels being higher in induced glial cells than in neurons. Future experiments could address with more appropriate techniques (e.g. electrophysiological recordings) the possibility of optically activating neurons with alloswitch-1, either directly or through the activation of astrocytes.

Overall, these results indicated that optical modulation through alloswitch-1 was also possible with endogenous $mGlu_5$ receptors, thus suggesting potential activity in physiological conditions.

5 Alloswitch-1 controls motility in *X. tropicalis*

In the previous sections we showed that alloswitch-1 allows control of both heterologous and native $mGlu_5$ receptors. In the perspective of using this optical switch in more physiological conditions or for therapeutic purposes, we needed to examine eventual effects of alloswitch-1 in living animals. All experiments in animals were done by Dr. Kay Eckelt, a former post-doc in our group.

We decided to use *Xenopus tropicalis* tadpoles because they are transparent at early developmental stages. This allows the delivery of light throughout the whole body, with no need for complicate implants of optical fibers, as required for mammals. Moreover, the putative mGlu₅ gene product shares high homology with the rat mGlu₅ in the TMD, where allosteric modulators are known to bind GPCRs (Pittolo *et al.* 2014).

We established a behavioral assay to monitor tadpole motility under different light conditions (**Figure 48**). In basal conditions and after the addition of either 25 μ M alloswitch-1, 100 μ M fenobam or vehicle, all groups showed similar motility. We then applied cycles of violet and green light to the animals. During violet illumination, control animals increased their motility, whereas tadpole movement was almost abolished in alloswitch-1 treated animals. After green illumination, the tadpoles recovered their basal motility, and the light-dependent behaviour induced by alloswitch-1 treatment was reversible for at least three violet-green light cycles. In contrast, fenobam treated animals showed normal swimming at both light wavelengths, although at slower rates than control animals, much probably as a result of the mGlu₅ inhibition.

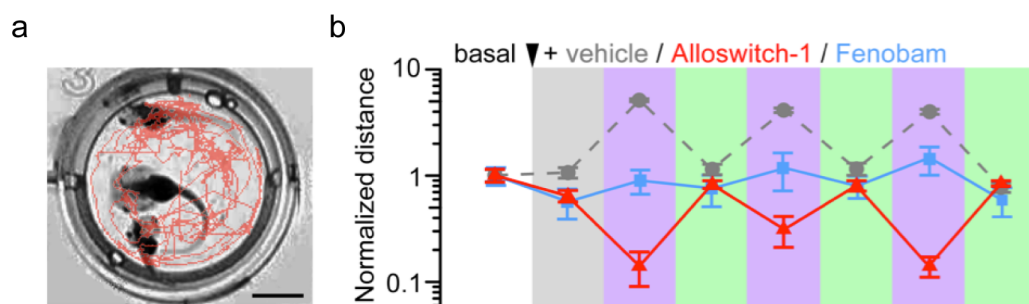


Figure 48 | Alloswitch-1 allows optical control of motility in wild type *X. tropicalis* tadpoles.

(a) Overlay image showing *X. tropicalis* tadpoles and their trajectories (red) during a behavioral experiment. Scale bar, 5 mm. (b) Quantification of tadpole motility as normalized distance before (basal) and after treatment (arrowhead; 25 μ M alloswitch-1, 100 μ M fenobam, vehicle; n = 20, 13 and 33 groups, respectively) and in different light conditions after treatment (dark, gray box; violet or green light, colored boxes). Values represent mean \pm s.e.m. from at least three independent experiments. Differences in motility are significant compared to baseline for vehicle or alloswitch-1–treated animals under violet ($p \leq 0.004$) but not green light. Reproduced from Pittolo, Gomez-Santacana *et al.* 2014.

Finally, the behavioral studies were repeated 24 hours after washing out alloswitch-1, and no differences in motility were found between animals previously treated with alloswitch-1 and control animals, as well as no dead animals, behavioral abnormalities or other signs of toxicity.

To conclude, alloswitch-1 was non-toxic at the tested concentrations and times (24 h), and allowed controlling the motility of wild type tadpoles with light. This suggests a potential to optically control mGlu₅ in a physiological context *in vivo*.

Chapter 2

Following a genuine medicinal chemistry approach, we included in a high throughput screening done in Montpellier by Dr. Xavier Rovira (IGF, Montpellier, France) not only the compounds described in the previous chapter, but also reaction intermediates and compounds derived from other ongoing projects in our laboratory. Luckily, one of these reaction intermediates was found to work as an optical switch for mGlu₄ receptors. In the following chapter we present this compound, which we named G4optoNAM, and its optopharmacological characterization in both *in vitro* and *in vivo* assays.

1 Photochemistry and pharmacology of G4optoNAM

The UV-visible absorption spectra of G4optoNAM analyzed in DMSO (**Figure 49b**) showed that this molecule is a red-shifted azobenzene-based compound. Its absorption peaked as a wide band in the blue wavelength range (420 to 460 nm), and illumination with 430-nm light promoted a nice isomerization of *trans*-G4optoNAM to the *cis* isomer. This change was reversed by applying red light (630 nm).

The UV-visible absorption spectra recorded in buffer (**Figure 49c**) revealed that G4optoNAM is a fast-relaxing azobenzene-based switch. During thermal relaxation, the half-life of the *cis* isomer was estimated to be around 8 ms. Interestingly, this should enable 'photodriving' the system with a single light wavelength.

The synthesis of the molecule and its photochemical characterization was done by Dr. Ana Trapero, a former PhD student in the group of Dr. Amadeu Llebaria and a post-doc at IBEC, as a precursor of a photoswitchable tethered ligand of ionotropic glutamate receptors analogous to MAG and GluAzo (**Section 3.2** of the **Introduction**).

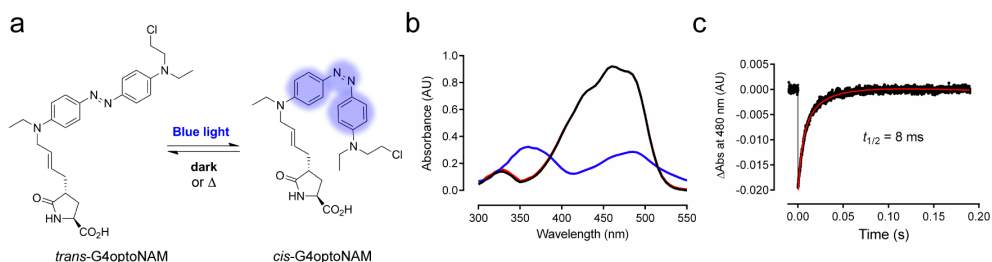


Figure 49 | G4optoNAM absorption is dynamically regulated by a single light wavelength.

(a) Schematics illustrating *trans*-to-*cis* photoisomerization of G4optoNAM under blue light (420–460 nm), and *cis*-to-*trans* fast relaxation in dark conditions. (b) Absorbance spectrum of G4optoNAM in DMSO in dark conditions (black line) and after illumination with 430 nm light for 3 min (blue line) or 630 nm light for 1 min (red line). (c) *Trans*-to-*cis* photoisomerization of G4optoNAM (50 μ M, PBS:DMSO 98:2) after a single ns laser pulse at $\lambda_{\text{exc}} = 355$ nm ($t = 0$), and *cis*-to-*trans* thermal relaxation occurring in the dark with a half-life of 8 ms. Red line corresponds to monoexponential fitting of the experimental data. Reproduced from Rovira *et al.* (submitted).

We next examined the effect of *trans*-G4optoNAM on mGlu₄ by IP-One HTRF assay (**Figure 50**), which revealed that the molecule in its relaxed configuration is an allosteric antagonist of both basal and agonist-mediated mGlu₄ activation.

These results were obtained by establishing dose-response relationships of the agonist L-AP4 in presence of G4optoNAM (**Figure 50a**). Increasing concentrations of the molecule induced a reduction of the efficacy and potency of the orthosteric ligand, as well as a decrease in the basal activity of the receptor, suggesting that G4optoNAM acted at the allosteric binding site of mGlu₄.

To fully test the possible allosteric activity of the molecule, we performed a series of experiments where the receptor was allosterically activated by a well-known ago-PAM, VU0155041 (Niswender *et al.* 2008), and competition with increasing concentrations of G4optoNAM was evaluated. This was done in either the wild type receptor (**Figure 50b**), a receptor containing a mutation that made it insensitive to glutamate (YADA, **Figure 50c**) or a truncated version that lacked the VFT domain where orthosteric agonists bind (**Figure 50d**).

The results confirmed that G4optoNAM could compete with the allosteric activation of mGlu₄, and the interaction of G4optoNAM with the receptor did not occur at the orthosteric ligand-binding site. Moreover, the observed decrease in basal activity became even more evident in the case of the truncated receptor, suggesting an inverse agonist effect similar to what observed for alloswitch-1 with mGlu₅.

The pharmacological characterization of the molecule in dark conditions with the IP-One assay was done entirely by Dr. Xavier Rovira (IGF, Montpellier, France).

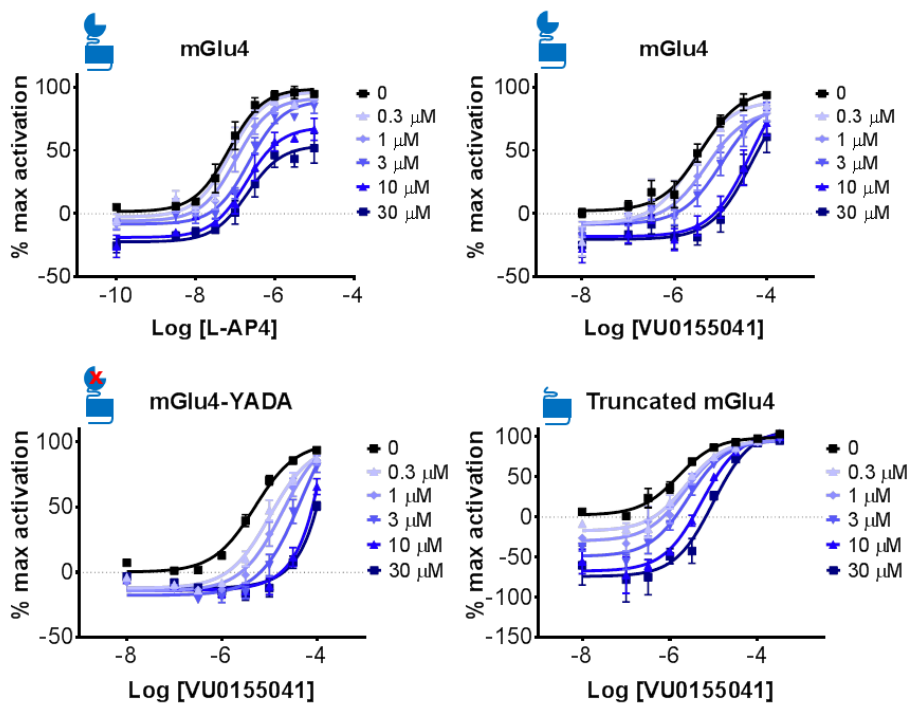


Figure 50 | G4optoNAM is a negative allosteric modulator of mGlu₄.

Dose-response curves of the orthosteric agonist L-AP4 or the allosteric agonist VU0155041 in presence of different doses of G4optoNAM in wild type (top graphs) or mutated mGlu₄ receptors (bottom graphs). mGlu₄-YADA is glutamate-insensitive (bottom left), whereas truncated mGlu₄ lacks the glutamate-binding VFT domain (bottom right). Reproduced from Rovira *et al.* (submitted).

Overall, pharmacological characterization of G4optoNAM highlighted that the molecule is a first-in-class NAM of mGlu₄, given there is no availability of such compounds commercially, in contrast with a high number of PAMs available for this mGlu subtype (Gregory and Conn 2015). Moreover, the photochemical characteristics of this compound make it even more interesting, anticipating the possibility of controlling optically native mGlu₄ receptors with a single, redshifted wavelength. With these premises, we proceeded to analyze the optopharmacological behaviour of G4optoNAM in calcium imaging experiments in individual cells.

2 Real-time optopharmacology of G4optoNAM

As in the case of alloswitch-1, the technique that we selected to measure the optical switching of G4optoNAM in real-time was imaging intracellular calcium in individual living cells. Since signaling initiated by mGlu₄ receptors is not directly coupled to variations in intracellular calcium, we co-transfected the cells with mGlu₄ and the chimeric G_{i/q}α protein, similar to what is done for IP-One experiments.

The application of either glutamate or L-AP4, another mGlu₄ agonist, resulted in robust, sustained increases in intracellular calcium in cells expressing both the transfected vectors (**Figure 51a** and **51b**), which returned to basal values soon after washout. We repeated the initial stimulation with the agonist three consecutive times, to determine consistently the activation of mGlu₄ receptors. Moreover, the average receptor response was used as a reference for normalization of all following responses.

Then, perfusion was stopped and G4optoNAM applied in the dark. About three minutes later, blue light (430 nm) was switched on in two consecutive illumination steps, but in most cases no light-induced responses were observed. Only occasionally this resulted in a sustained calcium rise, which decreased to basal soon after light was switched off.

When L-AP4 agonist was added again, now the presence of 10 μM G4optoNAM strongly inhibited the activation of the receptor by L-AP4 (quantified in **Figure 51b**). However, illumination with blue light immediately released the receptor activation induced by the presence of the agonist in solution. In the following dark period, the NAM effect of the optical switch was rapidly restored, as anticipated by its fast relaxation dynamics. This light-dependent activation was consistently reversible.

Because mGlu₄ NAMs are not available on the market, for control experiments we chose the non-selective orthosteric mGlu antagonist LY341495. As expected, this compound was able to inhibit the response to the agonist in the same experimental setup, but its inhibitory effect was not light-dependent.

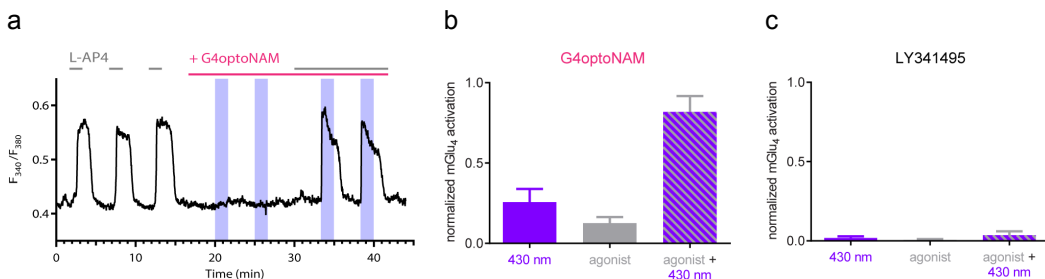


Figure 51 | Inhibition of mGlu₄ by G4optoNAM can be suspended with blue light.

(a) Time course of intracellular calcium (F_{340}/F_{380}) in an mGlu₄/G_{i/q} transfected cell, challenged with the agonist L-AP4 (0.3 μ M, grey bars), in absence or presence of G4optoNAM (10 μ M, magenta bar). Blue boxes indicate illumination at 430 nm. (b, c) Quantification of agonist (1 μ M L-AP4) and light (430 nm) dependent mGlu₄ activation in presence of G4optoNAM (b, 10 μ M, n=12) or LY341495 (c, 100 μ M, n=3) from experiments as exemplified in (a). Mean \pm s.e.m., normalized to the baseline response (average of the three initial applications of agonist). Differences in receptor activation are significant compared to baseline during application of G4optoNAM for 430-nm light ($p < 0.05$) and L-AP4 ($p < 0.001$), and during LY341495 for L-AP4 ($p < 0.1$).

Also, different agonist concentrations were used, to check for possible variability in the cell response (Figure 52). When challenging the receptors with lower concentrations of L-AP4 (300 nM), the response to the agonist in the presence of 10 μ M G4optoNAM seemed to be even lower than what observed at 1 μ M L-AP4, consistent with the relative proportion of agonist and NAM in solution. Remarkably, the normalized receptor activation induced by light in the presence of 300 nM L-AP4 and 10 μ M G4optoNAM was not only higher than that induced in the presence of 1 μ M L-AP4, but even exceeded the activation of the *naïve* cell recorded at the beginning of the experiment. This could either be due to an unknown mechanism at play, maybe faster desensitization of the receptor at higher agonist concentrations, or derive from the already mentioned effect of glutamate accumulation in the extracellular medium. However, G4optoNAM could not be tested during continuous perfusion, due to the limited amount of compound available.

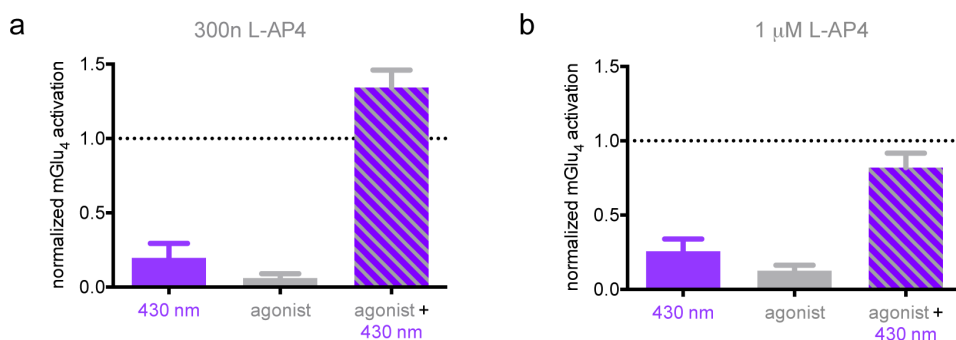


Figure 52 | Inhibition of mGlu₄ by G4optoNAM changes with agonist concentration and light.

Quantification of mGlu₄ activation in presence of different amounts of the orthosteric agonist L-AP4 (300 nM in a, n = 11; 1 μ M in b, n = 12) from experiments as exemplified in Figure 51a. Data presented as mean \pm s.e.m., normalized to the baseline response (average of the three initial applications of agonist).

In this first round of experiments we had also included a washout step at the end of the incubation of G4optoNAM, which we have not shown in the previous figure and we show hereafter (Figure 53). After washout, we perfused the agonist again, with the intention of demonstrating the full recovery of the receptor response. Unexpectedly, an equal

amount of agonist failed to induce a response equivalent to the initial one, and by repeating the illumination with blue light, most (although not all) cells still showed some degree of optical activation. This suggested a permanent effect of G4optoNAM over mGlu₄ receptors, which we will discuss in the following section.

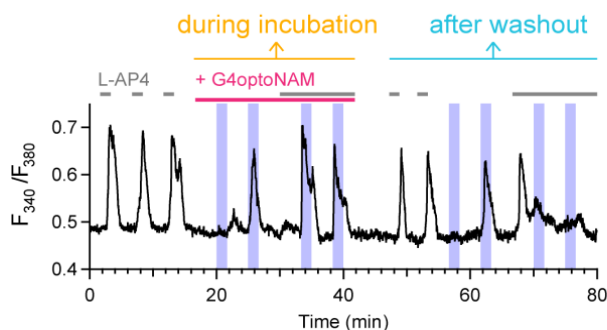


Figure 53 | Representative trace of a full-length real-time experiment including incubation and washout of G4optoNAM.

Time course of intracellular calcium (F_{340}/F_{380}) in an mGlu₄/G_{iq} transfected cell loaded with Fura-2, challenged with the agonist L-AP4 (0.3 μ M, grey bars), in absence or presence of G4optoNAM (10 μ M, magenta bar), with the same protocol for agonist application and illumination repeated after its washout. Blue boxes indicate illumination at 430 nm.

3 Probing the duration of G4optoNAM binding

The chemical structure of G4optoNAM was interesting because it contained a 2-chloroethyl substituent at one of the nitrogen atoms flanking the azobenzene moiety. Anticancer drugs presenting similar structure were demonstrated to exert their effect by crosslinking DNA thanks to the chloroethyl substituted nitrogen (Gandhi 2002), and molecules exploiting the same mechanism were designed as covalent ligands of class A GPCRs (Weichert and Gmeiner 2015).

Based on the first evidence of permanent effects of G4optoNAM over mGlu₄, we hypothesized that the same reactivity could exist between our optical switch and the receptor. We quantified the optical activation of mGlu₄-expressing cells during application of G4optoNAM and after its washout (**Figure 54g** and **54j**, respectively), which confirmed that the light-dependency of the NAM effect in the mGlu₄ expressing cells was maintained even after extensive washout (minimum 5 times the volume plus 5 minutes washout perfusion) of the allosteric ligand. Notably, the response to the agonist was slightly recovered after washout of G4optoNAM, as if the efficacy and this

was reflected in a diminished response to light. These observations indicate that, even if G4optoNAM were able to permanently bind the receptor, the efficacy or kinetics of such a conjugation would be limited or slow, or its effects over long timescales reversible (for example due to internalization and degradation of the labeled receptors).

For comparison, we next tested a photoswitchable but non-reactive G4optoNAM analogue, which should be unable to react chemically with the receptor residues. This molecule was synthesized by Dr. Ana Trapero (iQAC-CSIC, Barcelona) by substituting the reactive chlorine atom with an inert hydroxyl group (compound **2**, or G4optoNAM-OH; **Figure 54b**).

This chemical substitution resulted in an mGlu₄ NAM of lower potency (data not shown), so that all experiments were done by adding 30 μM of the compound. During its incubation, 'G4optoNAM-OH' provided a light-dependent inhibition of the receptor that was comparable to the one observed in cells treated with G4optoNAM (**Figure 54h**). In contrast, after washout of the inert compound the response of the cells was fully recovered to values similar to the initial ones, but no receptor activation was obtained during illumination (**Figure 54k**). To summarize, only the compound presenting the reactive chlorine was able to induce a long-term sensitization of the cells to light, thus suggesting that a chemical reaction was taking place between G4optoNAM and the receptor.

Finally, we repeated the same experiments using the non-photoswitchable and non-reactive mGlu antagonist LY341495 (**Figure 54c**). As expected, the compound fully inhibited mGlu₄ when bath-applied (**Figure 54i**), and after its washout the response to the agonist was fully recovered (**Figure 54l**). No optical responses were seen in cells treated with LY341495 at any time point.

The relationship between optical activation of mGlu₄ during incubation and after washout of either the reactive or inert G4optoNAM was plotted for individual cells (**Figure 55**), and highlighted that the response after removal of the compounds was increased for cells treated with the chlorine-substituted optical switch.

To further test the ability of G4optoNAM to establish a permanent interaction with mGlu₄, we designed a new set of experiments (**Figure 56a**) whereby an exceeding amount (30 μM) of either the reactive (**b, d**) or inert compound (**c, e**) was incubated during 10 minutes prior to any experimental procedure (including loading of the cells with the calcium indicator). After thorough washout of the compounds, we challenged the cells with 430-nm light and increasing concentrations of L-AP4.

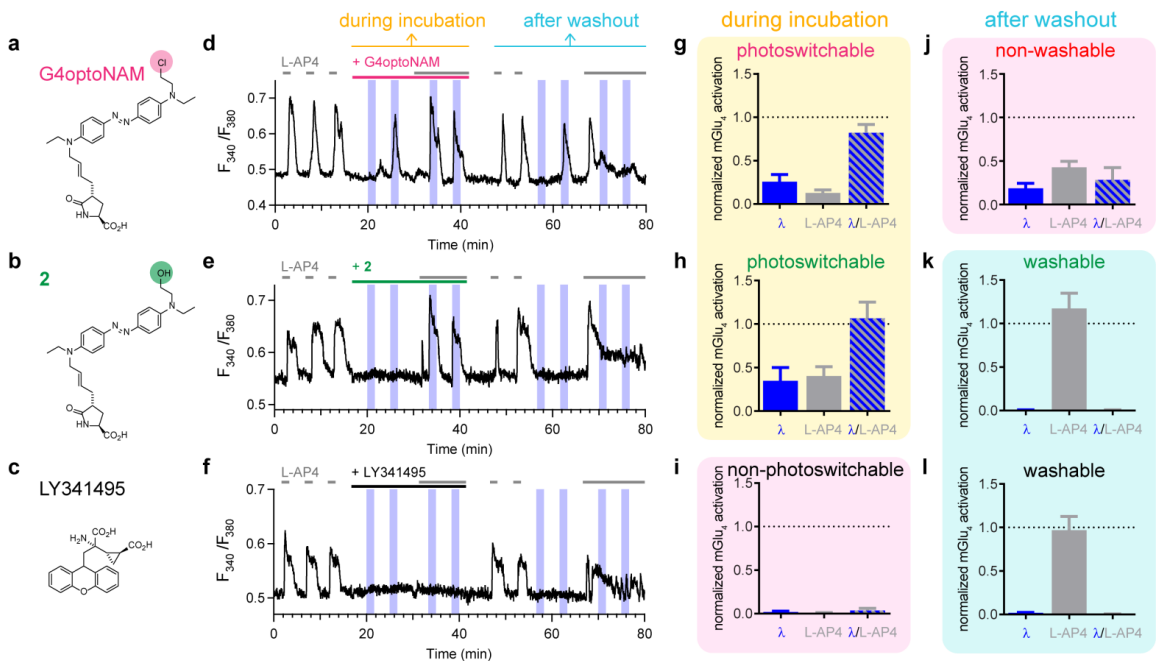


Figure 54 | G4optoNAM and the –OH substituted compound allow optical control of mGlu₄, but only G4optoNAM effects is permanent.

(a-c) Structures and nomenclature of the tested antagonists of mGlu₄. G4optoNAM (a) contains an azobenzene for the optical control of the molecule, and a chlorine atom that can react with receptor residues. Compound 2 (b) is equivalent to G4optoNAM, but the chlorine atom is substituted with a non-reactive hydroxyl group. LY341495 (c) is a non-photoswitchable non-reactive general antagonist of mGlu receptors.

(d-f) Time course of intracellular calcium dynamics expressed as fluorescence ratio (F_{340}/F_{380}) of the calcium indicator Fura-2 AM, in individual HEK tsA201 cells expressing mGlu₄ and the calcium signaling-transducer $G_{\beta\gamma q}\alpha$ protein. The cells were stimulated with the mGlu₄ agonist L-AP4 (grey; 0.3 μ M, d; 1 μ M, e and f) three times to check for mGlu₄ expression and signal transduction. After that, they were challenged with the same amount of agonist, but during the incubation or after the washout of one of the mGlu₄ NAMs (10 μ M G4optoNAM, magenta, d; 30 μ M 2, green, e; 100 μ M LY341495, black, f). Blue boxes indicate 430-nm illumination. Perfusion was interrupted during NAM incubation.

(g-l) Quantification of intracellular calcium increases in response to 430 nm-light alone (λ), agonist (L-AP4), or the combination of the two (λ /L-AP4), during incubation (g-i) or after thorough washout (j-l) of the inhibitors (G4optoNAM, g and j; compound 2, h and k; LY341495, i and l). The yellow box (g, h) highlights the typical behavior of the photoswitchable mGlu₄ NAMs G4optoNAM and 2. Their activity as mGlu₄ NAMs is observed in the reduced response to the agonist compared to the initial response. Moreover, as they are photoswitchable, they allow activating mGlu₄ by simply illuminating with 430-nm light even in the absence of agonist (λ), but to a bigger extent in presence of both light and agonist (λ /L-AP4). The light-blue box (k, l) indicates that the inhibitory and/or light-dependent activities of compound 2 and LY341495 over mGlu₄ are suppressed after washout. Red boxes (i, j) highlight either effects on mGlu₄ receptors that are non-photoswitchable (LY341495, i) or that do not disappear upon washout (G4optoNAM, j). Mean \pm s.e.m., normalized to the average mGlu₄ response to three initial applications of agonist. G4optoNAM, n = 12 cells (g, j); compound 2, n = 11 (h, k); LY341495, n = 3 (i, l). Reproduced from Rovira *et al.* (submitted).

G4optoNAM vs G4optoNAM-OH

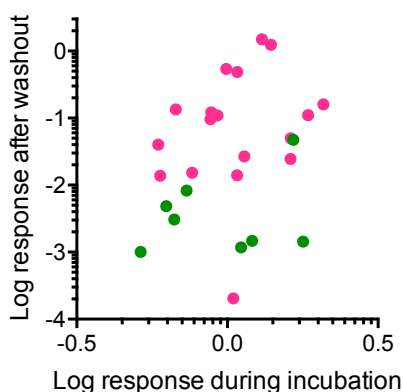


Figure 55 | Cell-by-cell analysis of the optical responses of cells treated with G4optoNAM and the –OH substituted compound.

Log values of the normalized receptor activation in presence of both agonist (1 μ M L-AP4) and illumination (430 nm) for experiments done as shown in **Figure 54d** and **54e**, for G4optoNAM (magenta; n=) and the –OH substituted compound (green). The optical response of a cell during incubation of the indicated compound is plotted against the optical response of the cell after its washout, to highlight residual optical activation of mGlu₄ receptors.

Each concentration of agonist was applied in dark conditions, and after that light was switched on and off two times to assess optical responses. Strikingly, only cells previously incubated with the chlorine containing optical switch displayed strong but reversible activation upon illumination (example trace in **Figure 56c**). In contrast, pre-treatment with the –OH substituted compound failed to induce light-dependent responses in all cells tested and regardless the concentration of the agonist (example trace in **Figure 56c**). Dose-response to agonist calculated either for dark conditions or under blue light showed that G4optoNAM treated cells reached maximal mGlu₄ activation in light conditions (**Figure 56d**), whereas G4optoNAM-OH treated cells responded to agonist in a dose-dependent manner but not to light (**Figure 56e**).

Altogether, these results point to a stable interaction being established between G4optoNAM and mGlu₄ receptors. However, this requires further investigation to be confirmed, for example by means of direct determination of the covalent conjugation sites in the purified or isolated receptor using mass spectrometry

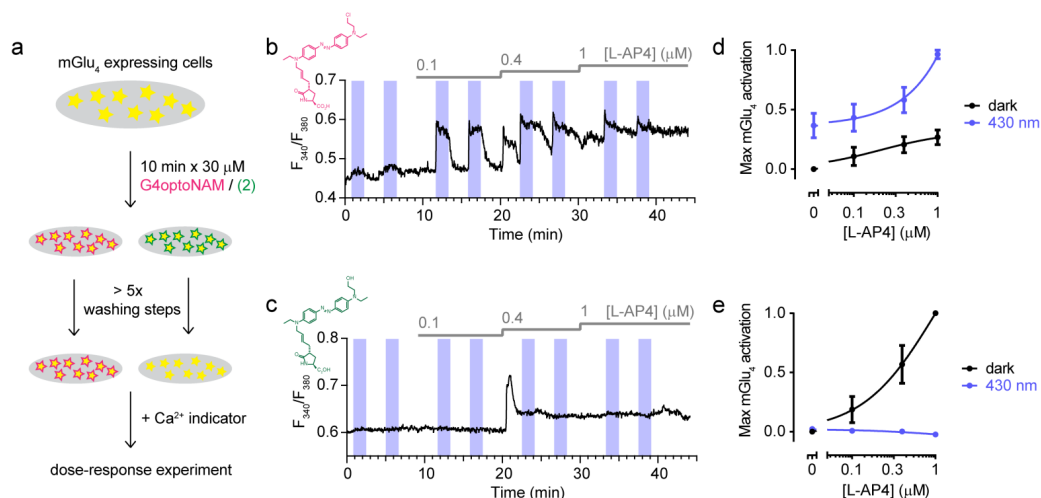


Figure 56 | Pre-incubation of cells with G4optoNAM and extensive washout do not eliminate inhibition of mGlu₄ and responsiveness to light.

(a) Schematics illustrating the pre-incubation protocol and experimental outcomes. HEK tsA201 cells overexpressing mGlu₄ and G_{i/o}α protein (yellow stars) were incubated with a solution containing 30 μM G4optoNAM (magenta) or the –OH substituted compound **2** (green), to allow binding of the NAM to the mGlu₄ receptors, and any possible reaction. After 10 minutes, the compounds were removed and the cells washed extensively. The first washing steps were done with washing solution containing 2% DMSO, to maximize solubility and removal of the compounds. Then, the cells were loaded with the calcium indicator Fura-2 AM during 30 min, and after this were ready for dose-response experiments shown in **b** and **c**. (**b**, **c**) Time course of calcium indicator fluorescence ratio (F_{340}/F_{380}) from individual cells, challenged with light (430 nm, blue boxes) and application of increasing concentrations of agonist (grey lines; 0.1, 0.4, and 1 μM L-AP4), after pre-incubation with 30 μM G4optoNAM (**a**) or compound **2** (**b**). Responses to light were observed in cells previously treated with the chloride-containing G4optoNAM, but not with the –OH substituted compound **2**.

(**d**, **e**) Quantification of intracellular calcium increases from experiments exemplified in **b** and **c**, respectively, displayed as mean ± s.e.m. and normalized to the maximum calcium increase observed cell by cell ($n \geq 5$ cells). The calcium increases observed immediately after application of agonist and before light illumination were quantified as responses of the mGlu₄ receptors in the dark. Calcium variations were discarded after the maximum response was reached (in panels **b** and **c**, after 0.4 μM L-AP4). Pre-incubation with G4optoNAM (**d**), did not allow a full activation of mGlu₄ in dark conditions with respect to illumination with 430 nm-light, suggesting that the compound was still exerting an inhibitory effect over mGlu₄. Responses to light were seen even in the absence of mGlu₄ agonist (0 μM L-AP4). Instead, pre-incubation with compound **2** (**e**) allowed a full dose-response to L-AP4 in dark conditions, and gave no responses to light at any concentration of agonist. Reproduced from Rovira *et al.* (submitted).

We did controls in untransfected HEK cells for both real-time-incubation and pre-incubation experiments (**Figure 57a** and **57b**, respectively). As expected, no optical responses comparable to the ones observed with photoswitchable compounds emerged from these trials.

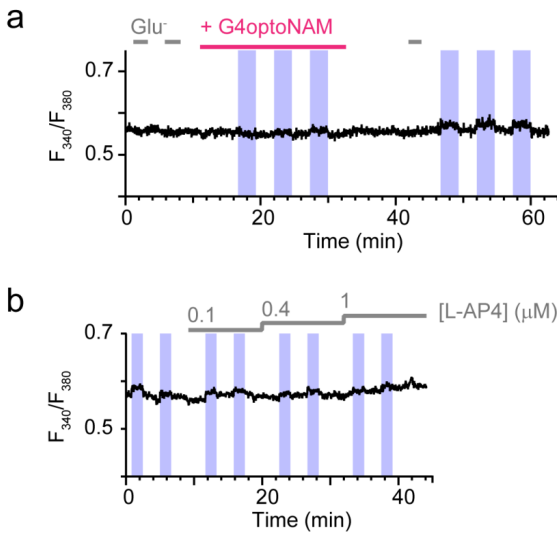


Figure 57 | Non-transfected cells do not respond to mGlu₄ agonists, light, or G4optoNAM.

Time course of calcium indicator fluorescence ratio (F_{340}/F_{380}) in wild type HEK tsA201 cells loaded with Fura-2 AM, in *naïve* cells (a) or cells pre-treated with 30 μM G4optoNAM (b) during 10 minutes. Traces represent experiments conducted as controls of those displayed in **Figures 54** and **56**, respectively, and described in the corresponding figure legends. We did not observe variations in intracellular calcium following application of mGlu₄ agonists (grey, 50 μM glutamate, a; 0.1, 0.4, and 1 μM L-AP4, b), 430-nm light (blue boxes), G4optoNAM (10 μM ,

a), or a combination of compounds and illumination in either experimental setup. We observed small increases in fluorescence ratio in correspondence with 430-nm light periods, which were however not comparable with the typical calcium increases in response to receptor activation in mGlu₄ and G_{i/q} α protein transfected cells.

The effects of a non-photoswitchable allosteric agonist (agoPAM, VU0155041) in calcium imaging experiments with mGlu₄/G_{i/q} α -transfected cells is shown in **Figure 58**. The agoPAM generated a sustained intracellular response in the absence of orthosteric activation. It is worth pointing out that small fluctuations in intracellular calcium were normally observed during prolonged activation of mGlu₄.

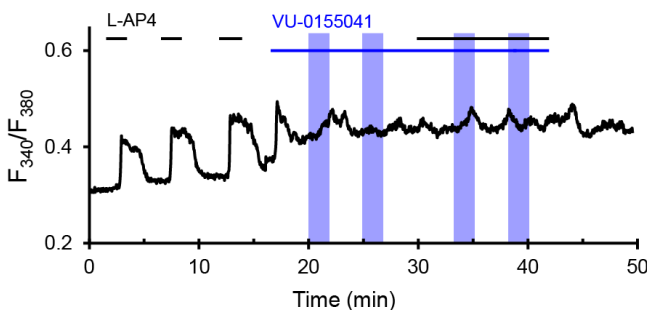


Figure 58 | Effect of non-photoswitchable agoPAMs on mGlu₄ signaling.

Time course of intracellular calcium (F_{340}/F_{380}) in a HEK cell transfected with mGlu₄/G_{i/q}. Black lines represent agonist application (300 nM L-AP4), and the blue line addition of the mGlu₄ agoPAM VU-0155041 (10 μM). Illumination with 430-nm light is represented by color boxes. Perfusion was switched off just prior to the addition of the agoPAM.

In the present section we demonstrate that G4optoNAM acts at the allosteric binding site of mGlu₄ by inhibiting receptor activation, and this inhibition can be interrupted optically by illuminating with blue light, and quickly restored soon after light has been switched off. Receptor activation in presence of this optical switch and of light is robust and reversible, and is facilitated by the presence of the orthosteric agonist. Moreover, the presence of a chloroethyl substituent flanking the azobenzene makes the light-sensitization induced by this molecule over mGlu₄-expressing cells long lasting. However, we still need to confirm the nature of this stable interaction between G4optoNAM and its target receptor with more appropriate analysis tools. In the next section we will demonstrate the *in vivo* potential of this optical switch.

4 G4optoNAM and alloswitch-1 in Zebrafish embryos

We finally tested G4optoNAM in dark or light conditions *in vivo* by monitoring locomotion of zebrafish *larvae* with an Opto-Zebrabox setup (**Figure 59a**). Small aquatic animals like *Xenopus* tadpoles and zebrafish larvae have the advantage of being translucent and allowing straightforward delivery of light, expressing mGlu receptors homologues and allowing high throughput behavioural analysis with commercial measurement and analysis systems. Optimization of the technique for coupling with a light source and the experiments shown here were done by Dr. Xavier Rovira (IGF, Montpellier, France).

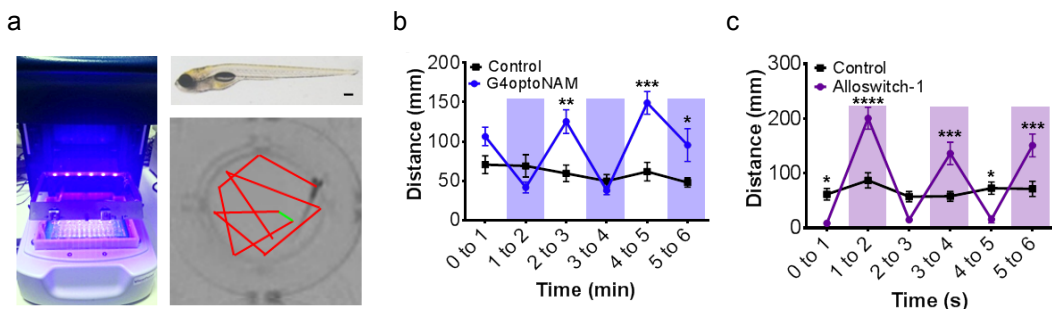


Figure 59 | G4optoNAM and alloswitch-1 control zebrafish *larvae* motility with different light wavelengths and with opposite tendencies.

(a) The Opto-Zebrabox setup allows monitoring zebrafish *larvae* locomotion in 96-well plates during illumination (scale bar 200 μ m). Red line represents the trajectory of an animal into a well. (b-c) Measure of the distance traveled by zebrafish embryos in a well per unit of time (1 min) in dark conditions or under illumination with blue (430 nm, b) or violet light (380 nm, c). Color boxes represent light periods. The effects of 10 μ M G4optoNAM (b) and alloswitch-1 (c) over zebrafish motility were light-dependent but showed opposing trends.

Data correspond to mean \pm s.e.m. of 12 animals in experiments performed over two different days. Statistical differences from control are denoted for adjusted p-values as follows: *p < 0.05, **p < 0.01, ***p < 0.001, and ****p < 0.0001. Reproduced from Rovira *et al.* (submitted).

Zebrafish treated with G4optoNAM (10 μ M, **Figure 59c**) showed increased locomotion compared to control animals, which was reversed to baseline upon illumination with 430-nm light. The opposite situation was observed in animals treated with alloswitch-1 (**Figure 59c**), with measured free-swimming distance comparable to control animals or lower in dark conditions, but significantly higher under 380-nm light.

As already mentioned, all mGlu receptors are involved in the modulation of synaptic transmission, but while activation of mGlu₄ receptors acts at the presynaptic terminal to reduce neurotransmitter release, activation of postsynaptic mGlu₅ facilitates synaptic transmission. Therefore, the differential effects observed by treating zebrafish with G4optoNAM or alloswitch-1 are in accordance with the opposed biological roles of their target receptors.

Chapter 3

The design and synthesis of alloswitch-1 was straightforward and successful as described in **Chapter 1**. However, by azologization of both amides in the parent compound we had obtained also another photochromic molecule (**Figure 24c**). This was inactive at mGlu₅, and mainly differed from alloswitch-1 for bearing an azobenzene instead of a phenylazopyridine. We observed that the presence of a pyridine is common among many mGlu₅ NAMs and PAMs (Gregory *et al.* 2012). With the objective of synthesizing a library of optical switches for mGlu₅, we decided to maintain the phenylazopyridine core of alloswitch-1, and modify the chemical substituents around this core to see how these changes affected the affinity of the ligand for mGlu₅, or its photochemical or optopharmacological properties. All compounds were synthesized by Xavier Gómez i Santacana (iQAC-CSIC), who also characterized their photochemical and IP accumulation properties.

1 Description of the library of alloswitches

We designed derivatives of alloswitch-1 (also indicated as **1a** in this chapter) where the external phenyl ring of the original molecule was substituted with more bulky phenyl rings (**1b** and **1c**, containing an additional chloride atom in position 4, and a benzophenone, respectively), aliphatic moieties (**1d**, **1e**, and **1f**, substituted with methyl, isopropyl, and cyclohexyl), less bulky phenyl groups (**1g** and **1h**, phenyl and 2-fluorophenyl), a heterocyclic ring (**1i**, thiazole), a pyridine (**1j**, **1k**, and **1l**, with the nitrogen in positions 2, 3 and 4, respectively), a bulky N-benzoylbenzamido substituent (**5**), and a 2-fluorophenyl urea (**6**). We also explored the effect of changing the pyridine in alloswitch-1 for a phenyl ring (compound **2**), since we had hypothesized that this part of the

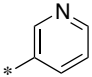
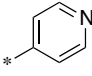
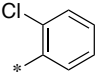
molecule was important for activity in mGlu₅. Finally, from compound **1j**, which interestingly presents a symmetric 2-pyridine at both ends, we changed the methoxy substituent in the central phenyl from position 3 to position 2 (**3a**), or removed it (**3c**). All compounds and the structures of their substituents are listed in **Table 8**, together with the results of photochemical and optopharmacological characterization.

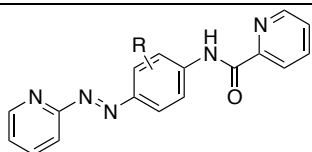
Table 8 | Structures, photochemical and optopharmacological properties of alloswitches.

1 X = N

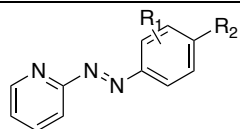
2 X = CH

Comp.	R	Max abs (nm)	PIS*	t _{1/2} (s)	IC ₅₀ ± sem (nM)	PPS**
1a		374	5	54	297 ± 77	5.1
1b		372	4	25	904 ± 82	7.1
1c		377	3	19	1884 ± 44	1.7
1d		374	4	489	183 ± 36	3.7
1e		374	4	556	30 ± 4	3.7
1f		377	5	353	76 ± 12	4.8
1g		377	4	71	180 ± 28	4.1
1h		375	3	65	308 ± 43	4.1
1i		377	4	41	328 ± 18	2.5
1j		382	4	134	309 ± 5	2.9

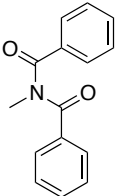
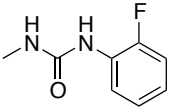
1k		373	1	15	356 ± 57	1.3
1l		372	1	13	1025 ± 257	1.2
2		366	5	187	4667 ± 392	2.5



Comp.	R	Max abs (nm)	PIS*	t _{1/2} (s)	IC ₅₀ ± sem (nM)	PPS**
3a	2-OMe	385	5	75	31661 ± 3601	n.m.
3c	H	358	5	322	3209 ± 269	n.m.



R₁ = 3-OMe

Comp.	R ₂	Max abs (nm)	PIS*	t _{1/2} (s)	IC ₅₀ ± sem (nM)	PPS**
5		329	3	46	1477 ± 265	3.3
6		387	5 [§]	10 [§]	2184 ± 663 [§]	12.3 [§]

* photoisomerization score (PIS), describes the effectiveness of the photoswitch from the change in *trans/cis* absorption spectra, on a scale 0 to 5

** photoinduced potency shift (PPS), describes the effectiveness of the photoswitch in IP-One assays, calculated as the ratio between IC₅₀ in dark and light conditions

[§] measured after illumination at 400 instead of 380 nm

n.m. not measurable (very high)

2 Photochemistry of alloswitches

Absorption peak of the trans isomer

Xavier Gómez i Santacana acquired the UV-Vis absorption spectra of all compounds of the alloswitch series by HPLC coupled to a PDA and a mass spectrometer, in aqueous buffer at pH 7.4 mixed with acetonitrile. This allowed separating the *trans* and *cis* isomers of the alloswitches by chromatography, acquiring the pure UV-Vis absorption spectrum of the *trans* and the *cis* isomer and determining their mass. From this analysis we could conclude that the majority of *trans*-alloswitches had absorption peaks at wavelengths similar or lower than that of alloswitch-1, except **6** that displayed a mildly redshifted peak at almost 390 nm (**Table 8**, column 3). Notably, this compound contains a urea, which is more electron-donating than the original amide. This is probably what causes the redshift in the absorption spectrum of **6**.

Effectiveness of trans-to-cis photoisomerization

Xavier Gómez i Santacana acquired the UV-Vis absorption spectra of all compounds at 25 μ M in DMSO before and after illumination with violet light (380 nm). This was used to identify the effectiveness of *trans*-to-*cis* photoisomerization of the different alloswitches, and was expressed as the 'photoisomerization score' (PIS, see **Table 8**, column 4). The compounds that were found to display the best PIS were alloswitch-1 (**1a**), **1f**, **2**, **3a**, and **3c**. When illuminated at 400 nm, compound **6** also displayed one of the highest PIS.

Thermal relaxation kinetics

Xavier Gómez i Santacana measured the thermal relaxation of all compounds, according to what described for alloswitch-1 in **Chapter 1** (**Table 8**, column 5). Compounds **1k** and **1l**, where the third phenyl ring of alloswitch-1 was substituted with a pyridine with meta- and para- nitrogens, displayed faster relaxation kinetics (< 20 s) than the symmetric pyridine in the ortho position (**1j**, 134 s). Other fast relaxing substituents are benzophenone (**1c**) and urea (**6**). Fast relaxation kinetics imply that the use of these optical switches would require almost constant illumination for maintaining the molecules in their *cis* configuration. In contrast, the half-life of thermal relaxation becomes much longer with substitution with aliphatic groups (**1d-f**) or removal of the 3-methoxyl (**3c**). Slow relaxing alloswitches do not need continuous irradiation, because once they reach the photostationary state they remain longer in the *cis* configuration. This represents an

advantage when photoisomerization relies on violet light, whose continuous irradiation could be harmful for cells and tissues.

3 Optopharmacology of alloswitches – IP-One assay

Xavier Gómez i Santacana performed all the IP-One assays at the IGF (Montpellier, France) under the supervision of Dr. Xavier Rovira, and obtained dose-response relationships for all compounds in dark conditions and under violet light (380 nm, except **6** that was illuminated at 400 nm). The calculated IC_{50} for experiments conducted in the dark are reported in **Table 8** (column 6), together with the 'photo-induced potency shift' (PPS, column 7) that represents the IC_{50} ratio between the dark and light conditions, and gives an idea of the efficacy of the photoswitch in the IP-One assay. The results are striking, since almost all compounds were active as mGlu₅ NAMs, with nanomolar potency in line with the precursor alloswitch-1 (**1d**, **1g-k**) or even higher for the methyl and isopropyl substitutions (**1e-f**). All other compounds showed micromolar potency, which however was above 5 μ M only for the 2-OMet symmetric pyridine (**3a**). For compound **2**, where the phenylazopyridine was substituted by an azobenzene, the potency is 5 μ M, which confirms our expectations about the importance of this group for the effective binding to mGlu₅. Moreover, an interesting effect was observed in another kind of assay, where **2** induced only partial inhibition of mGlu₅. This again could be related to the lack of the azopyridine moiety, but this possibility won't be discussed here. The shift in potency upon illumination with violet light (PPS) was observed at variable extents for all compounds, with no correlation to their potency in dark conditions. However, we did not detect significant ameliorations compared to alloswitch-1, which already showed very good photoswitching in cell assays. In this aspect, the compounds showing best performance were **1b**, **3c**, and **6** (when illuminated with 400 nm).

4 Real-time optopharmacology of alloswitches

We performed real-time calcium imaging experiments, similar to what described in **Chapter 1** for alloswitch-1, for all alloswitches plus another phenylazopyridine-containing mGlu₅ NAM (see **Section 4.1**). These experiments with the library of alloswitches were aimed at identifying the best compounds and the optimal wavelengths for optical

activation of mGlu₅. Therefore, after the usual violet-green light cycles applied to verify reversibility of the switch, we added a series of light periods of different wavelengths and build wavelength-response relationships for all the compounds in the series. In **Section 4.2** we exemplify our experimental approach by focusing on two compounds of the series (**3c** and **1f**), whereas the entire set of results is presented in **Section 4.3**.

4.1 SIB-1757

Strikingly, SIB-1757 (Varney *et al.* 1999) had emerged during the initial bibliographic search for ‘azologizable’ allosteric modulators of mGlu receptors being an mGlu₅ NAM that already included in its structure a phenylazopyridine (**Figure 60a**, ref. We tested SIB-1757 in calcium imaging experiments similar to what was done for alloswitch-1, and although the molecule showed a weak but clear NAM activity on mGlu₅-expressing cells (at 10 but not 1 μ M, **Figure 60c** shows a representative trace from 10 μ M experiments), we could not observe any light dependency in its inhibition of the receptor. This result was confirmed by the lack of change in the absorption spectrum of the molecule upon illumination (**Figure 60b**), which could be due to either ineffective photoisomerization or superfast relaxation kinetics that could not be detected with our analysis system.

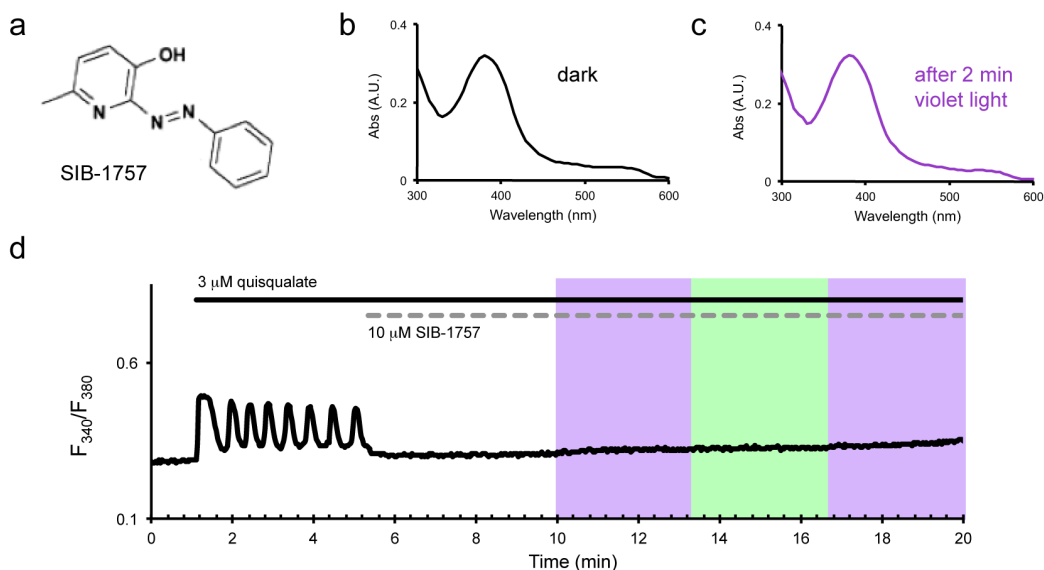


Figure 60 | The azo-containing mGlu₅ NAM SIB-1757 is not photoswitchable.

(a) Structure of the mGlu₅ NAM SIB-1757, composed by aryl and phenyl rings separated by an azo. (b) Absorption spectra of 25 μ M SIB-1757 in DMSO, in dark conditions and after illumination

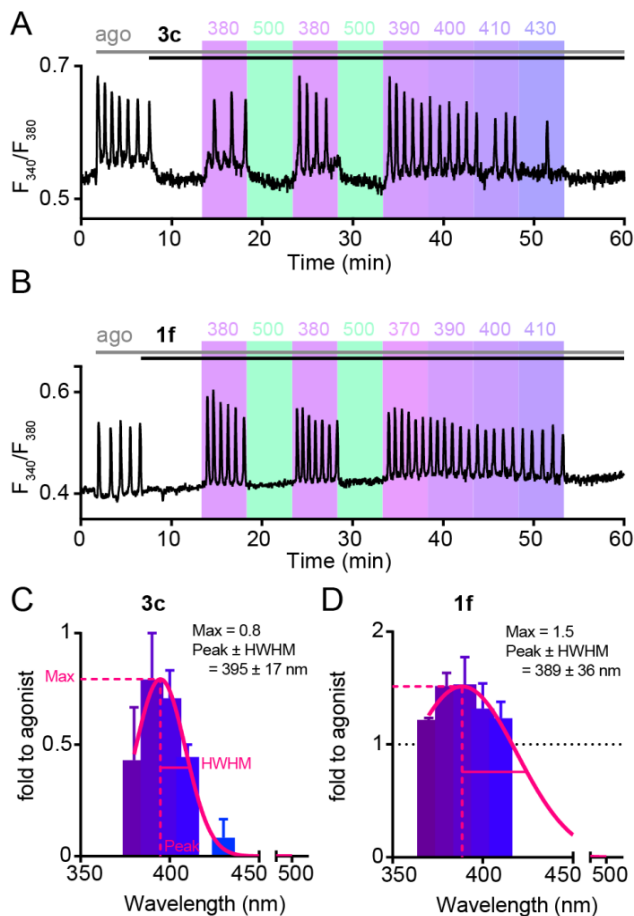
with 380-nm light. (c) Time course of intracellular calcium in an HEK cell overexpressing mGlu₅, loaded with Fura-2 and challenged with agonist (3 μM quisqualate) to induce calcium oscillations, and inhibited by 10 μM SIB-1757, in both dark conditions and under illumination with violet or green light (in order: 380/500/380-nm light; 0.5 s illumination every other 2 s; total duration of light periods was 3.3 min).

4.2 Wavelength-response relationship of alloswitches

We selected compounds **3c** and **1f** as representatives for exemplifying the experimental setup used for real-time calcium imaging of alloswitches. These compounds emerged from endpoint experiments as the ones displaying best photoswitching or highest potency and best photoswitching.

The real-time calcium imaging of mGlu₅-expressing HEK tsA201 cells was done as usual, the cells stimulated with the orthosteric agonist (3 μM quisqualate) for about 7 minutes to produce calcium oscillations. After this, an alloswitch was added, at a fixed concentration of 1 μM, to silence the receptor responses. After about 7 more minutes, the usual violet-green light cycles were applied, to verify the efficacy of the *trans*-to-*cis* transition in releasing the receptor activity, and its reversibility by green light. After this, we applied a series of light periods of diverse wavelengths, above and below the absorption peak of the *trans* isomer for each compound in steps of 10 or 20 nm (see examples of experiments in **Figure 61a** and **61b**). We counted the oscillatory frequency of cells for each treatment and light condition, and normalized it to the initial response to the agonist for comparison between different cells and compounds. From these data we selected the responses measured under different illuminations to build wavelength-response relationships (**Figure 61c** and **61d**), which we fit to a Gaussian function to infer the three parameters that define the curve. One was the light wavelength at which the maximum activation was obtained (Peak), then the extent of this maximum receptor activation expressed as fold to agonist (Maximum), and finally the half-width at half-maximum (HWHM), which represents a measure of how wide is the range of wavelengths that allow half the maximum receptor activation. In other words, we identified a range of wavelengths for the best photoisomerization of the compound, and the plasticity in the receptor response.

Figure 61 | Light-dependency of mGlu₅ inhibition by compounds **1f and **3c**.**



(a-b) Fluorescence ratio (F_{340}/F_{380}) over time of calcium indicator Fura-2 loaded in mGlu₅-expressing HEK cells. Cells were challenged with an mGlu₅ agonist (ago, grey line, 3 μ M quisqualate), 1 μ M of compound (a) **3c** or (b) **1f** (black lines), and with different illumination wavelengths (six, ranging between 370 and 500 nm) indicated by color boxes and corresponding numbers above. (c-d) Quantification of the light-induced receptor activity in the presence of (c) **3c** or (b) **1f** at indicated illumination wavelengths. Data are mean \pm s.e.m. of the normalized calcium oscillation frequency. Frequency of calcium oscillations during an illumination period (5 min) was calculated as number of oscillations per minute, and normalized to the initial response to the agonist. Peak, full width at half maximum (FWHM; HWHM is half FWHM) and maximum (Max) values were inferred by fitting a Gaussian function (magenta curve) to the data shown in graph.

We can observe in **Figure 61a** and **61b** that both **3c** and **1f** inhibited the calcium oscillations initiated by the agonist, and could switch them on and off reversibly when illuminated with violet and green light. However, the range of wavelengths for the optical activation of mGlu₅ was narrower for compound **3c**, indicating that optical activation of mGlu₅ with this compound is only possible at well-defined wavelengths. In contrast, optical activation of mGlu₅ by compound **1f** admits illumination with more diverse wavelengths.

Moreover, the maximum receptor response induced by **3c** was lower than those observed with **1f**, indicating that **3c** could barely restore optically the full receptor response whereas optical activation of mGlu₅ with **1f** even exceeded the initial receptor response. However, this could be due to the low amount of compound used with respect to its potency. In fact, we used **3c** at a concentration well below its potency as measured with IP-One assays (1 μ M compound against a potency of almost 5 μ M). Therefore, the

results observed here could derive from an incomplete occupancy of the receptors by the optical switch, which then could induce a limited or partial receptor response.

Hereafter we show the wavelength-response relationships for the entire library of alloswitches (**Figure 62**) and the list of parameters inferred from the Gaussian fitting of the data (**Table 9**).

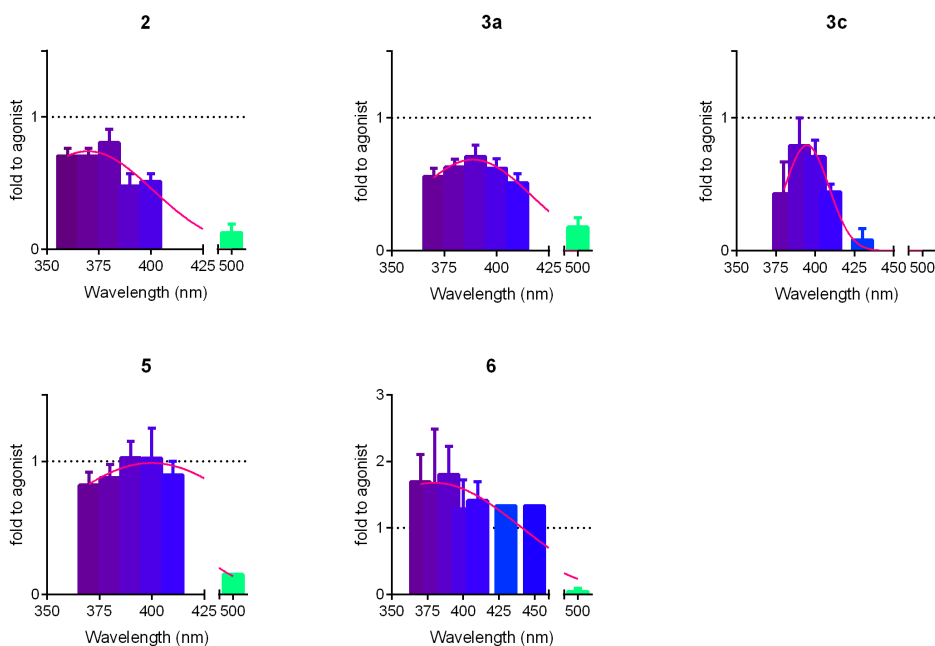


Figure 62 | Wavelength-activity relationship for all compounds in single-cell experiments.

Normalized light-induced activity spectrum of HEK tsA201 cells expressing mGlu₅ and treated with agonist (3 μ M quisqualate) plus 1 μ M of compounds indicated on top of graphs. Data were obtained by calculating the frequency of calcium oscillation during calcium imaging experiments in individual cells loaded with the calcium indicator Fura-2 AM, and conducted as exemplified in **Figure 61a** and **61b**. Frequency of calcium oscillations was calculated as number of oscillations per minute during an illumination period (5 min), and normalized to the initial response to the agonist (fold to agonist). Data are represented as mean or mean \pm s.e.m. of the normalized activity, and fitted to a Gaussian function using Prism 6.01 (GraphPad) to infer maximum (maximum activation of the receptor, as fold to agonist), peak (wavelength at which the maximum is obtained), and half width at half maximum (HWHM; half the range of wavelengths at which the activation of the receptor is half the maximum) of the curve. A list of the obtained values can be found in **Table 9**.

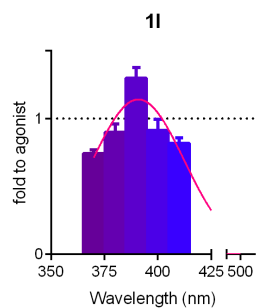
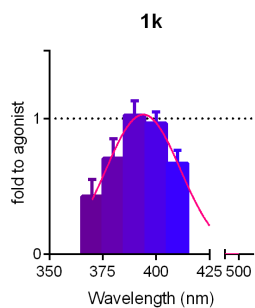
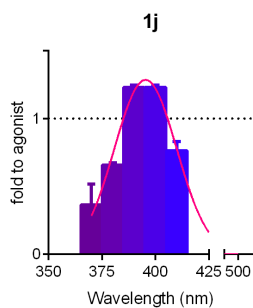
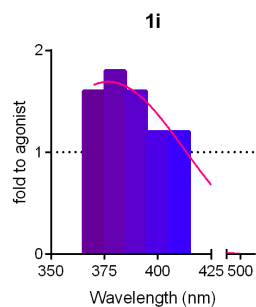
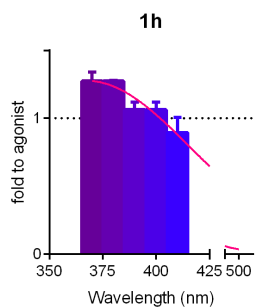
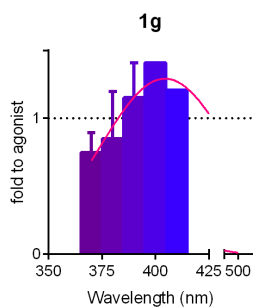
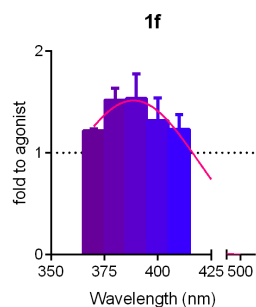
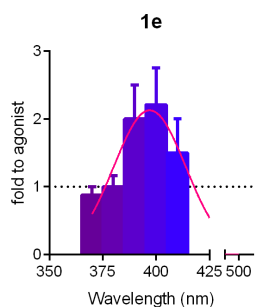
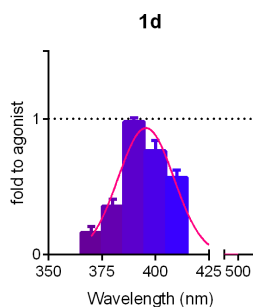
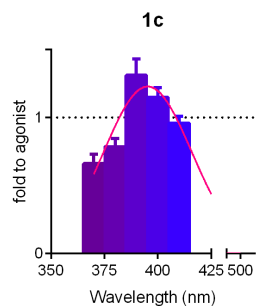
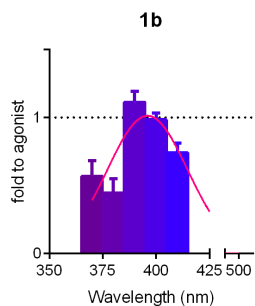
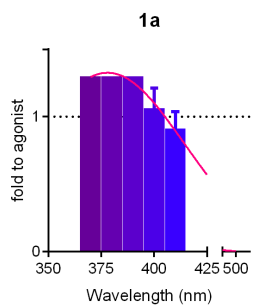


Table 9 | Summary of parameters inferred from the Gaussian fitting of single-cell data shown in Figure 61c and 61d.

Compound	Maximum (fold to agonist)	Peak (nm)	FWHM* (nm)	HWHM (nm)
1a	1.33	378	85	43
1b	1.01	396	44	22
1c	1.23	395	49	24
1d	0.93	396	31	15
1e	2.13	397	40	20
1f	1.51	389	72	36
1g	1.29	405	72	36
1h	1.28	368	116	58
1i	1.69	377	81	42
1j	1.29	395	34	17
1k	1.03	394	41	21
1l	1.14	391	51	25
2	0.74	370	73	37
3a	0.69	389	66	33
3c	0.79	395	33	17
5	0.99	400	119	59
6	1.68	380	143	72

*FWHM = 2 × HWHM

All compounds showed reversible photoisomerization at violet and green light illuminations, although the NAM effect of compounds **2**, **3a**, **5** and **6** was not complete, as we can observe by a residual receptor activity under green illumination (500 nm, **Figure 62**). These data are in accordance with the IC₅₀ obtained with the IP-One assay, which showed that **5** and **6** were NAMs in the micromolar range, and **2** and **3a** the less potent among the library. Moreover, all compound displayed quite different wavelength-response spectra, which were reflected in a variety of Peak, Maximum and HWHM parameters. We summarized graphically these three parameters for the entire library in **Figure 63**.

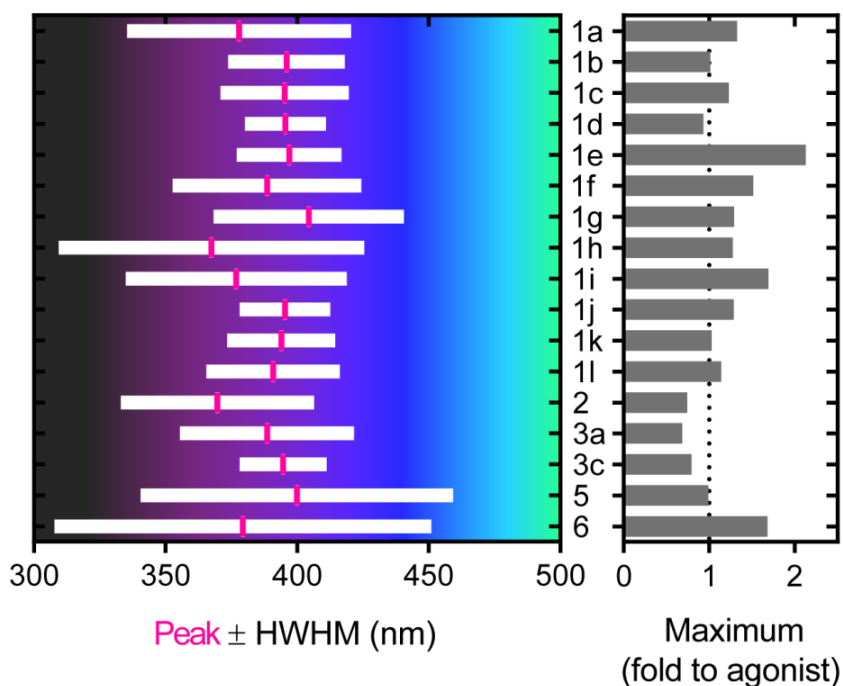


Figure 63 | Outline of wavelength-activity relationship in single-cell experiments for all compounds.

In the left graph, magenta bars indicate the illumination wavelength (Peak) at which the maximum light-induced receptor activity is obtained for the compounds indicated on the right axis. White bars represent the range of wavelengths at which the light-induced activity is equal to half the maximum response or more (half width at half maximum, HWHM). The maximum amplitude of the light-induced receptor activity is reported in the graph on the right, and expressed as times the response to agonist of the naïve receptors.

These three parameters (peak, HWHM, and maximum) describe the Gaussian fitting performed for all compounds on the original data from single-cell experiments, as shown for compounds **1f** and **3c** in **Figure 61c** and **61d**. Original data were obtained from calcium imaging experiments in individual cells (done as described in **Figure 61** and **61b**) by calculating the frequency of calcium oscillations in response to the agonist (quisqualate, 3 μM) and in presence of 1 μM of the indicated compound and of different illumination wavelengths, and finally normalized to the initial response to the agonist.

This figure should be looked at as a guide for the fast identification of the basic features of each alloswitch of the series, that are (1) the wavelength for best photoisomerization at which the maximum receptor activation is reached (Peak), (2) a range of wavelengths for which photoactivation of the receptor occurs satisfactorily (FWHM), and the maximum amount of receptor activation that can be achieved optically (Maximum). The ranking of the compounds following this classification is listed in **Table 10**.

Table 10 | Compound ranking by wavelength of maximum receptor activation (Peak), wavelength range for half-maximum activation (FWHM), and optical receptor activation (Max).

Peak	(nm)	FWHM	(nm)	Max	% R act.
1g	405	1d	31	1e	213
5	400	3c	33	1i	169
1e	397	1j	34	6	168
1b	396	1e	40	1f	151
1d	396	1k	41	1a	133
1c	395	1b	44	1g	129
1j	395	1c	49	1j	129
3c	395	1l	51	1h	128
1k	394	3a	66	1c	123
1l	391	1f	72	1l	114
1f	389	1g	72	1k	103
3a	389	2	73	1b	101
6	380	1i	81	5	99
1a	378	1a	85	1d	93
1i	377	1h	116	3c	79
2	370	5	119	2	74
1h	368	6	143	3a	69

FWHM = full width at half maximum; % R act. = % receptor activation

We have at our disposal an array of compounds displaying different combinations of these characteristics, which makes these molecules highly versatile, depending on the application required. For instance, if our experiment consists in the use of an optical switch in combination with a calcium indicator, but the indicator is excited at a similar wavelength than the optical switch, then we will prefer an alloswitch that has a narrow FWHM, so that the probability of interference between the optical switch and the calcium indicator is minimized. Instead, if we just want to stimulate the optical switch, but we dispose of a limited set of illumination wavelengths, and these do not correspond to the peak of the optical switch, we will choose an alloswitch with a wider FWHM, to be sure we can photoswitch it despite the limited availability of light sources.

Chapter 4

In **Chapters 1** and **2** we demonstrated that both alloswitch-1 and G4optoNAM can be switched on and off successfully in living organisms. We achieved this by illuminating the animals with an external LED light source, which is a very simple and cost-effective illumination method. However, the successful penetration of light was accomplished because we did the experiments at developmental stages whereby the animals were still translucent. This tradeoff goes at the expenses of biological significance of the results, and limited the study of the *in vivo* properties of our optical switches to fish and amphibians. In contrast, in intact nervous tissues, both *in vitro* (*i.e.* in brain slices) and *in vivo*, light is scattered and its penetration is limited. One possibility to overcome these difficulties is illuminating in the NIR range and using pulsed lasers to excite two-photon absorption processes like fluorescence and uncaging. These illumination conditions are required to penetrate through biological samples with minimal scattering and to achieve *in vivo* imaging of neuronal structures (Svoboda and Yasuda 2006) and excitation of optical switches (Carroll *et al.* 2015; Izquierdo-Serra *et al.* 2014; Matsuzaki *et al.* 2001). In this last chapter we consider the importance of photoswitching the optical switches described in the previous chapters with high spatial precision in the three dimensions, in the perspective of future applications in intact tissues or *in vivo*. Our main objective was to demonstrate that alloswitch-1 could be photoisomerized by using two-photon excitation (2PE), which would constitute the first demonstration that improving the spatial resolution of freely diffusible reversible optical switches is possible.

1 Two-photon excitation of alloswitch-1 in HEK cells

We used a laser scanning microscope setup (Leica TCS SP5 MP Confocal system) equipped with a pulsed IR laser (MaiTai Wide Band) whose power can be adjusted in less than 0.5 s, but has a much longer delay for changing the wavelength (~ 2 s/10 nm). So it would be advantageous to use the same wavelength for both measuring calcium and exciting alloswitch-1 (at low and high power, respectively). We thus expressed mGlu₅-eYFP in HEK cells and loaded them with the calcium indicator Fura-2, which has a good absorption under pulsed NIR light (Xu *et al.* 1996). We performed real-time two-photon calcium imaging at different light wavelengths in the NIR range (760 to 820 nm, with 20 nm steps). We did this during continuous stimulation with the orthosteric mGlu₅ agonist quisqualate (3 μ M), to check if the intracellular calcium oscillations initiated by mGlu₅ could be displayed by 2P calcium imaging with Fura-2 within the wavelength range expected for 2PE of alloswitch-1 ($390 \times 2 = 780$ nm; **Figure 64**).

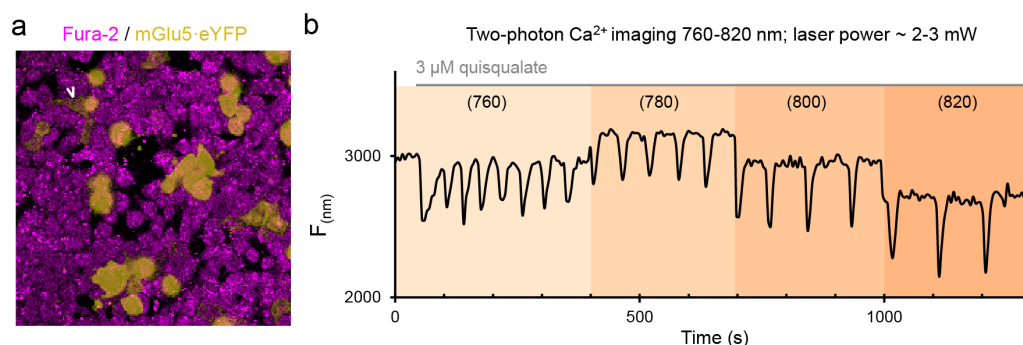


Figure 64 | Two-photon calcium imaging of mGlu₅-induced oscillations.

(a) Two-photon image of Fura-2 (magenta, 780 nm) overlapped with a one-photon image of eYFP fluorescence (yellow, 514 nm) to highlight cells expressing mGlu₅-eYFP. (b) Time course of two-photon calcium imaging at 760, 780, 800, and 820 nm (numbers in parenthesis and colored boxes) from an individual cell expressing mGlu₅ (white arrowhead in a) and challenged with the mGlu₅ agonist quisqualate (3 μ M, grey line).

In these control experiments we observed that the low laser power used for 2P calcium imaging was compatible with our model at all light wavelengths tested, since calcium oscillations were detected for the entire duration of mGlu₅ stimulation. However, basal fluorescence values and amplitude of the peaks varied during the stimulation. This was attributed to the different fluorescence and dynamic range of the calcium indicator at different excitation wavelengths, rather to real changes in intracellular calcium. In fact,

these artifacts can be observed in the sharp changes in basal fluorescence upon wavelength tuning, especially at longer wavelengths. Therefore, we interpreted qualitatively the amplitude of the calcium peaks when measuring the effectiveness of the 2PE of alloswitch-1.

Then, we set up 2PE experiments where a number of frames of 2P calcium imaging were followed by some frames of 2P calcium imaging intercalated with a high-power 2P scanning of the field of view at the same wavelength as used for imaging, until low-power 2P calcium imaging was restored for the rest of the experiment. This was done to induce the excitation of alloswitch-1 during the high-power scanning, and to simultaneously monitor the time course of intracellular calcium, before, during, and after 2PE.

We designed this protocol in the software controlling the TCF SP5 Confocal microscope (Leica Microsystems) and run a simulation of the real experiment with a fluorescent blue plastic slide (Chroma) normally used for calibration (**Figure 65**).

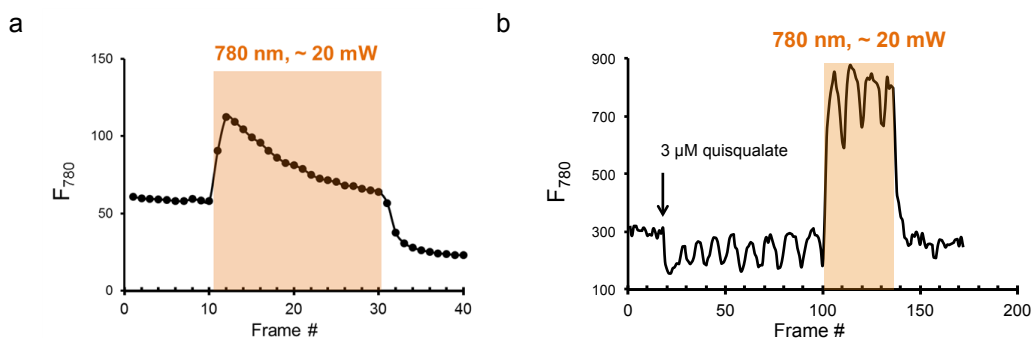


Figure 65 | Artifact observed in 2PE experiments.

Readout of two-photon imaging ($\lambda = 780 \text{ nm}$, 345 ms, power = 3 mW) of (a) a fluorescent blue plastic slide (Chroma) and (b) the calcium indicator Fura-2 loaded in an mGlu₅-expressing cell. Orange box represents two-photon excitation ($\lambda = 780 \text{ nm}$, 4.453 s, power = 20 mW; 2PE, see **Materials & Methods**), which for panel a started after acquisition of frame 10 and lasted 20 more frames. The scans were acquired every out of 5 s before and after 2PE, and out of around 7 s during 2PE for both images. (b) The mGlu₅ agonist quisqualate was added at timepoint indicated by the arrow.

This control evidenced an artifact (possibly a bug in the software that controls the microscope, or a slowly-decaying fluorescence process) whereby during 2PE (scanning at high-power) we detected increased fluorescence readout in the images scanned at low power. This increase reached a maximum at the second frame after 2PE was started, and slowly decreased and almost reached the basal fluorescence by the end of the 2PE period (which lasted here 20 frames). A similar increase in fluorescence was

observed during calcium imaging of a cell loaded with Fura-2, but was unable to mask the intracellular calcium oscillations induced by activation of mGlu₅ receptors (**Figure 65b**). Therefore, for 2P calcium imaging experiments in living cells we took into account this artifact, although we decided not to subtract it from the raw images in order to avoid any unnecessary manipulation of the original data.

Finally, we challenged mGlu₅-eYFP-transfected cells with agonist and alloswitch-1, and induced the photoisomerization of alloswitch-1 with both 2PE at 780 nm and, after a recovery time in the dark, 1PE at 405 nm (**Figure 66a** and **66b**), and vice versa (**Figure 66c** and **66d**). Note that the 405 nm continuous wave laser has a wavelength that is close to the alloswitch-1 isomerization maximum (390 nm) and is within the range for successful photoconversion of the molecule (**Figure 62**).

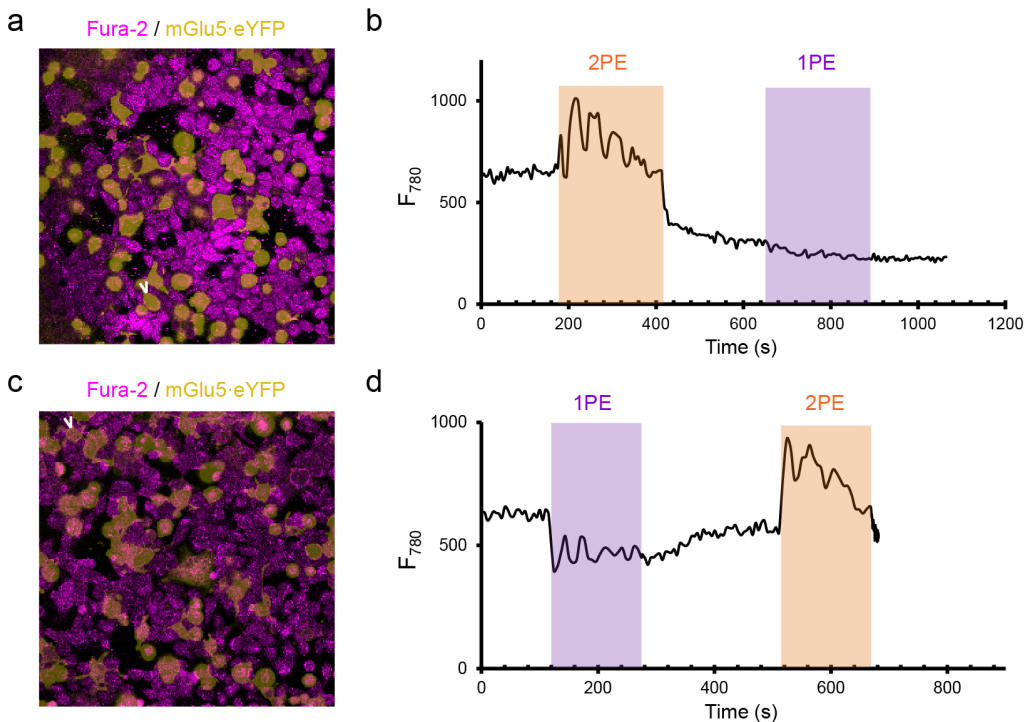


Figure 66 | Two-photon calcium imaging of mGlu₅-induced oscillations.

(a, c) Two-photon images of Fura-2 (magenta, 780 nm) overlapped with one-photon images of eYFP fluorescence (yellow, 514 nm) to identify mGlu₅-eYFP-expressing cells. (b, d) Time course of 2P imaging of Fura-2 in cells indicated by white arrowheads in a and c, respectively, and previously incubated with agonist (3 μ M quisqualate) and alloswitch-1 (1 μ M). Orange and violet boxes indicate 2PE at 780 nm (20 mW) and 1PE at 405 nm (20% nominal power in b and 10% in d), respectively.

The results indicated that by two-photon excitation at 780 nm we were able to selectively induce calcium oscillations in cells that expressed mGlu₅ receptors. The periodicity of

these oscillations was in line with the frequency of calcium events that we usually observed in HEK cells (about one event per minute). Moreover, we never observed calcium oscillations in cells that did not express mGlu₅, as inferred from eYFP images. These evidences strongly suggest that the oscillations observed during 2PE are due to an optical activation of mGlu₅ receptors thanks to *trans*-to-*cis* photoisomerization of alloswitch-1. However, we were not able to see control 1PE in the same cells after 2PE was over and a period in the dark had allowed the thermal relaxation of the compound. Since we observed a huge decrease in the basal fluorescence of the calcium indicator after 2PE was over, we hypothesized that during the scan at high power the indicator was bleached, and this impeded the subsequent detection of calcium oscillations. Therefore we repeated the same experiment but inverting the order between 1PE and 2PE (**Figure 66c** and **66d**). In this second case we were able to observe mGlu₅ activation at both one and two photons in the same mGlu₅-expressing cell. We repeated 2PE of alloswitch-1 at different wavelengths, ranging 760 to 820 nm in steps of 20 nm, and we quantified the light-dependency of the oscillatory frequency, as well as the onset time between the beginning of 2PE and the appearance of the first calcium peak (**Figure 67**).

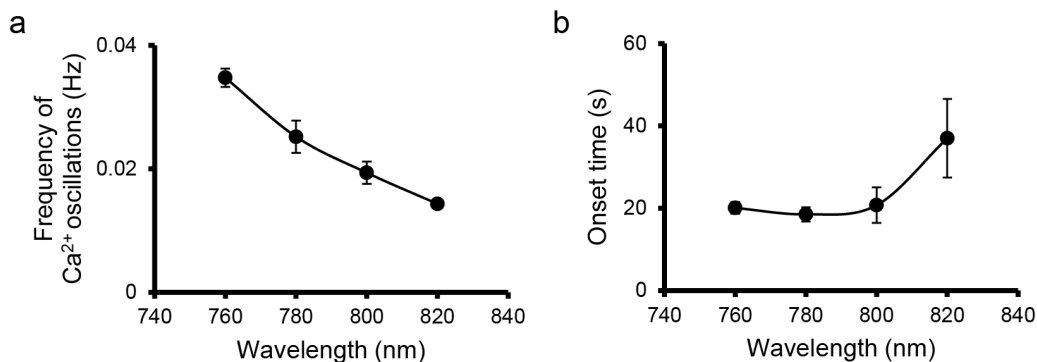


Figure 67 | Wavelength-dependence of frequency and onset time of calcium responses at 2PE of alloswitch-1.

(a) Frequency of calcium oscillations and (b) onset time of the first calcium peak during 2PE of alloswitch-1 at indicated wavelengths. Data are represented as mean \pm s.e.m.; $n = 4, 8, 3$ and 5 cells for $\lambda = 760, 780, 800$ and 820 nm, respectively. Only cells displaying two or more oscillations were analysed.

From these graphs we infer that the wavelength leading to faster 2PE oscillations of alloswitch-1 is 760 nm out of the wavelengths we tested. Moreover, we observed an inverse correlation between frequency of calcium oscillations and onset time of the first

peak The shortest the time needed to photoisomerize alloswitch-1, the highest the optical activation of mGlu₅.

2 Two-photon excitation of other alloswitches

We tested some other members of the alloswitch series, with the aim of identifying functionally compounds with better 2PE properties than alloswitch-1. In order to test a diversity of properties of alloswitches, we selected 4 compounds: **1j**, with properties similar to alloswitch-1 but containing a second polar pyridine, **1d**, the only compound lacking the third ring, **1c**, that contains a benzophenone and could act as a sensitizer for 2PE (Cai *et al.* 2005; Vendrell-Criado *et al.* 2013), and **6**, which is the compound with more red-shifted photoisomerization.

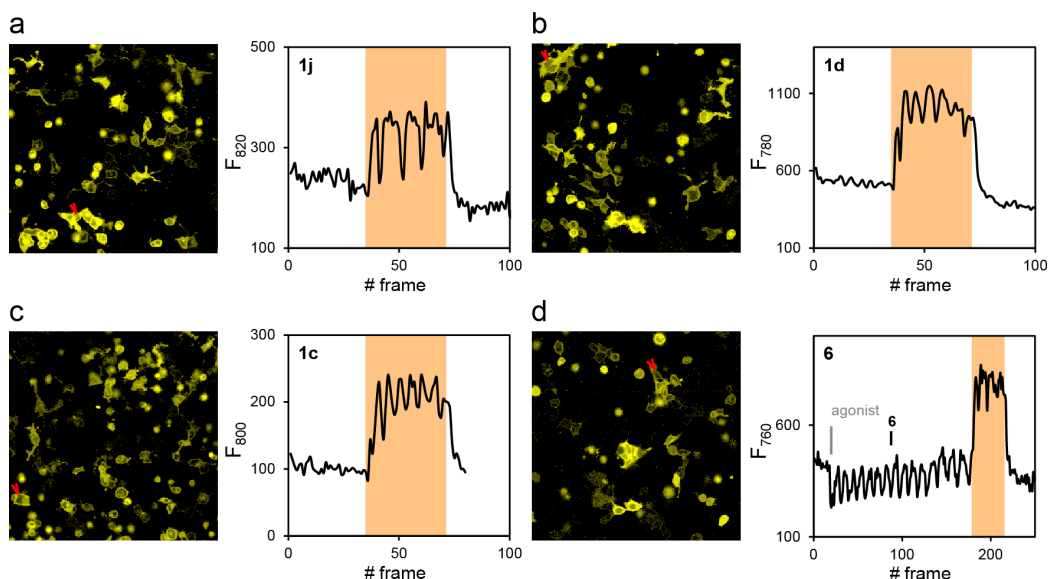


Figure 68 | Alloswitches 1j, 1d, 1c can be excited with different light wavelengths in the NIR part of the spectrum.

(a-d) Two-photon excitation (2PE, orange boxes) of alloswitches **1j** (a, 820nm), **1d** (b, 780 nm), **1c** (c, 800 nm), and **6** (d, 760 nm) in mGlu₅-eYFP expressing HEK cells loaded with the calcium indicator Fura-2. In the left part of each panel are shown eYFP fluorescence images, with imaged cells indicated by a red arrowhead. (a-c) The mGlu₅ agonist (3 μ M quisqualate) and the indicated compound were added at least 15 minutes before starting the experiments. (d) Alloswitch **6** failed to inhibit agonist-induced calcium oscillations. Timepoints for addition of agonist and **6** are indicated by a grey and black line, respectively. All alloswitches were applied at the same concentration (1 μ M).

We observed 2PE of 3 out of 4 alloswitches tested, at different NIR wavelengths as indicated in **Figure 68**. The general character of 2PE switching of azobenzenes (and azopyridines in particular) is evident from these results, although further experiments are needed to quantify the exact oscillatory frequency and onset time for each alloswitch, to allow quantitative comparisons among different compounds.

3 Axial resolution with two-photon excitation of alloswitch-1

The last objective of this thesis was to demonstrate the axial control of photostimulation that can be obtained by two-photon excitation of diffusible azobenzene-based compounds. To test this, we set up an experiment where cells expressing mGlu₅ were treated with agonist and alloswitch-1, and sequential light stimulations at one or two-photon were done by setting the focal plane at different positions of the z axis, beginning far from the cells and getting closer to the plane where the cells were in focus (**Figure 69b**). This would probe the ability of 1PE compared to 2PE of alloswitch-1 for the optical control of mGlu₅ at the micrometer range.

Since 2PE of alloswitch-1 at 780 nm is in the range of absorption of the calcium indicator we used so far (Fura-2), long imaging times and high-intensity 2PE at such wavelength provoke extensive bleaching of Fura-2, as observed in previous experiments (**Figure 66b**), which complicates long-term measurements of intracellular calcium. As an alternative, we used the genetically-encoded calcium indicator GCaMP6s instead of Fura-2, whose absorption at 780 nm is limited and should be stable over long recording times (Tian *et al.* 2009). Increased fluorescence of GCaMP6s indicates rises in intracellular calcium.

A preliminary result of such experiment is shown in **Figure 69c**, which evidences that photoswitching of mGlu₅-dependent calcium oscillations in the presence of alloswitch-1 occurs regardless of the focal plane for 1PE. Instead, 2PE of alloswitch-1 is achieved only at the focal plane (0 μm), whereas at 10 or 30 μm above the cells the blockade of calcium oscillations by alloswitch-1 is maintained. Further experiments are needed to quantify the efficiency of 2PE compared to 1PE, and to determine whether optical activation of mGlu₅ can be achieved with subcellular resolution.

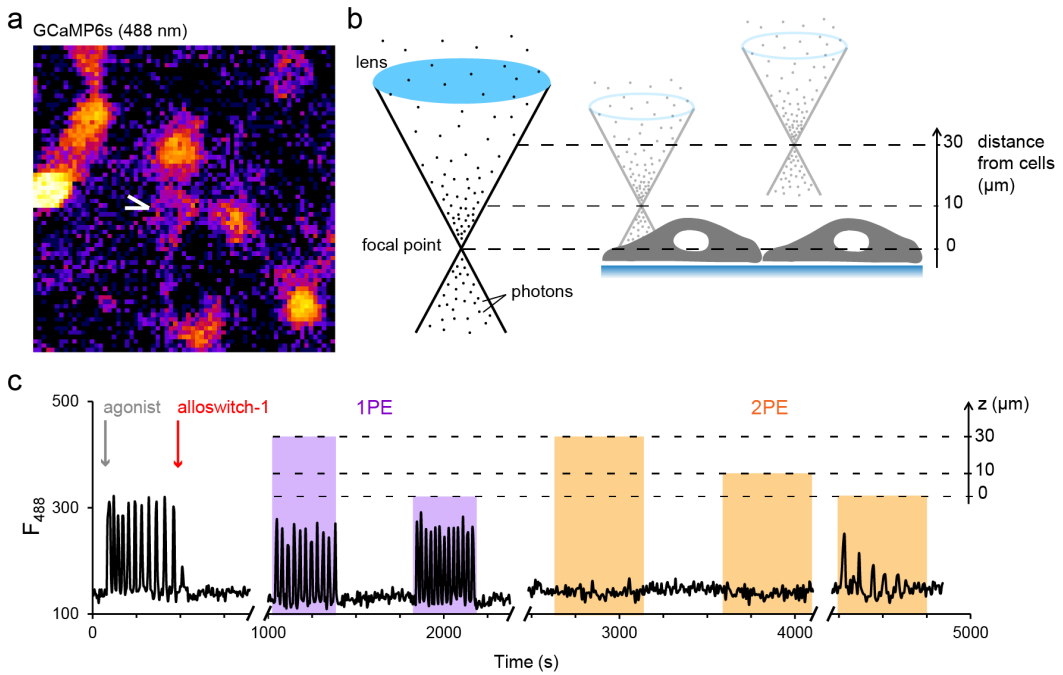


Figure 69 | Axial resolution with 2PE of alloswitch-1 is less than 10 μm .

(a) False color image of GCaMP6s fluorescence ($\lambda_{\text{exc}} = 488 \text{ nm}$) in GCaMP6s/mGlu₅-cotransfected HEK cells. (b) Schematics of the spatial compression of photons close to the focal point of an objective lens (left), and representation of the experimental setup in **c** for stimulation at different distances from the cell focal plane (right). (c) Time course of 1P imaging of GCaMP6s in the cell indicated by the white arrowhead in **a**. Intracellular calcium oscillations were induced with an mGlu₅ agonist (3 μM quisqualate, grey arrow), and stopped with the application of alloswitch-1 (1 μM , red arrow). Photoisomerization of alloswitch-1 was induced with one (1PE) and two-photon excitation (2PE) at distances from the focal plane indicated by the right axis (z , μm). Violet and orange boxes indicate 1PE at 405 nm and 2PE at 780 nm, respectively.

DISCUSSION

Optical tools for both probing and controlling the activity of neurons with light have seen a great expansion in the last few years. The interest of scientists in developing such tools comes from the precision offered by light in obtaining information about how biological systems function with highest temporal and spatial resolution.

The use of light for probing the activity of a neuron or a neuronal protein relies on one hand on fluorescent chemical indicators or naturally fluorescent proteins that can sense calcium, voltage, or other variable properties of excitable cells. On the other hand, it is based on fluorescent probes that emit light or undergo resonance energy transfer to probe the absolute or relative position of proteins or parts of a protein (Liu *et al.* 2015). At the neuronal activity level, such tools are still not comparable to what has been the elective tool for measuring the activation or inhibition patterns of neurons, which is electrophysiology (Newman *et al.* 2011). Instead, at the single protein level and especially for non-ion permeable proteins, these proteins have been recently engineered to couple their activation with changes in light emission, and these tools are probably the best indicators of protein activity in real-time (Lohse *et al.* 2012).

More recently, scientists conceived the idea of using light to actively manipulate the state of neuronal proteins, neurons, and circuits in the brain. Since its introduction, this became a major breakthrough in the field of neuroscience, given no other method provides such precision in activating this or that neuron. Genetically targeted naturally light-sensitive ion channels and pumps are the perfect candidates for the induction of electrical activity in particular sets of neurons and circuits with light, and the latest opsins are able to mimic the physiological activation of neurons with high fidelity, with the advantage of being neuron-type specific and of being operated remotely (Deisseroth 2011).

The selective activation of one class of neuronal proteins with light is more challenging, since there is not a universal method for photosensitizing a specific protein. Although there are general strategies available, either genetic, pharmacologic, or hybrid, these need to be adapted and optimized for every target protein, limiting the possibilities of optical activation of neuronal proteins (Kramer *et al.* 2013).

The work presented in this thesis is addressed at characterizing allosteric pharmacological tools for the control with light of mGlu₅ and mGlu₄, which are important neuronal receptors involved in the slow response to glutamate during synaptic activity (Scanziani *et al.* 1997a). We designed and synthesized such compounds in collaboration with the laboratory of medicinal chemistry lead by Dr. Amadeu Llebaria, at IQAC-CSIC, Barcelona, Spain. We selected azobenzene as the photochromic moiety to confer light sensitivity to our compounds thanks to its stability, reversibility, and the extensive literature available about its photochromic characteristics and the possibility of modifying them with the use of different chemical substituents (Szymański *et al.* 2013).

The results shown in **Chapter 1** demonstrate the design of a first-in-class photoswitchable NAM of mGlu₅, displaying high potency and selectivity, and whose negative allosteric activity over the target receptor could be reversibly switched on and off *in vitro* and *in vivo* with light. We did this through a novel design strategy dubbed 'azologization' (Schönberger *et al.* 2014), which consisted of searching the literature for allosteric modulators of mGlu receptors bearing two aryl groups linked by an amide bond, and substitute this for an azo bond. Since one out of two compounds synthesized by azologization of a described parent compound led to an active compound, we foresee that this approach may hold great promise for the straightforward synthesis of novel allosteric optical switches for the control of native GPCRs.

Alloswitch as a research tool

We demonstrated that alloswitch-1 is an optical switch with unprecedented characteristics, whose use over cells raised interesting questions that could not be raised by non-photoswitchable analogues (**Figure 36c**).

Still there are technical questions over this optical switch that must be clarified before it can be used as a research tool or in the clinics, such as its *cis/trans* composition at the photostationary state, the kinetics of binding and unbinding of both *trans* and *cis* isomers from the receptor, full pharmacological and toxicity profiles, bioavailability kinetics, *etc.* Once these technical questions will be solved, alloswitch-1 will provide a useful tool for

answering to mechanistic questions about mGlu receptors that could not be otherwise studied. It could help in shining light over the functional implication of binding and unbinding of a NAM on short (*e.g.* conformational changes and receptor desensitization) and long timescales (*e.g.* internalization and recycling of the receptor, rebound effect after prolonged inhibition).

Recently a model for orthosteric activation of mGlu receptors was proposed based on experimental data, whereby the continuous application of an agonist induced intermittent activation at fast rates (Vafabakhsh *et al.* 2015). Evidences were obtained by monitoring the conformational changes that occurred in the receptor VFT when switching from active to inactive state, and vice versa. How would an allosteric modulator act has not been explored yet, whether it would make this kinetics faster, slower, or unchanged. And assumed the receptor dynamics are fixed for a given class of compounds, what would happen if the allosteric modulator was withdrawn from the receptor before this had reached the time for inactivation? Would it induce a premature conformational change in the receptor, or would it rather comply with the rule?

The answer to these questions may require triggering receptor activity with super-fast optical switches, recording its functional responses by means of super-fast optical sensors, and finally the ability to perform those recordings at the individual receptor level.

Finally, the control offered by alloswitch-1 over astrocytes appears as the perfect tool for understanding the role of mGlu₅ receptors in astrocyte-to-neuron communication at the tripartite synapse. In fact, as already mentioned in the **Introduction** (page 34), “it is crucial to adapt the time and space domains of the experimental paradigm to fit the kinetics and properties of the astrocytes in a given physiological condition” (Panatier and Robitaille 2015).

Alloswitch-1 as a therapeutic tool

The dichotomy between the therapeutic effect of a drug and its toxicity over off-target tissues has always been a major problem in pharmacology (Langer 1998). The highest selectivity that modern pharmacology can provide (ligands that are active only at a certain receptor subtype or heteromer combination) may be not sufficient to specifically target receptors expressed in different tissues or organs, if the drug is systemically administered. Although targeted delivery and triggered release of drugs are strategies that partially improve drug safety, they completely lack control over what happens to the drug once it has been released close to the site of action (*e.g.* the drug can diffuse to tissues other than the target one).

The spatiotemporal precision of optical switches could be used to circumvent the limitations of conventional drugs. First, because they could decrease the side effects by being made available only at the site where the drug is needed by focal illumination. Second, by switching the active drug on and off as required they would admit more precise dosing patterns, like an all-optical measuring cap. Third, they could potentially improve the therapeutic effect if pulsatile doses were known to be more physiological or therapeutically effective than continuous activation for a given receptor and pathology (e.g. for neurotransmitter release, see page 187 for critical discussion). In this sense, alloswitch-1 is a proof of concept for direct non-invasive allosteric control of endogenous GPCRs, which are prerequisites for therapeutic applications (Rogan and Roth 2011). Moreover, recent technical improvements made it possible to illuminate deep brain areas wirelessly (Kim *et al.* 2013), reducing the invasiveness of the latest techniques, and preparing the field for the translation of optopharmacology to the clinics.

A shortcoming of alloswitch-1 is its activity in the *trans* configuration, which limits strongly the spatial localization of its effects. In order to reduce side effects, a light-regulated drug should be administered in its inactive form, and made active only where needed by illumination with an appropriate wavelength. To do this, we would need optical switches to be *cis*-on compounds, or the *cis* isoform to be more stable than the *trans* one. Another concern involves the wavelength needed for photoisomerization of alloswitch-1, which is in the deep-violet wavelength range. These are very energetic radiations, which are associated with cell damage. Therefore, a redshift in the wavelength used for photoisomerization is desirable for therapeutic applications of our optical switch. Both these issues could be addressed with chemical strategies that are nicely reviewed in (Beharry and Woolley 2011).

In the first chapter of this thesis we introduced the successful design of alloswitch-1, a first-in-class allosteric optical switch for a GPCR. In **Chapter 2** we presented G4optoNAM, which represents the first negative allosteric modulator targeting mGlu₄ receptors with high potency. This molecule is also an azobenzene-based optical switch, and displays a series of improvements compared to alloswitch-1.

Starting with its photochemical properties, the kinetics for the thermal relaxation of G4optoNAM are in the order of milliseconds, which implies that illumination with a single wavelength is sufficient for a reversible photoisomerization. This represents an advantage for its application in physiological systems where the delivery of two light wavelengths would be complicated. Moreover, thanks to the presence of push-pull

substituents flanking the azobenzene moiety of G4optoNAM, its absorption spectrum is redshifted compared to that of alloswitch-1. This means that less energetic, and therefore less damaging, wavelengths can be used to photoisomerize the compound to its *cis* isomer. As for *in vivo* applications where scattering in deep tissues limits the penetration of light, optimal wavelengths for isomerization would be red or infrared. The possibility of photoisomerizing G4optoNAM with blue light represents a first step towards this goal.

Another striking feature of G4optoNAM is its ability of establishing a long-term interaction with mGlu₄ receptors. Although this interaction requires further characterization, such a property would contribute to the spatial localization of the effects of this optical switch by creating a local concentration of G4optoNAM in the surroundings of the conjugation site. When this principle is applied to a drug, it allows using lower doses to obtain a higher effect and thus reducing side effects (Singh *et al.* 2011). This adds up to the advantages of using optical switches for localized therapies that were already mentioned in the discussion to **Chapter 1**.

One general observation regards emerging concepts about the difference between conventional drugs and optopharmacological tools for the activation of neuronal receptors.

Normally, conventional pharmacological ligands used in therapy or for research purposes are given in a single dose, and thereafter their activity on the receptor is regulated by the diffusion rate of the molecule in the organism or in solution, their clearance, and subjected to on and off rates for binding to and release from the receptor. These experimental conditions differ substantially from the reality of the physiological activation of a glutamate receptor, since the release of glutamate is not continuous, thanks to its quick clearance from the synaptic cleft and the extrasynaptic space. This fast clearance has been explained with the kiss-and-run model of vesicle fusion to the presynaptic membrane (Alabi and Tsien 2013), and the active transport of glutamate inside astrocytes through fast surface diffusion of glutamate transporters (Murphy-royal *et al.* 2015). This fast 'reset' of the glutamate concentration available for binding to the postsynaptic glutamate receptors not only admits the ms duration of the action potential and the high precision neuronal signaling through fast trains of action potentials, but also constantly changes the ligand concentration surrounding the postsynaptic receptors. This in turn modifies the binding and dissociation rates of glutamate, constantly alters

the equilibrium between active/inactive receptor states, and likely allows arbitrary conditioning of the receptor function and intracellular signaling.

This mechanism could be irrelevant for ionotropic receptors, which have very fast activation and inactivation modes, but could constitute a relevant issue in the activation of the slower metabotropic receptors. Indeed, many proteins work on a frequency-decoding basis; one classical example for this is the mode of action of CaMKII, which is preferentially activated by certain frequencies of calcium transients (De Koninck and Schulman 1998; Smedler and Uhlén 2014). Sustained and oscillating gene expressions were nicely demonstrated to lead to different biological outcomes (e.g. Hes1 oscillating or sustained expression lead to proliferation or differentiation, respectively; Isomura and Kageyama 2014). This is true also at the system level in the developing brain or during sleep, when correct functioning relies on oscillatory patterns of activity (Blankenship and Feller 2009).

It is clear then, that exogenous ligands that are applied continuously lead to a sustained receptor activation that does not resemble at all the endogenous activation of the receptor, which not only is transient, but much probably pulsatile. In the case of glutamate receptors, the importance of the temporal pattern of activation is demonstrated for instance during long-term synaptic plasticity by the evidence that induction protocols of different stimulation frequencies (high/low) lead to opposing plastic outcomes (LTP/LTD, **Figure 10**).

The importance of specific temporal patterns in glutamatergic activity is known for physiological processes that can be studied with electrophysiology. Pharmacology lacks the spatial and temporal precision of electrophysiology, and the local application of glutamate analogs, although minimally depending on diffusion, will probably lack the fast clearance of ligand concentration mediated by transporters.

Altogether, these considerations suggest that the use of exogenous ligands, although they have been extensively used as research tools and in the clinics, might not be the best approach, since these time-dependent aspects of their functioning have never been taken into account. A possible way of emulating these rapid transients in physiological glutamatergic transmission and regulation is by means of photoswitchable ligands. Instead of fast release of glutamate-containing vesicles to the synaptic cleft and glutamate transporter reuptake, photoswitchable ligands of glutamate receptors could be continuously present at the synapse, but transiently activated and deactivated with light at high spatial and temporal resolution.

The example traces presented in **Chapter 2** depicting mGlu₄ activation suggest that something similar to pulsatile activity can be achieved with optical switches that control neuronal receptors. Thanks to their ability in switching fast the receptor from the active to the inactive state in a dynamic way, they create patterns of activity that could not be observed with conventional drugs. Indeed, the application of optical switches combined with patterned illumination can lead to a paradoxical situation whereby a drug that works in one direction on the receptor can be driven optically to work in an exactly opposite direction. In other words, an inhibitor of one receptor can be used to trigger the receptor activation at a desired time point and for the desired duration simply by illumination. In contrast, the use of agonists or PAMs (as shown in **Figure 58**) leads to a continuous activation of the receptor that after the initial peak of activation could mean nothing to the neuron, at least at a molecular or cellular level. As discussed in the previous paragraphs, this does not resemble much how things work in the brain, where neurotransmitter receptors are not tonically activated, especially in the case of glutamate since this could lead to excitotoxicity and seizures.

In conclusion, optical switches for neuronal receptors and the ability to activate them transiently through light pulses could mimic better than conventional drugs how physiological receptor activity occurs, and might help unraveling their functioning or create new pharmacological paradigms for a more appropriate treatment of neuropathologies.

In **Chapter 3** we show the characterization of a library of phenylazopyridines that we designed as chemical variations to alloswitch-1, which was unexpectedly rich in compounds active at mGlu₅. All of them were negative modulators of the receptor, with potencies that ranged from high nanomolar to low micromolar. Obtaining such a high percentage of active hits in a screening of compounds usually takes long time for medicinal chemists. This unexpected success is probably explained by the fact that we were obliged to maintain the phenylazopyridine throughout the library of compounds, since this was the photoswitching core of alloswitches. In agreement with this, when we changed the phenylazopyridine for an azobenzene the NAM potency was disrupted (compound **2** in **Chapter 3**), indicating that this chemical scaffold plays an important role in the binding to mGlu₅.

The photochemical and optopharmacological characteristics of the series of alloswitches were quite diverse, and allowed a limited extent of generalization about which are the chemical strategies that allow the fine tuning of the characteristics of optical switches, in

terms of photoswitching behavior, relaxation kinetics, potency and optical activation of the target receptor. However, thanks to a thorough characterization of the compounds, we were able to create a detailed list of characteristics that can guide the user of alloswitches (just like a handbook) in the identification of the most appropriate alloswitch that fits its experimental needs for the optical control of mGlu₅ receptors.

As already discussed in the remarks to **Chapter 1**, redshifted and *cis*-ON compounds would be preferred for therapeutic applications of optical switches. In this library of compounds we only obtained one compound that was slightly redshifted, and none that was active in its *cis* configuration. This demonstrates that optimization of wavelengths or obtaining *cis*-on compounds are not straightforward processes, and deserve dedicated design strategies.

Finally, in **Chapter 4** we demonstrate for the first time the two-photon excitation of freely diffusible optical switches based on azobenzene, for alloswitch-1 and three more compounds of the alloswitch series. Pulsed illumination with NIR lasers is used for either imaging activity deep in 3D and scattering tissues, or to define a micrometric volume for optical activation of effector molecules such as for uncaging of neurotransmitters (Svoboda and Yasuda 2006). In the case of alloswitches, the small volume where 2PE occurs could in principle limit the optical activation of mGlu₅, which is mediated by the exit of *cis*-alloswitch-1 from the allosteric binding pocket inside the mGlu₅ TMD. In fact, diffusion of the *trans* isoforms from outside the volume of 2PE could immediately replace the outgoing *cis*-isoforms in the TMD and block the intracellular signaling downstream of mGlu₅. Therefore, the results we obtained were in part unexpected, and further characterization of the mechanisms at play here is needed to fully understand the dynamics of 2PE of mGlu₅ receptors.

Although these experiments were limited to 2D cell cultures, the axial control demonstrated so far for alloswitch-1 (corresponding to a resolution of at least 10 μm) has the average size of the soma of astrocytes, whose area is estimated around 100 μm² (Torres-Platas *et al.* 2011), and neurons, between 50 and 90 μm² (Meitzen *et al.* 2011). Therefore these results constitute an initial step towards the high-resolution spatial-specific activation of mGlu receptors. Ongoing studies in 3D tissues (brain slices or *in vivo*) will clarify the real potential for the optical modulation of mGlu receptors at high spatial resolution.

Overall, the work presented in this thesis shows for the first time the design and characterization of optical switches for the allosteric and remote control of native mGlu receptors *in vitro* and *in vivo* with light. This advance broadens the availability of optical tools to manipulate mGlu receptors with high temporal and spatial resolution, and represents a step towards the development of optopharmacological tools for the innovative treatment of neuropathologies with light.

CONCLUSIONS

1. By replacing an amide by an azo group in an allosteric modulator of mGlu receptors we obtain the phenylazopyridine alloswitch-1, which is a potent, selective, robustly photoisomerizable allosteric optical switch that allows reversibly photocontrolling mGlu₅ receptors *in vitro* and *in vivo*.
2. Alloswitch-1 is the first allosteric optical switch to be described targeting a GPCR, and its unique characteristics raise interesting questions about the functioning of mGlu₅ receptors.
3. Thanks to its *in vivo* activity and drug-like properties, it constitutes a proof-of-principle for future therapeutics based on allosteric and reversible optical switches.
4. We identified G4optoNAM, an allosteric optical switch for the control of mGlu₄ receptors *in vitro* and *in vivo*, using a classical medicinal chemistry approach based on screening a compound library.
5. Compared to alloswitch-1, G4optoNAM has more redshifted excitation wavelength and faster thermal relaxation, which makes it a better choice for less invasive single-wavelength optical therapeutics.
6. We demonstrate a prolonged interaction between G4optoNAM and its target receptors, which suggests intriguing possibilities for chemical strategies to improve the spatial localization of the drug effects.
7. Both alloswitch-1 and G4optoNAM contribute to the knowledge about the functions of mGlu₅ and mGlu₄ receptors, since they induce opposing effects over the locomotion of zebrafish, consistent with their established biological role.
8. By screening a series of alloswitch-1 derivatives with diverse chemical substitutions, we identified a family of phenylazopyridine derivatives having satisfactory photochemical and optopharmacological characteristics and active as mGlu₅ NAMs.

9. We establish charts for the identification of the diverse photochemical and optopharmacological characteristics among the library of alloswitches.
10. We demonstrate the two-photon excitation of alloswitch-1 and some of its derivatives. This is the first evidence that optical control of freely diffusible allosteric modulators of GPCRs is possible with NIR light.
11. We show the 2PE of alloswitch-1 with an axial resolution as good as 10 μm , which opens up interesting possibilities for its use in intact tissues and *in vivo* with unprecedented tissue depth and spatial resolution.
12. In summary, we generated several azobenzene-based tools for the optical activation of mGlu receptors that enable novel pharmacological modes, and could help solving old questions in pharmacology and make new ones arise.

Resum en català

Títol de la tesi:

Desenvolupament de lligands al·lostèrics per modular mitjançant la llum receptors neuronals, de forma remota i no-invasiva

En el sistema nerviós els esdeveniments es desenvolupen en l'escala temporal dels milisegons, i els processos que tenen lloc en neurones i cèl·lules gliars presenten compartimentalitzacions microscòpiques. Aquesta organització determina uns patrons d'activitat ben definits temporalment i espacial, els quals permeten el precís funcionament del sistema nerviós per tal de transmetre, integrar i processar la informació d'una forma ràpida i específica. Per entendre millor la forma en la que aquests patrons estan organitzats en el temps i l'espai, calen noves eines que permetin superar les limitacions espaciotemporals de les tecnologies existents per l'observació passiva o l'activa manipulació del sistema nerviós. Una de les estratègies més potents i precises per activar i inactivar proteïnes neuronals es basa en la seva fotosensibilització, per tal de poder-les controlar mitjançant la precisió espai-temporal incomparable que la llum ofereix. Tantmateix, la llum representa l'eina preferida per observar amb detall els esdeveniments al sistema nerviós.

En la introducció a aquest treball de tesi presentem les eines òptiques disponibles per detectar (sensors) o induir (commutadors) l'activitat d'una família de proteïnes neuronals denominades receptors metabotòpics de glutamat (mGlu). Estem interessats en aquests receptors per la importància que tenen com moduladors de la

neurotransmissió, i el seu rol en el desenvolupament de neuropatologies. La possibilitat d'expandir el ventall d'eines optofarmacològiques que permeten un control farmacològic d'aquests receptors neuronals amb llum, de forma remota i no invasiva, va ser el punt d'inici d'aquest treball de recerca.

1 Receptors metabotòpics de glutamat (mGlu)

El glutamat és el principal neurotransmissor excitatori del sistema nerviós central. Els receptors de glutamat es classifiquen en ionotròpics i metabotòpics (mGlu). Els vuit membres de la família de mGlu són receptors acoblats a proteïna G (G protein-coupled receptors, GPCR) de classe C, amb estructura semblant, que conté principalment un domini extracel·lular (venus fly trap, VFT) per la unió del lligand ortostèric (glutamat), un domini format pels set segments transmembrana (transmembrane domain, TMD), que transmet l'arribada de la senyal extracel·lular al domini intracel·lular (C-terminal domain, CTD), el qual activa la proteïna G. Els vuit mGlu es divideixen en tres grups. Els de grup I (mGlu₁ i mGlu₅) estan localitzats majoritàriament al terminal postsinàptic, i la seva activació per part del lligand endogen (glutamat) activa la senyalització intracel·lular mitjançant inositol fosfats (IPs) i calci, i finalment afavoreix la neurotransmissió. Per contra, els mGlu de grup II (mGlu₂ i mGlu₃) i de grup III (mGlu₄, mGlu₆, mGlu₇ i mGlu₈) es troben normalment al terminal presinàptic, i la seva activació porta a una reducció en la producció de AMP cíclic (cAMP), i finalment de l'alliberament de neurotransmissor. Els mGlu₃ i mGlu₅ s'expressen també als astròcits, unes cèl·lules de la glia que també poden modular la comunicació entre neurones. S'ha demostrat que tots els mGlu estan fisiològicament implicats en els importants processos de plasticitat sinàptica de curta i llarga durada, i que les disfuncions dels mGlu estan relacionades amb patologies del sistema nerviós. Els fàrmacs que s'han desenvolupat pels mGlu són principalment moduladors al·lostèrics, els quals s'uneixen al TMD i actuen modulant l'activació del receptor per part del lligands ortostèrics (que s'uneixen al VFT). L'interès pels moduladors al·lostèrics es deu principalment a la selectivitat amb la que permeten modular els diferents subtipus de mGlu, ja que la seqüència dels receptors al voltant del lloc d'unió al·lostèric al TMD està menys conservada entre diferents subtipus que el VFT. Alhora, aquest lloc d'unió es troba endinsat en els receptors i ofereix un accés restringit, que dificulta la identificació de moduladors al·lostèrics amb una estructura adequada per poder accedir a aquest lloc d'unió. Per exemple, encara no hi ha moduladors al·lostèrics negatius amb potència nanomolar dirigits al mGlu₄.

2 Sensors òptics per mGlu

La gran majoria dels sensors òptics es basen en el marcatge de proteïnes amb sondes de fluorescència. Això permet la localització dels mGlu mitjançant microscòpia de fluorescència. Aquestes sondes poden ser anticossos marcats amb fluorocroms, lligands fluorescents, o bé proteïnes autofluorescents o marcades amb fluorocroms amb les que es fusionen genèticament els receptors. Això permet també monitorar els moviments dels receptors, sols o en relació amb altres proteïnes. Avenços recents en la resolució òptica d'aquests microscopis permeten augmentar la resolució espaciotemporal amb la que es detecten els receptors. Un exemple de tècnica de seccionament òptic de la imatge que permet millorar la resolució espacial és l'estimulació per dos fotons, que utilitza làsers pulsats a 80MHz (Ti:safir) i longituds d'ona vermelles o infraroges (700-1000nm) per excitar fotoelectrons en un volum molt petit en el centre del pla focal. L'estimulació per dos fotons es pot fer servir alhora per produir fluorescència i isomerització de fotocommutadors en volums molt reduïts.

Una classe de sensors òptics desenvolupada recentment es fa servir per monitoritzar els canvis conformacionals que guien l'activació dels receptors i el començament de la senyalització intracel·lular. Aquests són els biosensors basats en el fenomen de la transmissió d'energia de resonància Förster (FRET), que han sigut fonamentals per revelar les dinàmiques de funcionament dels mGlu amb elevada resolució espaciotemporal. Altres sensors òptics més clàssics són els que es fan servir per revelar la senyalització intracel·lular dels mGlu, i es basen en indicadors químics de segons missatgers com ara el calci o els IPs. Altres indicadors òptics es basen en proteïnes fluorescents sensibles a segons missatgers.

3 Commutadors òptics per mGlu

Els commutadors disponibles pel control amb llum de receptors mGlu es poden classificar en tres grups: els optogenètics, els optofarmacogenètics, i els optofarmacològics. Els primers dos requereixen una modificació genètica del receptor, que és complicada en la perspectiva de aplicacions terapèutiques en humans. En canvi, la tercera estratègia només implica la modificació d'un fàrmac per tal de fer-lo sensible a la llum, i així permetre la fotosensibilització d'una proteïna nativa. En aquesta última i més interessant classe trobem uns lligands ortostèrics de mGlu, o bé engabiats amb un protector químic fotolàbil, o bé units a un grup químic fotoisomeritzable. El primer tipus de compost s'allibera per llum, generant un lligand actiu de forma irreversible. Aquesta

irreversibilitat limita les aplicacions d'aquest tipus de commutador, ja que així es perd el control temporal sobre l'efecte del fàrmac un cop s'hagi produït el seu alliberament.

En el segon cas, al glutamat està lligat un grup anomenat azobenzè, que pot commutar reversiblement entre configuracions de propietats molt diferent (*trans* i *cis*) mitjançant llum de diferents colors. Aquesta fotoisomerització fa que el compost pateixi un canvi de geometria, polaritat i/o de distància entre els seus extrems, i en conseqüència es vegi alterada l'accessibilitat del lligand al lloc de unió amb el receptor. Cal destacar que en el moment de començar aquest treball no existia cap modulador al·lostèric de GPCRs regulat per llum.

Objectius

Ens proposem els següents objectius, considerant els avantatges que ofereix el fotocontrol de proteïnes i l'escassetat d'eines optofarmacològiques pel control òptic i reversible dels receptors mGlu, així com la importància fisiològica de modular al·lostèricament aquestes proteïnes neuronals per entendre els mecanismes d'acció d'aquests receptors, i la possibilitat d'aplicar aquestes eines optofarmacològiques per tractar malalties relacionades:

1. dissenyar i caracteritzar els primers moduladors al·lostèrics de mGlu controlats per llum: alloswitch-1 i G4optoNAM, descrits als **Capítols 1 i 3**.

2. sintetitzar i caracteritzar una llibreria de compostos derivats de l'alloswitch-1, amb l'objectiu d'entendre quines són les característiques òptimes per la creació de fotocommutadors al·lostèrics de receptors mGlu (**Capítol 2**).

3. demostrar la fotoconversió d'alloswitch-1 amb estimulació de dos fotons, per tal d'augmentar amb estratègies òptiques la resolució espacial amb la que es poden activar els fotocommutadors reversibles (**Capítol 4**).

Capítol 1

En el primer capítol es descriu el disseny, la síntesi i la caracterització d'alloswitch-1, un fotocommutador al·lostèric capaç d'activar receptors mGlu₅ amb llum de forma reversible.

Capítol 2

En el segon capítol mostrem la caracterització de G4optoNAM, un fotocommutador al·lostèric actiu en receptors mGlu₄ i de llarga durada.

Capítol 3

En el tercer capítol s'estudia una llibreria de compostos derivats del precursor alloswitch-1 amb diverses substitucions químiques, que mantene l'activitat com a NAM de mGlu₅, i presenten característiques fotofísiques i optofarmacològiques variades.

Capítol 4

En l'últim capítol demostrem la capacitat d'alloswitch-1 i d'alguns membres seleccionats de la llibreria de alloswitches de fotoisomeritzar de *trans* a *cis* amb il·luminació de dos fotons.

Conclusions

1. Mitjançant l'analogia amb l'azobenzè d'un modulador al·lostèric dels receptors mGlu es va obtenir un fotocommutador al·lostèric potent, selectiu que permet controlar de forma reversible amb llum els receptors mGlu₅ *in vitro* i *in vivo*. Hem anomenat aquest compost alloswitch-1.
2. Alloswitch-1 va ser el primer commutador òptic al·lostèric descrit que es dirigeix a un GPCR, i les seves característiques úniques van permetre plantejar preguntes interessants sobre el funcionament dels receptors mGlu₅.
3. Gràcies a la seva activitat, selectivitat i control amb llum *in vivo*, constitueix una prova de principi per a futurs fàrmacs fotoregulats amb potencial terapèutic .
4. Amb un enfocament més tradicional de química mèdica, hem identificat un commutador òptic al·lostèric per al control dels receptors de mGlu₄ *in vitro* i *in vivo*.
5. G4optoNAM isomeritza amb longituds d'ona més llargues que l'alloswitch-1 i la seva relaxació és més ràpida, el que permet utilitzar-lo amb un sol color i menor fototoxicitat.
6. Es va observar una interacció perllongada entre G4optoNAM i el seu receptor diana, el que suggereix estratègies químiques interessants per millorar la localització espacial dels efectes dels fàrmacs.
7. Tant alloswitch-1 com G4optoNAM contribueixen al coneixement sobre la funció biològica dels receptors mGlu₅ i mGlu₄, com demostren els efectes oposats d'aquests compostos sobre la locomoció de peix zebra.

8. Hem identificat diversos derivats de l'alloswitch-1 que tot i les substitucions químiques són actius en mGlu₅ i presenten característiques fotofísiques i optofarmacològiques satisfactòries.
9. Hem catalogat la llibreria de alloswitches d'acord amb les seves característiques fotofísiques i optofarmacològiques.
10. Hem demostrat la isomerització d'alloswitch-1 i la regulació del seu efecte farmacològic mitjançant l'excitació a dos fotons. Això fa possible l'ús de moduladors al·lostèrics lliurement difusibles per activar òpticament receptors GPCR en teixit intacte i *in vivo*, amb una resolució espacial sense precedents.
11. En conclusió, hem generat diverses eines per a l'activació òptica dels receptors mGlu que han obert noves metodologies farmacològiques per a l'estudi de la fisiopatologia del sistema nerviós.

APPENDIX

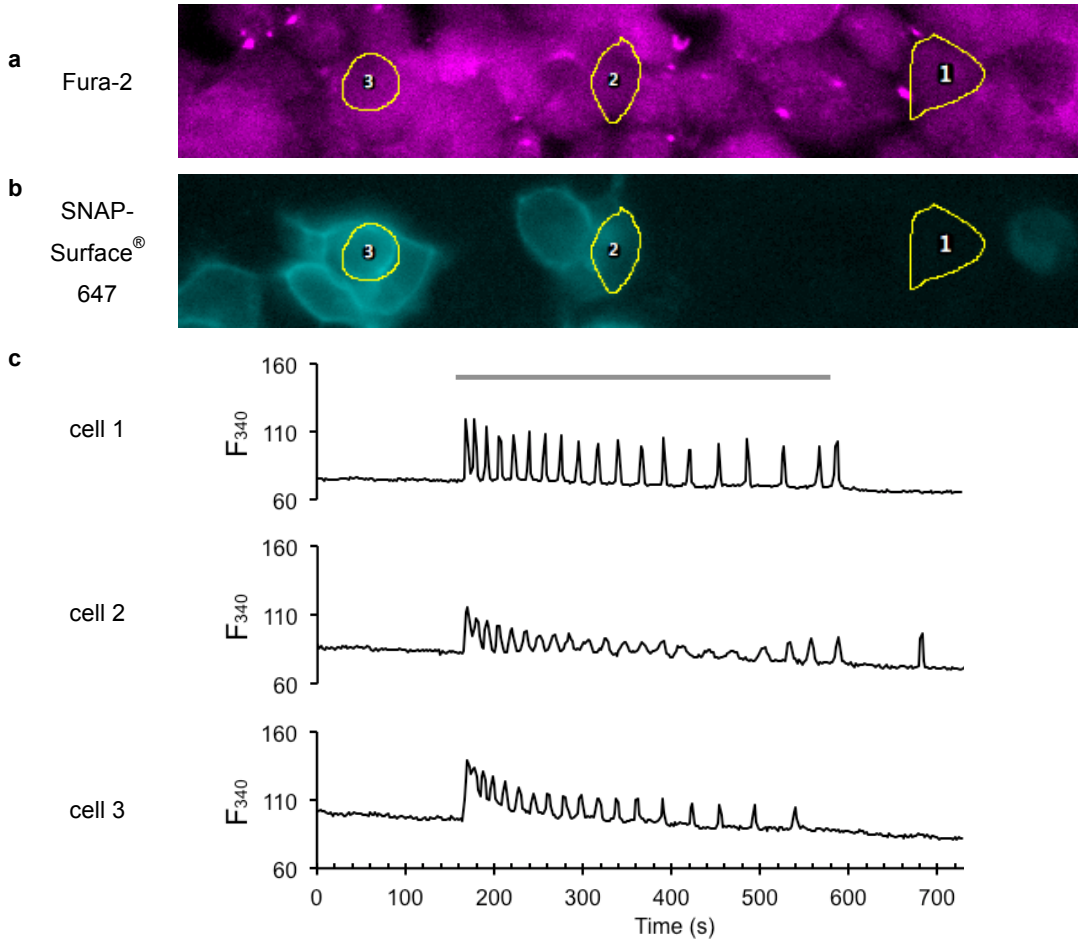


Figure A1 | Frequency of calcium oscillations does not correlate with levels of surface receptors in mGlu₅-SNAP-expressing HEK cells.

(a-b) Images of Fura-2 fluorescence (excitation at 340 nm, **a**) and mGlu₅-SNAP receptors labeled with the SNAP-Surface® 647 fluorophore (logarithmic transform of the original fluorescence, **b**), overlaid with profiles of analyzed cells in yellow. (c) Time course of intracellular calcium (Fura-2 excited at 340 nm) from cells indicated in **a** and **b**, and challenged with an mGlu₅ agonist (3 μM quisqualate, grey line).

I. Expression of mGlu₅ and oscillatory frequency

According to Nash and colleagues (Nash *et al.* 2002), expression levels of mGlu₅ receptors determine the frequency of agonist-induced Ca²⁺ oscillations. We made a series of experiments in an effort for identifying the appropriate levels of mGlu₅ expression that paired to satisfactory calcium oscillations in transfected HEK cells.

We expressed mGlu₅-SNAP-tag receptors and incubated the cells with the specific substrate for fluorescent labeling of the SNAP-tag of receptors present at the cell surface, SNAP-Surface[®] 647, following manufacturer's instructions (CisBio Bioassays). The reaction mix for labeling the receptors was put in solution together with the calcium indicator Fura-2 AM (**Figure A1a**), and incubated as explained in the **Materials & Methods** Section. The coverslips were then rinsed and mounted on the imaging chamber for calcium imaging with an IX70 inverted microscope (Olympus), a UApo/340 oil 40×/1.35-NA objective, and a Polychrome V monochromator as light source. After recording basal calcium levels, we challenged the cells with the addition of 3 μM quisqualate to induce activation of mGlu₅ receptors and intracellular calcium signaling. Before and after each experiment, we used a dichroic Q660lp beam splitter and a HQ700/75m emitter (Chroma Technology) with 647-nm light to image SNAP-tagged receptors at the cell surface.

Unfortunately, with the methods in our hands we could not establish any correlation between the expression level of mGlu₅-SNAP at the cell surface and the frequency of calcium oscillations in response to agonist. In fact, in one experiment we can observe three cells with very different levels of mGlu₅ at their plasma membrane (**Figure A1b**, note that the image represents a logarithmic transform of the original fluorescence) showing very similar frequencies of calcium oscillations (**Figure A1c**).

This could mean either that in our expression system receptor levels are not linked to the oscillatory frequency, or that labeling of surface receptors is not a good estimate of the total amount of receptors expressed by a cell. Quisqualate is known to cross the plasma membrane and act also on mGlu₅ receptors from intracellular compartments (Jong *et al.* 2009; Kumar *et al.* 2008). In fact, we don't know what is the contribution to calcium oscillation of the intracellular mGlu₅ receptors, which were not labeled in our assay. These experiments could be repeated using different labeling methods (to differentially target surface, intracellular, or all receptors present on the cell) and/or different agonists (able/unable to cross the membrane).

II. Phenotypes of mGlu₅ calcium responses

The data presented in this thesis from calcium imaging experiments in individual cells expressing mGlu₅ only take into account cells displaying oscillatory behavior for the entire duration of mGlu₅ activation. However, calcium oscillations only represent one of response phenotypes that are obtained by activating mGlu₅ receptors. In **Table A1** we classify these calcium responses as non-responding (NR), single-peak (SP), desensitizing (D), oscillatory (O), peak-and-plateau (PP), according to Bradley *et al.* (2009), and we provide examples of such response phenotypes.

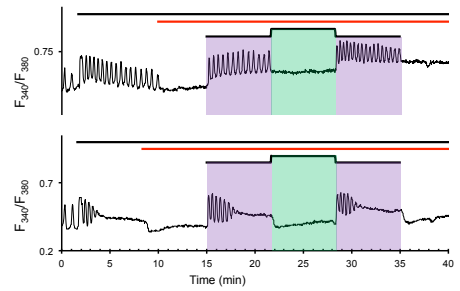
Table A1 | Observed phenotypes of calcium responses in mGlu₅-expressing HEK cells.

response phenotype	name	description	Example trace
Single-peak	SP	One initial peak	
Desensitizing	D	Two or more peaks, but then silenced before the end of the stimulation	
Oscillatory	O	Stably oscillating Can undergo some degree of desensitization (decrease in the oscillatory frequency)	
Peak-and-plateau	PP	Initial calcium rise (peak) followed by a steady-state Ca ²⁺ increase (plateau)	

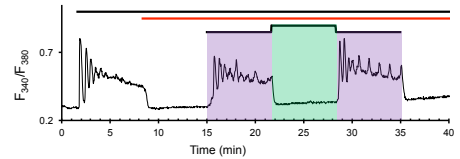
Other

X

Spontaneously
responding



Peaks over a plateau



...

Example traces of calcium imaging experiments were from mGlu₅-expressing HEK tsA201 cells loaded with the calcium indicator Fura-2 (F_{340}/F_{380}), and stimulated with 3 μ M of the mGlu₅ agonist quisqualate and with 1 μ M alloswitch-1 (black and red lines respectively). Illumination with violet (390 nm) and green light (490 nm) was at times indicated by violet and green boxes.

III. Rebound effect after persistent inactivation of mGlu₅

A series of experiments presented in **Chapter 1** left some open questions about the ‘apparent PAM’ effect of alloswitch-1. This effect is observed when cells expressing mGlu₅ are incubated with *trans*-alloswitch-1 (in dark conditions or under green illumination), and then the block imposed by the *trans*-NAM is suddenly withdrawn by illumination with violet light, which induces *cis*-alloswitch-1 (see **Figure 30**). In **Chapter 1** we demonstrated that *cis*-alloswitch-1 is not a PAM of mGlu₅ (**Figure 37**), and that a relatively fast washout of a non-optical NAM of mGlu₅ fails in inducing such a ‘rebound activation’ of the receptor after persistent inhibition (**Figure 40**).

We present here some experiments that we did in an attempt to clarify the reasons for these observations.

Effect of increasing the time of persistent inactivation of mGlu₅ by trans-alloswitch-1

As already mentioned in **Chapter 1**, we only observed rebound effect in cells where violet light was switched on after a period of time in which alloswitch-1 had been in contact with the cells in dark conditions or under green illumination. We hypothesized that during this time *trans*-alloswitch-1 could be dynamically changing the response properties of mGlu₅ receptors or cells. In this case, the extent of the rebound effect should then depend on the duration of the contact between *trans*-alloswitch-1 and the cells.

To demonstrate this, we repeated experiments equivalent to those presented in **Figure 30**, but decreasing more and more the time between the addition of alloswitch-1 and illumination with violet light. This progressively reduced the ‘incubation time’ in which the cells were exposed to *trans*-alloswitch-1 before this was photoisomerized to *cis*-alloswitch-1 by violet illumination. Example traces of calcium oscillations in cells with different ‘incubation times’ are shown in **Figure A2 a-e**, and the quantification of normalized responses is shown in **Figure A2 f**.

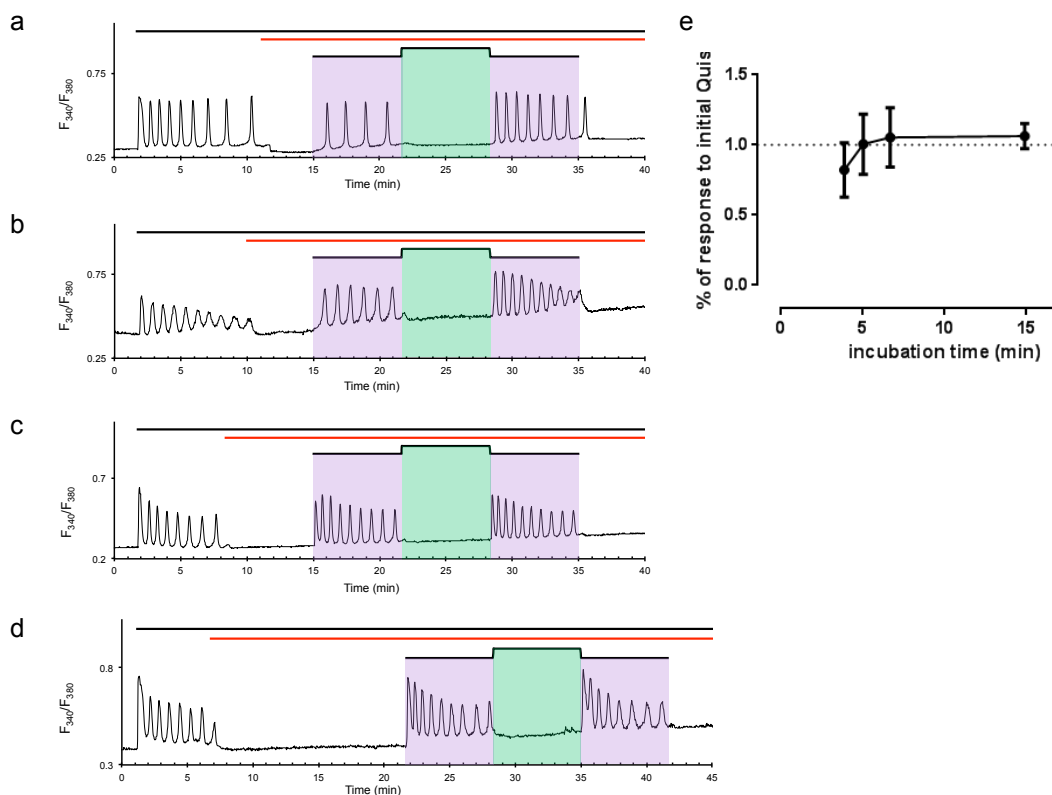


Figure A2 | Effect of different times of persistent inactivation of mGlu₅ on the rebound effect.

(a-e) Time course of intracellular calcium in mGlu₅-expressing HEK tsA201 cells, loaded with Fura-2 and stimulated with 3 μ M quisqualate and 1 μ M alloswitch-1 (black and red lines respectively), and illuminated with violet and green light at times indicated by violet and green boxes in figure. Time of alloswitch-1 incubation before violet illumination was 0, 3.3, 5, 6.7, and 15 min for panels a to e. For all experiments except the 15-min incubation, violet illumination was started at minute 15. (f) Quantification of calcium oscillations during the first period of violet illumination for cells incubated for indicated times with *trans*-alloswitch-1, normalized by the initial response to agonist.

We observed a tendency for the rebound response to be reduced for shorter incubation times. Moreover, it seemed to reach a maximum with incubations of 5 minutes. We hypothesized that these slow dynamics could be attributed to receptor resensitization by trafficking and recycling, rather than to a regulation of its activation and inactivation dynamics. To test this hypothesis, we repeated similar experiments in absence or presence of a membrane traffic inhibitor.

Effect of blocking protein trafficking

Dynasore was initially discovered as an inhibitor of dynamin (Macia *et al.* 2006), and was later described to interfere with membrane traffic (Preta *et al.* 2015). We used it in our

experiments in combination with alloswitch-1, with the aim of blocking the recycling of mGlu₅ during the period of persistent inactivation operated by *trans*-alloswitch-1.

Example traces of calcium responses in mGlu₅-expressing cells stimulated with quisqualate and alloswitch-1 together with dynasore, and challenged with violet and green light cycles are shown in **Figure A3**. These results highlighted that, in contrast to our hypothesis, by inhibiting receptor trafficking we obtained an increase in the rebound effect. This was observed especially in the case of cells showing a single-peak of intracellular calcium in response to mGlu₅ activation (**Figure A3c**).

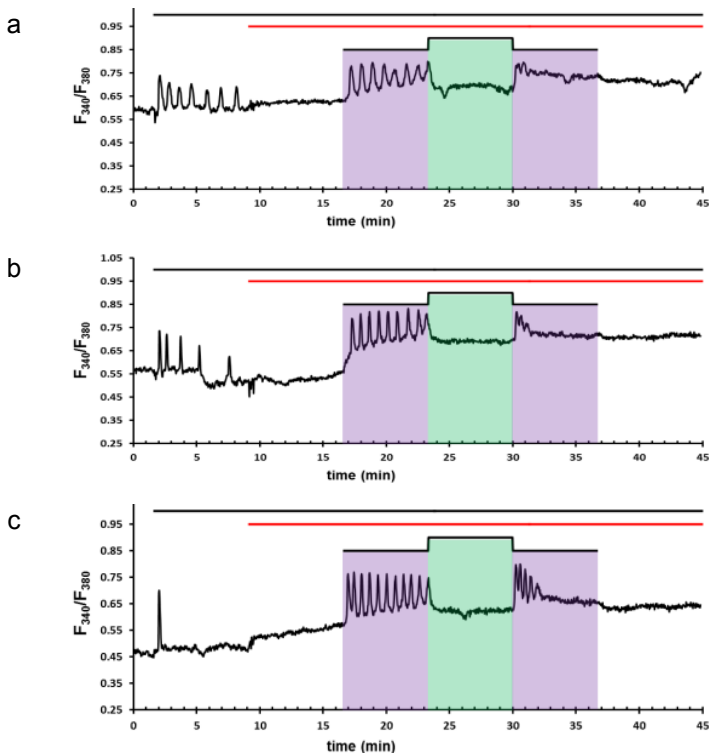


Figure A3 | Effect of blocking membrane traffic during persistent inhibition on the rebound effect.

(a-c) Time course of intracellular calcium in mGlu₅-expressing HEK tsA201 cells, stimulated with 3 μ M quisqualate (black line) and a mix of 1 μ M alloswitch-1 and 80 μ M dynasore (red line). Illumination with violet (390 nm, 1 out of 2 s) and green (490 nm, 0.1 out of 2 s) light was switched on and off as indicated by colored boxes. In all experiments, violet light was switched on at minute 16.7. We selected two cells with oscillatory response (a, b) and displaying different frequencies, and a cell with single-peak response (c).

To check the effect of dynasore on mGlu₅ receptors not treated with Allosiwthch-1, we repeated these experiments with vehicle (0.1% DMSO). A comparison of all results from

experiments both in presence and absence of dynasore, for both cells treated with alloswitch-1 and vehicle is displayed in **Figure A4**.

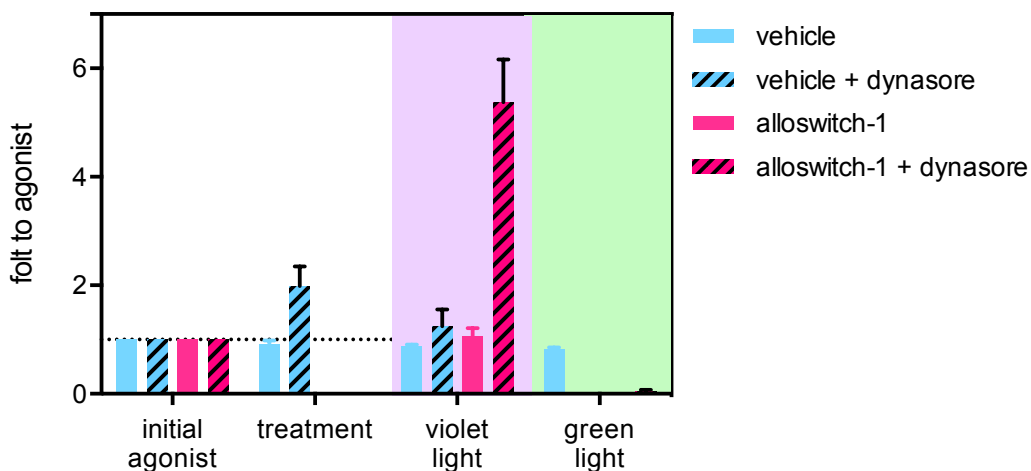


Figure A4 | Effect of blocking membrane traffic on optical mGlu₅ responses.

Response of mGlu₅-expressing HEK tsA201 cells to 3 μ M quisqualate, quantified as number of calcium peaks over time and normalized by the initial response to the agonist (initial agonist). We compare here the responses of four groups of cells from experiments similar to those exemplified in **Figure A3**, and now treated with vehicle (0.1% DMSO) or alloswitch-1 (1 μ M) in absence or presence of the inhibitor of membrane traffic dynasore (80 μ M). Calcium responses were counted during four consecutive time periods, corresponding to: initial response to the agonist, addition of vehicle/alloswitch-1/dynasore (treatment), illumination with violet or green light, indicated by colored boxes. Data are represented as mean \pm s.e.m.; n = 4, 22, 10, and 15 cells for, respectively, vehicle, vehicle + dynasore, alloswitch-1, and alloswitch-1 + dynasore.

From this quantification we observe that calcium oscillations are increased by treatment with dynasore alone. These results indicate that dynasore was either interfering with calcium signaling or even with the mGlu₅ receptor itself. All these scenarios are possible. Dynasore is a small chemical molecule which could have unexpected affinities for many proteins in the cellular environment. Moreover, it was shown to interfere with no selectivity over membrane traffic, since it acts at several branch points of the trafficking machinery. A better understanding of whether and how alloswitch-1 regulates receptor trafficking could come from experiments repeated with inhibitors of specific parts of the internalization and recycling pathway that receptors undergo following activation or inhibition. Many of such molecules are commercially available, and a review of cellular components implicated in endocytic recycling and vesicle recycling by Rab-GTPases can be found in Grant and Donaldson (2009) and Stenmark (2009).

Also, internalization and trafficking of fluorescently labeled mGlu₅ receptors (like mGlu₅-eYFP or mGlu₅-SNAP) could be monitored with microscopy techniques such as TIRF, to track vesicle docking and internalization, or FRAP, to observe the lateral motility of receptors on the cell surface.

IV. Abbreviations

1PE	One-photon excitation
2PE	Two-photon excitation
5-HT	5-hydroxytryptamine (serotonin)
AC	adenylate cyclase
ACh	Acetylcholine
AMPA	α -amino-3-hydroxy-5-methyl-4-isoxazolepropionic acid
AMPA	AMPA receptor
BRET	bioluminescence resonance energy transfer
CA1 or CA3/ DG	cornus ammonis 1 or 3/ dentate gyrus
Ca ²⁺	calcium
CaM	calmodulin (Ca ²⁺ -modulated protein)
CaMK	Ca ²⁺ /CaM-dependent kinase
cAMP	cyclic adenosin monophosphate
cGMP	cyclic guanosin monophosphate
CI-AMPA	see CP-AMPA
CNS	central nervous system
CP-AMPA/CI-AMPA	calcium permeable/impermeable AMPA receptors
CRD	cysteine-rich domain
CTD	C-terminal domain
DA	dopamine
DAG	diacylglycerol
eCB	endocannabinoid
EPSC	excitatory post-synaptic current
ER	endoplasmic reticulum
FRET	fluorescence resonance energy transfer
GABA	γ -Aminobutyric acid
GIRK	G protein-gated inward rectifying potassium channels
GluA1	AMPA subunit 1 (forms Ca ²⁺ -permeable homomers)
GluA2	AMPA subunit 2 (usually Ca ²⁺ -impermeable)
GPCR	G protein-coupled receptor
GRK	GPCR kinase
GTP	guanosine triphosphate
iGlu	ionotropic glutamate (receptors)
InsP3	inositol phosphate-3 (receptor)
IP (or InsP)	inositol phosphate

IP ₁	inositol monophosphate
IP ₂	1,4-bisphosphate
IP ₃	inositol 1,4,5-triphosphate
LTP or LTD	long-term potentiation or depression
mGlu	metabotropic glutamate (receptors)
NAM	negative allosteric modulator
NGF	nerve growth factor
NMDA	<i>N</i> -Methyl-D-aspartate
NMDAR	NMDA receptor
PALM	photoactivated localization microscopy
PAM	positive allosteric modulator
PDE	phosphodiesterase
PI3K/AKT/mTOR	phosphatidylinositol 3-kinase / protein kinase B / mammalian target of rapamycin
PIP ₂	phosphatidylinositol 4,5-bisphosphate
PKA	protein kinase cAMP-dependent
PKC	protein kinase Ca ²⁺ -dependent
PLC	phospholipase C
PP1	protein phosphatase 1
PP2	protein phosphatase 2
PSD	postsynaptic density
RAS/MAPK/ERK	Ras / mitogen-activated protein kinase / extracellular signal-regulated kinases
RGS	regulator of G protein signaling
SAM	silent allosteric modulator
SNAP-25	synaptosomal-associated protein 25
SNARE	soluble NSF Attachment Protein REceptor
SNc, SNr	substantia nigra pars compacta, substantia nigra pars reticulata
SORM	stochastic optical reconstruction microscopy
STED	stimulated emission depletion
t-LTD	timing-dependent LTD
TGFβ	tumor growth factor β
TMD	transmembrane domain
trFRET	time-resolved FRET
TRPM1	transient receptor potential cation channel subfamily M member 1
VFT	venus flytrap (domain)

AKNOWLEDGEMENTS

En una tesi de doctorat, en cinc anys de feina, amb dos jefes, molts col·laboradors, companys i amics, tinc moltes persones a agrair per haver arribat a posar punt final a aquest projecte de la meva vida.

Gràcies a Xavi, 'el meu quimic', sense tu no tindria tesi! I sense les teves bromes seria una 'piciulute' una mica menys contenta. Ana Ester Roser Joan i tots els quimics per haver-me acollit tant bè un estiu al iQac... Gràcies especialment a Amadeu, per haver-me mostrat que es pot ser un jefe genial i ahora tenir tant bon cor com tu el tens!

Gràcies a tota la penya de Bellvitge: Mercè per les hores de bipolaritat compartides 'en la cueva' i per ser un petit crack, Nuri per que ets la nostra incorregible optimista i futura alcaldesa, Aida per la teua divertida ironia, Miquel per donar-nos tant material de discussió a l'hora de dinar! Antoni, per donar-nos en canvi a tots tanta feina, i pels mesos passats al pis. Ari, por contagiar toda tu energía siempre, y escuchar todos nuestros 'porfiiiiii'. Marisabel, por haberme enseñado tantas cosas al llegar al lab. Kay, gracias por tu ayuda con 'los ranas'! Gracias a las mil Annas del lab de la Ana, Santi por que eres mi compañero de tesis hasta el final y una enciclopedia con patas, y por haberme desapretado unos cuantos tornillos, Natalia por haberme hecho reir tanto. Gràcies al Pere per haver donat el impuls pels ultims experiments, pero sobretot... gracias a la niña PubMed y el niño Haver!

Gracias a la otra mitad del lab, los del parc: Andrés y Juanma, por ser un par de friquis muy divertidos y por las conversaciones científicas antisistema, Montse Marta y Berta, por cederme vuestros ordenadores con una sonrisa y reir sobre las peripecias de mi doctorado.

Gràcies Pau, per ser un jefe tant humà com n'hi han pocs, i per haver-me firmat unes quantes fulles en blanc (en tots sentits). M'has sabut guiar sempre donant-me plena llibertat, i això m'ha fet creixer immensament com a científica i com a persona!

Gràcies al Xavi Rovira per fer-me de guia a Montpeller i ser tant generós. Gràcies a l'Anna Lladó per aguantar-me amb les meves punkeries i ajudar-me sempre amb les meves necessitats especials. Gracias a Ari en Elche por todas las horas pasadas a oscuras para sacar esos resultados tan emocionantes. Quería agradecer también a Fernando Aguado por sus consejos con los astrocitos, y a los de la cuarta por dejarnos siempre invadir su agitador.

Un gracias especial a Carlos Avendaño, por haberme hecho descubrir el mundo de la investigación con todo el entusiasmo que te caracteriza.

También quería agradecer a todos los que hicisteis que estos años pasaran tan rápido, con bromas, risas, sonrisas, palabras buenas y malas, birras de chino, birras de paqui, las mailing list del viernes, gracias al gato del raval por haber sido durante mucho tiempo una referencia tan imponente e inmóvil. Gracias Fra, mi gran amiga de Barcelona, mi hermana del alma, que me has enseñado a vivir el presente y que el futuro se cambia. Gracias a la familia de Barcelona, Luca Laura Guido Giaime, Cinzia e Lucia, Ale Cris Violeta Sonia, a los que seguís aquí y los que ya os habéis ido... sin vosotros no hubiera aguantado esta tesis!

Gràcies Iris i Chus per haver sigut tant pacients escoltant i corregint els meus primers passos amb la vostra llengua. El resum en català és per vosaltres! Tot i que no m'espero que el llegiu, que si no al Chus li donarà mal de cap abans d'arribar a 'optofarmacologia'.

Grazie alle befane, Giuliusk Any Cami Emi, siete sempre con me ovunque vada con il suono delle vostre risate nelle orecchie! Grazie a Pio e a Letizia, di voi invece ho il suono delle voci nella testa sempre pronto a rallegrarmi.

Infine grazie a tutta la mia grande famiglia, *a les storís de none Marie*, ai miei fratelli, ma specialmente ai miei genitori, so che il vostro sostegno incondizionato e il vostro aiuto non mi mancherà mai. Devo a voi tutto quello che sono e che ho, e un po' di più...

BIBLIOGRAPHY

- Abe T, Sugihara H, Nawa H, Shigemoto R, Mizuno N and Nakanishi S (1992): Molecular characterization of a novel metabotropic glutamate receptor mGluR5 coupled to inositol phosphate/Ca²⁺ signal transduction. *Journal of Biological Chemistry* 267, 13361-13368
- Adamantidis AR, Zhang F, Aravanis AM, Deisseroth K and de Lecea L (2007): Neural substrates of awakening probed with optogenetic control of hypocretin neurons. *Nature* 450, 420-424. <http://dx.doi.org/10.1038/nature06310>
- Adesnik H, Nicoll RA and England PM (2005): Photoinactivation of native AMPA receptors reveals their real-time trafficking. *Neuron* 48, 977-985. <http://dx.doi.org/10.1016/j.neuron.2005.11.030>
- Airan RD, Thompson KR, Fenno LE, Bernstein H and Deisseroth K (2009): Temporally precise in vivo control of intracellular signalling. *Nature* 458, 1025-1029. <http://dx.doi.org/10.1038/nature07926>
- Alabi AA and Tsien RW (2013): Perspectives on kiss-and-run: role in exocytosis, endocytosis, and neurotransmission. *Annu Rev Physiol* 75, 393-422. <http://dx.doi.org/10.1146/annurev-physiol-020911-153305>
- Alberts B, Johnson A, Lewis J, Raff M, Roberts K and Walter P (2002) *Molecular Biology of the Cell*. Garland Science, New York.
- Albizu L, Cottet M, Kralikova M, Stoev S, Seyer R, Brabet I, Roux T, Bazin H, Bourrier E, Lamarque L, Breton C, Rives M-L, Newman A, Javitch J, Trinquet E, Manning M, Pin J-P, Mouillac B and Durroux T (2010): Time-resolved FRET between GPCR ligands reveals oligomers in native tissues. *Nature chemical biology* 6, 587-594. <http://dx.doi.org/10.1038/nchembio.396>
- Alexander GM and Godwin DW (2006): Metabotropic glutamate receptors as a strategic target for the treatment of epilepsy. *Epilepsy Res* 71, 1-22. <http://dx.doi.org/10.1016/j.eplepsyres.2006.05.012>
- Alexander GM, Rogan SC, Abbas AI, Armbruster BN, Pei Y, Allen JA, Nonneman RJ, Hartmann J, Moy SS, Nicoletis MA, McNamara JO and Roth BL (2009): Remote control of neuronal activity in transgenic mice expressing evolved G protein-coupled receptors. *Neuron* 63, 27-39. <http://dx.doi.org/10.1016/j.neuron.2009.06.014>
- Allen NJ (2014): Astrocyte Regulation of Synaptic Behavior. *Annual Review of Cell and Developmental Biology* 30, 439-463. <http://dx.doi.org/10.1146/annurev-cellbio-100913-013053>
- Amalric M, Lopez S, Goudet C, Fisone G, Battaglia G, Nicoletti F, Pin JP and Acher FC (2013): Group III and subtype 4 metabotropic glutamate receptor agonists: discovery and pathophysiological applications in Parkinson's disease. *Neuropharmacology* 66, 53-64. <http://dx.doi.org/10.1016/j.neuropharm.2012.05.026>
- Ambrosio M and Lohse MJ (2011) Kinetics and Mechanisms of GPCR Activation. In *G Protein-Coupled Receptors : From Structure to Function* (Giraldo J & Pin J-P eds.). The Royal Society of Chemistry, Cambridge.
- Ango F, Prézeau L, Muller T, Tu JC, Xiao B, Worley PF, Pin JP, Bockaert J and Fagni L (2001): Agonist-independent activation of metabotropic glutamate receptors by the intracellular protein Homer. *Nature* 411, 962-965. <http://dx.doi.org/10.1038/35082096>
- Aramori I and Nakanishi S (1992): Signal transduction and pharmacological characteristics of a metabotropic glutamate receptor, mGluR1, in transfected CHO cells. *Neuron* 8, 757-765
- Araque A, Carmignoto G, Haydon PG, Oliet SHR, Robitaille R and Volterra A (2014): Gliotransmitters travel in time and space. *Neuron* 81, 728-739. <http://dx.doi.org/10.1016/j.neuron.2014.02.007>

- Araque A, Parpura V, Sanzgiri RP and Haydon PG (1999): Tripartite synapses: glia, the unacknowledged partner. *Trends Neurosci* 22, 208-215
- Arizono M, Bannai H, Nakamura K, Niwa F, Enomoto M, Matsu-Ura T, Miyamoto A, Sherwood MW, Nakamura T and Mikoshiba K (2012): Receptor-selective diffusion barrier enhances sensitivity of astrocytic processes to metabotropic glutamate receptor stimulation. *Science Signaling* 5, ra27-ra27. <http://dx.doi.org/10.1126/scisignal.2002498>
- Aronica E, Gorter JA, Ijst-Keizers H, Rozemuller AJ, Yankaya B, Leenstra S and Troost D (2003): Expression and functional role of mGluR3 and mGluR5 in human astrocytes and glioma cells: opposite regulation of glutamate transporter proteins. *Eur J Neurosci* 17, 2106-2118
- Atkinson PJ, Young KW, Ennion SJ, Kew JN, Nahorski SR and Challiss RA (2006): Altered expression of G(q/11alpha) protein shapes mGlu1 and mGlu5 receptor-mediated single cell inositol 1,4,5-trisphosphate and Ca(2+) signaling. *Mol Pharmacol* 69, 174-184. <http://dx.doi.org/10.1124/mol.105.014258>
- Atwood BK, Lovinger DM and Mathur BN (2014): Presynaptic long-term depression mediated by Gi/o-coupled receptors. *Trends in Neurosciences*, 1-11. <http://dx.doi.org/10.1016/j.tins.2014.07.010>
- Auerbach BD, Osterweil EK and Bear MF (2011): Mutations causing syndromic autism define an axis of synaptic pathophysiology. *Nature* 480, 63-68. <http://dx.doi.org/10.1038/nature10658>
- Awad H, Hubert GW, Smith Y, Levey AI and Conn PJ (2000): Activation of metabotropic glutamate receptor 5 has direct excitatory effects and potentiates NMDA receptor currents in neurons of the subthalamic nucleus. *J Neurosci* 20, 7871-7879
- Axelrod D, Burghardt TP and Thompson NL (1984): Total internal reflection fluorescence. *Annu Rev Biophys Bioeng* 13, 247-268. <http://dx.doi.org/10.1146/annurev.bb.13.060184.001335>
- Bahamonde MI, Taura J, Paoletta S, Gakh AA, Chakraborty S, Hernando J, Jacobson KA and Gorostiza P (2014): Photomodulation of G Protein-Coupled Adenosine Receptors by a Novel Light-Switchable Ligand. *ACS Bioconjugate Chemistry* 25, 1847-1854. <http://dx.doi.org/10.1021/bc5003373>
- Banghart MR, Mourou A, Fortin DL, Yao JZ, Kramer RH and Trauner D (2009): Photochromic blockers of voltage-gated potassium channels. *Angew Chem Int Ed Engl* 48, 9097-9101. <http://dx.doi.org/10.1002/anie.200904504>
- Bartels E, Wassermann NH and Erlanger BF (1971): Photochromic activators of the acetylcholine receptor. *Proc Natl Acad Sci U S A* 68, 1820-1823
- Battaglia G, Bruno V, Pisani A, Centonze D, Catania MV, Calabresi P and Nicoletti F (2001): Selective blockade of type-1 metabotropic glutamate receptors induces neuroprotection by enhancing gabaergic transmission. *Mol Cell Neurosci* 17, 1071-1083. <http://dx.doi.org/10.1006/mcne.2001.0992>
- Bazin H, Trinquet E and Mathis G (2002): Time resolved amplification of cryptate emission: a versatile technology to trace biomolecular interactions. *Journal of biotechnology* 82, 233-250
- Bear MF, Huber KM and Warren ST (2004): The mGluR theory of fragile X mental retardation. *Trends in Neurosciences* 27, 370-377. <http://dx.doi.org/10.1016/j.tins.2004.04.009>
- Becker JA, Clesse D, Spiegelhalter C, Schwab Y, Le Merrer J and Kieffer BL (2014): Autistic-like syndrome in mu opioid receptor null mice is relieved by facilitated mGluR4 activity. *Neuropsychopharmacology* 39, 2049-2060. <http://dx.doi.org/10.1038/npp.2014.59>
- Beharry Aa and Woolley GA (2011): Azobenzene photoswitches for biomolecules. *Chemical Society reviews* 40, 4422-4437. <http://dx.doi.org/10.1039/c1cs15023e>
- Beiert T, Bruegmann T and Sasse P (2014): Optogenetic activation of Gq signalling modulates pacemaker activity of cardiomyocytes. *Cardiovasc Res* 102, 507-516. <http://dx.doi.org/10.1093/cvr/cvu046>
- Bellone C, Lüscher C and Mameli M (2008): Mechanisms of synaptic depression triggered by metabotropic glutamate receptors. *Cellular and molecular life sciences : CMLS* 65, 2913-2923. <http://dx.doi.org/10.1007/s00018-008-8263-3>
- Benjamin ER, Haftl SL, Xanthos DN, Crumley G, Hachicha M and Valenzano KJ (2004): A miniaturized column chromatography method for measuring receptor-mediated inositol phosphate accumulation. *Journal of biomolecular screening* 9, 343-353. <http://dx.doi.org/10.1177/1087057103262841>
- Beqollari D and Kammermeier PJ (2010): Venus fly trap domain of mGluR1 functions as a dominant negative against group I mGluR signaling. *J Neurophysiol* 104, 439-448. <http://dx.doi.org/10.1152/jn.00799.2009>
- Berger JV, Dumont AO, Focant MC, Vergouts M, Sternotte A, Calas AG, Goursaud S and Hermans E (2012): Opposite regulation of metabotropic glutamate receptor 3 and metabotropic glutamate receptor 5 by inflammatory stimuli in cultured microglia and astrocytes. *Neuroscience* 205, 29-38. <http://dx.doi.org/10.1016/j.neuroscience.2011.12.044>
- Berlin S, Carroll EC, Newman ZL, Okada HO, Quinn CM, Rockwell NC, Martin SS, Lagarias JC and Isacoff EY (2015): Photoactivatable genetically encoded calcium indicators for targeted neuronal imaging. *Nature Methods* 12. <http://dx.doi.org/10.1038/nmeth.3480>
- Bernardinelli Y, Randall J, Janett E, Nikonenko I, König S, Jones EV, Flores CE, Murai KK, Bochet CG, Holtmaat A and Muller D (2014): Activity-dependent structural plasticity of perisynaptic astrocytic domains promotes excitatory synapse stability. *Current Biology* 24, 1679-1688. <http://dx.doi.org/10.1016/j.cub.2014.06.025>
- Berridge MJ, Bootman MD and Roderick HL (2003): Calcium signalling: dynamics, homeostasis and remodelling. *Nature reviews. Molecular cell biology* 4, 517-529. <http://dx.doi.org/10.1038/nrm1155>

- Betzig E, Patterson GH, Sougrat R, Lindwasser OW, Olenych S, Bonifacino JS, Davidson MW, Lippincott-schwartz J and Hess HF (2006): Imaging Intracellular Fluorescent Proteins at Nanometer Resolution. *Science* 313, 1642-1646. <http://dx.doi.org/10.1126/science.1127344>
- Bhakar AL, Dölen G and Bear MF (2012): The Pathophysiology of Fragile X (and What It Teaches Us about Synapses). *Annual Review of Neuroscience* 35, 417-443. <http://dx.doi.org/10.1146/annurev-neuro-060909-153138>
- Blackmer T, Larsen EC, Bartleson C, Kowalchuk JA, Yoon E-J, Preiner AM, Alford S, Hamm HE and Martin TFJ (2005): G protein betagamma directly regulates SNARE protein fusion machinery for secretory granule exocytosis. *Nature Neuroscience* 8, 421-425. <http://dx.doi.org/10.1038/nn1423>
- Blankenship AG and Feller MB (2009): Mechanisms underlying spontaneous patterned activity in developing neural circuits. *Nature Reviews Neuroscience* 11, 18-29. <http://dx.doi.org/10.1038/nrn2759>
- Bleakman D, Alt A and Nisenbaum ES (2006): Glutamate receptors and pain. *Semin Cell Dev Biol* 17, 592-604. <http://dx.doi.org/10.1016/j.semcdb.2006.10.008>
- Boer K, Encha-Razavi F, Sinico M and Aronica E (2010): Differential distribution of group I metabotropic glutamate receptors in developing human cortex. *Brain Research* 1324, 24-33. <http://dx.doi.org/10.1016/j.brainres.2010.02.005>
- Bojkowska K, Santoni de Sio F, Barde I, Offner S, Verp S, Heinis C, Johnsson K and Trono D (2011): Measuring in vivo protein half-life. *Chemistry & biology* 18, 805-815. <http://dx.doi.org/10.1016/j.chembiol.2011.03.014>
- Boyden ES, Zhang F, Bamberg E, Nagel G and Deisseroth K (2005): Millisecond-timescale, genetically targeted optical control of neural activity. *Nat Neurosci* 8, 1263-1268. <http://dx.doi.org/10.1038/nn1525>
- Brabet I, Parmentier ML, De Colle C, Bockaert J, Acher F and Pin JP (1998): Comparative effect of L-CCG-I, DCG-IV and gamma-carboxy-L-glutamate on all cloned metabotropic glutamate receptor subtypes. *Neuropharmacology* 37, 1043-1051
- Bradley SJ and Challiss RAJ (2012): G protein-coupled receptor signalling in astrocytes in health and disease: A focus on metabotropic glutamate receptors. *Biochemical Pharmacology* 84, 249-259. <http://dx.doi.org/10.1016/j.bcp.2012.04.009>
- Bradley SJ, Watson JM and Challiss RA (2009): Effects of positive allosteric modulators on single-cell oscillatory Ca²⁺ signaling initiated by the type 5 metabotropic glutamate receptor. *Mol Pharmacol* 76, 1302-1313. <http://dx.doi.org/10.1124/mol.109.059170>
- Brakeman PR, Lanahan AA, O'Brien R, Roche K, Barnes CA, Hagan RL and Worley PF (1997): Homer: a protein that selectively binds metabotropic glutamate receptors. *Nature* 386, 284-288. <http://dx.doi.org/10.1038/386284a0>
- Breyse N, Baunez C, Spooren W, Gasparini F and Amalric M (2002): Chronic but not acute treatment with a metabotropic glutamate 5 receptor antagonist reverses the akinetic deficits in a rat model of parkinsonism. *J Neurosci* 22, 5669-5678. <http://dx.doi.org/20026513>
- Brock C, Oueslati N, Soler S, Boudier L, Rondard P and Pin J-P (2007): Activation of a dimeric metabotropic glutamate receptor by intersubunit rearrangement. *The Journal of biological chemistry* 282, 33000-33008. <http://dx.doi.org/10.1074/jbc.M702542200>
- Broichhagen J, Frank JA and Trauner D (2015): A Roadmap to Success in Photopharmacology. *Accounts of Chemical Research*, 150623154001000-150623154001000. <http://dx.doi.org/10.1021/acs.accounts.5b00129>
- Bruno V, Battaglia G, Casabona G, Copani A, Caciagli F and Nicoletti F (1998): Neuroprotection by glial metabotropic glutamate receptors is mediated by transforming growth factor-beta. *J Neurosci* 18, 9594-9600
- Cabello N, Gandía J, Bertarelli DCG, Watanabe M, Lluís C, Franco R, Ferré S, Luján R and Ciruela F (2009): Metabotropic glutamate type 5, dopamine D2 and adenosine A_{2a} receptors form higher-order oligomers in living cells. *Journal of Neurochemistry* 109, 1497-1507. <http://dx.doi.org/10.1111/j.1471-4159.2009.06078.x>
- Cahalan MD, Parker I, Wei SH and Miller MJ (2002): Two-photon tissue imaging: seeing the immune system in a fresh light. *Nature reviews. Immunology* 2, 872-880. <http://dx.doi.org/10.1038/nri935>
- Cai X, Sakamoto M, Fujitsuka M and Majima T (2005): Higher triplet excited states of benzophenones and bimolecular triplet energy transfer measured by using nanosecond-picosecond two-color/two-laser flash photolysis. *Chemistry* 11, 6471-6477. <http://dx.doi.org/10.1002/chem.200500463>
- Caldwell JH, Herin GA, Nagel G, Bamberg E, Scheschonka A and Betz H (2008): Increases in intracellular calcium triggered by channelrhodopsin-2 potentiate the response of metabotropic glutamate receptor mGluR7. *J Biol Chem* 283, 24300-24307. <http://dx.doi.org/10.1074/jbc.M802593200>
- Callaway EM and Katz LC (1993): Photostimulation using caged glutamate reveals functional circuitry in living brain slices. *Proc Natl Acad Sci U S A* 90, 7661-7665
- Caraci F, Battaglia G, Sortino MA, Spampinato S, Molinaro G, Copani A, Nicoletti F and Bruno V (2012): Metabotropic glutamate receptors in neurodegeneration/neuroprotection: still a hot topic? *Neurochemistry International* 61, 559-565. <http://dx.doi.org/10.1016/j.neuint.2012.01.017>
- Carrasco S and Mérida I (2007): Diacylglycerol, when simplicity becomes complex. *Trends in biochemical sciences* 32, 27-36. <http://dx.doi.org/10.1016/j.tibs.2006.11.004>

- Carroll EC, Berlin S, Levitz J, Kienzler Ma, Yuan Z, Madsen D, Larsen DS and Isacoff EY (2015): Two-photon brightness of azobenzene photoswitches designed for glutamate receptor optogenetics. *Proceedings of the National Academy of Sciences*, 201416942-201416942. <http://dx.doi.org/10.1073/pnas.1416942112>
- Castillo PE (2012): Presynaptic LTP and LTD of excitatory and inhibitory synapses. *Cold Spring Harbor Perspectives in Biology* 4. <http://dx.doi.org/10.1101/cshperspect.a005728>
- Chen CC, Lu HC and Brumberg JC (2012): mGluR5 knockout mice display increased dendritic spine densities. *Neuroscience Letters* 524, 65-68. <http://dx.doi.org/10.1016/j.neulet.2012.07.014>
- Chevalyre V, Heifets BD, Kaeser PS, Südhof TC, Purpura DP and Castillo PE (2007): Endocannabinoid-Mediated Long-Term Plasticity Requires cAMP/PKA Signaling and RIM1 α . *Neuron* 54, 801-812. <http://dx.doi.org/10.1016/j.neuron.2007.05.020>
- Chevalier A, Hardouin J, Renard PY and Romieu A (2013): Universal dark quencher based on "clicked" spectrally distinct azo dyes. *Org Lett* 15, 6082-6085. <http://dx.doi.org/10.1021/ol402972y>
- Chiamulera C, Epping-Jordan MP, Zocchi A, Marcon C, Cottiny C, Tacconi S, Corsi M, Orzi F and Conquet F (2001): Reinforcing and locomotor stimulant effects of cocaine are absent in mGluR5 null mutant mice. *Nature Neuroscience* 4, 873-874. <http://dx.doi.org/10.1038/nn0901-873>
- Chiarini-Garcia H, Melo C. M R, Ghiran C I and Walker JM (2011) *Light microscopy: methods and protocols*.
- Choi KY, Chung S and Roche KW (2011): Differential binding of calmodulin to group I metabotropic glutamate receptors regulates receptor trafficking and signaling. *The Journal of neuroscience : the official journal of the Society for Neuroscience* 31, 5921-5930. <http://dx.doi.org/10.1523/JNEUROSCI.6253-10.2011>
- Ciccarelli R, Di Iorio P, Bruno V, Battaglia G, D'Alimonte I, D'Onofrio M, Nicoletti F and Caciagli F (1999): Activation of A(1) adenosine or mGlu3 metabotropic glutamate receptors enhances the release of nerve growth factor and S-100 β protein from cultured astrocytes. *Glia* 27, 275-281
- Ciruela F, Vilardaga JP and Fernández-Dueñas V (2010) Lighting up multiprotein complexes: Lessons from GPCR oligomerization, pp. 407-415.
- Collingridge GL, Peineau S, Howland JG and Wang YT (2010): Long-term depression in the CNS. *Nat Rev Neurosci* 11, 459-473. <http://dx.doi.org/10.1038/nrn2867>
- Conn PJ, Battaglia G, Marino MJ and Nicoletti F (2005): Metabotropic glutamate receptors in the basal ganglia motor circuit. *Nature reviews. Neuroscience* 6, 787-798. <http://dx.doi.org/10.1038/nrn1763>
- Conn PJ, Christopoulos A and Lindsley CW (2009a): Allosteric modulators of GPCRs: a novel approach for the treatment of CNS disorders. *Nature reviews. Drug discovery* 8, 41-54. <http://dx.doi.org/10.1038/nrd2760>
- Conn PJ, Lindsley CW and Jones CK (2009b): Activation of metabotropic glutamate receptors as a novel approach for the treatment of schizophrenia. *Trends Pharmacol Sci* 30, 25-31. <http://dx.doi.org/10.1016/j.tips.2008.10.006>
- Conquet F, Bashir ZI, Davies CH, Daniel H, Ferraguti F, Bordi F, Franz-Bacon K, Reggiani A, Matarese V and Condé F (1994): Motor deficit and impairment of synaptic plasticity in mice lacking mGluR1. *Nature* 372, 237-243. <http://dx.doi.org/10.1038/372237a0>
- Conti V, Aghaie A, Cilli M, Martin N, Caridi G, Musante L, Candiano G, Castagna M, Fairen A, Ravazzolo R, Guenet J-L and Puliti A (2006): *crv4*, a mouse model for human ataxia associated with kyphoscoliosis caused by an mRNA splicing mutation of the metabotropic glutamate receptor 1 (*Grm1*). *International journal of molecular medicine* 18, 593-600
- Cornell-Bell AH, Finkbeiner SM, Cooper MS and Smith SJ (1990): Glutamate induces calcium waves in cultured astrocytes: long-range glial signaling. *Science* 247, 470-473
- Corti C, Aldegheri L, Somogyi P and Ferraguti F (2002): Distribution and synaptic localisation of the metabotropic glutamate receptor 4 (mGluR4) in the rodent CNS. *Neuroscience* 110, 403-420. [http://dx.doi.org/10.1016/S0306-4522\(01\)00591-7](http://dx.doi.org/10.1016/S0306-4522(01)00591-7)
- Cosgrove KE, Galván EJ, Barrionuevo G and Meriney SD (2011): mGluRs modulate strength and timing of excitatory transmission in hippocampal area CA3. *Molecular Neurobiology* 44, 93-101. <http://dx.doi.org/10.1007/s12035-011-8187-z>
- Costantini LM and Snapp EL (2013): Fluorescent proteins in cellular organelles: serious pitfalls and some solutions. *DNA and cell biology* 32, 622-627. <http://dx.doi.org/10.1089/dna.2013.2172>
- Cottet M, Faklaris O, Falco A, Trinquet E, Pin J-P, Mouillac B and Durroux T (2013): Fluorescent ligands to investigate GPCR binding properties and oligomerization. *Biochemical Society transactions* 41, 148-153. <http://dx.doi.org/10.1042/BST20120237>
- Cottet M, Faklaris O, Maurel D, Scholler P, Doumazane E, Trinquet E, Pin JP and Durroux T (2012): BRET and time-resolved FRET strategy to study GPCR oligomerization: From cell lines toward native tissues. *Frontiers in Endocrinology* 3, 1-14. <http://dx.doi.org/10.3389/fendo.2012.00092>
- Coutinho V, Kavanagh I, Sugiyama H, Tones MA and Henley JM (2001): Characterization of a metabotropic glutamate receptor type 5-green fluorescent protein chimera (mGluR5-GFP): pharmacology, surface expression, and differential effects of Homer-1a and Homer-1c. *Mol Cell Neurosci* 18, 296-306. <http://dx.doi.org/10.1006/mcne.2001.1031>
- Cryan JF, Kelly PH, Neijt HC, Sansig G, Flor PJ and van Der Putten H (2003): Antidepressant and anxiolytic-like effects in mice lacking the group III metabotropic glutamate receptor mGluR7. *The European journal of neuroscience* 17, 2409-2417

- Cui-Wang T, Hanus C, Cui T, Helton T, Bourne J, Watson D, Harris KM and Ehlers MD (2012): Local zones of endoplasmic reticulum complexity confine cargo in neuronal dendrites. *Cell* 148, 309-321. <http://dx.doi.org/10.1016/j.cell.2011.11.056>
- D'Antoni S, Berretta A, Bonaccorso CM, Bruno V, Aronica E, Nicoletti F and Catania MV (2008): Metabotropic glutamate receptors in glial cells. *Neurochemical research* 33, 2436-2443. <http://dx.doi.org/10.1007/s11064-008-9694-9>
- Damijonaitis A, Broichhagen J, Urushima T, Hüll K, Nagpal J, Laprell L, Schönberger M, Woodmansee DH, Rafiq A, Sumser MP, Kummer W, Gottschalk A and Trauner D (2015): AzoCholine Enables Optical Control of Alpha 7 Nicotinic Acetylcholine Receptors in Neural Networks. *ACS Chemical Neuroscience*, 150327112428002-150327112428002. <http://dx.doi.org/10.1021/acschemneuro.5b00030>
- Darnell JC and Klann E (2013): The translation of translational control by FMRP: therapeutic targets for FXS. *Nature Neuroscience* 16, 1530-1536. <http://dx.doi.org/10.1038/nn.3379>
- Davis MJ, Iancu OD, Acher FC, Stewart BM, Eiwaz Ma, Duvoisin RM and Raber J (2013): Role of mGluR4 in acquisition of fear learning and memory. *Neuropharmacology* 66, 365-372. <http://dx.doi.org/10.1016/j.neuropharm.2012.07.038>
- De Koninck P and Schulman H (1998): Sensitivity of CaM kinase II to the frequency of Ca²⁺ oscillations. *Science* 279, 227-230
- de Novellis V, Mariani L, Palazzo E, Vita D, Marabese I, Scafuro M, Rossi F and Maione S (2005): Periaqueductal grey CB1 cannabinoid and metabotropic glutamate subtype 5 receptors modulate changes in rostral ventromedial medulla neuronal activities induced by subcutaneous formalin in the rat. *Neuroscience* 134, 269-281. <http://dx.doi.org/10.1016/j.neuroscience.2005.03.014>
- de Paulis T, Hemstapat K, Chen Y, Zhang Y, Saleh S, Alagille D, Baldwin RM, Tamagnan GD and Conn PJ (2006): Substituent effects of N-(1,3-diphenyl-1H-pyrazol-5-yl)benzamides on positive allosteric modulation of the metabotropic glutamate-5 receptor in rat cortical astrocytes. *Journal of medicinal chemistry* 49, 3332-3344. <http://dx.doi.org/10.1021/jm051252j>
- De Pittà M, Brunel N and Volterra A (2015): Astrocytes: Orchestrating synaptic plasticity? *Neuroscience*. <http://dx.doi.org/10.1016/j.neuroscience.2015.04.001>
- Dean KM and Palmer AE (2014): Advances in fluorescence labeling strategies for dynamic cellular imaging. *Nature chemical biology* 10, 512-523. <http://dx.doi.org/10.1038/nchembio.1556>
- Deisseroth K (2011): Optogenetics. *Nature Methods* 8, 26-29. <http://dx.doi.org/10.1038/nmeth.f.324>
- Deisseroth K (2015): Optogenetics: 10 years of microbial opsins in neuroscience. *Nature Neuroscience* 18, 1213-1225. <http://dx.doi.org/10.1038/nn.4091>
- Denk W, Strickler JH and Webb WW (1990): Two-photon laser scanning fluorescence microscopy. *Science (New York, N.Y.)* 248, 73-76
- Devaraju P, Sun M-Y, Myers TL, Lauderdale K and Fiacco Ta (2013): Astrocytic group I mGluR-dependent potentiation of astrocytic glutamate and potassium uptake. *Journal of neurophysiology* 109, 2404-2414. <http://dx.doi.org/10.1152/jn.00517.2012>
- DeWire SM, Ahn S, Lefkowitz RJ and Shenoy SK (2007): β -Arrestins and Cell Signaling. *Annual Review of Physiology* 69, 483-510. <http://dx.doi.org/10.1146/annurev.physiol.69.022405.154749>
- Doherty AJ, Coutinho V, Collingridge GL and Henley JM (1999): Rapid internalization and surface expression of a functional, fluorescently tagged G-protein-coupled glutamate receptor. *Biochem J* 341 (Pt 2), 415-422
- Doré AS, Okrasa K, Patel JC, Serrano-Vega M, Bennett K, Cooke RM, Errey JC, Jazayeri A, Khan S, Tehan B, Weir M, Wiggan GR and Marshall FH (2014): Structure of class C GPCR metabotropic glutamate receptor 5 transmembrane domain. *Nature* 511, 557-562. <http://dx.doi.org/10.1038/nature13396>
- Doumazane E, Scholler P, Fabre L, Zwier JM, Trinquet E, Pin J-P and Rondard P (2013): Illuminating the activation mechanisms and allosteric properties of metabotropic glutamate receptors. *Proceedings of the National Academy of Sciences of the United States of America* 110, E1416-1425. <http://dx.doi.org/10.1073/pnas.1215615110>
- Doumazane E, Scholler P, Zwier JM, Trinquet E, Rondard P and Pin J-P (2011): A new approach to analyze cell surface protein complexes reveals specific heterodimeric metabotropic glutamate receptors. *FASEB journal : official publication of the Federation of American Societies for Experimental Biology* 25, 66-77. <http://dx.doi.org/10.1096/fj.10-163147>
- Dunayevich E, Erickson J, Levine L, Landbloom R, Schoepp DD and Tollefson GD (2008): Efficacy and tolerability of an mGlu2/3 agonist in the treatment of generalized anxiety disorder. *Neuropsychopharmacology* 33, 1603-1610. <http://dx.doi.org/10.1038/sj.npp.1301531>
- Dutar P, Vu HM and Perkel DJ (1999): Pharmacological characterization of an unusual mGluR-evoked neuronal hyperpolarization mediated by activation of GIRK channels. *Neuropharmacology* 38, 467-475. [http://dx.doi.org/10.1016/S0028-3908\(98\)00206-8](http://dx.doi.org/10.1016/S0028-3908(98)00206-8)
- Duvoisin RM, Zhang C and Ramonell K (1995): A novel metabotropic glutamate receptor expressed in the retina and olfactory bulb. *The Journal of neuroscience : the official journal of the Society for Neuroscience* 15, 3075-3083
- El Moustaine D, Granier S, Doumazane E, Scholler P, Rahmeh R and Bron P (2012): Distinct roles of metabotropic glutamate receptor dimerization in agonist activation and G-protein coupling. <http://dx.doi.org/10.1073/pnas.1205838109/-/DCSupplemental.www.pnas.org/cgi/doi/10.1073/pnas.1205838109>

- Ellis-Davies GCR (2007): Caged compounds: photorelease technology for control of cellular chemistry and physiology. *Nature Methods* 4, 619-628. <http://dx.doi.org/10.1038/nmeth1072>
- Emile L, Mercken L, Apiou F, Pradier L, Bock MD, Menager J, Clot J, Doble A and Blanchard JC (1996): Molecular cloning, functional expression, pharmacological characterization and chromosomal localization of the human metabotropic glutamate receptor type 3. *Neuropharmacology* 35, 523-530
- Engers DW, Field JR, Le U, Zhou Y, Bolinger JD, Zamorano R, Blobaum AL, Jones CK, Jadhav S, Weaver CD, Conn PJ, Lindsley CW, Niswender CM and Hopkins CR (2011): Discovery, synthesis, and structure-activity relationship development of a series of N-(4-acetamido)phenylpicolinamides as positive allosteric modulators of metabotropic glutamate receptor 4 (mGlu(4)) with CNS exposure in rats. *J Med Chem* 54, 1106-1110. <http://dx.doi.org/10.1021/jm101271s>
- Enz R (2012) Structure of metabotropic glutamate receptor C-terminal domains in contact with interacting proteins.
- Eroglu C and Barres Ba (2010): Regulation of synaptic connectivity by glia. *Nature* 468, 223-231. <http://dx.doi.org/10.1038/nature09612>
- Fagni L, Ango F, Perroy J and Bockaert J (2004): Identification and functional roles of metabotropic glutamate receptor-interacting proteins. *Seminars in cell & developmental biology* 15, 289-298. <http://dx.doi.org/10.1016/j.semcdb.2003.12.018>
- Fatemi SH and Folsom TD (2011): Dysregulation of fragile x mental retardation protein and metabotropic glutamate receptor 5 in superior frontal cortex of individuals with autism: a postmortem brain study. *Molecular autism* 2, 6-6. <http://dx.doi.org/10.1186/2040-2392-2-6>
- Fazio F, Notartomaso S, Aronica E, Storto M, Battaglia G, Vieira E, Gatti S, Bruno V, Biagioni F, Gradini R, Nicoletti F and Di Marco R (2008): Switch in the expression of mGlu1 and mGlu5 metabotropic glutamate receptors in the cerebellum of mice developing experimental autoimmune encephalomyelitis and in autptic cerebellar samples from patients with multiple sclerosis. *Neuropharmacology* 55, 491-499. <http://dx.doi.org/10.1016/j.neuropharm.2008.06.066>
- Fernández-Suárez M and Ting AY (2008): Fluorescent probes for super-resolution imaging in living cells. *Nature reviews. Molecular cell biology* 9, 929-943. <http://dx.doi.org/10.1038/nrm2531>
- Ferraguti F and Shigemoto R (2006): Metabotropic glutamate receptors. *Cell and Tissue Research* 326, 483-504. <http://dx.doi.org/10.1007/s00441-006-0266-5>
- Ferre S, Karcz-Kubicha M, Hope BT, Popoli P, Burgueno J, Gutierrez MA, Casado V, Fuxe K, Goldberg SR, Lluís C, Franco R and Ciruela F (2002): Synergistic interaction between adenosine A2A and glutamate mGlu5 receptors: implications for striatal neuronal function. *Proc Natl Acad Sci U S A* 99, 11940-11945. <http://dx.doi.org/10.1073/pnas.172393799>
- Finlay C and Duty S (2014): Therapeutic potential of targeting glutamate receptors in Parkinson's disease. *Journal of neural transmission (Vienna, Austria : 1996)* 121, 861-880. <http://dx.doi.org/10.1007/s00702-014-1176-4>
- Fino E, Araya R, Peterka DS, Salierno M, Etchenique R and Yuste R (2009): RuBi-Glutamate: Two-Photon and Visible-Light Photoactivation of Neurons and Dendritic spines. *Frontiers in neural circuits* 3, 2-2. <http://dx.doi.org/10.3389/neuro.04.002.2009>
- Fino E and Yuste R (2011): Dense inhibitory connectivity in neocortex. *Neuron* 69, 1188-1203. <http://dx.doi.org/10.1016/j.neuron.2011.02.025>
- Flor PJ, Lindauer K, Püttner I, Rüegg D, Lukic S, Knöpfel T and Kuhn R (1995a): Molecular cloning, functional expression and pharmacological characterization of the human metabotropic glutamate receptor type 2. *The European journal of neuroscience* 7, 622-629
- Flor PJ, Lukic S, Ruegg D, Leonhardt T, Knöpfel T and Kuhn R (1995b): Molecular cloning, functional expression and pharmacological characterization of the human metabotropic glutamate receptor type 4. *Neuropharmacology* 34, 149-155
- Fourgeaud L, Bessis AS, Rossignol F, Pin JP, Olivo-Marin JC and Hemar A (2003): The metabotropic glutamate receptor mGluR5 is endocytosed by a clathrin-independent pathway. *J Biol Chem* 278, 12222-12230. <http://dx.doi.org/10.1074/jbc.M205663200>
- Francesconi A and Duvoisin RM (2004): Divalent cations modulate the activity of metabotropic glutamate receptors. *Journal of neuroscience research* 75, 472-479. <http://dx.doi.org/10.1002/jnr.10853>
- Frank RAW, McRae AF, Pocklington AJ, van de Lagemaat LN, Navarro P, Croning MDR, Komiyama NH, Bradley SJ, Challiss RAJ, Armstrong JD, Finn RD, Malloy MP, MacLean AW, Harris SE, Starr JM, Bhaskar SS, Howard EK, Hunt SE, Coffey AJ, Ranganath V, Deloukas P, Rogers J, Muir WJ, Deary IJ, Blackwood DH, Visscher PM and Grant SGN (2011): Clustered coding variants in the glutamate receptor complexes of individuals with schizophrenia and bipolar disorder. *PLoS one* 6, e19011-e19011. <http://dx.doi.org/10.1371/journal.pone.0019011>
- Fridy PC, Li Y, Keegan S, Thompson MK, Nudelman I, Scheid JF, Oeffinger M, Nussenzweig MC, Fenyö D, Chait BT and Rout MP (2014): A robust pipeline for rapid production of versatile nanobody repertoires. *Nature Methods* 11, 1253-1260. <http://dx.doi.org/10.1038/nmeth.3170>
- Fu Y, Liao H-W, Do MTH and Yau K-W (2005): Non-image-forming ocular photoreception in vertebrates. *Current opinion in neurobiology* 15, 415-422. <http://dx.doi.org/10.1016/j.conb.2005.06.011>
- Gallagher SM, Daly CA, Bear MF and Huber KM (2004): Extracellular signal-regulated protein kinase activation is required for metabotropic glutamate receptor-dependent long-term depression in hippocampal area CA1.

- The Journal of neuroscience : the official journal of the Society for Neuroscience* 24, 4859-4864. <http://dx.doi.org/10.1523/JNEUROSCI.5407-03.2004>
- Gandhi V (2002): Metabolism and mechanisms of action of bendamustine: rationales for combination therapies. *Semin Oncol* 29, 4-11
- Gandía J, Lluís C, Ferré S, Franco R and Ciruela F (2008) Light resonance energy transfer-based methods in the study of G protein-coupled receptor oligomerization, pp. 82-89.
- Gao C, Tronson NC and Radulovic J (2013): Modulation of behavior by scaffolding proteins of the post-synaptic density. *Neurobiology of Learning and Memory* 105, 3-12. <http://dx.doi.org/10.1016/j.nlm.2013.04.014>
- Gasparini F, Lingenhöhl K, Stoehr N, Flor PJ, Heinrich M, Vranesic I, Biollaz M, Allgeier H, Heckendorn R, Urwyler S, Varney Ma, Johnson EC, Hess SD, Rao SP, Saccaan AI, Santori EM, Veliçelebi G and Kuhn R (1999): 2-Methyl-6-(phenylethynyl)-pyridine (MPEP), a potent, selective and systemically active mGlu5 receptor antagonist. *Neuropharmacology* 38, 1493-1503. [http://dx.doi.org/10.1016/S0028-3908\(99\)00082-9](http://dx.doi.org/10.1016/S0028-3908(99)00082-9)
- Gerachshenko T, Blackmer T, Yoon E-J, Bartleson C, Hamm HE and Alford S (2005): Gbetagamma acts at the C terminus of SNAP-25 to mediate presynaptic inhibition. *Nature Neuroscience* 8, 597-605. <http://dx.doi.org/10.1038/nn1439>
- Gereau RW and Heinemann SF (1998): Role of Protein Kinase C Phosphorylation in Rapid Desensitization of Metabotropic Glutamate Receptor 5. *Neuron* 20, 143-151. [http://dx.doi.org/10.1016/S0896-6273\(00\)80442-0](http://dx.doi.org/10.1016/S0896-6273(00)80442-0)
- Gereau RW and Swanson G (2008) *The Glutamate Receptors*. Humana Press.
- Geurts JJ, Wolswijk G, Bo L, van der Valk P, Polman CH, Troost D and Aronica E (2003): Altered expression patterns of group I and II metabotropic glutamate receptors in multiple sclerosis. *Brain* 126, 1755-1766. <http://dx.doi.org/10.1093/brain/awg179>
- Gomez J, Mary S, Brabet I, Parmentier ML, Restituito S, Bockeaert J and Pin JP (1996): Coupling of metabotropic glutamate receptors 2 and 4 to G alpha 15, G alpha 16, and chimeric G alpha q/i proteins: characterization of new antagonists. *Mol Pharmacol* 50, 923-930
- González-Maeso J, Ang RL, Yuen T, Chan P, Weisstaub NV, López-Giménez JF, Zhou M, Okawa Y, Callado LF, Milligan G, Gingrich Ja, Filizola M, Meana JJ and Sealfon SC (2008): Identification of a serotonin/glutamate receptor complex implicated in psychosis. *Nature* 452, 93-97. <http://dx.doi.org/10.1038/nature06612>
- Gordon GRJ, Iremonger KJ, Kantevari S, Ellis-Davies GCR, MacVicar BA and Bains JS (2009): Astrocyte-Mediated Distributed Plasticity at Hypothalamic Glutamate Synapses. *Neuron* 64, 391-403. <http://dx.doi.org/10.1016/j.neuron.2009.10.021>
- Gorostiza P and Isacoff E (2007): Optical switches and triggers for the manipulation of ion channels and pores. *Molecular bioSystems* 3, 686-704. <http://dx.doi.org/10.1039/b710287a>
- Gorostiza P and Isacoff EY (2008): Optical switches for remote and noninvasive control of cell signaling. *Science* 322, 395-399. <http://dx.doi.org/10.1126/science.1166022>
- Gorshkov K and Zhang J (2014): Visualization of cyclic nucleotide dynamics in neurons. *Frontiers in Cellular Neuroscience* 8, 1-13. <http://dx.doi.org/10.3389/fncel.2014.00395>
- Goudet C, Gaven F, Kniazeff J, Vol C, Liu J, Cohen-Gonsaud M, Acher F, Prêzeau L and Pin JP (2004): Heptahelical domain of metabotropic glutamate receptor 5 behaves like rhodopsin-like receptors. *Proceedings of the National Academy of Sciences of the United States of America* 101, 378-383. <http://dx.doi.org/10.1073/pnas.0304699101>
- Goudet C, Magnaghi V, Landry M, Nagy F, Gereau Iv RW and Pin JP (2009): Metabotropic receptors for glutamate and GABA in pain. *Brain Research Reviews* 60, 43-56. <http://dx.doi.org/10.1016/j.brainresrev.2008.12.007>
- Gourine AV, Kasymov V, Marina N, Tang F, Figueiredo MF, Lane S, Teschemacher AG, Spyer KM, Deisseroth K and Kasparov S (2010): Astrocytes control breathing through pH-dependent release of ATP. *Science* 329, 571-575. <http://dx.doi.org/10.1126/science.1190721>
- Grant BD and Donaldson JG (2009): Pathways and mechanisms of endocytic recycling. *Nat Rev Mol Cell Biol* 10, 597-608. <http://dx.doi.org/10.1038/nrm2755>
- Graves AR, Moore SJ, Bloss EB, Mensh BD, Kath WL and Spruston N (2012): Hippocampal Pyramidal Neurons Comprise Two Distinct Cell Types that Are Countermodulated by Metabotropic Receptors. *Neuron* 76, 776-789. <http://dx.doi.org/10.1016/j.neuron.2012.09.036>
- Gray NW, Fourgeaud L, Huang B, Chen J, Cao H, Oswald BJ, Hémar A and McNiven MA (2003): Dynamin 3 Is a Component of the Postsynapse, Where it Interacts with mGluR5 and Homer. *Current Biology* 13, 510-515. [http://dx.doi.org/10.1016/S0960-9822\(03\)00136-2](http://dx.doi.org/10.1016/S0960-9822(03)00136-2)
- Gregory KJ and Conn PJ (2015): Molecular Insights into Metabotropic Glutamate Receptor Allosteric Modulation. *Molecular Pharmacology* 88, 188-202
- Gregory KJ, Noetzel MJ, Rook JM, Vinson PN, Stauffer SR, Rodriguez aL, Emmitte Ka, Zhou Y, Chun aC, Felts aS, Chauder Ba, Lindsley CW, Niswender CM and Conn PJ (2012): Investigating Metabotropic Glutamate Receptor 5 Allosteric Modulator Cooperativity, Affinity, and Agonism: Enriching Structure-Function Studies and Structure-Activity Relationships. *Molecular Pharmacology* 82, 860-875. <http://dx.doi.org/10.1124/mol.112.080531>

- Grienberger C and Konnerth A (2012): Imaging calcium in neurons. *Neuron* 73, 862-885. <http://dx.doi.org/10.1016/j.neuron.2012.02.011>
- Groc L and Choquet D (2006): AMPA and NMDA glutamate receptor trafficking: multiple roads for reaching and leaving the synapse. *Cell and Tissue Research* 326, 423-438. <http://dx.doi.org/10.1007/s00441-006-0254-9>
- Gross G, Junge J, Mora R, Kwon HB, Olson CA, Takahashi T, Liman E, Ellis-Davies GR, McGee A, Sabatini B, Roberts R and Arnold D (2013): Recombinant Probes for Visualizing Endogenous Synaptic Proteins in Living Neurons. *Neuron* 78, 971-985. <http://dx.doi.org/10.1016/j.neuron.2013.04.017>
- Grynkiewicz G, Poenie M and Tsien RY (1985): A new generation of Ca²⁺ indicators with greatly improved fluorescence properties. *J. Biol. Chem.* 260, 3440-3450
- Gubellini P, Melon C, Dale E, Doller D and Kerkerian-Le Goff L (2014): Distinct effects of mGlu4 receptor positive allosteric modulators at corticostriatal vs. striatopallidal synapses may differentially contribute to their antiparkinsonian action. *Neuropharmacology* 85, 166-177. <http://dx.doi.org/10.1016/j.neuropharm.2014.05.025>
- Gulyás G, Tóth JT, Tóth DJ, Kurucz I, Hunyady L, Balla T and Várnai P (2015): Measurement of Inositol 1,4,5-Trisphosphate in Living Cells Using an Improved Set of Resonance Energy Transfer-Based Biosensors. *PLoS one* 10, e0125601-e0125601. <http://dx.doi.org/10.1371/journal.pone.0125601>
- Hainmüller T, Kriegstein K, Kulik A and Bartos M (2014): Joint CP-AMPA and group I mGlu receptor activation is required for synaptic plasticity in dentate gyrus fast-spiking interneurons. *Proceedings of the National Academy of Sciences* 111, 13211-13216. <http://dx.doi.org/10.1073/pnas.1409394111>
- Han JS and Neugebauer V (2005): mGluR1 and mGluR5 antagonists in the amygdala inhibit different components of audible and ultrasonic vocalizations in a model of arthritic pain. *Pain* 113, 211-222. <http://dx.doi.org/10.1016/j.pain.2004.10.022>
- Haustein MD, Kracun S, Lu XH, Shih T, Jackson-Weaver O, Tong X, Xu J, Yang XW, O'Dell TJ, Marvin JS, Ellisman MH, Bushong Ea, Looger LL and Khakh BS (2014): Conditions and constraints for astrocyte calcium signaling in the hippocampal mossy fiber pathway. *Neuron* 82, 413-429. <http://dx.doi.org/10.1016/j.neuron.2014.02.041>
- Hayashi MK, Tang C, Verpelli C, Narayanan R, Stearns MH, Xu R-M, Li H, Sala C and Hayashi Y (2009): The postsynaptic density proteins Homer and Shank form a polymeric network structure. *Cell* 137, 159-171. <http://dx.doi.org/10.1016/j.cell.2009.01.050>
- Heifets BD and Castillo PE (2009): Endocannabinoid signaling and long-term synaptic plasticity. *Annu Rev Physiol* 71, 283-306. <http://dx.doi.org/10.1146/annurev.physiol.010908.163149>
- Hein P, Frank M, Hoffmann C, Lohse MJ and Bunemann M (2005): Dynamics of receptor/G protein coupling in living cells. *EMBO J* 24, 4106-4114. <http://dx.doi.org/10.1038/sj.emboj.7600870>
- Hell SW and Wichmann J (1994): Breaking the diffraction resolution limit by stimulated emission: stimulated-emission-depletion fluorescence microscopy. *Optics letters* 19, 780-782. <http://dx.doi.org/10.1364/OL.19.000780>
- Hermann D and Schneider M (2012): Potential protective effects of cannabidiol on neuroanatomical alterations in cannabis users and psychosis: a critical review. *Curr Pharm Des* 18, 4897-4905
- Hink MA, Griep RA, Borst JW, van Hoek A, Eppink MH, Schots A and Visser AJ (2000): Structural dynamics of green fluorescent protein alone and fused with a single chain Fv protein. *The Journal of biological chemistry* 275, 17556-17560. <http://dx.doi.org/10.1074/jbc.M001348200>
- Hlavackova V, Zabel U, Frankova D, Batz J, Hoffmann C, Prezeau L, Pin JP, Blahos J and Lohse MJ (2012): Sequential Inter- and Intrasubunit Rearrangements During Activation of Dimeric Metabotropic Glutamate Receptor 1. *Science Signaling* 5, ra59-ra59. <http://dx.doi.org/10.1126/scisignal.2002720>
- Holbro N, Grunditz A and Oertner TG (2009): Differential distribution of endoplasmic reticulum controls metabotropic signaling and plasticity at hippocampal synapses. *Proceedings of the National Academy of Sciences of the United States of America* 106, 15055-15060. <http://dx.doi.org/10.1073/pnas.0905110106>
- Hölscher C, Schmid S, Pilz PKD, Sansig G, van der Putten H and Plappert CF (2004): Lack of the metabotropic glutamate receptor subtype 7 selectively impairs short-term working memory but not long-term memory. *Behavioural brain research* 154, 473-481. <http://dx.doi.org/10.1016/j.bbr.2004.03.015>
- Hölscher C, Schmid S, Pilz PKD, Sansig G, van der Putten H and Plappert CF (2005): Lack of the metabotropic glutamate receptor subtype 7 selectively modulates Theta rhythm and working memory. *Learning & memory (Cold Spring Harbor, N.Y.)* 12, 450-455. <http://dx.doi.org/10.1101/lm.98305>
- Hou L and Klann E (2004): Activation of the phosphoinositide 3-kinase-Akt-mammalian target of rapamycin signaling pathway is required for metabotropic glutamate receptor-dependent long-term depression. *The Journal of neuroscience : the official journal of the Society for Neuroscience* 24, 6352-6361. <http://dx.doi.org/10.1523/JNEUROSCI.0995-04.2004>
- Hu J-H, Park JM, Park S, Xiao B, Dehoff MH, Kim S, Hayashi T, Schwarz MK, Haganir RL, Seeburg PH, Linden DJ and Worley PF (2010): Homeostatic scaling requires group I mGluR activation mediated by Homer1a. *Neuron* 68, 1128-1142. <http://dx.doi.org/10.1016/j.neuron.2010.11.008>
- Hu J-H, Yang L, Kammermeier PJ, Moore CG, Brakeman PR, Tu J, Yu S, Petralia RS, Li Z, Zhang P-W, Park JM, Dong X, Xiao B and Worley PF (2012): Preso1 dynamically regulates group I metabotropic glutamate receptors. *Nature Neuroscience* 15, 836-844. <http://dx.doi.org/10.1038/nn.3103>

- Huang B, Babcock H and Zhuang X (2010): Breaking the diffraction barrier: Super-resolution imaging of cells. *Cell* 143, 1047-1058. <http://dx.doi.org/10.1016/j.cell.2010.12.002>
- Huber KM, Gallagher SM, Warren ST and Bear MF (2002): Altered synaptic plasticity in a mouse model of fragile X mental retardation. *Proceedings of the National Academy of Sciences of the United States of America* 99, 7746-7750. <http://dx.doi.org/10.1073/pnas.122205699>
- Huber KM, Kayser MS and Bear MF (2000): Role for rapid dendritic protein synthesis in hippocampal mGluR-dependent long-term depression. *Science (New York, N.Y.)* 288, 1254-1257. <http://dx.doi.org/10.1126/science.288.5469.1254>
- Ikeda SR (1996): Voltage-dependent modulation of N-type calcium channels by G-protein beta gamma subunits. *Nature* 380, 255-258. <http://dx.doi.org/10.1038/380255a0>
- Irannejad R, Tomshine JC, Tomshine JR, Chevalier M, Mahoney JP, Steyaert J, Rasmussen SGF, Sunahara RK, El-Samad H, Huang B and von Zastrow M (2013): Conformational biosensors reveal GPCR signalling from endosomes. *Nature* 495, 534-538. <http://dx.doi.org/10.1038/nature12000>
- Irvine RF and Schell MJ (2001): Back in the water: the return of the inositol phosphates. *Nature reviews. Molecular cell biology* 2, 327-338. <http://dx.doi.org/10.1038/35073015>
- Isomura A and Kageyama R (2014): Ultradian oscillations and pulses: coordinating cellular responses and cell fate decisions. *Development* 141, 3627-3636. <http://dx.doi.org/10.1242/dev.104497>
- Ito M (1989): Long-term depression. *Annu Rev Neurosci* 12, 85-102. <http://dx.doi.org/10.1146/annurev.ne.12.030189.000505>
- Izquierdo-Serra M, Gascón-Moya M, Hirtz JJ, Pittolo S, Poskanzer KE, Ferrer È, Alibés R, Busqué F, Yuste R, Hernando J and Gorostiza P (2014): Two-photon neuronal and astrocytic stimulation with azobenzene-based photoswitches. *Journal of the American Chemical Society* 136, 8693-8701. <http://dx.doi.org/10.1021/ja5026326>
- Jacob W, Gravius A, Pietraszek M, Nagel J, Belozertseva I, Shekunova E, Malysheva A, Greco S, Barberi C and Danysz W (2009): The anxiolytic and analgesic properties of fenobam, a potent mGlu5 receptor antagonist, in relation to the impairment of learning. *Neuropharmacology* 57, 97-108. <http://dx.doi.org/10.1016/j.neuropharm.2009.04.011>
- Jin D-Z, Xue B, Mao L-M and Wang JQ (2015): Metabotropic glutamate receptor 5 upregulates surface NMDA receptor expression in striatal neurons via CaMKII. *Brain Research*, 1-10. <http://dx.doi.org/10.1016/j.brainres.2015.07.053>
- Jin DZ, Guo ML, Xue B, Mao LM and Wang JQ (2013): Differential regulation of CaMKII α interactions with mGluR5 and NMDA receptors by Ca²⁺ in neurons. *Journal of Neurochemistry* 127, 620-631. <http://dx.doi.org/10.1111/jnc.12434>
- Johnson EC (2011): N-acetylaspartylglutamate is not demonstrated to be a selective mGlu₆ receptor agonist. *Journal of Neurochemistry* 119, 896-898. <http://dx.doi.org/10.1111/j.1471-4159.2011.07480.x>
- Jones CK, Bubser M, Thompson AD, Dickerson JW, Turle-Lorenzo N, Amalric M, Blobaum AL, Bridges TM, Morrison RD, Jadhav S, Engers DW, Italiano K, Bode J, Daniels JS, Lindsley CW, Hopkins CR, Conn PJ and Niswender CM (2012): The metabotropic glutamate receptor 4-positive allosteric modulator VU0364770 produces efficacy alone and in combination with L-DOPA or an adenosine 2A antagonist in preclinical rodent models of Parkinson's disease. *J Pharmacol Exp Ther* 340, 404-421. <http://dx.doi.org/10.1124/jpet.111.187443>
- Jones CK, Eberle EL, Peters SC, Monn JA and Shannon HE (2005): Analgesic effects of the selective group II (mGlu2/3) metabotropic glutamate receptor agonists LY379268 and LY389795 in persistent and inflammatory pain models after acute and repeated dosing. *Neuropharmacology* 49, 206-218. <http://dx.doi.org/10.1016/j.neuropharm.2005.05.008>
- Jones Sa, Shim S-H, He J and Zhuang X (2011): Fast, three-dimensional super-resolution imaging of live cells. *Nature Methods* 8, 499-508. <http://dx.doi.org/10.1038/nmeth.1605>
- Jong YJ, Sergin I, Purgert CA and O'Malley KL (2014): Location-dependent signaling of the group 1 metabotropic glutamate receptor mGlu5. *Mol Pharmacol* 86, 774-785. <http://dx.doi.org/10.1124/mol.114.094763>
- Jong YJ, Kumar V, apos and Malley KL (2009): Intracellular metabotropic glutamate receptor 5 (mGluR5) activates signaling cascades distinct from cell surface counterparts. *Journal of Biological Chemistry* 284, 35827-35838. <http://dx.doi.org/10.1074/jbc.M109.046276>
- Kammermeier PJ and Worley PF (2007): Homer 1a uncouples metabotropic glutamate receptor 5 from postsynaptic effectors. *Proceedings of the National Academy of Sciences of the United States of America* 104, 6055-6060. <http://dx.doi.org/10.1073/pnas.0608991104>
- Kammermeier PJ, Xiao B, Tu JC, Worley PF and Ikeda SR (2000): Homer Proteins Regulate Coupling of Group I Metabotropic Glutamate Receptors to N-Type Calcium and M-Type Potassium Channels. *J. Neurosci.* 20, 7238-7245
- Kammermeier PJ and Yun J (2005): Activation of metabotropic glutamate receptor 1 dimers requires glutamate binding in both subunits. *J Pharmacol Exp Ther* 312, 502-508. <http://dx.doi.org/10.1124/jpet.104.073155>
- Karlin A and Winnik M (1968): Reduction and specific alkylation of the receptor for acetylcholine. *Proc Natl Acad Sci U S A* 60, 668-674
- Karunaratne WKA, Giri L, Kalyanaraman V and Gautam N (2013): Optically triggering spatiotemporally confined GPCR activity in a cell and programming neurite initiation and extension. *Proceedings of the*

- National Academy of Sciences of the United States of America* 110, E1565-1574. <http://dx.doi.org/10.1073/pnas.1220697110>
- Kauer Ja and Malenka RC (2007): Synaptic plasticity and addiction. *Nature reviews. Neuroscience* 8, 844-858. <http://dx.doi.org/10.1038/nrn2234>
- Kawabata S, Kohara a, Tsutsumi R, Itahana H, Hayashibe S, Yamaguchi T and Okada M (1998): Diversity of calcium signaling by metabotropic glutamate receptors. *The Journal of biological chemistry* 273, 17381-17385
- Kawabata S, Tsutsumi R, Kohara A, Yamaguchi T, Nakanishi S and Okada M (1996): Control of calcium oscillations by phosphorylation of metabotropic glutamate receptors. *Nature* 383, 89-92. <http://dx.doi.org/10.1038/383089a0>
- Kelly L, Farrant M and Cull-Candy SG (2009): Synaptic mGluR activation drives plasticity of calcium-permeable AMPA receptors. *Nature Neuroscience* 12, 593-601. <http://dx.doi.org/10.1038/nn.2309>
- Kenny PJ (2009): Emerging therapeutic targets for the treatment of nicotine addiction. *Expert Rev Clin Pharmacol* 2, 221-225. <http://dx.doi.org/10.1586/ecp.09.6>
- Kepler A, Gendreizig S, Gronemeyer T, Pick H, Vogel H and Johnsson K (2003): A general method for the covalent labeling of fusion proteins with small molecules in vivo. *Nature biotechnology* 21, 86-89. <http://dx.doi.org/10.1038/nbt765>
- Kim CH, Braud S, Isaac JTR and Roche KW (2005a): Protein kinase C phosphorylation of the metabotropic glutamate receptor mGluR5 on Serine 839 regulates Ca²⁺ oscillations. *The Journal of biological chemistry* 280, 25409-25415. <http://dx.doi.org/10.1074/jbc.M502644200>
- Kim CH, Lee J, Lee J-Y and Roche KW (2008): Metabotropic Glutamate Receptors: Phosphorylation and Receptor Signaling. *Journal of neuroscience research* 86, 1-10. <http://dx.doi.org/10.1002/jnr>
- Kim J-M, Hwa J, Garriga P, Reeves PJ, RajBhandary UL and Khorana HG (2005b): Light-driven activation of beta 2-adrenergic receptor signaling by a chimeric rhodopsin containing the beta 2-adrenergic receptor cytoplasmic loops. *Biochemistry* 44, 2284-2292. <http://dx.doi.org/10.1021/bi048328i>
- Kim TI, McCall JG, Jung YH, Huang X, Siuda ER, Li Y, Song J, Song YM, Pao HA, Kim RH, Lu C, Lee SD, Song IS, Shin G, Al-Hasani R, Kim S, Tan MP, Huang Y, Omenetto FG, Rogers JA and Bruchas MR (2013): Injectable, cellular-scale optoelectronics with applications for wireless optogenetics. *Science* 340, 211-216. <http://dx.doi.org/10.1126/science.1232437>
- Kimmel CB, Ballard WW, Kimmel SR, Ullmann B and Schilling TF (1995): Stages of embryonic development of the zebrafish. *Dev Dyn* 203, 253-310. <http://dx.doi.org/10.1002/aja.1002030302>
- Kinney GG, Brien JaO, Lemaire W, Burno M, Bickel DJ, Clements MK, Chen T-b, Wisnoski DD, Lindsley CW, Tiller PR, Smith S, Jacobson Ma, Sur C, Duggan ME, Pettibone DJ, Conn PJ and Williams DL (2005): A Novel Selective Positive Allosteric Modulator of Metabotropic Glutamate Receptor Subtype 5 Has in Vivo Activity and Antipsychotic-Like Effects in Rat Behavioral Models. *The Journal of Pharmacology and Experimental Therapeutics* 313, 199-206. <http://dx.doi.org/10.1124/jpet.104.079244.tive>
- Kinon BJ, Zhang L, Millen BA, Osuntokun OO, Williams JE, Kollack-Walker S, Jackson K, Kryzhanovskaya L, Jarkova N and Group HS (2011): A multicenter, inpatient, phase 2, double-blind, placebo-controlled dose-ranging study of LY2140023 monohydrate in patients with DSM-IV schizophrenia. *J Clin Psychopharmacol* 31, 349-355. <http://dx.doi.org/10.1097/JCP.0b013e318218dcd5>
- Kiritoshi T, Sun H, Ren W, Stauffer SR, Lindsley CW, Conn PJ and Neugebauer V (2013): Modulation of pyramidal cell output in the medial prefrontal cortex by mGluR5 interacting with CB1. *Neuropharmacology* 66, 170-178. <http://dx.doi.org/10.1016/j.neuropharm.2012.03.024>
- Kitano M, Nakaya M, Nakamura T, Nagata S and Matsuda M (2008): Imaging of Rab5 activity identifies essential regulators for phagosome maturation. *Nature* 453, 241-245. <http://dx.doi.org/10.1038/nature06857>
- Klein Matthew E, Castillo Pablo E and Jordan Bryen A (2015): Coordination between Translation and Degradation Regulates Inducibility of mGluR-LTD. *Cell Reports* 10, 1459-1466. <http://dx.doi.org/10.1016/j.celrep.2015.02.020>
- Kniazeff J, Bessis A-s, Maurel D, Ansanay H, Prézeau L and Pin J-p (2004): Closed state of both binding domains of homodimeric mGlu receptors is required for full activity. *Nature structural & molecular biology* 11, 706-713. <http://dx.doi.org/10.1038/nsmb794>
- Knoflach F and Kemp JA (1998): Metabotropic glutamate group II receptors activate a G protein-coupled inwardly rectifying K⁺ current in neurones of the rat cerebellum. *J Physiol* 509 (Pt 2), 347-354
- Kramer RH, Mourot A and Adesnik H (2013): Optogenetic pharmacology for control of native neuronal signaling proteins. *Nature Neuroscience* 16, 816-823. <http://dx.doi.org/10.1038/nn.3424>
- Kuang D and Hampson DR (2006): Ion dependence of ligand binding to metabotropic glutamate receptors. *Biochemical and Biophysical Research Communications* 345, 1-6. <http://dx.doi.org/10.1016/j.bbrc.2006.04.064>
- Kumar V, Fahey PG, Jong YJl, Ramanan N and O'Malley KL (2012): Activation of intracellular metabotropic glutamate receptor 5 in striatal neurons leads to up-regulation of genes associated with sustained synaptic transmission including Arc/Arg3.1 protein. *Journal of Biological Chemistry* 287, 5412-5425. <http://dx.doi.org/10.1074/jbc.M111.301366>

- Kumar V, Jong YJl and O'Malley KL (2008): Activated nuclear metabotropic glutamate receptor mGlu5 couples to nuclear Gq/11 proteins to generate inositol 1,4,5-trisphosphate-mediated nuclear Ca²⁺ release. *Journal of Biological Chemistry* 283, 14072-14083. <http://dx.doi.org/10.1074/jbc.M708551200>
- Kunishima N, Shimada Y, Tsuji Y, Sato T, Yamamoto M, Kumasaka T, Nakanishi S, Jingami H and Morikawa K (2000): Structural basis of glutamate recognition by a dimeric metabotropic glutamate receptor. *Nature* 407, 971-977. <http://dx.doi.org/10.1038/35039564>
- Langer R (1998): Drug delivery and targeting. *Nature* 392, 5-10
- Lau CG and Zukin RS (2007): NMDA receptor trafficking in synaptic plasticity and neuropsychiatric disorders. *Nature reviews. Neuroscience* 8, 413-426. <http://dx.doi.org/10.1038/nrn2153>
- Lavialle M, Aumann G, Anlauf E, Pröls F, Arpin M and Derouiche A (2011): Structural plasticity of perisynaptic astrocyte processes involves ezrin and metabotropic glutamate receptors. *Proceedings of the National Academy of Sciences of the United States of America* 108, 12915-12919. <http://dx.doi.org/10.1073/pnas.1100957108>
- Lee H-K (2012): Ca²⁺-permeable AMPA receptors in homeostatic synaptic plasticity. *Frontiers in Molecular Neuroscience* 5, 1-11. <http://dx.doi.org/10.3389/fnmol.2012.00017>
- Lee HG, Zhu X, O'Neill MJ, Webber K, Casadesus G, Marlatt M, Raina AK, Perry G and Smith MA (2004): The role of metabotropic glutamate receptors in Alzheimer's disease. *Acta Neurobiol Exp (Wars)* 64, 89-98
- Lee JH, Lee J, Choi KY, Hepp R, Lee JY, Lim MK, Chatani-Hinze M, Roche PA, Kim DG, Ahn YS, Kim CH and Roche KW (2008): Calmodulin dynamically regulates the trafficking of the metabotropic glutamate receptor mGluR5. *Proc Natl Acad Sci U S A* 105, 12575-12580. <http://dx.doi.org/10.1073/pnas.0712033105>
- Lefkowitz RJ and Shenoy SK (2005): Transduction of receptor signals by beta-arrestins. *Science* 308, 512-517. <http://dx.doi.org/10.1126/science.1109237>
- Levitz J, Pantoja C, Gaub B, Janovjak H, Reiner A, Hoagland A, Schoppik D, Kane B, Stawski P, Schier AF, Trauner D and Isacoff EY (2013): Optical control of metabotropic glutamate receptors. *Nature Neuroscience* 16, 507-516. <http://dx.doi.org/10.1038/nn.3346>
- Lewandowicz A, Tyler PC, Evans GB, Furneaux RH and Schramm VL (2003): Achieving the ultimate physiological goal in transition state analogue inhibitors for purine nucleoside phosphorylase. *The Journal of biological chemistry* 278, 31465-31468. <http://dx.doi.org/10.1074/jbc.C300259200>
- Liao GY, Wagner DA, Hsu MH and Leonard JP (2001): Evidence for direct protein kinase-C mediated modulation of N-methyl-D-aspartate receptor current. *Mol Pharmacol* 59, 960-964
- Lipinski Ca, Lombardo F, Dominy BW and Feeney PJ (2001): Experimental and computational approaches to estimate solubility and permeability in drug discovery and development settings. *Advanced Drug Delivery Reviews* 23 (1997) 3. *Advanced Drug Delivery Reviews* 46, 3-26. [http://dx.doi.org/10.1016/S0169-409X\(00\)00129-0](http://dx.doi.org/10.1016/S0169-409X(00)00129-0)
- Liu F, Ma XH, Ule J, Bibb JA, Nishi A, DeMaggio AJ, Yan Z, Nairn AC and Greengard P (2001): Regulation of cyclin-dependent kinase 5 and casein kinase 1 by metabotropic glutamate receptors. *Proc Natl Acad Sci U S A* 98, 11062-11068. <http://dx.doi.org/10.1073/pnas.191353898>
- Liu Z, Lavis Luke D and Betzig E (2015): Imaging Live-Cell Dynamics and Structure at the Single-Molecule Level. *Molecular Cell* 58, 644-659. <http://dx.doi.org/10.1016/j.molcel.2015.02.033>
- Lodge D, Tidball P, Mercier MS, Lucas SJ, Hanna L, Ceolin L, Kritikos M, Fitzjohn SM, Sherwood JL, Bannister N, Volianskis A, Jane DE, Bortolotto ZA and Collingridge GL (2013): Antagonists reversibly reverse chemical LTD induced by group I, group II and group III metabotropic glutamate receptors. *Neuropharmacology* 74, 135-146. <http://dx.doi.org/10.1016/j.neuropharm.2013.03.011>
- Lohse MJ, Nuber S and Hoffmann C (2012): Fluorescence / Bioluminescence Resonance Energy Transfer Techniques to Study G-Protein-Coupled Receptor Activation and Signaling. *Pharmacological Reviews* 64, 299-336. <http://dx.doi.org/10.1124/pr.110.004309>
- Lopez JP, Lim R, Cruceanu C, Crapper L, Fasano C, Labonte B, Maussion G, Yang JP, Yerko V, Vigneault E, El Mestikawy S, Mechawar N, Pavlidis P and Turecki G (2014): miR-1202 is a primate-specific and brain-enriched microRNA involved in major depression and antidepressant treatment. *Nature medicine* 20, 764-768. <http://dx.doi.org/10.1038/nm.3582>
- Los GV, Encell LP, McDougall MG, Hartzell DD, Karassina N, Zimprich C, Wood MG, Learish R, Ohana RF, Urh M, Simpson D, Mendez J, Zimmerman K, Otto P, Vidugiris G, Zhu J, Darzins A, Klaubert DH, Bulleit RF and Wood KV (2008): HaloTag: a novel protein labeling technology for cell imaging and protein analysis. *ACS Chem Biol* 3, 373-382. <http://dx.doi.org/10.1021/cb800025k>
- Lu YM, Jia Z, Janus C, Henderson JT, Gerlai R, Wojtowicz JM and Roder JC (1997): Mice lacking metabotropic glutamate receptor 5 show impaired learning and reduced CA1 long-term potentiation (LTP) but normal CA3 LTP. *The Journal of neuroscience : the official journal of the Society for Neuroscience* 17, 5196-5205
- Luján R, Roberts JDB, Shigemoto R, Ohishi H and Somogyi P (1997): Differential plasma membrane distribution of metabotropic glutamate receptors mGluR1 α , mGluR2 and mGluR5, relative to neurotransmitter release sites. *Journal of Chemical Neuroanatomy* 13, 219-241. [http://dx.doi.org/10.1016/S0891-0618\(97\)00051-3](http://dx.doi.org/10.1016/S0891-0618(97)00051-3)
- Lüscher C and Huber KM (2010): Group 1 mGluR-dependent synaptic long-term depression: mechanisms and implications for circuitry and disease. *Neuron* 65, 445-459. <http://dx.doi.org/10.1016/j.neuron.2010.01.016>

- Lüscher C and Slesinger Pa (2010): Emerging roles for G protein-gated inwardly rectifying potassium (GIRK) channels in health and disease. *Nature Reviews Neuroscience* 11, 301-315. <http://dx.doi.org/10.1038/nrn2834>
- Macia E, Ehrlich M, Massol R, Boucrot E, Brunner C and Kirchhausen T (2006): Dynasore, a cell-permeable inhibitor of dynamin. *Dev Cell* 10, 839-850. <http://dx.doi.org/10.1016/j.devcel.2006.04.002>
- Mahato PK, Pandey S and Bhattacharyya S (2015): Differential effects of protein phosphatases in the recycling of metabotropic glutamate receptor 5. *Neuroscience* 306, 138-150. <http://dx.doi.org/10.1016/j.neuroscience.2015.08.031>
- Mameli M, Balland B, Lujan R and Luscher C (2007): Rapid synthesis and synaptic insertion of GluR2 for mGluR-LTD in the ventral tegmental area. *Science* 317, 530-533. <http://dx.doi.org/10.1126/science.1142365>
- Mannaioni G, Marino MJ, Valenti O, Traynelis SF and Conn PJ (2001): Metabotropic glutamate receptors 1 and 5 differentially regulate CA1 pyramidal cell function. *J Neurosci* 21, 5925-5934
- Marcaggi P, Mutoh H, Dimitrov D, Beato M and Knöpfel T (2009): Optical measurement of mGluR1 conformational changes reveals fast activation, slow deactivation, and sensitization. *Proceedings of the National Academy of Sciences of the United States of America* 106, 11388-11393. <http://dx.doi.org/10.1073/pnas.0901290106>
- Marino MJ, Williams DL, Jr., O'Brien JA, Valenti O, McDonald TP, Clements MK, Wang R, DiLella AG, Hess JF, Kinney GG and Conn PJ (2003): Allosteric modulation of group III metabotropic glutamate receptor 4: a potential approach to Parkinson's disease treatment. *Proc Natl Acad Sci U S A* 100, 13668-13673. <http://dx.doi.org/10.1073/pnas.1835724100>
- Martin R, Bajo-Graneras R, Moratalla R, Perea G and Araque A (2015): Circuit-specific signaling in astrocyte-neuron networks in basal ganglia pathways. *Science* 349, 730-734. <http://dx.doi.org/10.1126/science.aaa7945>
- Masseck Oa, Rubelowski JM, Spoida K and Herlitze S (2011): Light- and drug-activated G-protein-coupled receptors to control intracellular signalling. *Experimental physiology* 96, 51-56. <http://dx.doi.org/10.1113/expphysiol.2010.055517>
- Masseck OA, Spoida K, Dalkara D, Maejima T, Rubelowski JM, Wallhorn L, Deneris ES and Herlitze S (2014): Vertebrate cone opsins enable sustained and highly sensitive rapid control of Gi/o signaling in anxiety circuitry. *Neuron* 81, 1263-1273. <http://dx.doi.org/10.1016/j.neuron.2014.01.041>
- Masu M, Iwakabe H, Tagawa Y, Miyoshi T, Yamashita M, Fukuda Y, Sasaki H, Hiroi K, Nakamura Y and Shigemoto R (1995): Specific deficit of the ON response in visual transmission by targeted disruption of the mGluR6 gene. *Cell* 80, 757-765
- Matosin N and Newell Ka (2013): Metabotropic glutamate receptor 5 in the pathology and treatment of schizophrenia. *Neuroscience and Biobehavioral Reviews* 37, 256-268. <http://dx.doi.org/10.1016/j.neubiorev.2012.12.005>
- Matsu-ura T, Michikawa T, Inoue T, Miyawaki A, Yoshida M and Mikoshiba K (2006): Cytosolic inositol 1,4,5-trisphosphate dynamics during intracellular calcium oscillations in living cells. *Journal of Cell Biology* 173, 755-765. <http://dx.doi.org/10.1083/jcb.200512141>
- Matsuzaki M, Ellis-Davies GC, Nemoto T, Miyashita Y, Iino M and Kasai H (2001): Dendritic spine geometry is critical for AMPA receptor expression in hippocampal CA1 pyramidal neurons. *Nature Neuroscience* 4, 1086-1092. <http://dx.doi.org/10.1038/nn736>
- Matsuzaki M, Honkura N, Ellis-Davies GC and Kasai H (2004): Structural basis of long-term potentiation in single dendritic spines. *Nature* 429, 761-766. <http://dx.doi.org/10.1038/nature02617>
- Matta Ja, Ashby MC, Sanz-Clemente A, Roche KW and Isaac JTR (2011): mGluR5 and NMDA receptors drive the experience- and activity-dependent NMDA receptor NR2B to NR2A subunit switch. *Neuron* 70, 339-351. <http://dx.doi.org/10.1016/j.neuron.2011.02.045>
- Maurel D, Comps-Agrar L, Brock C, Rives ML, Bourrier E, Ayoub MA, Bazin H, Tinel N, Durroux T, Prezeau L, Trinquet E and Pin JP (2008): Cell-surface protein-protein interaction analysis with time-resolved FRET and snap-tag technologies: application to GPCR oligomerization. *Nat Methods* 5, 561-567. <http://dx.doi.org/10.1038/nmeth.1213>
- Maurel D, Kniazeff J, Mathis G, Trinquet E, Pin J-P and Ansanay H (2004): Cell surface detection of membrane protein interaction with homogeneous time-resolved fluorescence resonance energy transfer technology. *Analytical biochemistry* 329, 253-262. <http://dx.doi.org/10.1016/j.ab.2004.02.013>
- Meitzen J, Pflipsen KR, Stern CM, Meisel RL and Mermelstein PG (2011): Measurements of neuron soma size and density in rat dorsal striatum, nucleus accumbens core and nucleus accumbens shell: differences between striatal region and brain hemisphere, but not sex. *Neurosci Lett* 487, 177-181. <http://dx.doi.org/10.1016/j.neulet.2010.10.017>
- Mellman I (1992): The importance of being acid: the role of acidification in intracellular membrane traffic. *J Exp Biol* 172, 39-45
- Mercier MS and Lodge D (2014): Group III metabotropic glutamate receptors: pharmacology, physiology and therapeutic potential. *Neurochemical research* 39, 1876-1894. <http://dx.doi.org/10.1007/s11064-014-1415-y>

- Michalon A, Sidorov M, Ballard TM, Ozmen L, Spooren W, Wettstein JG, Jaeschke G, Bear MF and Lindemann L (2012): Chronic pharmacological mGlu5 inhibition corrects fragile X in adult mice. *Neuron* 74, 49-56. <http://dx.doi.org/10.1016/j.neuron.2012.03.009>
- Miesenböck G, De Angelis Da and Rothman JE (1998): Visualizing secretion and synaptic transmission with pH-sensitive green fluorescent proteins. *Nature* 394, 192-195. <http://dx.doi.org/10.1038/28190>
- Miller S, Romano C and Cotman CW (1995): Growth factor upregulation of a phosphoinositide-coupled metabotropic glutamate receptor in cortical astrocytes. *The Journal of neuroscience : the official journal of the Society for Neuroscience* 15, 6103-6109
- Mitchell SJ and Silver RA (2000): Glutamate spillover suppresses inhibition by activating presynaptic mGluRs. *Nature* 404, 498-502. <http://dx.doi.org/10.1038/35006649>
- Miyashita T, Shao YR, Chung J, Pourzia O and Feldman DE (2013): Long-term channelrhodopsin-2 (ChR2) expression can induce abnormal axonal morphology and targeting in cerebral cortex. *Frontiers in neural circuits* 7, 8-8. <http://dx.doi.org/10.3389/fncir.2013.00008>
- Miyawaki A (2011): Development of probes for cellular functions using fluorescent proteins and fluorescence resonance energy transfer. *Annual review of biochemistry* 80, 357-373. <http://dx.doi.org/10.1146/annurev-biochem-072909-094736>
- Miyawaki a, Llopis J, Heim R, McCaffery JM, Adams Ja, Ikura M and Tsien RY (1997): Fluorescent indicators for Ca²⁺ based on green fluorescent proteins and calmodulin. *Nature* 388, 882-887. <http://dx.doi.org/10.1038/42264>
- Moghaddam B and Javitt D (2012): From Revolution to Evolution: The Glutamate Hypothesis of Schizophrenia and its Implication for Treatment. *Neuropsychopharmacology* 37, 4-15. <http://dx.doi.org/10.1038/npp.2011.181>
- Moldrich RX, Aprico K, Diwakarla S, O'Shea RD and Beart PM (2002): Astrocyte mGlu(2/3)-mediated cAMP potentiation is calcium sensitive: studies in murine neuronal and astrocyte cultures. *Neuropharmacology* 43, 189-203
- Moreno JL, Muguruza C, Umali A, Mortillo S, Holloway T, Pilar-cuéllar F, Mocci G, Seto J, Callado LF, Neve RL, Milligan G, Sealfon SC, López-giménez JF, Meana JJ and Benson DL (2012): Identification of Three Residues Essential for (5-HT 2A □ mGlu2) Receptor Heteromerization and Its Psychoactive Behavioral Function *. 287, 44301-44319. <http://dx.doi.org/10.1074/jbc.M112.413161>
- Morishima Y, Miyakawa T, Furuyashiki T, Tanaka Y, Mizuma H and Nakanishi S (2005): Enhanced cocaine responsiveness and impaired motor coordination in metabotropic glutamate receptor subtype 2 knockout mice. *Proceedings of the National Academy of Sciences of the United States of America* 102, 4170-4175. <http://dx.doi.org/10.1073/pnas.0500914102>
- Morishita W, Marie H and Malenka RC (2005): Distinct triggering and expression mechanisms underlie LTD of AMPA and NMDA synaptic responses. *Nature Neuroscience* 8, 1043-1050. <http://dx.doi.org/10.1038/nn1506>
- Mourof A, Fehrentz T, Le Feuvre Y, Smith CM, Herold C, Dalkara D, Nagy F, Trauner D and Kramer RH (2012): Rapid optical control of nociception with an ion-channel photoswitch. *Nature Methods* 9, 396-402. <http://dx.doi.org/10.1038/nmeth.1897>
- Mourof A, Kienzler MA, Banghart MR, Fehrentz T, Huber FME, Stein M, Kramer RH and Trauner D (2011): Tuning photochromic ion channel blockers. *ACS Chemical Neuroscience* 2, 536-543. <http://dx.doi.org/10.1021/cn200037p>
- Mukherjee S and Manahan-Vaughan D (2013): Role of metabotropic glutamate receptors in persistent forms of hippocampal plasticity and learning. *Neuropharmacology* 66, 65-81. <http://dx.doi.org/10.1016/j.neuropharm.2012.06.005>
- Mundell SJ, Matharu AL, Pula G, Roberts PJ and Kelly E (2001): Agonist-induced internalization of the metabotropic glutamate receptor 1a is arrestin- and dynamin-dependent. *J Neurochem* 78, 546-551
- Murphy-royal C, Dupuis JP, Varela Ja, Panatier A, Pinson B, Baufreton J, Groc L and Oliet SHR (2015): Surface diffusion of astrocytic glutamate transporters shapes synaptic transmission. 18. <http://dx.doi.org/10.1038/nn.3901>
- Muto T, Tsuchiya D, Morikawa K and Jingami H (2007): Structures of the extracellular regions of the group II/III metabotropic glutamate receptors. *Proceedings of the National Academy of Sciences of the United States of America* 104, 3759-3764. <http://dx.doi.org/10.1073/pnas.0611577104>
- Nagel G, Szellas T, Huhn W, Kateriya S, Adeishvili N, Berthold P, Ollig D, Hegemann P and Bamberg E (2003): Channelrhodopsin-2, a directly light-gated cation-selective membrane channel. *Proc Natl Acad Sci U S A* 100, 13940-13945. <http://dx.doi.org/10.1073/pnas.1936192100>
- Nakahara K, Okada M and Nakanishi S (1997): The metabotropic glutamate receptor mGluR5 induces calcium oscillations in cultured astrocytes via protein kinase C phosphorylation. *Journal of Neurochemistry* 69, 1467-1475
- Nakajima Y, Iwakabe H, Akazawa C, Nawa H, Shigemoto R, Mizuno N and Nakanishi S (1993): Molecular characterization of a novel retinal metabotropic glutamate receptor mGluR6 with a high agonist selectivity for L-2-amino-4-phosphobutyrate. *J Biol Chem* 268, 11868-11873
- Nakamoto M, Nalavadi V, Epstein MP, Narayanan U, Bassell GJ and Warren ST (2007): Fragile X mental retardation protein deficiency leads to excessive mGluR5-dependent internalization of AMPA receptors.

- Proceedings of the National Academy of Sciences of the United States of America* 104, 15537-15542. <http://dx.doi.org/10.1073/pnas.0707484104>
- Nash MS, Schell MJ, Atkinson PJ, Johnston NR, Nahorski SR and John Challiss RA (2002): Determinants of metabotropic glutamate receptor-5-mediated Ca²⁺ and inositol 1,4,5-trisphosphate oscillation frequency: Receptor density versus agonist concentration. *Journal of Biological Chemistry* 277, 35947-35960. <http://dx.doi.org/10.1074/jbc.M205622200>
- Nash MS, Young KW, Challiss RA and Nahorski SR (2001): Intracellular signalling. Receptor-specific messenger oscillations. *Nature* 413, 381-382. <http://dx.doi.org/10.1038/35096643>
- Neugebauer V (2001): Peripheral metabotropic glutamate receptors: fight the pain where it hurts. *Trends in Neurosciences* 24, 550-552
- Newman RH, Fosbrink MD and Zhang J (2011): Genetically encodable fluorescent biosensors for tracking signaling dynamics in living cells. *Chemical Reviews* 111, 3614-3666. <http://dx.doi.org/10.1021/cr100002u>
- Nickols HH and Conn JP (2014): Development of allosteric modulators of GPCRs for treatment of CNS disorders. *Neurobiology of Disease* 61, 55-71. <http://dx.doi.org/10.1016/j.nbd.2013.09.013>
- Nicoletti F, Bockaert J, Collingridge GL, Conn PJ, Ferraguti F, Schoepp DD, Wroblewski JT and Pin JP (2011): Metabotropic glutamate receptors: From the workbench to the bedside. *Neuropharmacology* 60, 1017-1041. <http://dx.doi.org/10.1016/j.neuropharm.2010.10.022>
- Nicoletti F, Bruno V, Ngomba RT, Gradini R and Battaglia G (2015): Metabotropic glutamate receptors as drug targets: what's new? *Current Opinion in Pharmacology* 20, 89-94. <http://dx.doi.org/10.1016/j.coph.2014.12.002>
- Nikolenko V, Poskanzer KE and Yuste R (2007): Two-photon photostimulation and imaging of neural circuits. *Nature Methods* 4, 943-950. <http://dx.doi.org/10.1038/nmeth1105>
- Nikolenko V, Watson BO, Araya R, Woodruff A, Peterka DS and Yuste R (2008): SLM Microscopy: Scanless Two-Photon Imaging and Photostimulation with Spatial Light Modulators. *Front Neural Circuits* 2, 5. <http://dx.doi.org/10.3389/neuro.04.005.2008>
- Nishi A, Liu F, Matsuyama S, Hamada M, Higashi H, Nairn AC and Greengard P (2003): Metabotropic mGlu5 receptors regulate adenosine A2A receptor signaling. *Proc Natl Acad Sci U S A* 100, 1322-1327. <http://dx.doi.org/10.1073/pnas.0237126100>
- Niswender CM and Conn PJ (2010): Metabotropic glutamate receptors: physiology, pharmacology, and disease. *Annual review of pharmacology and toxicology* 50, 295-322. <http://dx.doi.org/10.1146/annurev.pharmtox.011008.145533>
- Niswender CM, Johnson KA, Weaver CD, Jones CK, Xiang Z, Luo Q, Rodriguez AL, Marlo JE, de Paulis T, Thompson AD, Days EL, Nalywajko T, Austin CA, Williams MB, Ayala JE, Williams R, Lindsley CW and Conn PJ (2008): Discovery, characterization, and antiparkinsonian effect of novel positive allosteric modulators of metabotropic glutamate receptor 4. *Molecular Pharmacology* 74, 1345-1358. <http://dx.doi.org/10.1124/mol.108.049551>
- Noetzel MJ, Gregory KJ, Vinson PN, Manka JT, Stauffer SR, Lindsley CW, Niswender CM, Xiang Z and Conn PJ (2013): A novel metabotropic glutamate receptor 5 positive allosteric modulator acts at a unique site and confers stimulus bias to mGlu5 signaling. *Molecular Pharmacology* 83, 835-847. <http://dx.doi.org/10.1124/mol.112.082891>
- Noetzel MJ, Rook JM, Vinson PN, Cho HP, Days E, Zhou Y, Rodriguez AL, Lavreysen H, Stauffer SR, Niswender CM, Xiang Z, Daniels JS, Jones CK, Lindsley CW, Weaver CD and Conn PJ (2012): Functional impact of allosteric agonist activity of selective positive allosteric modulators of metabotropic glutamate receptor subtype 5 in regulating central nervous system function. *Mol Pharmacol* 81, 120-133. <http://dx.doi.org/10.1124/mol.111.075184>
- Noguchi J, Nagaoka A, Watanabe S, Ellis-Davies GCR, Kitamura K, Kano M, Matsuzaki M and Kasai H (2011): In vivo two-photon uncaging of glutamate revealing the structure-function relationships of dendritic spines in the neocortex of adult mice. *The Journal of physiology* 589, 2447-2457. <http://dx.doi.org/10.1113/jphysiol.2011.207100>
- Nomura A, Shigemoto R, Nakamura Y, Okamoto N, Mizuno N and Nakanishi S (1994): Developmentally regulated postsynaptic localization of a metabotropic glutamate receptor in rat rod bipolar cells. *Cell* 77, 361-369
- Nordquist RE, Durkin S, Jaeschke G and Spooren W (2007): Stress-induced hyperthermia: effects of acute and repeated dosing of MPEP. *Eur J Pharmacol* 568, 199-202. <http://dx.doi.org/10.1016/j.ejphar.2007.04.034>
- Nørskov-Lauritsen L, Thomsen ARB and Bräuner-Osborne H (2014): G protein-coupled receptor signaling analysis using homogenous time-resolved Förster resonance energy transfer (HTRF®) technology. *International Journal of Molecular Sciences* 15, 2554-2572. <http://dx.doi.org/10.3390/ijms15022554>
- Nussinov R and Tsai C-J (2013): Allostery in disease and in drug discovery. *Cell* 153, 293-305. <http://dx.doi.org/10.1016/j.cell.2013.03.034>
- O'Connor V, El Far O, Bofill-Cardona E, Nanoff C, Freissmuth M, Karschin A, Airas JM, Betz H and Boehm S (1999): Calmodulin dependence of presynaptic metabotropic glutamate receptor signaling. *Science* 286, 1180-1184

- Oh E, Maejima T, Liu C, Deneris E and Herlitze S (2010): Substitution of 5-HT1A receptor signaling by a light-activated G protein-coupled receptor. *J Biol Chem* 285, 30825-30836. <http://dx.doi.org/10.1074/jbc.M110.147298>
- Oh WC, Hill TC and Zito K (2013): Synapse-specific and size-dependent mechanisms of spine structural plasticity accompanying synaptic weakening. *Proceedings of the National Academy of Sciences of the United States of America* 110, E305-312. <http://dx.doi.org/10.1073/pnas.1214705110>
- Oh Won C, Parajuli Laxmi K and Zito K (2015): Heterosynaptic Structural Plasticity on Local Dendritic Segments of Hippocampal CA1 Neurons. *Cell Reports* 10, 162-169. <http://dx.doi.org/10.1016/j.celrep.2014.12.016>
- Okamoto N, Hori S, Akazawa C, Hayashi Y, Shigemoto R, Mizuno N and Nakanishi S (1994): Molecular characterization of a new metabotropic glutamate receptor mGluR7 coupled to inhibitory cyclic AMP signal transduction. *Journal of Biological Chemistry* 269, 1231-1236
- Olde Loohuis NFM, Ba W, Stoerchel PH, Kos A, Jager A, Schrott G, Martens GJM, van Bokhoven H, Nadif Kasri N and Aschrafi A (2015): MicroRNA-137 Controls AMPA-Receptor-Mediated Transmission and mGluR-Dependent LTD. *Cell Reports* 11, 1876-1884. <http://dx.doi.org/10.1016/j.celrep.2015.05.040>
- Palazzo E, Marabese I, de Novellis V, Rossi F and Maione S (2014): Spinal metabotropic glutamate receptors: a target for pain relief and beyond. *The European journal of neuroscience* 39, 444-454. <http://dx.doi.org/10.1111/ejn.12398>
- Palczewski K (2006): G protein-coupled receptor rhodopsin. *Annual review of biochemistry* 75, 743-767. <http://dx.doi.org/10.1146/annurev.biochem.75.103004.142743>
- Palma-Cerda F, Auger C, Crawford DJ, Hodgson ACC, Reynolds SJ, Cowell JK, Swift KaD, Cais O, Vyklicky L, Corrie JET and Ogden D (2012): New caged neurotransmitter analogs selective for glutamate receptor sub-types based on methoxy-nitroindoline and nitrophenylethoxycarbonyl caging groups. *Neuropharmacology* 63, 624-634. <http://dx.doi.org/10.1016/j.neuropharm.2012.05.010>
- Palmer MJ, Irving AJ, Seabrook GR, Jane DE and Collingridge GL (1997): The group I mGlu receptor agonist DHPG induces a novel form of LTD in the CA1 region of the hippocampus. *Neuropharmacology* 36, 1517-1532
- Panatier a and Robitaille R (2015): Astrocytic mGluR5s and the tripartite synapse. *Neuroscience*, 1-6. <http://dx.doi.org/10.1016/j.neuroscience.2015.03.063>
- Panatier A, Vallée J, Haber M, Murai KK, Lacaille J-C and Robitaille R (2011): Astrocytes are endogenous regulators of basal transmission at central synapses. *Cell* 146, 785-798. <http://dx.doi.org/10.1016/j.cell.2011.07.022>
- Paoletti P, Bellone C and Zhou Q (2013): NMDA receptor subunit diversity: impact on receptor properties, synaptic plasticity and disease. *Nature reviews. Neuroscience* 14, 383-400. <http://dx.doi.org/10.1038/nrn3504>
- Papagiakoumou E, Bègue A, Leshem B, Schwartz O, Stell BM, Bradley J, Oron D and Emiliani V (2013): Functional patterned multiphoton excitation deep inside scattering tissue. *Nature Photonics* 7, 274-278. <http://dx.doi.org/10.1038/nphoton.2013.9>
- Park JM, Hu J-H, Milshteyn A, Zhang P-W, Moore CG, Park S, Datko MC, Domingo RD, Reyes CM, Wang XJ, Etzkorn FA, Xiao B, Szumlinski KK, Kern D, Linden DJ and Worley PF (2013): A prolyl-isomerase mediates dopamine-dependent plasticity and cocaine motor sensitization. *Cell* 154, 637-650. <http://dx.doi.org/10.1016/j.cell.2013.07.001>
- Parmentier-Batteur S, Hutson PH, Menzel K, Uslaner JM, Mattson BA, O'Brien JA, Magliaro BC, Forest T, Stump CA, Tynebor RM, Anthony NJ, Tucker TJ, Zhang XF, Gomez R, Huszar SL, Lambeng N, Faure H, Le Poul E, Poli S, Rosahl TW, Rocher JP, Hargreaves R and Williams TM (2014): Mechanism based neurotoxicity of mGlu5 positive allosteric modulators--development challenges for a promising novel antipsychotic target. *Neuropharmacology* 82, 161-173. <http://dx.doi.org/10.1016/j.neuropharm.2012.12.003>
- Patil ST, Zhang L, Martenyi F, Lowe SL, Jackson KA, Andreev BV, Avedisova AS, Bardenstein LM, Gurovich IY, Morozova MA, Mosolov SN, Neznanov NG, Reznik AM, Smulevich AB, Tochilov VA, Johnson BG, Monn JA and Schoepp DD (2007): Activation of mGlu2/3 receptors as a new approach to treat schizophrenia: a randomized Phase 2 clinical trial. *Nat Med* 13, 1102-1107. <http://dx.doi.org/10.1038/nm1632>
- Pekhletski R, Gerlai R, Overstreet LS, Huang XP, Agopyan N, Slater NT, Abramow-Newerly W, Roder JC and Hampson DR (1996): Impaired cerebellar synaptic plasticity and motor performance in mice lacking the mGluR4 subtype of metabotropic glutamate receptor. *The Journal of neuroscience : the official journal of the Society for Neuroscience* 16, 6364-6373
- Pelkey KA, Lavezzari G, Racca C, Roche KW and McBain CJ (2005): mGluR7 is a metaplastic switch controlling bidirectional plasticity of feedforward inhibition. *Neuron* 46, 89-102. <http://dx.doi.org/10.1016/j.neuron.2005.02.011>
- Pelkey KA, Yuan X, Lavezzari G, Roche KW and McBain CJ (2007): mGluR7 undergoes rapid internalization in response to activation by the allosteric agonist AMN082. *Neuropharmacology* 52, 108-117. <http://dx.doi.org/10.1016/j.neuropharm.2006.07.020>
- Peng Y, Zhao J, Gu QH, Chen RQ, Xu Z, Yan JZ, Wang SH, Liu SY, Chen Z and Lu W (2010): Distinct trafficking and expression mechanisms underlie LTP and LTD of NMDA receptor-mediated synaptic responses. *Hippocampus* 20, 646-658. <http://dx.doi.org/10.1002/hipo.20654>

- Perea G and Araque A (2007): Astrocytes potentiate transmitter release at single hippocampal synapses. *Science (New York, N.Y.)* 317, 1083-1086. <http://dx.doi.org/10.1126/science.1144640>
- Perea G, Yang A, Boyden ES and Sur M (2014): Optogenetic astrocyte activation modulates response selectivity of visual cortex neurons in vivo. *Nat Commun* 5, 3262. <http://dx.doi.org/10.1038/ncomms4262>
- Perroy J, Raynaud F, Homburger V, Rousset MC, Telley L, Bockaert J and Fagni L (2008): Direct interaction enables cross-talk between ionotropic and group I metabotropic glutamate receptors. *Journal of Biological Chemistry* 283, 6799-6805. <http://dx.doi.org/10.1074/jbc.M705661200>
- Petersen OH, Michalak M and Verkhratsky A (2005): Calcium signalling: Past, present and future. *Cell Calcium* 38, 161-169. <http://dx.doi.org/10.1016/j.ceca.2005.06.023>
- Petralia RS, Wang YX, Niedzielski AS and Wenthold RJ (1996): The metabotropic glutamate receptors, MGLUR2 and MGLUR3, show unique postsynaptic, presynaptic and glial localizations. *Neuroscience* 71, 949-976. [http://dx.doi.org/10.1016/0306-4522\(95\)00533-1](http://dx.doi.org/10.1016/0306-4522(95)00533-1)
- Pierce KL and Lefkowitz RJ (2001): Classical and new roles of beta-arrestins in the regulation of G-protein-coupled receptors. *Nature reviews. Neuroscience* 2, 727-733. <http://dx.doi.org/10.1038/35094577>
- Pierce KL, Premont RT and Lefkowitz RJ (2002): Seven-transmembrane receptors. *Nature reviews. Molecular cell biology* 3, 639-650. <http://dx.doi.org/10.1038/nrm908>
- Piers TM, Kim DH, Kim BC, Regan P, Whitcomb DJ and Cho K (2012): Translational Concepts of mGluR5 in Synaptic Diseases of the Brain. *Frontiers in Pharmacology* 3, 199-199. <http://dx.doi.org/10.3389/fphar.2012.00199>
- Pilc A, Chaki S, Nowak G and Witkin JM (2008): Mood disorders: regulation by metabotropic glutamate receptors. *Biochem Pharmacol* 75, 997-1006. <http://dx.doi.org/10.1016/j.bcp.2007.09.021>
- Pilc A, Wierońska JM and Skolnick P (2013): Glutamate-based antidepressants: preclinical psychopharmacology. *Biological Psychiatry* 73, 1125-1132. <http://dx.doi.org/10.1016/j.biopsych.2013.01.021>
- Pin JPP and Duvoisin R (1995): The metabotropic glutamate receptors: Structure and functions. *Neuropharmacology* 34, 1-26. [http://dx.doi.org/10.1016/0028-3908\(94\)00129-G](http://dx.doi.org/10.1016/0028-3908(94)00129-G)
- Pinheiro PS and Mulle C (2008): Presynaptic glutamate receptors: physiological functions and mechanisms of action. *Nature reviews. Neuroscience* 9, 423-436. <http://dx.doi.org/10.1038/nrn2379>
- Pitsikas N (2014): The metabotropic glutamate receptors: potential drug targets for the treatment of anxiety disorders? *European Journal of Pharmacology* 723, 181-184. <http://dx.doi.org/10.1016/j.ejphar.2013.12.019>
- Pittolo S, Gómez-Santacana X, Eckelt K, Rovira X, Dalton J, Goudet C, Pin J-P, Llobet A, Giraldo J, Llebaria A and Gorostiza P (2014): A photochromic allosteric modulator to control an endogenous G protein-coupled receptor with light. *Nature chemical biology* (In press), 1-5. <http://dx.doi.org/10.1038/nchembio.1612>
- Poisik OV, Mannaioni G, Traynelis S, Smith Y and Conn PJ (2003): Distinct functional roles of the metabotropic glutamate receptors 1 and 5 in the rat globus pallidus. *J Neurosci* 23, 122-130
- Polosukhina A, Litt J, Tochitsky I, Nemargut J, Sychev Y, De Kouchkovsky I, Huang T, Borges K, Trauner D, Van Gelder RN and Kramer RH (2012): Photochemical Restoration of Visual Responses in Blind Mice. *Neuron* 75, 271-282. <http://dx.doi.org/10.1016/j.neuron.2012.05.022>
- Pomierny-Chamióło L, Rup K, Pomierny B, Niedzielska E, Kalivas PW and Filip M (2014): Metabotropic glutamatergic receptors and their ligands in drug addiction. *Pharmacology & therapeutics* 142, 281-305. <http://dx.doi.org/10.1016/j.pharmthera.2013.12.012>
- Porter RH, Jaeschke G, Spooren W, Ballard TM, Buttelmann B, Kolczewski S, Peters JU, Prinssen E, Wichmann J, Vieira E, Muhlemann A, Gatti S, Mutel V and Malherbe P (2005): Fenobam: a clinically validated nonbenzodiazepine anxiolytic is a potent, selective, and noncompetitive mGlu5 receptor antagonist with inverse agonist activity. *J Pharmacol Exp Ther* 315, 711-721. <http://dx.doi.org/10.1124/jpet.105.089839>
- Preta G, Cronin JG and Sheldon IM (2015): Dynasore - not just a dynamin inhibitor. *Cell Communication and Signaling* 13, 1-7. <http://dx.doi.org/10.1186/s12964-015-0102-1>
- Quiocho FA (1990): Atomic structures of periplasmic binding proteins and the high-affinity active transport systems in bacteria. *Philos Trans R Soc Lond B Biol Sci* 326, 341-351; discussion 351-342
- Rau H (1990) Photoisomerization of Azobenzenes. In *Photochemistry and photophysics* (Rabek JF ed.). CRC Press, Boca Raton.
- Redfern CH, Coward P, Degtyarev MY, Lee EK, Kwa AT, Hennighausen L, Bujard H, Fishman GI and Conklin BR (1999): Conditional expression and signaling of a specifically designed Gi-coupled receptor in transgenic mice. *Nat Biotechnol* 17, 165-169. <http://dx.doi.org/10.1038/6165>
- Regehr WG (2012): Short-term presynaptic plasticity. *Cold Spring Harbor Perspectives in Biology* 4, 1-19. <http://dx.doi.org/10.1101/cshperspect.a005702>
- Reiner A, Levitz J and Isacoff EY (2015): Controlling ionotropic and metabotropic glutamate receptors with light: principles and potential. *Current Opinion in Pharmacology* 20, 135-143. <http://dx.doi.org/10.1016/j.coph.2014.12.008>
- Remus TP, Zima AV, Bossuyt J, Bare DJ, Martin JL, Blatter LA, Bers DM and Mignery GA (2006): Biosensors to measure inositol 1,4,5-trisphosphate concentration in living cells with spatiotemporal resolution. *J Biol Chem* 281, 608-616. <http://dx.doi.org/10.1074/jbc.M509645200>

- Ritter SL and Hall Ra (2009): Fine-tuning of GPCR activity by receptor-interacting proteins. *Nature reviews. Molecular cell biology* 10, 819-830. <http://dx.doi.org/10.1038/nrm2803>
- Roda A, Pasini P, Mirasoli M, Michelini E and Guardigli M (2004): Biotechnological applications of bioluminescence and chemiluminescence. *Trends Biotechnol* 22, 295-303. <http://dx.doi.org/10.1016/j.tibtech.2004.03.011>
- Rogan SC and Roth BL (2011): Remote control of neuronal signaling. *Pharmacol Rev* 63, 291-315. <http://dx.doi.org/10.1124/pr.110.003020>
- Romano C, Yang WL and O'Malley KL (1996): Metabotropic glutamate receptor 5 is a disulfide-linked dimer. *J Biol Chem* 271, 28612-28616
- Rondard P, Goudet C, Kniazeff J, Pin JP and Prézeau L (2011): The complexity of their activation mechanism opens new possibilities for the modulation of mGlu and GABAB class C G protein-coupled receptors. *Neuropharmacology* 60, 82-92. <http://dx.doi.org/10.1016/j.neuropharm.2010.08.009>
- Rook JM, Noetzel MJ, Pouliot Wa, Bridges TM, Vinson PN, Cho HP, Zhou Y, Gogliotti RD, Manka JT, Gregory KJ, Stauffer SR, Dudek FE, Xiang Z, Niswender CM, Daniels JS, Jones CK, Lindsley CW and Conn PJ (2013): Unique signaling profiles of positive allosteric modulators of metabotropic glutamate receptor subtype 5 determine differences in vivo activity. *Biological Psychiatry* 73, 501-509. <http://dx.doi.org/10.1016/j.biopsych.2012.09.012>
- Rook JM, Xiang Z, Lv X, Ghoshal A, Dickerson JW, Bridges TM, Johnson KA, Foster DJ, Gregory KJ, Vinson PN, Thompson AD, Byun N, Collier RL, Bubser M, Nedelcovych MT, Gould RW, Stauffer SR, Daniels JS, Niswender CM, Lavreysen H, Mackie C, Conde-Ceide S, Alcazar J, Bartolomé-Nebreda JM, Macdonald GJ, Talpos JC, Steckler T, Jones CK, Lindsley CW and Conn PJ (2015): Biased mGlu5-Positive Allosteric Modulators Provide In Vivo Efficacy without Potentiating mGlu5 Modulation of NMDAR Currents. *Neuron* 86, 1029-1040. <http://dx.doi.org/10.1016/j.neuron.2015.03.063>
- Rust MJ, Bates M and Zhuang X (2006): Sub-diffraction-limit imaging by stochastic optical reconstruction microscopy (STORM). *Nat Methods* 3, 793-795. <http://dx.doi.org/10.1038/nmeth929>
- Sansig G, Bushell TJ, Clarke VR, Rozov A, Burnashev N, Portet C, Gasparini F, Schmutz M, Klebs K, Shigemoto R, Flor PJ, Kuhn R, Knoepfel T, Schroeder M, Hampson DR, Collett VJ, Zhang C, Duvoisin RM, Collingridge GL and van Der Putten H (2001): Increased seizure susceptibility in mice lacking metabotropic glutamate receptor 7. *The Journal of neuroscience : the official journal of the Society for Neuroscience* 21, 8734-8745
- Sato M, Ueda Y, Shibuya M and Umezawa Y (2005): Locating inositol 1,4,5-trisphosphate in the nucleus and neuronal dendrites with genetically encoded fluorescent indicators. *Analytical chemistry* 77, 4751-4758. <http://dx.doi.org/10.1021/ac040195j>
- Sato M, Ueda Y and Umezawa Y (2006): Imaging diacylglycerol dynamics at organelle membranes. *Nat Methods* 3, 797-799. <http://dx.doi.org/10.1038/nmeth930>
- Scanziani M (2002): Competing on the edge. *Trends Neurosci* 25, 282-283
- Scanziani M and Häusser M (2009): Electrophysiology in the age of light. *Nature* 461, 930-939. <http://dx.doi.org/10.1038/nature08540>
- Scanziani M, Salin PA, Vogt KE, Malenka RC and Nicoll RA (1997a): Use-dependent increases in glutamate concentration activate presynaptic metabotropic glutamate receptors. *Nature* 385, 630-634. <http://dx.doi.org/10.1038/385630a0>
- Scanziani M, Salin PA, Vogt KE, Malenka RC and Nicoll RA (1997b): Use-dependent increases in glutamate concentration activate presynaptic metabotropic glutamate receptors. *Nature* 385, 630-634. <http://dx.doi.org/10.1038/385630a0>
- Schafer DP, Lehrman EK, Kautzman AG, Koyama R, Mardinly AR, Yamasaki R, Ransohoff RM, Greenberg ME, Barres BA and Stevens B (2012): Microglia Sculpt Postnatal Neural Circuits in an Activity and Complement-Dependent Manner. *Neuron* 74, 691-705. <http://dx.doi.org/10.1016/j.neuron.2012.03.026>
- Schnabel R, Kilpatrick IC and Collingridge GL (1999): An investigation into signal transduction mechanisms involved in DHPG-induced LTD in the CA1 region of the hippocampus. *Neuropharmacology* 38, 1585-1596
- Schoepp DD, Wright RA, Levine LR, Gaydos B and Potter WZ (2003): LY354740, an mGlu2/3 receptor agonist as a novel approach to treat anxiety/stress. *Stress* 6, 189-197. <http://dx.doi.org/10.1080/1025389031000146773>
- Schönberger M, Damijonaitis A, Zhang Z, Nagel D and Trauner D (2014): Development of a new photochromic ion channel blocker via azologization of fomocaine. *ACS Chemical Neuroscience* 5, 514-518. <http://dx.doi.org/10.1021/cn500070w>
- Schönberger M and Trauner D (2014): A Photochromic Agonist for μ -Opioid Receptors. *Angewandte Chemie (International ed. in English)* 53, 3264-3267. <http://dx.doi.org/10.1002/anie.201309633>
- Schwartz TW and Holst B (2007): Allosteric enhancers, allosteric agonists and ago-allosteric modulators: where do they bind and how do they act? *Trends in Pharmacological Sciences* 28, 366-373. <http://dx.doi.org/10.1016/j.tips.2007.06.008>
- Serge A, Fourgeaud L, Hemar A and Choquet D (2003): Active surface transport of metabotropic glutamate receptors through binding to microtubules and actin flow. *Journal of cell science* 116, 5015-5022. <http://dx.doi.org/10.1242/jcs.00822>
- Sergé A, Fourgeaud L, Hémar A and Choquet D (2002): Receptor activation and homer differentially control the lateral mobility of metabotropic glutamate receptor 5 in the neuronal membrane. *The Journal of*

- neuroscience : the official journal of the Society for Neuroscience* 22, 3910-3920. <http://dx.doi.org/20026331>
- Sheffler DJ, Wenthur CJ, Bruner JA, Carrington SJ, Vinson PN, Gogi KK, Blobaum AL, Morrison RD, Vamos M, Cosford ND, Stauffer SR, Daniels JS, Niswender CM, Conn PJ and Lindsley CW (2012): Development of a novel, CNS-penetrant, metabotropic glutamate receptor 3 (mGlu3) NAM probe (ML289) derived from a closely related mGlu5 PAM. *Bioorg Med Chem Lett* 22, 3921-3925. <http://dx.doi.org/10.1016/j.bmcl.2012.04.112>
- Shen Y, Rampino MA, Carroll RC and Nawy S (2012): G-protein-mediated inhibition of the Trp channel TRPM1 requires the Gbetagamma dimer. *Proc Natl Acad Sci U S A* 109, 8752-8757. <http://dx.doi.org/10.1073/pnas.1117433109>
- Shigemoto R, Kinoshita A, Wada E, Nomura S, Ohishi H, Takada M, Flor PJ, Neki A, Abe T, Nakanishi S and Mizuno N (1997): Differential presynaptic localization of metabotropic glutamate receptor subtypes in the rat hippocampus. *J Neurosci* 17, 7503-7522
- Shigemoto R, Kulik A, Roberts JD, Ohishi H, Nusser Z, Kaneko T and Somogyi P (1996): Target-cell-specific concentration of a metabotropic glutamate receptor in the presynaptic active zone. *Nature* 381, 523-525. <http://dx.doi.org/10.1038/381523a0>
- Singh J, Petter RC, Baillie Ta and Whitty A (2011): The resurgence of covalent drugs. *Nature reviews. Drug discovery* 10, 307-317. <http://dx.doi.org/10.1038/nrd3410>
- Siuda ER, Copits BA, Schmidt MJ, Baird MA, Al-Hasani R, Planer WJ, Funderburk SC, McCall JG, Gereau RWt and Bruchas MR (2015): Spatiotemporal control of opioid signaling and behavior. *Neuron* 86, 923-935. <http://dx.doi.org/10.1016/j.neuron.2015.03.066>
- Slawinska A, Wieronska JM, Stachowicz K, Marciniak M, Lason-Tyburkiewicz M, Gruca P, Papp M, Kusek M, Tokarski K, Doller D and Pilc A (2013): The antipsychotic-like effects of positive allosteric modulators of metabotropic glutamate mGlu4 receptors in rodents. *Br J Pharmacol* 169, 1824-1839. <http://dx.doi.org/10.1111/bph.12254>
- Smedler E and Uhlén P (2014) Frequency decoding of calcium oscillations, pp. 964-969.
- Snyder EM, Philpot BD, Huber KM, Dong X, Fallon JR and Bear MF (2001): Internalization of ionotropic glutamate receptors in response to mGluR activation. *Nature Neuroscience* 4, 1079-1085. <http://dx.doi.org/10.1038/nn746>
- Snyder MA and Gao WJ (2013): NMDA hypofunction as a convergence point for progression and symptoms of schizophrenia. *Front Cell Neurosci* 7, 31. <http://dx.doi.org/10.3389/fncel.2013.00031>
- Sohya K, Kameyama K, Yanagawa Y, Obata K and Tsumoto T (2007): GABAergic neurons are less selective to stimulus orientation than excitatory neurons in layer II/III of visual cortex, as revealed by in vivo functional Ca²⁺ imaging in transgenic mice. *The Journal of neuroscience : the official journal of the Society for Neuroscience* 27, 2145-2149. <http://dx.doi.org/10.1523/JNEUROSCI.4641-06.2007>
- Spoida K, Masseck OA, Deneris ES and Herlitze S (2014): Gq/5-HT_{2c} receptor signals activate a local GABAergic inhibitory feedback circuit to modulate serotonergic firing and anxiety in mice. *Proc Natl Acad Sci U S A* 111, 6479-6484. <http://dx.doi.org/10.1073/pnas.1321576111>
- Spooren WP, Vassout A, Neijt HC, Kuhn R, Gasparini F, Roux S, Porsolt RD and Gentsch C (2000): Anxiolytic-like effects of the prototypical metabotropic glutamate receptor 5 antagonist 2-methyl-6-(phenylethynyl)pyridine in rodents. *The Journal of Pharmacology and Experimental Therapeutics* 295, 1267-1275
- Sridharan R, Zuber J, Connelly SM, Mathew E and Dumont ME (2014): Fluorescent approaches for understanding interactions of ligands with G protein coupled receptors. *Biochim Biophys Acta* 1838, 15-33. <http://dx.doi.org/10.1016/j.bbamem.2013.09.005>
- Stawski P, Sumser M and Trauner D (2012): A photochromic agonist of AMPA receptors. *Angewandte Chemie - International Edition* 51, 5748-5751. <http://dx.doi.org/10.1002/anie.201109265>
- Stein M, Breit A, Fehrentz T, Gudermann T and Trauner D (2013): Optical control of TRPV1 channels. *Angewandte Chemie* 52, 9845-9848. <http://dx.doi.org/10.1002/anie.201302530>
- Stein M, Middendorp SJ, Carta V, Pejo E, Raines DE, Forman Sa, Sigel E and Trauner D (2012): Azopropofols: photochromic potentiators of GABA(A) receptors. *Angewandte Chemie* 51, 10500-10504. <http://dx.doi.org/10.1002/anie.201205475>
- Stenmark H (2009): Rab GTPases as coordinators of vesicle traffic. *Nature reviews. Molecular cell biology* 10, 513-525. <http://dx.doi.org/10.1038/nrm2728>
- Stone T (1988): NMDA receptors and ligands in the vertebrate CNS. *Progress in Neurobiology* 30, 333-368. [http://dx.doi.org/10.1016/0301-0082\(88\)90027-5](http://dx.doi.org/10.1016/0301-0082(88)90027-5)
- Stone TW and Burton NR (1988): NMDA receptors and ligands in the vertebrate CNS. *Prog Neurobiol* 30, 333-368
- Sun W, McConnell E, Pare JF, Xu Q, Chen M, Peng W, Lovatt D, Han X, Smith Y and Nedergaard M (2013): Glutamate-dependent neuroglial calcium signaling differs between young and adult brain. *Science* 339, 197-200. <http://dx.doi.org/10.1126/science.1226740>
- Svoboda K and Yasuda R (2006): Principles of Two-Photon Excitation Microscopy and Its Applications to Neuroscience. *Neuron* 50, 823-839. <http://dx.doi.org/10.1016/j.neuron.2006.05.019>

- Swanson CJ, Bures M, Johnson MP, Linden A-M, Monn JA and Schoepp DD (2005): Metabotropic glutamate receptors as novel targets for anxiety and stress disorders. *Nature reviews. Drug discovery* 4, 131-144. <http://dx.doi.org/10.1038/nrd1630>
- Szymański W, Beierle JM, Kistemaker HaV, Velema Wa and Feringa BL (2013): Reversible photocontrol of biological systems by the incorporation of molecular photoswitches. *Chemical Reviews* 113, 6114-6178. <http://dx.doi.org/10.1021/cr300179f>
- Takahashi T, Forsythe ID, Tsujimoto T, Barnes-Davies M and Onodera K (1996): Presynaptic calcium current modulation by a metabotropic glutamate receptor. *Science (New York, N.Y.)* 274, 594-597. <http://dx.doi.org/10.1126/science.274.5287.594>
- Tamaru Y, Nomura S, Mizuno N and Shigemoto R (2001): Distribution of metabotropic glutamate receptor mGluR3 in the mouse CNS: differential location relative to pre- and postsynaptic sites. *Neuroscience* 106, 481-503
- Tanimura A, Morita T, Nezu A, Shitara A, Hashimoto N and Tojyo Y (2009): Use of fluorescence resonance energy transfer-based biosensors for the quantitative analysis of inositol 1,4,5-trisphosphate dynamics in calcium oscillations. *Journal of Biological Chemistry* 284, 8910-8917. <http://dx.doi.org/10.1074/jbc.M805865200>
- Tanimura A, Nezu A, Morita T, Turner RJ and Tojyo Y (2004): Fluorescent biosensor for quantitative real-time measurements of inositol 1,4,5-trisphosphate in single living cells. *The Journal of biological chemistry* 279, 38095-38098. <http://dx.doi.org/10.1074/jbc.C400312200>
- Tateyama M and Kubo Y (2006): Dual signaling is differentially activated by different active states of the metabotropic glutamate. *Proceedings of the National Academy of Sciences* 103
- Thomas U (2002): Modulation of synaptic signalling complexes by Homer proteins. *J Neurochem* 81, 407-413
- Thomsen WJ and Behan DP (2007): G protein-coupled receptors. *Comprehensive medicinal chemistry II*, 771-826
- Tian L, Hires SA, Mao T, Huber D, Chiappe ME, Chalasani SH, Petreanu L, Akerboom J, McKinney Sa, Schreier ER, Bargmann CI, Jayaraman V, Svoboda K and Looger LL (2009): Imaging neural activity in worms, flies and mice with improved GCaMP calcium indicators. *Nature Methods* 6, 875-881. <http://dx.doi.org/10.1038/nmeth.1398>
- Torres-Platas SG, Hercher C, Davoli MA, Maussion G, Labonte B, Turecki G and Mechawar N (2011): Astrocytic hypertrophy in anterior cingulate white matter of depressed suicides. *Neuropsychopharmacology* 36, 2650-2658. <http://dx.doi.org/10.1038/npp.2011.154>
- Trehan A, Rotgers E, Coffey ET, Huhtaniemi I and Rivero-Müller A (2014): CANDLES, an assay for monitoring GPCR induced cAMP generation in cell cultures. *Cell communication and signaling : CCS* 12, 70-70. <http://dx.doi.org/10.1186/s12964-014-0070-x>
- Tsai HH, Li H, Fuentealba LC, Molofsky aV, Taveira-Marques R, Zhuang H, Tenney a, Murnen aT, Fancy SPJ, Merkle F, Kessaris N, Alvarez-Buylla a, Richardson WD and Rowitch DH (2012): Regional Astrocyte Allocation Regulates CNS Synaptogenesis and Repair. *Science* 337, 358-362. <http://dx.doi.org/10.1126/science.1222381>
- Tsien RY (1980): New calcium indicators and buffers with high selectivity against magnesium and protons: design, synthesis, and properties of prototype structures. *Biochemistry* 19, 2396-2404
- Tsien RY (1981): A non-disruptive technique for loading calcium buffers and indicators into cells. *Nature* 290, 527-528. <http://dx.doi.org/10.1038/290527a0>
- Tsukiji S, Miyagawa M, Takaoka Y, Tamura T and Hamachi I (2009): Ligand-directed tosyl chemistry for protein labeling in vivo. *Nat Chem Biol* 5, 341-343. <http://dx.doi.org/10.1038/nchembio.157>
- Tu JC, Xiao B, Naisbitt S, Yuan JP, Petralia RS, Brakeman P, Doan A, Aakalu VK, Lanahan Aa, Sheng M and Worley PF (1999): Coupling of mGluR/Homer and PSD-95 complexes by the Shank family of postsynaptic density proteins. *Neuron* 23, 583-592. [http://dx.doi.org/10.1016/S0896-6273\(00\)80810-7](http://dx.doi.org/10.1016/S0896-6273(00)80810-7)
- Turrigiano GG (2008): The Self-Tuning Neuron: Synaptic Scaling of Excitatory Synapses. *Cell* 135, 422-435. <http://dx.doi.org/10.1016/j.cell.2008.10.008>
- Ueda Y, Kwok S and Hayashi Y (2013): Application of FRET probes in the analysis of neuronal plasticity. *Frontiers in neural circuits* 7, 163-163. <http://dx.doi.org/10.3389/fncir.2013.00163>
- Urwyler S (2011): Allosteric modulation of family C G-protein-coupled receptors: from molecular insights to therapeutic perspectives. *Pharmacological Reviews* 63, 59-126. <http://dx.doi.org/10.1124/pr.109.002501.59>
- Vafabakhsh R, Levitz J and Isacoff EY (2015): Conformational dynamics of a class C G-protein-coupled receptor. *Nature*. <http://dx.doi.org/10.1038/nature14679>
- van Wyk M, Pielecka-Fortuna J, Löwel S and Kleinlogel S (2015): Restoring the ON Switch in Blind Retinas: Opto-mGluR6, a Next-Generation, Cell-Tailored Optogenetic Tool. *PLOS Biology* 13, e1002143-e1002143. <http://dx.doi.org/10.1371/journal.pbio.1002143>
- Varney Ma, Cosford ND, Jachec C, Rao SP, Sacaan a, Lin FF, Bleicher L, Santori EM, Flor PJ, Allgeier H, Gasparini F, Kuhn R, Hess SD, Veliçelebi G and Johnson EC (1999): SIB-1757 and SIB-1893: selective, noncompetitive antagonists of metabotropic glutamate receptor type 5. *The Journal of Pharmacology and Experimental Therapeutics* 290, 170-181

- Vendrell-Criado V, Rodriguez-Muniz GM, Yamaji M, Lhiaubet-Vallet V, Cuquerella MC and Miranda MA (2013): Two-photon chemistry from upper triplet states of thymine. *J Am Chem Soc* 135, 16714-16719. <http://dx.doi.org/10.1021/ja408997j>
- Verkhusha VV and Lukyanov Ka (2004): The molecular properties and applications of Anthozoa fluorescent proteins and chromoproteins. *Nature biotechnology* 22, 289-296. <http://dx.doi.org/10.1038/nbt943>
- Vilardaga JP, Bunemann M, Krasel C, Castro M and Lohse MJ (2003): Measurement of the millisecond activation switch of G protein-coupled receptors in living cells. *Nat Biotechnol* 21, 807-812. <http://dx.doi.org/10.1038/nbt838>
- Volgraf M, Gorostiza P, Numano R, Kramer RH, Isacoff EY and Trauner D (2006): Allosteric control of an ionotropic glutamate receptor with an optical switch. *Nat Chem Biol* 2, 47-52. <http://dx.doi.org/10.1038/nchembio756>
- Volgraf M, Gorostiza P, Szobota S, Helix MR, Isacoff EY and Trauner D (2007): Reversibly caged glutamate: a photochromic agonist of ionotropic glutamate receptors. *J Am Chem Soc* 129, 260-261. <http://dx.doi.org/10.1021/ja067269o>
- Wang X, Lou N, Xu Q, Tian G-F, Peng WG, Han X, Kang J, Takano T and Nedergaard M (2006): Astrocytic Ca²⁺ signaling evoked by sensory stimulation in vivo. *Nature Neuroscience* 9, 816-823. <http://dx.doi.org/10.1038/nn1703>
- Weichert D and Gmeiner P (2015): Covalent molecular probes for class A G protein-coupled receptors: advances and applications. *ACS Chem Biol* 10, 1376-1386. <http://dx.doi.org/10.1021/acschembio.5b00070>
- Westin L, Reuss M, Lindskog M, Aperia A and Brismar H (2014): Nanoscopic spine localization of Norbin, an mGluR5 accessory protein. *BMC neuroscience* 15, 45-45. <http://dx.doi.org/10.1186/1471-2202-15-45>
- Wilkinson KA and Henley JM (2011): Analysis of metabotropic glutamate receptor 7 as a potential substrate for SUMOylation. *Neuroscience Letters* 491, 181-186. <http://dx.doi.org/10.1016/j.neulet.2011.01.032>
- Willard SS and Koochekpour S (2013): Glutamate , Glutamate Receptors , and Downstream Signaling Pathways. *Int J Biol Sci* 9, 948-959. <http://dx.doi.org/10.7150/ijbs.6426>
- Wood MR, Hopkins CR, Brogan JT, Conn PJ and Lindsley CW (2011): "Molecular switches" on mGluR allosteric ligands that modulate modes of pharmacology. *Biochemistry* 50, 2403-2410. <http://dx.doi.org/10.1021/bi200129s>
- Wroblewska B, Wroblewski JT, Pshenichkin S, Surin A, Sullivan SE and Neale JH (2002): N-Acetylaspartylglutamate Selectively Activates mGluR3 Receptors in Transfected Cells. *Journal of Neurochemistry* 69, 174-181. <http://dx.doi.org/10.1046/j.1471-4159.1997.69010174.x>
- Wu H, Wang C, Gregory KJ, Han GW, Cho HP, Xia Y, Niswender CM, Katritch V, Meiler J, Cherezov V, Conn PJ and Stevens RC (2014): Structure of a class C GPCR metabotropic glutamate receptor 1 bound to an allosteric modulator. *Science (New York, N.Y.)* 344, 58-64. <http://dx.doi.org/10.1126/science.1249489>
- Xiao B, Tu JC, Petralia RS, Yuan JP, Doan A, Breder CD, Ruggiero A, Lanahan AA, Wenthold RJ and Worley PF (1998): Homer regulates the association of group 1 metabotropic glutamate receptors with multivalent complexes of homer-related, synaptic proteins. *Neuron* 21, 707-716
- Xu C, Zipfel W, Shear JB, Williams RM and Webb WW (1996): Multiphoton fluorescence excitation: new spectral windows for biological nonlinear microscopy. *Proceedings of the National Academy of Sciences of the United States of America* 93, 10763-10768. <http://dx.doi.org/10.1073/pnas.93.20.10763>
- Xu C and Zipfel WR (2015): Multiphoton excitation of fluorescent probes. *Cold Spring Harb Protoc* 2015, 250-258. <http://dx.doi.org/10.1101/pdb.top086116>
- Yin S and Niswender CM (2014): Progress toward advanced understanding of metabotropic glutamate receptors: structure, signaling and therapeutic indications. *Cellular signalling* 26, 2284-2297. <http://dx.doi.org/10.1016/j.cellsig.2014.04.022>
- Yin S, Noetzel MJ, Johnson Ka, Zamorano R, Jalan-Sakrikar N, Gregory KJ, Conn PJ and Niswender CM (2014): Selective actions of novel allosteric modulators reveal functional heteromers of metabotropic glutamate receptors in the CNS. *The Journal of neuroscience : the official journal of the Society for Neuroscience* 34, 79-94. <http://dx.doi.org/10.1523/JNEUROSCI.1129-13.2014>
- Yokoi M, Kobayashi K, Manabe T, Takahashi T, Sakaguchi I, Katsuura G, Shigemoto R, Ohishi H, Nomura S, Nakamura K, Nakao K, Katsuki M and Nakanishi S (1996): Impairment of hippocampal mossy fiber LTD in mice lacking mGluR2. *Science (New York, N.Y.)* 273, 645-647
- Yue L, Pawlowski M, Dellal SS, Xie A, Feng F, Otis TS, Bruzik KS, Qian H and Pepperberg DR (2012): Robust photoregulation of GABAA receptors by allosteric modulation with a propofol analogue. *Nature Communications* 3, 1095-1095. <http://dx.doi.org/10.1038/ncomms2094>
- Yuste R and Bonhoeffer T (2001): Morphological changes in dendritic spines associated with long-term synaptic plasticity. *Annu Rev Neurosci* 24, 1071-1089. <http://dx.doi.org/10.1146/annurev.neuro.24.1.1071>
- Zaccolo M and Pozzan T (2002): Discrete microdomains with high concentration of cAMP in stimulated rat neonatal cardiac myocytes. *Science (New York, N.Y.)* 295, 1711-1715. <http://dx.doi.org/10.1126/science.1069982>
- Zhang XL, Upreti C and Stanton PK (2011): Gbetagamma and the C terminus of SNAP-25 are necessary for long-term depression of transmitter release. *PloS one* 6, e20500. <http://dx.doi.org/10.1371/journal.pone.0020500>

- Zhou XL, Karlsson C ... and Goldman D (2013): Loss of metabotropic glutamate receptor 2 escalates alcohol consumption *Proceedings of the National Academy of Sciences of the United States of America* 110, 16963-16968. <http://dx.doi.org/10.1073/pnas.1309839110>
- Zonta M, Angulo MC, Gobbo S, Rosengarten B, Hossmann K-A, Pozzan T and Carmignoto G (2003): Neuron-to-astrocyte signaling is central to the dynamic control of brain microcirculation. *Nature Neuroscience* 6, 43-50. <http://dx.doi.org/10.1038/nn980>



Institute for Bioengineering of Catalonia



UNIVERSITAT DE
BARCELONA